Host Cell-Specific Folding of the Neuronal Nicotinic Acetylcholine Receptor α7 and α8 Subunits.

Sandra T. Cooper

A thesis presented for the degree of Doctor of Philosophy to the University of London

May 1998

The Wellcome Laboratory for Molecular Pharmacology, Department of Pharmacology, University College, London, WC1E 6BT.

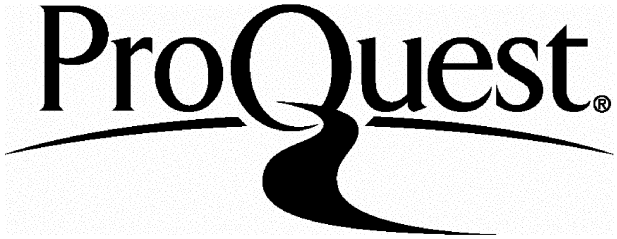

Abstract

The α7 and α8 nicotinic acetylcholine receptor (nAChR) subunits when expressed in *Xenopus* oocytes, form functional homo-oligomeric ion channels which are potently inhibited by the nicotinic antagonist α-bungarotoxin (αBTX). However, expression of the rat α7 and chick α8 subunits in several mammalian cell lines demonstrates that the folding of α7 and α8 into a conformation able to bind αBTX or conformation-sensitive antibodies, is critically dependent on the host cell type. In all cell lines, production of α7 (~58 kDa) or α8 (~57 kDa) subunit protein was verified by metabolic labelling and immunoprecipitation using subunit-specific antibodies which recognise linear epitopes. In contrast, for both α7 and α8 subunits, antibodies which recognise conformation-dependent extracellular epitopes fail to detect subunit protein in cell lines which fail to produce nicotinic radioligand binding, implying that these subunits are misfolded. The α7 subunit was expressed in a panel of nine mammalian cell lines from neuronal (N1E-115, NCB-20, Neuro2A, NG108-15, PC12, SH-SY5Y) and non-neuronal (HEK293, CHO, COS-7) origins. However, elevated levels of αBTX-binding could be detected in only two (PC12 and SH-SY5Y) of the nine cell lines examined. The α8 subunit was expressed in three cell lines (HEK293, GH_4C_1, SH-SY5Y) and readily formed αBTX-binding sites in a polyclonal SH-SY5Y-α8 cell line and when transiently expressed in GH_4C_1 cells. Saturation binding revealed that α8 nAChRs expressed in transfected GH_4C_1-α8 cells bind epibatidine with high affinity (K_D=0.24 ± 0.4 nM) although no specific αBTX or epibatidine binding could be detected in transfected HEK293-α8 cells. HEK293 cells which fail to correctly fold the α7 and α8 nAChR subunits form functional cell surface rat muscle nAChRs and homo-oligomeric 5-HT_3 receptors. In addition, chimaeric subunits encoding the N-terminal region of α7 or α8 and the C-terminal domain of the 5-HT_3 receptor were expressed very efficiently in all cell lines examined. These results implicate the C-terminal domain of α7 and α8 in the cell-type specific folding and further chimeras need to be generated to more precisely determine which region mediates this effect.

Contents

List of figures

Abbreviations

5-HT	5-hydroxytryptamine
5-HT_3R	5-hydroxytryptamine receptor, Type 3
α-BTX	α-bungarotoxin
ACh	Acetylcholine
ADH	alcohol dehydrogenase
ATP	adenosine triphosphate
BES	*N,N*-bis (2-hydroxyethyl) -2-aminoethanesulfonic acid buffered saline
B_{max}	maximal binding level
BOSC 23	human kidney fibroblast
BSA	bovine serum albumin
CHO	hamster ovary fibroblast
CIAP	calf intestinal alkaline phosphatase
CMV	cytomegalovirus
COS7	monkey kidney fibroblast
CPBG	1-*m*-chlorophenyl biguanide
DDF	[^{3}H-p-(*N*, *N*-dimethylamino)-benzenediazonium fluoroborate]
dNTP	deoxynucleotide triphosphate
ddNTP	dideoxynucleotide triphosphate
DHβE	dihydro-β-erythroidine
DMEM	Dulbecco's modified Eagle's medium
DMPP	1,1-dimethyl-4-phenylpiperazinium iodide
DMSO	dimethylsulphoxide
dNTP	deoxynucleotide triphosphate
DTT	dithiothreitol
EC_{50}	median effective concentration
EDTA	ethylenediaminetetraacetic acid
EndoF	N-endoglycoside F

EndoH	N-endoglycoside H
FITC	fluoroscein isothiocyanate
Fura 2-AM	Fura 2-acetoxymethyl ester
G418	geneticin G418 sulphate
$GABA_AR$	γ-aminobutyric acid receptor, Type A
GH_4C_1	rat pituitary cell line
HBSS	Hanks buffered saline solution
HEK293	human embryonic kidney fibroblast
HEPES	*N*-2-hydroxyethylpiperazine-*N*-2-ethanesulphonic acid
k_D	equilibrium binding constant
kDa	kilodalton
LBbroth	Luria-Bettani medium
LB	lysis buffer
mAb	monoclonal antibody
MBTA	[^{3}H-4- (N-maleimido)-benzyltrimethylammonium]
MEA	methanethiosuphonate ethylammonium
MLA	methyllycaconitine
MOPS	(3-*N* -morpholino propanesulphonic acid)
MQ	milli-Q
MT	metallothionein
nAChR	nicotinic acetylcholine receptor
NCB20	mouse neuroblastoma/rat brain hybrid cell line
NEM	*N* -ethylmaleimide
Neuro-2A	mouse neuroblastoma cell line
NG108-15	mouse neuroblastoma/rat glioma hybrid cell line
n_H	Hill Coefficient
NIE-115	mouse neuroblastoma cell line
ONPG	*o*-nitrophenyl-β-D-galactopyranoside
PBS	phosphate buffered saline

PC12	rat adrenal phaeochromocytoma cell line
PCR	polymerase chain reaction
PEI	polyethylenimine
PFA	paraformaldehyde
PMSF	phenylmethylsulfonyl fluoride
Rd-BTX	rhodamine-conjugated α-bungarotoxin
SCG	superior cervical ganglia
SDS	sodium dodecyl sulphate
SDS-PAGE	SDS polyacrylamide gel electrophoresis
SH-SY5Y	human neuroblastoma cell line
SV40	Simian virus
U	units

Introduction

1.0 Introduction

The neurotransmitter acetylcholine has two distinct sites of action within the vertebrate central nervous system. One site is also activated by muscarine and blocked by atropine and is termed "muscarinic", whereas the other site is activated by nicotine and blocked by curare and is termed "nicotinic". Muscarinic acetylcholine receptors are integral membrane glycoproteins which belong to a large superfamily of G-protein coupled receptors (for reviews see Caulfield, 1993; Wess, 1996). Each member of this superfamily is composed of a single, large polypeptide chain which contain seven putative transmembrane domains and tranduces agonist or sensory stimulus via the activation of heterotrimeric guanine nucleotide binding proteins (G-proteins) (Kolbilka, 1992). Muscarinic acetylcholine receptors are relatively slow transmitters of external signals requiring the activation of downstream signal transducers such as adenylyl cyclase, phospholipase C, D and A_2, and guanylyl cylclase to mediate their effect through the subsequent release of cellular second messengers such as cyclic adenosine mono-phosphate (cAMP), inositol 1,4,5-triphosphate (IP_3), diacylglycerol (DAG), arachidonic acid and cyclic guanine mono-phosphate (cGMP) (Caulfield, 1993; Felder, 1995).

In contrast, nicotinic acetylcholine receptors (nAChRs) are ligand-gated ion channels which directly mediate an immediate depolarizing effect in response to ACh (for review see Claudio, 1989). Nicotinic acetylcholine receptors belong to a large family of neurotransmitter-gated ion channels which also includes γ-aminobutyric acid Type A ($GABA_A$) receptors (Barnard *et al.*, 1987; Schofield *et al.*, 1987), glycine receptors (Grenningloh *et al.*, 1987), the serotonin 5-HT_3 (5-hydroxytryptamine Type 3) receptor (Maricq *et al.*, 1991) and an invertebrate glutamate-gated chloride channel (Cully *et al.*, 1994). All members of this ligand-gated ion channel family share sequence similarities and form oligomeric ion channel complexes, made up of subunits with four putative transmembrane domains, which bind specific

neurotransmitters and conduct ions across the plasma membrane. The ACh and serotonin (5-HT_3) ion channels conduct cations and are classified as "excitatory", whereas the $GABA_A$, glycine receptors and the invertebrate glutamate-gated chloride channel conduct anions and are classified as "inhibitory" .

1.1 The nicotinic acetylcholine receptor (nAChR)

1.1.1 The nAChR of electric organ

The electric organs of the marine *Torpedo californica* ray and the freshwater electric eel (*Electrophorous electricus*) are composed of rows or columns of cells termed electroplaques or electrocytes which are modified muscle cells. The electroplaques are innervated and are very densely packed with rows of nAChRs providing an abundant source for nAChR isolation (Karlin and Cowburn, 1973; Weill *et al.*, 1974). The snake toxin α-bungarotoxin (αBTX) (Lee and Chang, 1966), isolated from the venom of the Elipadae snake *Bungarus multicintus* (a Malayan banded krait), is a potent nicotinic antagonist and binds almost irreversibly to the *Torpedo* nAChR (Changeux *et al.*, 1970). The specific high affinity binding of αBTX to the nAChR has been exploited in the extensive characterization of the nAChR which has revealed many of its biochemical and pharmacological properties (Popot and Changeux, 1984).

The nAChR of electric organ is a transmembrane pentameric glycoprotein (Brisson and Unwin, 1985) composed of four different subunits α, β, γ and δ which were named according to their increasing apparent molecular weights of approximately 40 kilodaltons (kDa), 48 kDa, 58 kDa and 64 kDa, respectively (Hucho *et al.*, 1976). The native nAChRs isolated from *Torpedo* exist as a pentameric monomer of ~250kDa and a disulphide-linked dimer of ~500kDa which migrate on a sucrose gradient with sedimentation coefficients of 9S and 13S, respectively (Gibson *et al.*, 1976; Reynolds and Karlin, 1978). By affinity labelling of the nAChR with an alkylating agent [^{3}H]-MBTA ([^{3}H]-4-(*N*-maleimido)-benzyltrimethylammonium), or

with [^{3}H]-bromo-acetylcholine, the α subunits were identified as containing the ligand binding site and it was shown that there were two ligand-binding sites per receptor molecule (Reiter *et al.*, 1972; Weill *et al.*, 1974; Kao *et al.*, 1984; Karlin, 1991) (see Section 1.2.2). Given the apparent molecular weights of the subunits, it was established that the native nAChR is a pentamer assembled with the stoichiometry $\alpha_2\beta\gamma\delta$ (Reynolds and Karlin, 1978).

1.1.2 The nAChR of the vertebrate neuromuscular junction

Several lines of evidence suggested that the nAChR from electric organ was highly homologous to the nAChR located at the synapse of the neuromuscular junction. The purified mammalian muscle nAChR was found to sediment with a similar buoyant density to the nAChR from electric organ and consist of four subunit components (Froehner, 1977). A 45 kDa and a 49 kDa component (which both produced identical peptide maps and probably represents differently glycosylated species of the same protein) could be affinity labelled with [^{3}H]-MBTA (Froehner, 1977). Monoclonal antibodies raised against individual *Torpedo* nAChR subunits crossreacted with mammalian muscle nAChR subunits (Lindstrom, 1978; Lindstrom, 1979) and it was possible to induce an auto-immune response in rats against their own nAChR by injection of any of the four Torpedo nAChR subunits (Lindstrom, 1978).

Over the last 50 years, electrophysiologists have studied neurotransmission at the muscle endplate and the gating, conductance and desensitization properties of the muscle-type nicotinic acetylcholine receptor have been well defined (Peper *et al.*, 1982; Sakmann and Neher, 1984; Colquhoun and Ogden, 1988). At the vertebrate neuromuscular junction, the nAChR is located on the post synaptic membrane and mediates synaptic transmission between nerve and muscle. Upon stimulation of the motor neurone, when an action potential reaches the motor nerve ending, vesicles containing ACh fuse to the presynaptic membrane and release ACh into the synaptic cleft. Within a few microseconds the local concentration of ACh rapidly reaches 0.1-

1.0mM (Katz and Miledi, 1977). ACh molecules diffuse about 50 nm to the post-synaptic membrane which is densely packed with nAChRs. Two molecules of ACh bind per receptor molecule on the extracellular side of the membrane (Adams, 1981). Upon binding of ACh, the nAChRs undergo a conformational change and the ion channel opens allowing cations (principally sodium ions but also potassium and calcium) to flow through the plasma membrane. This results in depolarization of the muscle cell and eventually muscle contraction. The entire process, from the activation of the motor neurone by an action potential, to contraction of the muscle fibre, occurs in under 100μs (Adams, 1981; Peper *et al.*, 1982). Activation by ACh is terminated within a few milliseconds as ACh diffuses away and is rapidly hydrolyzed by acetylcholinesterase (Katz and Miledi, 1977).

1.1.3 Cloning and expression of the nAChR of electric organ and muscle

In 1981, a landmark experiment successfully expressed assembled *Torpedo* nAChRs in *Xenopus* oocyes (Sumikawa *et al.*, 1981). Amphibian oocytes had been previously used for the translation of foreign mRNA and found to successfully generate proteins which were correctly post-translationally modified and secreted (Gurdon *et al.*, 1971; Lane *et al.*, 1979). Sumikawa and colleagues isolated mRNA from the electric organ of *Torpedo* and used this crude preparation to inject *Xenopus* oocytes. Biochemical analysis of injected oocytes revealed the presence of the four α, β, γ, and δ *Torpedo* nAChR subunits which had undergone signal peptide cleavage and were glycosylated (Sumikawa *et al.*, 1981). Sucrose gradient centrifugation and surface αBTX-binding experiments showed that the four subunits were assembled into a oligomeric complex which migrated with a sedimentation coefficient of 9S (the *Torpedo* nAChR did not form a dimer in oocytes) and was successfully exported and inserted into the plasma membrane. Shortly afterwards, a second report used established electrophysiological techniques to show that the nAChRs expressed at the cell surface of *Torpedo* mRNA-injected oocytes were functional and formed channels with similar ionic properties to that of native electric organ nAChRs (Barnard *et al.*, 1982).

Since then an enormous amount of progress has been made and genes encoding the subunits of the *Torpedo* nAChR were cloned (Noda *et al.*, 1982; Claudio *et al.*, 1983; Noda *et al.*, 1983c). Recombinant *Torpedo* nAChRs were heterologously expressed in *Xenopus* oocytes (Mishina *et al.*, 1984; Kurosaki *et al.*, 1987) and later in mouse fibroblasts (Claudio *et al.*, 1987) and the pharmacological properties of these receptors were found to closely resemble the functional characteristics of the native nAChR from electric organ.

cDNA probes derived from *Torpedo* sequences were used to isolate the genes encoding the highly homologous muscle nAChR located at the neuromuscular junction (Noda *et al.*, 1983a; LaPolla *et al.*, 1984; Nef *et al.*, 1984; Tanabe *et al.*, 1984) which were also expressed in *Xenopus* oocytes (Boulter *et al.*, 1986b) and mammalian fibroblasts (Blount and Merlie, 1989; Forsayeth *et al.*, 1990; Gu *et al.*, 1990).

During the process of screening different mammalian libraries for muscle nAChR cDNA clones, a novel γ-like subunit was discovered and termed ε (Takai *et al.*, 1985). Electrophysiological analysis revealed that the channel properties of nAChRs expressed in oocytes injected with α, β, γ and δ subunits resembled the low conductance nAChR channels typical of foetal muscle, whereas nAChRs formed following injection of α, β, δ, and ε subunits exhibited the high conductance properties reminiscent of nAChR channels at the adult endplate (Mishina *et al.*, 1986). The nicotinic AChR in mammalian muscle was found to exist in two forms. Both species share common α, β and δ subunits, but the γ subunit expressed in embryonic (and denervated) muscle is exchanged in a developmental switch to a homologous ε subunit in adult muscle.

1.1.4 The neuronal nicotinic acetylcholine receptors

The most well characterised neuronal nicotinic cholinergic transmission is located at the motor neurone-Renshaw cell synapse within the spinal cord (Curtis and Ryall, 1966; Belcher and Ryall, 1977), but many neurons within the brain and in autonomic ganglia respond to applications of nicotine or ACh. During the period when αBTX was being used to characterise the nAChR of *Torpedo* and muscle, high affinity αBTX-binding sites were detected in brain and ganglia (Green *et al.*, 1973; Hunt and Schmidt, 1978). Surprisingly, ganglia which responded to nicotine, and possessed [^{125}I]-αBTX-binding sites, were not inhibited by applications of αBTX. Furthermore, an antiserum raised against the *Torpedo* nAChR was shown to block responses elicited by nicotine on rat phaeochromocytoma (PC-12) cells, but failed to precipitate the αBTX-binding component (Patrick and Stallcup, 1977a; Patrick and Stallcup, 1977b). On the basis of these observations, it was proposed that the αBTX-binding component and the functional nAChR present on the ganglia may be different proteins (Patrick and Stallcup, 1977a; Oswald and Freeman, 1981).

Due to the cross-reactivity of the *Torpedo* nAChR antisera with the nicotinic receptor on PC-12 cells, it was suggested that the "neuronal-type" nAChR must be structurally homologous, and cDNA probes based on sequences from *Torpedo* and muscle nAChR subunits might be used to identify genes encoding neuronal nAChR subunits. In 1986, the first neuronal nicotinic α subunit was cloned from a rat PC12 cDNA library (Boulter *et al.*, 1986a) and the first neuronal nAChR was immunopurified from chick brain using a monoclonal antibody raised against *Torpedo* α (mAb35) (Whiting and Lindstrom, 1986b).

To date, the screening of cDNA libraries and recombinant DNA technology has identified eleven genes which encode neuronal-type nAChR subunits (Figure 1.1.1) (for review see Sargent, 1993; McGehee and Role, 1995). These neuronal nAChR subunits all exhibit high sequence homology to *Torpedo* and muscle nAChR genes

Figure 1.1.1. Summary of the cloned rat neuronal nAChR subunits. Data modified from Sargent *et al*, 1993.

Subunit	Probe	Mature Peptide (Da)	Amino Acids	Consensus N-linked Glycosylation Sites	Conserved Cysteines	Homology	Reference
α2	chick α2	55 500	484	29, 79, 185	133, 147, 197, 198	α1/48%	Wada *et al.*, 1988
α3	mouse α1	54 800	474	24, 141	128, 142, 192, 193	α1/52%, α2/58%	Boulter *et al.*, 1986
α4	rat α3 mouse α1	67 100	600	24, 141	128, 142, 192, 193	α1/53%, α2/68% α3/59%	Boulter *et al.*, 1987 Goldman *et al.*, 1987
α5	rat β3	48 800	424	112, 140, 186	127, 141, 191, 192	α1-α4/44-55%	Boulter *et al.*, 1990
α6	PCR	53 300	463	24, 141	66, 128, 142, 192, 193	α3/59% α2, α4/49% α1, α5/41%, 45% β2-β4/43-47%	Lamar *et al.*, 1990
α7	PCR(based on chick α7, α8)	54 200	480	24, 68, 111	116, 128, 142 200, 201	α2-α5/31-37% β2-β4/31-37%	Séguéla *et al.*, 1993
α8* (Chick)	Chick α7	55 200	481	24, 111	116, 128, 142 190, 191	α7/82%	Schoepfer *et al.*, 1990
α9	PCR (based on rat α7)	~52 000	457		133, 147, 197 198	α8, α8/38% α2-α6/36-39%	Elgoyhen *et al.*, 1994
β2	rat α3	54 300	475	26, 141	128, 142	β1/45% α1-α5/44-50%	Deneris *et al.*, 1988
β3	rat α3	50 200	434	26, 141	128, 142	β1, β2/40%, 44% α1/45% α2-α4/50-56% α5/68%	Deneris *et al.*, 1989
β4	rat β2	53 300	475	132, 146	132, 146	β2/64% β1, β3/43%, 44% α1-α5/43-52%	Duvoisin *et al.*, 1989 Boulter *et al.*, 1990

* No mammalian homologue of chick α8 has been identified.

and possess two cysteine residues which align to the disulphide linked Cys-128 and Cys-142 residues located within the extracellular N-terminal domain of *Torpedo* α (Kao and Karlin, 1986). Eight genes are designated as α-type (α2 - α9), based on whether they contain an additional pair of conserved adjacent cysteine residues that are found in all α subunits of muscle and electric organ (aligning at positions 192 and 193 of *Torpedo* α) and are thought to form part of the ligand-binding domain (Kao *et al.*, 1984; Kao and Karlin, 1986; Dennis *et al.*, 1988) (see Section 1.2.2).

The remaining three subunits are termed β-type (β2 - β4), not because they most closely resemble β1, but because they lack the conserved adjacent cysteine residues (aligning to Cys 192 and Cys 193 of *Torpedo* α). However, both rat β2 and β4 can substitute for rat muscle β1 when coexpressed with α1, γ and δ subunits in *Xenopus* oocytes (Deneris *et al.*, 1988; Duvoisin *et al.*, 1989) although β3 is unable to substitute for β1 in this manner.

Analysis of cloned neuronal nAChR subunits expressed in *Xenopus* oocytes reveals that when α2, α3 or α4 is expressed in combination with either β2 or β4 subunits, functional ion channels are generated which are activated by ACh (Boulter *et al.*, 1987; Ballivet *et al.*, 1988; Deneris *et al.*, 1988; Wada *et al.*, 1988; Papke *et al.*, 1989). No functional channels were detected following the injection of pairwise combinations of α5, α6 or β3 with any other single subunit (Deneris *et al.*, 1989; Couturier *et al.*, 1990b). However, more recently functional responses to ACh were obtained by the co-expression of chick and rat α6 subunits with human β4 in *Xenopus* oocytes (Gerzanich *et al.*, 1997). Interestingly, no functional nicotinic channels were detected when chick or rat α6 was expressed with the chick β2, β3 or β4 or the human β2 subunit. Each of the nicotinic channels formed by these pairwise combinations of neuronal subunits expressed in *Xenopus* oocytes possess distinct channel properties and pharmacological profiles and none were shown to be sensitive to the muscle and electric organ nicotinic antagonist αBTX.

In contrast to the other neuronal nAChR subunits, the α7, α8 and α9 subunits are able to form functional homo-oligomeric ion channels activated by ACh when expressed individually in *Xenopus* oocytes (Couturier *et al.*, 1990a; Elgoyhen *et al.*, 1994; Gerzanich *et al.*, 1994; Gotti *et al.*, 1994). The homo-oligomeric nAChRs also differ from other neuronal hetero-oligomeric channels in their sensitivity to nanomolar concentrations of the nicotinic antagonist αBTX (Couturier *et al.*, 1990a; Seguela *et al*, 1993 Elgoyhen *et al.*, 1994; Gerzanich *et al.*, 1994).

1.2 The structure of the nicotinic acetylcholine receptor

1.2.1 The primary structure of nAChR subunits

The primary amino-acid sequence of all nAChR subunits are approximately 40-50% homologous and are thought to have similar tertiary structures (see Figure 1.2.1). Sequence analysis indicate that there are four hydrophobic putative transmembrane domains which are termed M1-M4 and are highly conserved throughout the subunit family (Noda *et al.*, 1983b; Sargent, 1993). Each of the subunits are synthesized with a signal sequence which is cleaved to form the mature protein (Anderson and Blobel, 1981). The N-terminus constitutes a large hydrophilic extracellular domain which contains N-linked glycosylation sites (Nomoto *et al.*, 1986) and, in the case of the α subunits, the ligand-binding domain (Weill *et al.*, 1974). There is a large intracellular loop between transmembrane domains M3 and M4 which is phosphorylated at one or more sites in the muscle and Torpedo nAChR subunits (Huganir *et al.*, 1984; Ross *et al.*, 1987). The loops between the other proposed transmembrane domains are short, with only 20-25 residues each, and the short C-terminal fragment is also extracellular (as defined by the location of the *Torpedo* δ–δ disulphide bond) (Dunn *et al.*, 1986; McCrea *et al.*, 1987).

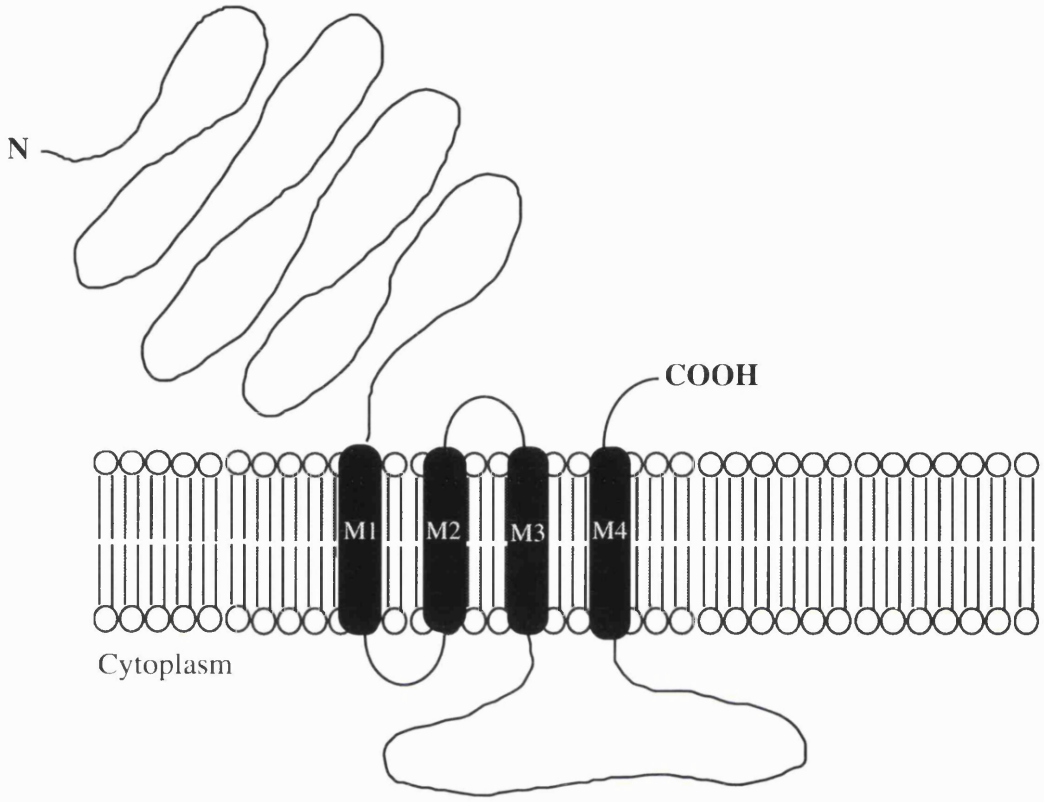

Figure 1.2.1. A model describing the predicted membrane topology of the nAChR subunit family. Each of the nAChR subunits has a large hydrophilic extracellular N-terminal domain which contains potential N-linked glycosylation sites and is disulphide linked in the muscle and electric organ nAChR. Each subunit gene encodes four hydrophobic putative transmembrane domains termed M1-M4. M1 to M3 are connected by short hydrophilic loops and there is a large intracellular loop between M3-M4. The nAChR subunits have a short carboxy-terminal tail, which is also extracellular.

1.2.2 Ligand-binding domain

It appears that the ligand-binding site of the nAChR is formed by amino acids from at least three regions of the extracellular domain of the α subunits, and in the case of the electric organ and muscle nAChR, is contributed to by residues from adjacent γ or δ subunits (Kao *et al.*, 1984; Kao and Karlin, 1986; Dennis *et al.*, 1988; Galzi *et al.*, 1990; Czajkowski and Karlin, 1991) (see Figue 1.2.2). The highly conserved adjacent cysteine residues (Cys-192 and Cys-193 of *Torpedo* α) used to designate α or β nomenclature in the neuronal nAChR subunit family, have been shown to contribute to the ligand-binding site of *Torpedo* α by affinity labelling with [^{3}H]-MBTA [^{3}H-4-(*N*-maleimido)-benzyltrimethylammonium] (Kao *et al.*, 1984), an alkylating agent which competitively inhibits ACh binding to the nAChR. Experiments using a small photo-affinity probe, DDF [^{3}H-p-(*N,N*-dimethylamino)-benzenediazonium fluoroborate], revealed that tyrosine (Tyr)-93, tryptophan (Trp)-149 and Tyr-190 are also labelled on the α subunit, indicating that there are at least three distinct regions involved in the ligand-binding domain of the α subunit (Dennis *et al.*, 1988; Galzi *et al.*, 1990). Tyrosine-190 is also covalently labelled by the coral toxin, lophotoxin, which is a competitive antagonist of the nAChR (Abramson *et al.*, 1989).

In addition to the conserved pair of adjacent cysteine residues, all other cloned α subunits except α5 have been shown to contain residues corresponding to Tyr-93, Trp-149 and Tyr-190 which have been implicated as contributing to the ligand binding site. The α5 subunit is atypical amongst α subunits in that it lacks both Tyr-93 and Tyr-190 (Boulter *et al.*, 1990; Couturier *et al.*, 1990b). The functional relevance of these changes are unknown but it is postulated that α5 may fulfil a more structural role in a nAChR. None of the five labelled amino acids implicated in the ligand-binding site are conserved in any cloned muscle or electric organ β1, γ, δ or ε subunits although in some instances homologues of Tyr-93 and Trp-149 are seen in β2, β3 and β4 neuronal nAChR subunits.

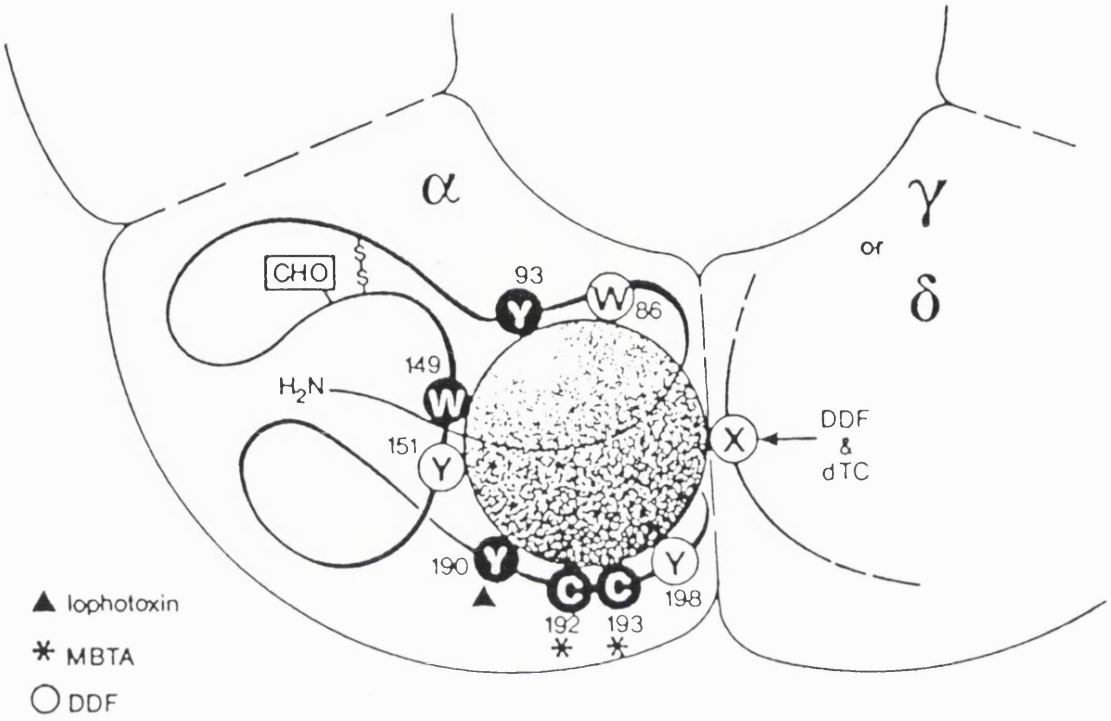

Figure 1.2.2. Model of the ligand binding domain of the nAChR from *Torpedo californica* electric organ (taken from Galzi *et al.*, 1991). Affinity labelling of the *Torpedo* nAChR reveals that the ligand binding domain of the nAChR is contributed to by amino acids from three regions within the extracellular N-terminal domain of the α subunit, and by residues from the δ or γ subunits. The model depicts the proposed folding of the N-terminal segment of the α-subunit. The sphere represents the space occupied by the competitive antagonist DDF. Filled circles denote residues clearly shown to be labelled by DDF and open circles denote residues for which evidence indicative of labelling was obtained. Amino acids specifically labelled with [^{3}H]-MBTA (*) and [^{3}H]-lophotoxin (▲) are shown. The X denotes residues from the δ and γ subunits which contribute to the ligand binding site. The disulphide bond linking α-Cys^{128} and α-Cys^{142} and the site of N-linked glycosylation at α-Asn^{141} are indicated.

The stoichiometry ($\alpha_2\beta\gamma\delta$) of the electric organ and muscle nAChR implies that it is asymmetric. This is supported by evidence that the two ligand-binding sites are non-identical and possess different affinities for different ligands, particularly ACh and tubocurarine (Damle *et al.*, 1978; Neubig and Cohen, 1979). Heterologous expression of *Torpedo* nAChR subunits in *Xenopus* oocyes (Kurosaki *et al.*, 1987) and of mouse muscle nAChR subunits in quail fibroblasts (Blount and Merlie, 1989) reveals that the α-subunit alone does not bind either ACh or tubocurarine with high affinity. However, expression of α and γ together generates a ligand-binding site which binds ACh with high affinity and tubocurarine with low affinity. Expression of α and δ generates a high affinity nicotine-binding site but binds ACh with low affinity. The combination of α and β does not result in high affinity binding of either ligand.

These results suggest that the γ and δ subunits contribute to the ligand-binding sites of the nAChR. Affinity labelling and mutational analysis indicate that several residues in the *Torpedo* δ-subunit (δ-Asp180, δ-Glu189 and δ-Trp57) and homologous amino acids in the *Torpedo* γ-subunit (γ-Asp174, γ-Glu183 and γ-Trp55) probably form part of the negatively charged subsite of the ligand-binding domain (Czajkowski and Karlin, 1991; Sine and Claudio, 1991a; Czajkowski *et al.*, 1993; Karlin, 1993). The subunits of neuronal nAChRs contain certain homologues of these residues found in δ and γ, including the neuronal α7 subunit. Mutagenesis of Trp54 in the α7 subunit, which aligns to δ–Trp57 and γ-Trp55 labelled by curare (Sine, 1993; Corringer *et al.*, 1995), suggest that it contributes to the ligand-binding site of the α7 homo-oligomer (Corringer *et al.*, 1995).

1.2.3 Stoichiometry and arrangement of subunits

The native nAChRs isolated from *Torpedo* exists as a pentameric monomer and disulphide-linked dimer where two nAChR complexes are joined via a disulphide

bond between the pentultimate cysteine residues of two adjacent δ subunits (DiPaola *et al.*, 1989). The nAChR monomer consists of four α, β, γ and δ subunits arranged with the stoichiometry $\alpha_2\gamma\delta\varepsilon$ (see Section 1.1.1). Electron microscopy was used to determine the relation of the α subunits to either the δ or β subunits to identify the arrangement of the subunits around the channel pore (Karlin *et al.*, 1983). The α subunits were identified by binding biotinylated cobra-toxin (a competitive antagonist of the nAChR) and avidin to the ligand-binding sites (Karlin *et al.*, 1983). The δ subunits were identified by the position of the disulphide bond between nAChR monomers in the native nAChR dimer. To identify β, the δ–δ disulphide bond was reduced and diamide was used to form a dimer crosslinked between β subunits (Hamilton *et al.*, 1979). The only possibilities which remain are the mirror image pair where γ lies between the two α subunits (Karlin *et al.*, 1983) (see Figure 1.2.3). This configuration is supported by evidence which indicates that the two ligand-binding sites are formed at the α/δ and α/γ subunit interfaces (Kurosaki *et al.*, 1987; Blount and Merlie, 1989; Pedersen and Cohen, 1990; Sine, 1993) (see Section 1.2.2). Which of these two possible conformations constitute the native nAChR of electric organ is still controversial.

Neuronal nAChRs immunoprecipitated from brain and ganglia have an apparent molecular weight of ~280-300 kDa and sediment with similar buoyant density (~10S) to that of the electric organ and muscle nAChR when analysed by sucrose gradient centrifugation (Whiting and Lindstrom, 1986b; Anand *et al.*, 1993b). The individual neuronal nAChR subunits range in mass from 49 kDa - 69 kDa and so presumably also exist as pentameric complexes. The typical stoichiometry of pairwise combinations of neuronal nAChRs is predicted by two separate approaches to be $(\alpha)_2(\beta)_3$ although the subunit arrangement of these nAChRs is uncharacterized. Ratiometric calculations from immunoprecipitations of metabolically labelled protein revealed that there was ~1.5 times more [^{35}S]-methionine present in the β subunits than in the α subunits following injection of α4 and β2 into *Xenopus* oocytes

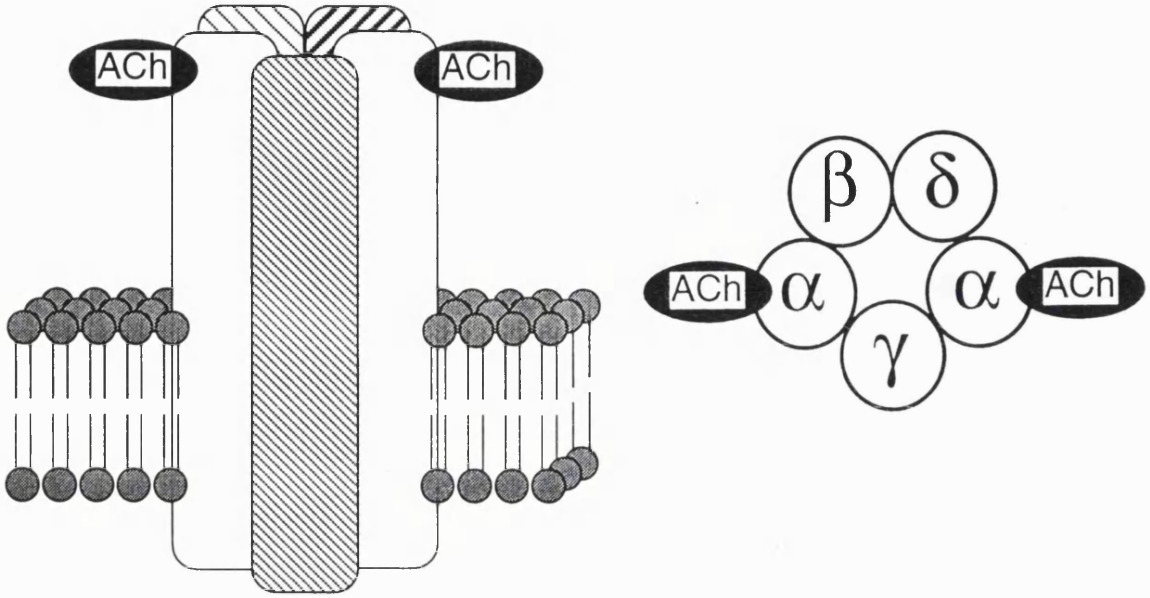

Figure 1.2.3. The structure and predicted stoichiometry of the nAChR of electic organ and muscle. The four α, β, δ and γ nAChR subunits oligomerize to form a membrane-spanning pentameric glycoprotein, with the stoichiometry α2βδγ. The five subunits form a ring of quasi-symmetry around a central ion channel. The α-subunits contain the agonist binding site which is contributed to by residues from adjacent δ or γ subunits. The arrangement of subunits whereby γ lies between the two α-subunits, is the predicted order of subunits around the channel pore.

(Anand *et al.*, 1991), or upon analysis of α4β2 stably expressed in mouse fibroblasts (Whiting *et al.*, 1991a). In addition, Cooper *et al* (1991) used site directed mutagenesis to alter residues within the M2 domain of the α4 and β2 subunits at sites which changed the single channel conductance of resulting nAChRs. Analysis of single-channel conductance populations of oocytes expressing wild-type α4 and β2 subunits in combination with mutant subunits also concluded that the predominant ratio of α:β subunits, in assembled α4β2 nAChRs, appeared to be 2:3 (Cooper *et al.*, 1991).

The homo-oligomeric neuronal α7 and α8 receptors are also thought to be pentameric (Anand *et al.*, 1993b; Gerzanich *et al.*, 1994; Palma *et al.*, 1996). Expression of α7 and α8 in *Xenopus* oocytes reveals that both subunits have an apparent molecular weight of ~60 kDa (shown by metabolic labelling and immunoprecipitation) and form complexes which sediment with a buoyant density of ~10S (shown by sucrose gradient sedimentation) (Anand *et al.*, 1993b; Gerzanich *et al.*, 1994). This is similar to the 9S sediment coefficient reported for the muscle and electric organ nAChR (Reynolds and Karlin, 1978) and indicates that α7 and α8 probably form pentameric complexes when expressed in oocytes (Anand *et al.*, 1993b; Gerzanich *et al.*, 1994).

This suggestion is supported by analysis of the kinetics of inhibition of the α7 homo-oligomer expressed in *Xenopus* oocytes, by methyllycaconitine (MLA) (Palma *et al.*, 1996). Methyllycaconitine (MLA) is an insecticide produced by delphiniums and is a potent antagonist of α7 nAChRs (Wonnacott *et al.*, 1993). Functional analysis of the α7 nAChR revealed that the onset and recovery of MLA blockade could be best described using a model based on 5 putative binding sites (Palma *et al.*, 1996). In contrast, inhibition of the α4β2 receptor expressed in oocytes by MLA was best described using an equation based on two ligand binding sites (Palma *et al.*, 1996).

1.2.4 The channel pore

The M2 domain of each of the nAChR subunits is thought play a major role in lining the channel pore and determining its conductance and selectivity (Imoto *et al.*, 1988; Revah *et al.*, 1991; Villarroel *et al.*, 1991; Akabas *et al.*, 1992; Galzi *et al.*, 1992). The M2 segments of all nAChR subunits are highly conserved and contain several interesting characteristics within their amino-acid compositions. In the nAChR there are negatively charged residues at either end of the M2 domain, a highly conserved leucine residue near the middle of the bilayer and a pattern of three small uncharged residues that repeat in every fourth position (see Figure 1.2.4) (Galzi *et al.*, 1990; Unwin, 1993). The functional effect of mutations within M2 have helped decipher what the role of these conserved amino-acid residues may be.

The amino-acids which line the pore of the channel were first identified by labelling with non-competitive inhibitors such as the open channel blocker chlorpromazine (see Figure 1.2.4) and QX-222 (Giraudat *et al.*, 1987a; Leonard *et al.*, 1988; Giraudat *et al.*, 1989; Revah *et al.*, 1990), or subsequently by systematic substitution of residues within the M2 domain of the mouse muscle α-subunit for cysteine residues (Akabas *et al.*, 1992). These mutant α subunits were expressed in *Xenopus* oocytes with wild-type β, γ, and δ subunits and subjected to functional analysis (Akabas *et al.*, 1992). In almost all cases, the mutant receptors were functional and oocytes were treated with a reactive sulphide-group specific compound (methanethiosulphonate ethylammonium, MEA) which covalently modifies cysteine residues and can be conducted by the channel. If residues within this membrane spanning region are modified by the compound (which is observed as changes in the agonist-induced current) then they must be exposed to the channel lumen. By treating the injected oocytes with MEA either prior to, or together with, the application of nicotinic agonists, it was possible to determine which residues are exposed to the channel lumen in the open or closed states, and their approximate location within the pore.

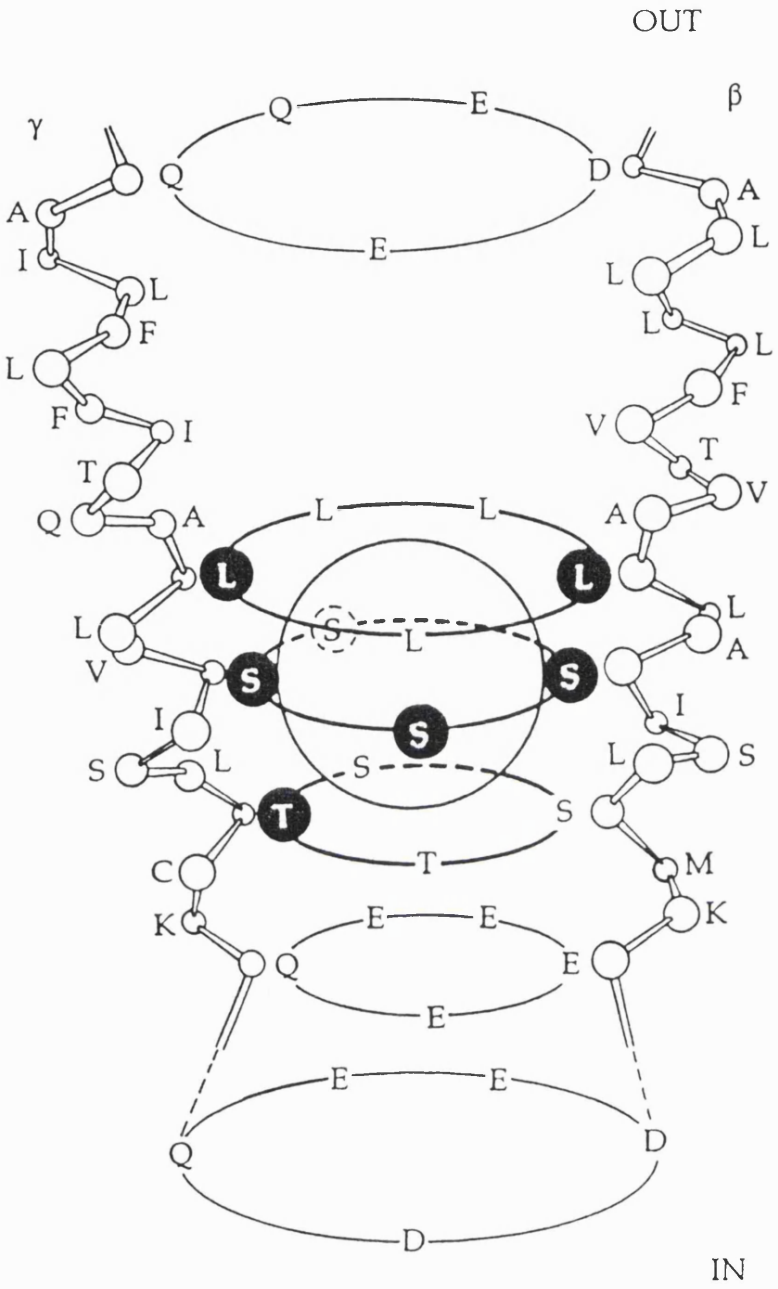

Figure 1.2.4. Model for the high-affinity binding site of the open channel blocker chlorpromazine (taken from Revah *et al.*, 1990). The sphere represents the space occupied by chlorpromazine. The M2 domains of the γ and β subunits are arranged as transmembrane α-helices depicting the α-carbons of the indicated amino-acids. The filled circles represent three rings of amino acids within the M2 domain of each subunit photolabelled by [^{3}H]-chlorpromazine, indicating that the M2 region is a component of the channel pore. The remaining circles represent rings of amino acids formed by negatively charged residues located at either end of the M2 domain of each subunit.

The negatively charged glutamate and aspartate residues at either end of the M2 domain have been shown to play a crucial role in the cation selectivity of the nAChR (Imoto *et al.*, 1988; Galzi *et al.*, 1992), although mutational analysis of these residues suggest that they are not the sole mechanism by which the nAChR screens for positively charged ions (Galzi *et al.*, 1992; Kienker *et al.*, 1994). Mutation of these residues to neutral amino acids generates functional nAChRs which are still selective for cations although mutation of the N-terminal Glu^{237} residue in the α7 homo-oligomer abolishes calcium permeability of the mutant receptor, without significantly altering other characteristics of the ACh response (Galzi *et al.*, 1992). However the mutation of a combination of residues in and around the M2 region of the homo-oligomeric neuronal α7 subunit, for residues contained in the M2 domain of the glycine receptor α1 subunit, results in the reversal from cationic to anionic selectivity (Galzi *et al.*, 1992). It was found that three simultaneous mutations were required for the reversal of ion selectivity; the insertion of an alanine or proline residue between Gly^{236} and Glu^{237} plus the substitution of the negatively charged Glu^{237} residue for alanine, both at the cytoplasmic end of the M2 domain, and an additional substitution of the Val^{251} residue for threonine within the membrane spanning domain.

It is proposed that the 3 groups of small uncharged amino-acids repeating every fourth residue within the putative M2 domain may form a sloping line along one face of an α-helix (Revah *et al*, 1990; Unwin, 1993). When five subunits come together to form a nAChR complex, these homologous residues from each of the subunits align to create rings which have been implicated in ion flow and channel conductance (Figure 1.2.4) (Bertrand *et al.*, 1991; Revah *et al.*, 1991; Villarroel *et al.*, 1991). The residue forming the ring nearest the cytoplasmic surface, sometimes referred to as the threonine ring, is important in modulating the conductance of the channel (Villarroel *et al.*, 1991). Point mutations at this residue revealed that the conductance of the channel is restricted by the amino-acid volume at this position (Villarroel *et al.*,

1991). The function of the rings formed by the 2 residues near the centre of the lipid bilayer is harder to define and may be more subtle. Mutations of these residues affect the binding of the open channel blocker QX-222 (Leonard *et al.*, 1988; Charnet *et al.*, 1990), but have little effect on conductance and ion flow.

The conserved leucine residue near the middle of the lipid bilayer seems to play a crucial role in regulating the flow of ions through the channel (Bertrand *et al.*, 1991; Revah *et al.*, 1991). When this residue in the homo-oligomeric α7 receptor is mutated to a residue of different size or polarity it has dramatic effects on the gating and desensitization rates of the mutant receptor (Bertrand *et al.*, 1991; Revah *et al.*, 1991). To some extent, mutations of residues in M1 have also been shown to effect gating or desensitization properties of the nAChR channel (Lo *et al.*, 1991; Akabas and Karlin, 1995). However, there is no evidence for residues from M1 contributing to the channel lining and it is possible they induce a steric effect by altering the alignment of residues in the adjacent M2 domain.

1.2.5 The 3-dimensional structure of the nAChR.

Electron microscopy of the *Torpedo* nAChR reveals that the five subunits are arranged in a ring of pseudo-symmetry around a central pore (Figure 1.2.5) (Toyoshima and Unwin, 1988; Mitra *et al.*, 1989; Unwin, 1993). The nAChR is a barrel-shaped cylinder of about 120Å in length (Figure 1.2.5). Its large extracellular domain of ~80Å in diameter extends about 65Å into the synaptic cleft and the intracellular tail around 15Å into the interior of the cell. The external mouth of the channel is about 25Å in diameter and is surrounded by walls of about the same thickness.

Recently the 3-dimensional structure of the *Torpedo* nAChR has been obtained by electron microscopy in both open and closed configurations to a resolution of 9Å

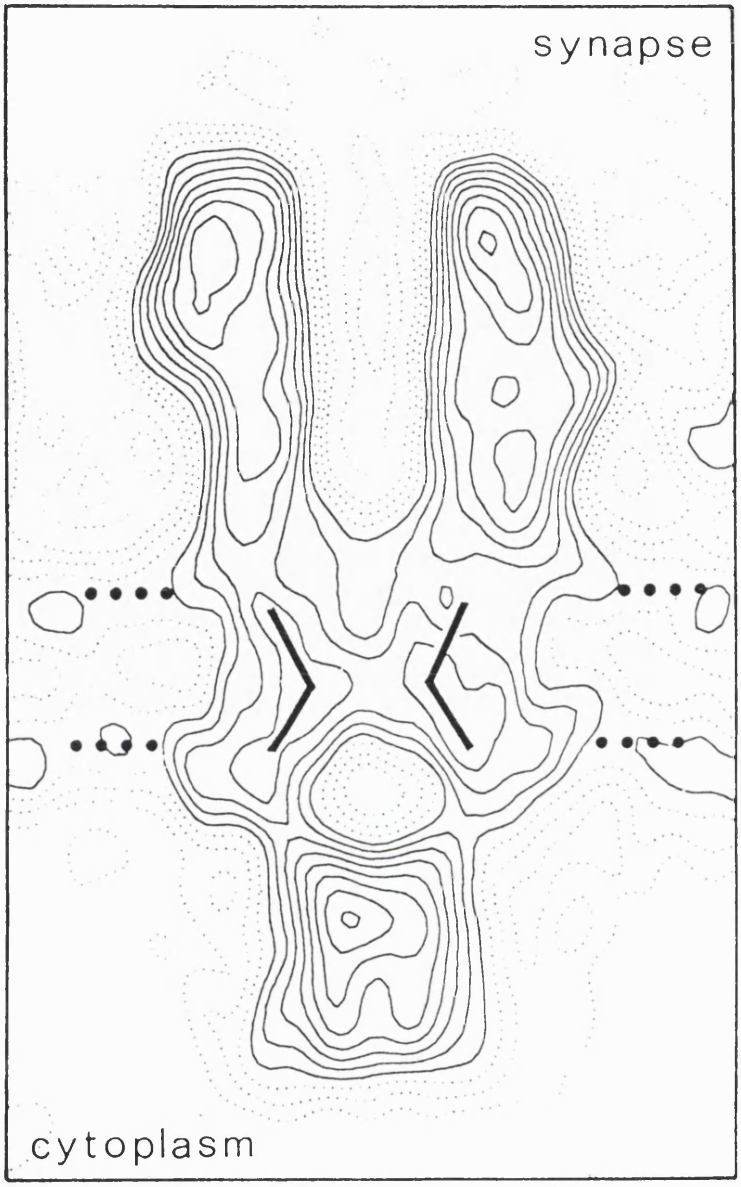

Unwin (1993) *J. Mol. Biol.* **229**, 1101-1124

Figure 1.2.5. Cross section through a three-dimensional image of the *Torpedo* nAChR by electron microscopy. The profile of the nAChR indicates that it forms an ion channel compex 120Å in length which extends 65Å into the synaptic cleft and 15Å into the cell interior. A central fluid-filled cavity approximately 25Å in diameter can be seen running the length of the extracelluar domain. The structure narrows as it crosses the lipid bilayer forming an area of density which presumably corresponds to the channel gate. The kinked rods within the membrane spanning domain represent the predicted conformation of the M2 domains of each subunit thought to line the channel pore. The associated 43K protein at the base of the nAChR is shown.

using a rapid mixing and freezing procedure (Unwin, 1993;1995). Furthermore, images of the *Torpedo* nAChR at a resolution of 7.5Å allow the distinct conformations of the α subunit to be resolved (Unwin, 1996). At this resolution it has been possible to begin to understand structure-function relationships and how the receptor works as an ion channel. By comparing the structural characteristics of the channel with what is known from mutational analysis of conserved residues in all nAChR subunits, it has been possible to propose what contributions protein domains, or even individual residues, make to the tertiary conformation and functional properties of the receptor molecule.

The extracellular part of the receptor has an irregular outer surface but a smooth inner surface resembling a tube (Unwin, 1993; 1995; 1996). The α subunits can be easily identified by a small cleft in their extracellular domains which are, presumably, the ligand-binding pockets. As the receptor passes through the middle of the bilayer, there is a pronounced constriction in diameter which is assumed to correspond to the channel gate. This membrane-spanning region reveals five rods of density which kink in the middle, pointing radially outwards on either side. The five rods presumably correspond to the five helical M2 transmembrane domains lining the channel pore.

Interestingly, the conserved leucine residues which have been implicated in channel gating, appear to align at about the same level in the sequence that would correspond to the kink in the helices. Unwin proposes that the side-chains from the five leucine residues could interconnect to create a barrier, that may form the gate, in the same manner that leucine residues between helices associate to form leucine zippers. Imaging of the nAChR in the open state shows that in the open channel, the kinked rods undergo a small rotation sideways, which opens the channel to approximately 9-10Å in diameter (Unwin, 1995). If the gating mechanism is provided by amino-acid side-chains, then this small rotation could pull the gate-forming sidechains away from

the centre of the pore and provide a possible mechanism for the rapid allosterically induced opening and closing of the ion channel.

1.3 The subunit composition of native neuronal nAChRs

1.3.1 Major nAChR subtype in brain

It was hoped that by biochemical characterization, and comparisons of the functional properties of nAChRs expressed by neurons and in heterologous expression systems, sufficient correlations would emerge to identify the subunit composition of native neuronal nAChR subtypes. Despite the array of pharmacological profiles and characteristics of neuronal nAChRs expressed in *Xenopus* oocytes, no combination of subunits produces channels which exactly match the properties of characterized nicotinic channels expressed in neurons (for reviews see Role, 1992; McGehee and Role, 1995). In addition, the distribution of the various neuronal nAChR subunit genes throughout the brain and nervous system has revealed a considerably complex pattern of expression. The α4 and β2 gene products are expressed widely throughout the brain and *in situ* hybridization studies reveal overlapping expression patterns of α2, α3, α4, α5, α7, β2, β3 and β4 subunits throughout various regions of the brain (Goldman *et al.*, 1987; Deneris *et al.*, 1989; Duvoisin *et al.*, 1989; Wada *et al.*, 1989; Morris *et al.*, 1990). Biochemical characterization of neuronal nAChR subtypes has provided some insights into the possible subunit composition of native nAChRs.

Several lines of biochemical evidence suggest the major nAChR species present in brain contains α4 and β2 subunits. Immunoprecipiation of nAChR subtypes from chick brain with an antibody raised against *Torpedo* nAChR (mAb35, which recognises the major immunogenic region of *Torpedo* α) purifies a complex which binds nicotine with high affinity (Whiting and Lindstrom, 1986a) and can be labelled with [^{3}H]-bromoacetylcholine (Whiting and Lindstrom, 1986b). The purifed material sediments on a sucrose gradient with a buoyant density of 10S and when resolved by

SDS (sodium dodecyl sulphate) polyacrylamide gel electrophoresis (SDS-PAGE), produces two protein bands of 49 kDa and 59 kDa (Whiting and Lindstrom, 1986a).

The purifed chick brain nAChR was used to generate mAb270 which immunoprecipitates more than 90% of the high-affinity [^{3}H]-nicotine-binding sites from solubilized chick brain extracts (Whiting and Lindstrom, 1986a). mAb270 cross reacts with both chick and rat brain nAChRs and immunopurifies a new band from chick brain of 75 kDa, in addition to the 49 kDa and 59 kDa bands, and also immunopurifies a 51 kDa and 79 kDa band from rat brain (Whiting *et al.*, 1987b). Western blotting showed that mAb270 recognizes both the 49 kDa and 51 kDa nAChR components from chick and rat, and N-terminal sequencing identified the neuronal nAChR β2 subunit (Nef *et al.*, 1988; Schoepfer *et al.*, 1988). N-terminal sequences of the 75 kDa protein were found to correspond to the α4 subunit (Whiting *et al.*, 1987a ; Nef *et al.*, 1988). The identity of the 59 kDa component is less certain but probably corresponds to the α2 gene product which is also thought to co-assemble with β2 in chick brain (Whiting *et al.*, 1987b).

Antisera raised against α4 or β2 fusion proteins are each able to precipitate more than 90% of the high-affinity [^{3}H]-cytisine-binding sites from solubilized rat brain extracts (Flores *et al.*, 1992). In addition, the α4-specific antisera removes virtually all of the β2 reactive protein from solibilized extracts and vice-versa. The pharmacological profile and electrophysiological characteristics of the α4β2 receptors expressed in *Xenopus* oocytes (Papke *et al.*, 1989; Charnet *et al.*, 1992) and mammalian fibroblasts (Whiting *et al.*, 1991a; Gopalakrishnan *et al.*, 1995b; Ragozzino *et al.*, 1997) resembles that obtained from brain preparations. In addition, more recent evidence has shown than deletion of the gene encoding β2 in transgenic mice results in the complete loss of high affinity nicotinic-binding sites in mouse brain (Picciotto *et al.*, 1995). Taken together, all of these results strongly suggest that both α4 and β2 are present in the major species of nAChR in brain.

Later reports suggest that the α5 gene product, also estimated to be ~50 kDa, may have been co-isolated by mAb35 during the immunopurification of nAChRs from chick brain (Whiting *et al.*, 1991b; Conroy *et al.*, 1992). The 49 kDa component immunopurified by mAb35 from chick brain was recognised by a monoclonal antibody (mAb210) and an antisera which both specifically recognise the α-subunits of *Torpedo* and muscle nAChR (Whiting and Lindstrom, 1986b). Because of these results, the β2 subunit recognised by mAb270 was originally designated as an α-subunit. However, mAb35 and mAb210 cross react with the α5 gene product and not the β2 subunit which is resolved to the same position following SDS-PAGE (Whiting *et al.*, 1991b; Conroy *et al.*, 1992). Moreover, two monoclonal antibodies raised against the nAChR immunopurified from chick brain (with mAb35) were specific for the α5 subunit and do not appear to recognise either the α4 or β2 subunits stably expressed in the M10 mouse fibroblast cell line (Conroy *et al.*, 1992). These results indicate that in chick brain, the α4 and β2 subunits may co-assemble with the α5 subunit. The possible co-assembly of α5 with α4 and β2 is supported by expression studies in *Xenopus* oocytes where co-expression of α5 together with α4 and β2, produced channels with different properties when compared to channels produced by expression of α4 and β2 alone (Ramirez-Latorre *et al.*, 1996).

The diversity of brain nAChR subtypes appears even more complex following reports generated by immunoprecipitation studies from rat cerebellum which implicate the presence of a small subset of nAChRs which contain four neuronal α4, β2, β3 and β4 subunits, presumably in a configuration reminiscent of the nAChR of electric organ and muscle (Forsayeth and Kobrin, 1997). To date, very little is known about the β3 subunit which does not form functional channels in *Xenopus* oocytes in pairwise combination with α2, α3 or α4 subunits (Deneris *et al.*, 1989). *In situ* hybridization reveals that both β3 and β4 are expressed in many regions of the brain, although with less widespread distributions compared with β2 (Deneris *et al.*, 1989; Duvoisin *et al.*, 1989; Dineley-Miller and Patrick, 1992; Willougby *et al.*, 1993). Rat cerebellum

nAChRs were immunoprecipitated with mAb270 (which recognises β2) and then blotted with antibodies specific for either β3 or β4. The antibodies clearly identified 60 kDa and 66 kDa components co-precipitating with β2 corresponding to the β3 and β4 subunits, respectively (Forsayeth and Kobrin, 1997). Transfection of the four neuronal α4, β2, β3 and β4 subunits into mammalian COS cells (monkey kidney fibroblasts) resulted in the appearence of receptor which binds nicotinic radoligands with high affinity. Competition binding experiments with nicotine and [^{3}H]-ACh showed that omission of any one of the four subunits altered the binding characteristics (either B_{max} or K_d) when compared to nAChRs formed following co-transfection of all four subunits together.

1.3.2 Major nAChR subtype in ganglia

Multiple neuronal nAChR subunit genes are also expressed in peripheral ganglia. RNAase protection assays and *in situ* hybridisation studies reveal that α3, α7 and β4 are widely expressed in autonomic ganglia in addition to α4, α5 and β2 nAChR subunits (Boyd *et al.*, 1988; Couturier *et al.*, 1990b; Klimaschewski *et al.*, 1994; Rust *et al.*, 1994). Several related cultured neuronal cell lines express a similar pattern of nAChR subunit expression (e.g. PC12, rat phaeochromocytoma; SH-SY5Y, human neuroblastoma) (Corriveau and Berg, 1993; Lukas *et al.*, 1993; Henderson *et al.*, 1994).

The purification of nAChRs from ciliary ganglia with mAb35 identified three protein bands of 49 kDa, 52 kDa and 60 kDa (Halvorsen and Berg, 1990) following SDS gel electrophoresis. Subsequently, immunoprecipiation and western blotting techniques have identified the 60 kDa protein as the α3 subunit, due to crossreactivity with several α3-specific antibodies (Schoepfer *et al.*, 1989; Vernallis *et al.*, 1993; Conroy and Berg, 1995). The 49 kDa component was identified as the α5 subunit and the 52 kDa protein was identified as the β4 subunit (Vernallis *et al.*, 1993; Conroy and Berg, 1995). Immunoprecipitation of receptors expressed on the surface of cultured

ciliary ganglia followed by immunoblotting techniques indicated that all three gene products (α3, α5 and β4) are assembled into nAChRs present on the cell surface (Vernallis *et al.*, 1993; Conroy and Berg, 1995). Further immunoprecipitation and western blot experiments revealed that a small subset of nAChRs expressed in ciliary ganglia appeared to contain β2 subunits (Conroy and Berg, 1995). The β2 gene product is also expressed in ciliary ganglia (Boyd *et al.*, 1988; Corriveau and Berg, 1993) and co-localises with the α5 gene product following SDS-PAGE (Conroy *et al.*, 1992). Coassembly of β2 with α3, β4 and α5 subunits expressed in ciliary ganglia was demonstrated by immunoprecipitaion with either mAb 270 or mAb B2-1, which recognise separate epitopes specific for the β2 subunit, followed by western blotting with antibodies specific for the α3, β4 and α5 subunits (Conroy and Berg, 1995).

1.3.3 The α-BTX-binding receptor of brain and ganglia.

The presence of neuronal α-BTX-binding sites was identified at a similar time when α-BTX was used in studies of the muscle and electric organ nAChR (Green *et al.*, 1973; Hunt and Schmidt, 1978). However, because α-BTX failed to block nicotinic responses of neurones (Patrick and Stallcup, 1977b; Carbonetto *et al.*, 1978), little effort at the time was put into their isolation and characterization. α-BTX-binding proteins were purified from chick optic lobe (Betz *et al.*, 1982; Norman *et al.*, 1982; Betz and Pfeiffer, 1984), chick brain (Conti-Tronconi *et al.*, 1985), chick retina (Betz *et al.*, 1982; Betz and Pfeiffer, 1984) and rat PC12 cells (Betz *et al.*, 1982; Betz and Pfeiffer, 1984), and found to be composed of 1-4 components. A predominant ~54-57kDa protein present in all preparations is labelled with α-BTX and bromo-acetylcholine (Betz *et al.*, 1982; Norman *et al.*, 1982; Betz and Pfeiffer, 1984) and used to obtain a partial N-terminal sequence which exhibited homology to other nAChRs (Conti-Tronconi *et al.*, 1985). By using an oligonucleotide based on this N-terminal sequence, a cDNA clone encoding the neuronal α7 subunit was isolated from a chick brain library (Schoepfer *et al.*, 1990). By re-screening the chick brain cDNA

library using the α7 cDNA sequence, the closely related α8 cDNA was also identified (Schoepfer *et al.*, 1990).

Purified α-BTX-binding receptors, and bacterially expressed fusion proteins containing the putative cytoplasmic loop regions of the α7 and α8 subunits, were used to generate a panel of monoclonal antibodies specific for the α-BTX-binding proteins of chick brain (Schoepfer *et al.*, 1990). About the same time, the α7 subunit was identified from a chick brain library using a cDNA probe based on N-terminal sequences of the chick α3 subunit (Couturier *et al.*, 1990a). Unlike all other previously cloned and expressed neuronal nAChRs, expression of α7 in *Xenopus* oocytes resulted in the formation of functional homo-oligomeric nicotinic channels which rapidly desensitized, displayed higher affinity for nicotine than acetylcholine and were blocked by nanomolar concentrations of α-BTX (Couturier *et al.*, 1990a).

The distribution of α7 transcripts in rat brain overlaps the pattern of [^{125}I]-αBTX-binding sites and does not correlate with the distribution of high affinity [^{3}H]-nicotine-binding sites (Clark *et al.*, 1985; Seguela *et al.*, 1993). *In situ* hybridization (Seguela *et al.*, 1993) and immunohistochemical analysis (Dominguez Del Toro *et al.*, 1994) of rat brain reveals the highest levels of α7 expression in the brainstem, hypothalamus, hippocampus, the olfactory regions and the amygdala. The α7 subunit is also widely expressed in peripheral ganglia (Listerud *et al.*, 1991; Klimaschewski *et al.*, 1994; Rust *et al.*, 1994).

The α8 subunit has been immunohistochemically localised in chick brain and retina (Britto *et al.*, 1992; Keyser *et al.*, 1993) although a mammalian homologue has yet to be identified. Immunoprecipitation experiments indicate that there are at least three classes of αBTX-binding nAChR expressed in chick. The subtype which predominates in the brain contains the α7 subunit (~70%) with a less abundant species containing both α7 and α8 subunits (~20%) (Gotti *et al.*, 1994). In chick

retina the predominant species of αBTX-binding nAChR contains the α8 subunit (~50-70%), an additional subtype containing both α7 and α8 (~10-17%), and a third subtype which contains only α7 subunits (~14-27%) (Keyser *et al.*, 1993; Gotti *et al.*, 1997).

1.4 The charactistics of neuronal nAChRs expressed in *Xenopus* oocytes.

1.4.1 The α-BTX insensitive neuronal nAChRs

The analysis of pairwise combinations of neuronal nAChR subunits expressed in *Xenopus* oocytes has revealed that each nAChR subtype possesses distinct pharmacological and ion channel properties. In many cases, multiple conductance classes are observed from co-expression of a single α and β subunit (Papke *et al.*, 1989; Papke and Heinmann, 1991; Charnet *et al.*, 1992). The hetero-oligomeric neuronal nAChRs are more permeable to calcium than their muscle counterparts, with a permeability ratio of P_{Ca}:P_{Na} = ~1.0-1.5, compared with P_{Ca}:P_{Na} = ~0.2 for skeletal muscle (Decker and Dani, 1990; Costa *et al.*, 1994). The calcium entry during channel openings is sufficient to trigger calcium-sensitive chloride channels in oocytes expressing α3β4 (Vernino *et al.*, 1992) and may activate second messenger pathways.

Both the α- and the β-subunits influence the ligand-binding affinites and channel properties of expressed nAChRs, perhaps in a similar manner as the δ and γ subunits contribute to the ligand binding site of the *Torpedo* nAChR (for review see McGhee and Role, 1995). Cytisine potently activates β4-containing receptors but is only a weak or partial agonist for β2-containing nAChRs (Papke and Heinemann, 1993). Similarly, the rat α3β4 receptor possesses a 10-fold higher sensitivity to ACh, and exhibits markedly longer burst times, than the rat α3β2 receptor expressed in *Xenopus*

oocytes (Papke and Heinmann, 1991). Nicotine potently activates chick α3β4 receptors but is only a weak partial agonist of chick α3β2 and even acts as a competitive antagonist of α3β2 when co-applied with ACh (Hussy *et al.*, 1994). However, nicotine acts as a full agonist on the rat α3β2 receptor and a single amino acid in the N-terminal domain of rat α3 (glutamine^{198}) when mutated to threonine, as found in chick α3, produced channels poorly activated by nicotine when co-expressed with rat β2. Rat α3β2 receptors are 55-fold more sensitive to the competitive antagonist dihydro-β-erythroidine than are α3β4 receptors (Harvey and Luetje, 1996). Both rat and chick α3β2 receptors are sensitive to blockade by neuronal bungarotoxin, whereas α3β4 receptors are not (Hussy *et al.*, 1994; Harvey and Luetje, 1996).

Recently the characteristics of triplet combinations of neuronal nAChR subunits expressed in *Xenopus* oocytes has been studied (Ramirez-Latorre *et al.*, 1996; Wang *et al.*, 1996; Sivilotti *et al.*, 1997). Pharmacological analysis of triplet combinatinations of neuronal nAChR subunits expressed in *Xenopus* oocytes demonstrates the participation of α5 subunits to functional nAChRs containing α3β2 and α3β4 (Wang *et al.*, 1996). Co-injection of α5 alters agonist sensitivites and increases desensitization rates of nAChR responses elicited from oocytes following injection of α3α5β2 and α3α5β4, compared with the properties of pairwise α3β2 and α3β4 combinations. This study confirms that nAChRs present at the surface membrane of injected oocytes contain the α5 subunit by cell surface labelling with radiolabelled antibodies and immunoprecipitation of tagged α5 subunits (Wang *et al.*, 1996). In addition, co-expression of α5 with α4 and β2 in *Xenopus* oocytes produces channels with 100-fold lower sensitivity to ACh and a much larger single channel conductance than observed with α4β2 receptors (Ramirez-Latorre *et al.*, 1996). Mutational analysis of residues within the M2 domain of the α5 subunit clearly demonstrated the contribution of residues from α5 to the channel pore (Ramirez-Latorre *et al.*, 1996). The single channel conductance of α3β4 receptors expressed in

Xenopus oocytes are also increased following the co-injection of α5, although not to the same extent as for the α4α5β2 combination (Sivilotti *et al.*, 1997).

1.4.2 The α-BTX sensitive neuronal nAChRs.

It was Couturier and co-workers (Couturier *et al.*, 1990a) who first demonstrated that a recently cloned chick α7 subunit could form functional homo-oligomeric channels when expressed in *Xenopus* oocytes which were blocked by nanonolar concentrations of αBTX. The α7 subunit had also been identified by Schoepfer *et al* (1990) based on the N-terminal sequence of a chick brain α-BTX-binding protein (Schoepfer *et al.*, 1990). The α7 sequence was used to identify the closely homologous α8 subunit (Schoepfer *et al.*, 1990), later also shown to form functional homo-oligomeric ion channels when expressed in *Xenopus* oocytes (Gerzanich *et al.*, 1994).

Mammalian homologues of the α7 subunit have been reported for rat (Seguela *et al.*, 1993), bovine (Garcia-Guzman *et al.*, 1995) and human (Peng *et al.*, 1994b) subtypes. To date, no mammalian homologue of α8 has been identified although it is widely expressed in chick brain and retina (Schoepfer *et al.*, 1990). There is no evidence from oocyte expression studies that α7 co-assembles with other nAChR subunits. Co-injection of α3, α5, β2, β3, β4, or muscle β1/γ/δ together with α7 does not produce channels which are pharmacologically distinguishable from channels produced by injection of α7 alone (Couturier *et al.*, 1990a; Seguela *et al.*, 1993). However, the characterization of receptor subtypes immunopurifed from chick brain and retina suggests that α7 and α8 may co-assemble *in vivo* (Keyser *et al.*, 1993; Gotti *et al.*, 1994; Gotti *et al.*, 1997).

Both the α7 and α8 nAChR channels when expressed in *Xenopus* oocytes form homo-oligomeric nicotinic channels which desensitize extremely rapidly and are highly permeable to calcium (Seguela *et al.*, 1993; Gerzanich *et al.*, 1994). The M1-M3 sequences of the α7 and α8 subunits are virtually identical with 100% sequence

homology within their M2 domains. Predictably, they appear to possess similar ionic permeabilities and conductances although they exhibit significantly different pharmacological properties with respect to ligand efficacy and binding affinity (Gerzanich *et al.*, 1994). The α8 homo-oligomeric receptors are overall more sensitive to agonists and less sensitive to antagonists than α7 (Gerzanich *et al.*, 1994). Acetylcholine, which activates α7 receptors with very low potency (EC_{50} = 112 μM), is as potent as nicotine or cytisine in activating α8 receptors (EC_{50} = 1.9 μM). DMPP (1,1-dimethyl-4-phenylpiperazinium), which is only a partial agonist on rat and chick α7 homo-oligomers, acts as a full agonist on α8 receptors. α-BTX, and to a slightly lesser extent curare, exhibit lower apparent affinities for α8 than for α7 homo-oligomers. Suprisingly atropine, a classical muscarinic antagonist, potently inhibits α8 homo-oligomers (IC_{50} = 0.4 μM) but also acts as an antagonist on α7 receptors (IC_{50} = 7.1 μM). Both α7 and α8 homo-oligomers are also sensitive to strychnine (IC_{50} of 0.5 μM and 0.8 μM, respectively), the classical glycine receptor antagonist.

A novel nicotinic α9 subunit was isolated by screening a rat genomic cDNA library at low stringency using α7 subunit cDNA as a probe (Elgoyhen *et al.*, 1994). α9 also forms functional homo-oligomeric channels activated by ACh and blocked by α-BTX when expressed in *Xenopus* oocytes, but exhibits an unusual pharmacology distinct from all other nAChRs. The α9 receptor displays a rapidly desensitizing peak response to ACh which plateaus to a slower desensitizing component. DMPP and the muscarinic agonist oxotremorine M, are able to elicit small responses from α9-injected oocyes but are only 5% as efficacious as ACh at maximal doses. Remarkably, nicotine does not elicit a response from α9-injected oocytes (or those co-injected with α9 plus β2 or β4) but inhibits the current elicited by applications of 10μM ACh (IC_{50} = 30 μM). ACh-induced currents are also inhibited by the nicotinic antagonist tubocurarine (IC_{50} = 0.3 μM), the muscarinic antagonist atropine (IC_{50} = 1.3 μM) and most potently by the glycine receptor antagonist strychnine (IC_{50} = 0.02

μM). Both α-BTX and neuronal BTX (both at 100 nM) are able to reversably block ACh-induced α9 responses.

Based on its primary sequence and activation by acetylcholine, the α9 subunit is a member of the nAChR subunit family. However, α9 is as distinct from the neuronal α7 and α8 subunits (38% amino-acid homology) as it is from the muscle α1 subunit (37% homology) or the neuronal α2-α6 subunits (36-39% homology) (Elgoyhen *et al.*, 1994). The structure of α9 gene differs from all other nicotinic subunit genes (for review see Le Novère and Changeux, 1995) which indicates that it may represent a divergent branch of the nAChR family. The pharmacological properties of α9 appeared to resemble the properties of acetylcholine-evoked responses in chick cochlear hair cells (Fuchs and Murrow, 1992; Erostegui *et al.*, 1994) and it was found that α9 expression is restricted almost exclusively to the cochlea with no evidence of expression in adult rat brain (Elgoyhen *et al.*, 1994).

Calcium entry through α7, α8 and α9 homo-oligomers expressed in *Xenopus* oocytes readily activates calcium-sensitive chloride channels in oocytes (Seguela *et al.*, 1993; Elgoyhen *et al.*, 1994; Gerzanich *et al.*, 1994). Intracellular calcium chelators such as BAPTA (1,2-bis(2-aminophenoxy)-ethane-N,N,N',N'-tetraacetic acid) (Elgoyhen *et al.*, 1994; Gerzanich *et al.*, 1994), or chloride channel blockers such as niflumic and flufenamic acid (Seguela *et al.*, 1993), inhibit more than 80% of the ACh-activated whole cell current obtained in oocytes expressing α7, α8 or α9 nAChRs. This suggests that each of the homo-oligomeric receptors is highly permeable to calcium and that a substantial fraction of the total current through oocyte membranes is due to calcium-activated chloride channels.

The calcium permeability of the α7 homo-oligomer is shown to be much greater than that for other nicotinic receptors with a permeability ratio of P_{Ca}:P_{Na} estimated to be 15-17 (Sands *et al.*, 1993; Seguela *et al.*, 1993). This exceeds the calcium

permeability of NMDA-type glutamate receptors (P_{Ca}:P_{Na} = ~7) (Mayer and Westbrook, 1987; Iino *et al.*, 1990). The mutation of the negatively charged Glu^{237} at the cytoplasmic end of the M2 domain was shown to drastically reduce calcium permeability of mutant α7 homo-oligomers and is thought to play a role in divalent cation permeability (Galzi *et al.*, 1992).

1.5 Correlations between the physiology of native and recombinant neuronal nAChRs

Analysis of the functional responses evoked by native neuronal nAChRs present in primary neurons has presented a complex pattern of functional properties with respect to subunit expression. Individual neuron populations throughout the central and peripheral nervous system exhibit multiple classes of nAChR channels (as defined by single channel conductances and channel kinetics) and distinct rank-order profiles of agonist activation (Aracava *et al.*, 1987; Moss *et al.*, 1989; Mathie *et al.*, 1991).

Rat hippocampal neurons express three distinct types of ACh-induced current which differ in channel kinetics, EC_{50} of ACh-activation and sensitivity to antagonists such as αBTX, dihydro-β-erythroidine (DHβE) and mecamylamine (Alkondon *et al.*, 1992; Alkondon and Albuquerque, 1993; Alkondon *et al.*, 1994). By comparisons of the kinetic and pharmacological properties of nicotinic currents evoked in hippocampal neurons to the properties of recombinant nAChR subtypes expressed in oocytes, it is thought that α7 is a component of the Type 1A rapidly densensitizing currents sensitive to αBTX, α4β2 subunits mediate the Type II slowly desensitizing currents blocked by DHβE and α3β4 constitutes Type III slowly densensitizing currents blocked by mecamylamine. In contrast to hippocampal neurons, multiple neuronal nAChR subunits are expressed in the interpeduncular nucleus where only one predominant channel class has been identified (Mulle *et al.*, 1991).

1.5.1 αBTX-insensitive neuronal nAChRs

An important experimental goal is to reproduce the functional and pharmacological characteristics of a given neuronal nicotinic subtype in a heterologous expression system. However, co-expression of the known α and β subtypes in pairwise combinations in *Xenopus* oocytes does not seem to reproduce exactly the channel properties of native preparations. Overall, expression of neuronal nAChR subtypes in *Xenopus* oocytes produces channels with similar but not identical pharmacological profiles and often with significantly lower single channel conductance than that observed in native sympathetic (SCG, superior cervical ganglia), parasympathetic (ciliary ganglia) and central neurons (hippocampal, habenula, interpeduncular nucleus) (for review see Role, 1993; McGehee and Role, 1995). Co-expression of α5 with α4 and β2 in oocytes increases the single channel conductance of nAChRs expressed from 24pS to 44pS (Ramirez-Latorre *et al.*, 1996) which is more typical of what is observed in central neurons (40 - 60 pS) (Mulle *et al.*, 1991; Brussard *et al.*, 1994).

Evidence using subunit-specific antisense oligonucleotides also indicate that the α5 subunit contributes to functional nAChRs on chick sympathetic neurons (Listerud *et al.*, 1991; Ramirez-Latorre *et al.*, 1996). Single channel recording of chick sympathetic neurons reveals three conductance classes of ~15, ~33 and ~53 pS. Treatment with α5-specific antisense oligonucleotides resulted in the selective deletion of the 53 pS conductance class, with no apparent effect on the 15 or 33 pS classes, whereas treatment with control oligonucleotides had no effect (Ramirez-Latorre *et al.*, 1996).

The pharmacological profile and single channel properties of the native nAChR expressed in rat superior cervical ganglia (SCG) have been well defined (Mathie *et al.*, 1991; Covernton *et al.*, 1994). The pharmacological profiles of the α3β4 nAChR

subtype expressed in *Xenopus* oocytes (Covernton *et al.*, 1994) and in mammalian fibroblasts (Wong *et al.*, 1995) most closely resembles that of the nAChR expressed in SCG neurons. However, the rank order of nicotinic agonist potency and single channel properties of α3β4 expressed in *Xenopus* oocyes are very distinct from what is observed in native SCG neurons. A small increase in the predominant single channel conductance is observed when α5 is co-injected with α3 and β4 into *Xenopus* oocytes (from ~22pS to ~25pS), but neither combination accurately reproduces the agonist profile, burst kinetics or predominant class of single channel conductance (~34-36pS) observed in rat superior cervical ganglia (Sivilotti *et al.*, 1997). A recent study has shown that a mammalian fibroblast cell line (mouse L-cells) stably expressing the α3β4 nAChR appears to express two classes of channel, one which resembles the ion channel properties of nAChRs expressed in SCG neurones (high conductance and short burst kinetics) and the other which is similar to the properties of α3β4 expressed in oocytes (low conductance and long open times) (Lewis *et al.*, 1997).

Another report documents a lack of correlation between the properties of several neuronal nAChR subtypes transiently expressed in human fibroblasts (BOSC 23 cells), and the same nAChR subunit combinations expressed in *Xenopus* oocytes (Ragozzino *et al.*, 1997). Expression of chick α4β2 in human fibroblasts produced two conductance classes (~22pS and ~42pS) (Ragozzino *et al.*, 1997) compared with a single low conductance class observed in oocytes (~20pS) (Ballivet *et al.*, 1988; Bertrand *et al.*, 1990). In addition, higher conductance classes of ~40-45pS were also observed for α3β4, α3β2 and α4β4 nAChR combinations expressed in human fibroblasts (Ragozzino *et al.*, 1997) which only exhibit low conductance classes (~18-21pS) when expressed in oocytes (Couturier *et al.*, 1990b; Gross *et al.*, 1991; Luetje and Patrick, 1991; Papke and Heinmann, 1991; Charnet *et al.*, 1992). These results suggest that different heterologous expression systems produce nAChRs with distinct ion channel properties. These expression systems may not faithfully reproduce the

environment in which native nAChRs are expressed, and whether this may be due to differences in post-translational modifications, receptor stoichiometries or even differences in the cytoskeletal or membrane environment is uncertain.

1.5.2 αBTX-sensitive neuronal nAChRs

The αBTX-binding nAChRs expressed in chick brain and optic lobe have been well chracterised biochemically (Keyser *et al.*, 1993; Gotti *et al.*, 1994; Gotti *et al.*, 1997), and the pharmacological profiles of α7 and α8 homo-oligomeric channels expressed in *Xenopus* oocytes (Amar *et al.*, 1993; Seguela *et al.*, 1993; Gerzanich *et al.*, 1994) correlate well with the characteristics of native α7 and α8 receptors immunopurified from the chick optic lobe (Anand *et al.*, 1993a; Anand *et al.*, 1993b; Gotti *et al.*, 1994; Gotti *et al.*, 1997) and native α7 receptors expressed in cultured SH-SY5Y cells (human neuroblastoma) (Peng *et al.*, 1994b). However, several differences in agonist and antagonist pharmacology exist between oocyte-expressed receptors and native αBTX-binding nAChRs (Anand *et al.*, 1993b; Peng *et al.*, 1994b). In addition, characterization of the single-channel properties of the α7 homo-oligomeric receptor demonstrates that the single channel conductance(s) of α7-homo-oligomers expressed in a mammalian cell line (two conductance states of ~19pS and ~31pS) (Ragozzino *et al.*, 1997) differs from that observed in oocytes (~45pS) (Revah *et al.*, 1991; Bertrand *et al.*, 1992; Galzi *et al.*, 1992).

The most well documented analysis of αBTX-sensitive nicotinic responses comes from studies of cultured rat hippocampal neurons where the α7 subunit is thought to comprise the nAChR mediating Type IA currents characterized by a rapid-activating and rapidly desensitizing high conductance channel, with a brief open time, that is highly permeable to calcium (Alkondon *et al.*, 1992; Castro and Albuquerque, 1993; Castro and Albuquerque, 1995). Type IA currents are sensitive to blockade by αBTX, MLA and α-conotoxin ImI which all act as specific antagonists of the α7 receptor (Couturier *et al.*, 1990a; Wonnacott *et al.*, 1993; Johnson *et al.*, 1995; Palma

et al., 1996). The pharmacological profile of activation of Type IA currents in hippocampal neurons is nicotine > cytisine > acetylcholine (Alkondon and Albuquerque, 1993), which is mimicked by the agonist profile of chick and rat α7 homomers expressed in *Xenopus* oocytes although the estimated activation affinity of cytisine and the efficacy of DMPP differ significantly (Seguela *et al.*, 1993; Gerzanich *et al.*, 1994). Nicotinic receptors which exhibit rapidly desensitizing, αBTX-sensitive responses typical of Type IA currents of hippocampal neurons have also been reported in rat olfactory bulb neurons (Alkondon and Albuquerque, 1994; Alkondon *et al.*, 1996), chick ciliary ganglia (Zhang *et al.*, 1994; Zhang *et al.*, 1996) and rat PC12 cells (Blumenthal *et al.*, 1997). Transgenic mice deficient in the α7 subunit lack the characteristic Type IA currents observed in hippocampal neurons, comfirming a role for the α7 subunit in the nAChR subtype which generates these responses (Orr Urtreger *et al.*, 1997).

1.6 The functional role of neuronal nAChRs *in vivo*

1.6.1 Neuronal nAChRs and tobacco dependence

The most obvious physiological role of the neuronal nAChRs is their mediation of nicotine-induced tobacco dependency. It has been demonstrated in rats that chronic exposure to nicotine results in an approximate two-fold upregulation of α4β2 high affinity [^{3}H]-nicotine-binding sites in the brain (Schwartz and Keller, 1983; Marks *et al.*, 1985; Schwartz and Keller, 1985; Flores *et al.*, 1992; Marks *et al.*, 1992) although this does not appear to be due to upreguation of subunit mRNA (Marks *et al.*, 1992) and may not be sufficient to overcome the persistent desensitization of expressed receptors (Wonnacott, 1990; Marks *et al.*, 1993). A similar upregulation of [^{3}H]-nicotine-binding sites has been observed in the brains of chronic smokers (Benwell *et al.*, 1988).

The upregulation of cell surface receptors in response to chronic desensitization appears to be an intrinsic property of the neuronal nAChR as it also occurs in mammalian cell lines stably expressing the recombinant α4β2 neuronal nAChR (Peng *et al.*, 1994a; Gopalakrishnan *et al.*, 1995b). The upregulation of recombinant α4β2 receptors is independent of subunit mRNA levels and appears to be exerted by post-transcriptional mechanisms involving reduced receptor turnover rates (Peng *et al.*, 1994a). Interestingly, the nicotine-induced upregulation of surface expressed human α4β2 nAChRs expressed in human fibroblasts (5-15 fold) was significantly higher than that observed for the chick α4β2 expressed in the M10 mouse L-cell line (2.5-fold). The EC_{50} value for the nicotine concentration required for receptor upregulation was calculated to be 0.2-0.5 μM (Peng *et al.*, 1994a; Gopalakrishnan *et al.*, 1995b) which may be physiologically significant because it correlates well to the approximate serum concentration of nicotine in chronic smokers (0.1-0.5μM) (Henningfield *et al.*, 1983; Benwell *et al.*, 1988) and is close to the concentration of nicotine required for activation of heterologously expressed α4β2 receptors (3.5μM) although much greater than the affinity of desensitized receptors for nicotine (4nM) (Peng *et al.*, 1994a).

Accumulating evidence indicates that tobacco smoking in humans and the self-administration of nicotine in rats may be associated with the reinforcement properties of dopamine release from dopaminergic neurons (Corrigall *et al.*, 1992; Dani and Heinemann, 1996; Rose and Corrigall, 1997). The actions of nicotine on dopaminergic neurons resembles that of other addictive drugs such as cocaine and amphetamines (Pontieri *et al.*, 1996; Merlo Pich *et al.*, 1997). The existence of high affinity [^{3}H]-nicotine binding sites on mesencephalic dopaminergic neurons has been demonstrated (Clarke and Pert, 1985) and nicotine has been shown to induce dopamine release from striatal synaptosome preparations (Rapier *et al.*, 1990; Grady *et al.*, 1992). Although the β2 subunit has been implicated in contributing to the

neuronal nAChR mediating nicotine-induced dopamine release (see Section 1.6.2) (Picciotto *et al.*, 1998), the potency ratio of cholinergic-stimulated dopamine release from striatal synaptosomes and its antagonist sensitivity do not implicate αBTX-sensitive receptors and also do not match the characteristics of α4β2 receptors (Grady *et al.*, 1992; Grady *et al.*, 1994). Recently, high levels of the α6 and β3 neuronal subunit mRNAs have been co-localized in catecholaminergic and dopaminergic neurons (Le Novère *et al.*, 1996) and may contribute to a neuronal nAChR implicated in the dopamine reward mechanisms of nicotine addiction. The α6 nAChR subunit exhibits a restricted pattern of expression and is highly homologous to the α3 subunit (61% identity), particularly in the domains implicated in contributing to the ligand-binding site.

1.6.2 Explorations of the role of neuronal nicotinic subunits by knock-out mutations

The physiological contribution of neuronal nAChR subtypes has been investigated in transgenic knock-out mice. Transgenic mice deficient in the β2 neuronal subunit are viable, feed and mate normally and present no drastic physiological or neurological defects (Picciotto *et al.*, 1995). The high-affinity [^{3}H]-nicotine-binding sites in the brain are completely absent in homozygous mutant mice with no apparent effect on the α-bungarotoxin-binding sites which persist. Mutant mice do not exhibit an enhanced performance on a passive-avoidance memory test following the adminstration of nicotine, and performed the task better than wild-type animals. β2-knockout mice were used to examine the contribution of the β2 subunit to neuronal nicotinic receptors involved in nicotine abuse and the reinforcement properties of dopamine release from mesolimbic dopaminergic neurons (Picciotto *et al.*, 1998). Unlike wild-type mice, nicotine did not increase dopamine release from the striatum of homozygous mutant mice and did not increase the frequency of discharge from dopaminergic neurons (Picciotto *et al.*, 1998). In addition, nicotine was unable to substitute for cocaine in maintaining self-administration of β2-mutant mice,

suggesting that β2 subunit is a component of the neuronal nAChR involved in modulating dopamine release and mediating the reinforcement properties of nicotine (Picciotto *et al.*, 1998). The analysis of the pharmacological and single channel properties of nicotinic responses from isolated neurons throughout the central and peripheral nervous system should provide invaluable insight into the contribution of β2 subunits to neuronal nAChRs and their physiological role *in vivo*.

Mice deficient in the neuronal α7 subunit were generated by deleting the last three exons of the α7 gene (encoding for the M2 transmembrane domain onwards) (Orr Urtreger *et al.*, 1997). The deletion leaves the coding region for the extracellular ligand-binding domain intact and the possibility of producing a truncated α7 protein in homozygous mutant mice. Northern blotting and immunoblotting techniques demonstrate the absence of detectable truncated α7 mRNA transcripts, or α7 protein, indicating that the resulting transcripts are unstable. Similarly to the β2-knock out mice, the α7 mutant mice feed and mate normally, they grow to normal size and do not appear to possess any obvious physical or neurological deficit. However, the homozygous mutant mice are completely lacking in high-affinity [^{125}I]-αBTX-binding sites but possess identical distributions of high-affinity [^{3}H]-nicotine binding sites compared to wild-type mice. The α7 mutant mice exhibited a hypersynchronous E.E.G. (electroencephalogram) bursting rhythym which may illustrate a possible role in the regulation of firing activity in the brain (Orr Urtreger *et al.*, 1996). α7 null mice also lack the characteristic, rapidly desensitizing, nicotinic current in hippocampal neurons (Orr Urtreger *et al.*, 1997). This confirms previous suggestions the α7 subunit constitutes or is a component of this nAChR in the hippocampus (Alkondon *et al.*, 1992; Alkondon and Albuquerque, 1993; Albuquerque *et al.*, 1997).

1.6.3 Neuronal nAChRs and neurological disorders

Familial nocturnal epilepsies have been linked to point mutations within the α4 nAChR subunit. Two familial mutations have been mapped and found to correspond

to mutations within the M2 transmembrane domain of the α4 subunit; the substitution of serine^{248} to phenylalanine (Steinlein *et al.*, 1995) and an insertion of a leucine residue at position 260 (Steinlein *et al.*, 1997). The aligned residue of α4-serine^{248} in *Torpedo* α has been identified as being exposed to the channel lumen (Giraudat *et al.*, 1987b; Revah *et al.*, 1990). Mutation of the human α4 gene and expression of α4(S248F)β2 in *Xenopus* oocytes produces a receptor with a twofold increase in affinity for ACh and fivefold increase in desensitization rate, compared with wildtype $\alpha_4\beta_2$ (Weiland *et al.*, 1996). The same mutation in the α7 homo-oligomer (at the aligned threonine^{244}) also resulted in drastic changes in receptor desensitization and affinity for ACh. Generating the insertional mutation in α4 (+Leu260) and functional analysis of the mutated α4 coexpressed with β2 in oocytes, revealed a 12-fold increase in affinity for ACh.

A significant reduction in cholinergic transmission and neuronal nAChR density is associated with Alzheimer's disease, Parkinson's disease and other chronic neurodegenerative disease (Whitehouse *et al.*, 1988; Lange *et al.*, 1993; Perry *et al.*, 1995). Treatment with nicotine appears to provide some therapeutic relief in these diseases, as well as in Tourette's syndrome and schizophrenia (Jones *et al.*, 1992; Levin *et al.*, 1996; Shytle *et al.*, 1996). Due to the non-specific and addictive nature of nicotine, the development of subunit specific agonists for therapeautic treatment of disease is paramount.

The α7 nAChR subunit has also been implicated in the pathology of schizophrenia as a reduction in the number of αBTX-binding sites has been observed in the post-mortem brains of schizophrenics (Freedman *et al.*, 1995). Recently the gene locus involved in a hereditary defect resulting in an impaired response to paired auditory stimuli, characteristic in schizophrenic patients, was investigated in nine families with multiple cases of schizophrenia. The gene locus of the auditory defect was mapped to a chromosome 15 locus (15q13-14), the same site as the neuronal α7 nAChR subunit

gene (Freedman *et al.*, 1997). In addition, a susceptibility locus implicated in juvenile myoclonic epilepsy is mapped to a similar region near the α7 gene locus on chromosome 15q (Elmslie *et al.*, 1997)

1.6.4 The role of neuronal nAChRs as pre-synaptic modulators of synaptic function

The postsynaptic transmission mediated by neuronal nAChRs in the spinal cord at the motor neuron-Renshaw cell synapse (Curtis and Ryall, 1966; Belcher and Ryall, 1977) and at efferent synapses in the cochlea (Fuchs and Murrow, 1992; Elgoyhen *et al.*, 1994; Erostegui *et al.*, 1994) have been well documented. Synaptic currents predominantly generated by αBTX-sensitive receptors have also been reported in chick ciliary ganglia (Zhang *et al.*, 1996). Surprisingly, unlike nAChRs recognised by mAb35 (α5 and α3) there is no evidence for αBTX-binding sites on the postsynaptic membrane of ciliary ganglia (Loring *et al.*, 1985; Conroy and Berg, 1995; Wilson Horch and Sargent, 1995). Instead, immunohistochemistry indicates that the αBTX-receptors are located adjacent to postsynaptic membrane thickenings on the soma in perisynaptic clusters on short dendrites which emanate from the cell body (Wilson Horch and Sargent, 1995). However, Zhang *et al* (1996) demonstrate that this population of perisynaptic receptors are capable of generating synaptic current which is specifically blocked by αBTX and MLA, and that transmitter released from presynaptic terminals could plausibly have time to reach these perisynaptic clusters within the time-frame of observed current activation (Zhang *et al.*, 1996). Experiments were conducted using acetylcholinesterase inhibitors in an attempt to prolonge the lifetime of ACh diffusion. This treatment increased the amplitude of the slowly decaying αBTX-insensitive currents, but had no effect on the rapidly desensitizing, αBTX-sensitive component indicating that extending the activity of ACh did not activate a greater number of perisynaptic αBTX-sensitive nAChRs. Recent reports show that choline acts a selective agonist of α7-containing

nAChRs on rat hippocampal, thalamic and olfactory bulb neurons as well as in rat PC12 cells (Alkondon *et al.*, 1997). However, the threshold choline concentration required for activation of α7-containing receptors was >100μM with an EC_{50} of 1.6mM, an order of magnitude greater than that for ACh.

There are remarkably few reports of synaptic transmission elicited by neuronal nAChRs in the brain. Recently, compelling evidence has been generated for a postsynaptic role mediated by α7-containing receptors located on the soma of stratum radiatum interneurons in the hippocampus (Jones and Yakel, 1997; Frazier *et al.*, 1998). αBTX and MLA were able to inhibit the ACh-induced synaptic responses observed in hippocampal interneurons indicating the involvment of nAChRs containing the α7 subunit.

There is considerable evidence suggesting that the predominant role of neuronal nAChRs in the brain may be involved in more subtle modulatory effects by acting pre-synaptically (Role and Berg, 1996; Wonnacott, 1997). The calcium permeability of nAChRs could be a mechanism which allows nAChRs to modulate release of other neurotransmitters without triggering endplate potentials. Many of the neuronal nAChRs detected in brain preparations seem to be located presynaptically (Clarke *et al.*, 1986; Swanson *et al.*, 1987), with evidence for presynaptic terminal receptors on dopamine (Clarke and Pert, 1985), GABA (Lena *et al.*, 1993), catecholamine and serotonin (Schwartz *et al.*, 1984) neurons, and the specific targeting of synthesized nAChRs by axonal transport to terminal fields of the optic tectum (Henley *et al.*, 1986). There is accumulating evidence for nAChR modulation of synaptic transmission by regulating neurotransmitter release (Rapier *et al.*, 1990; Grady *et al.*, 1992). Studies performed on chick brain (McGehee *et al.*, 1995), rat hippocampal neurons (Gray *et al.*, 1996) and rat olfactory bulb neurons (Alkondon *et al.*, 1996) have all demonstrated that presynaptic α7-containing nAChRs located on glutamatergic neurons facilitate glutamate release and activation of synaptic

transmission which can be blocked by αBTX or MLA. In addition, nicotine has been shown to increase the frequency of spontaneous $GABA_A$-mediated inhibitory postsynaptic currents in chick brain (McMahon *et al.*, 1994b; McMahon *et al.*, 1994a).

Neuronal nAChRs may also have a role in regulating neurite outgrowth (Pugh and Berg, 1994). Applications of nicotine to isolated ciliary ganglia was shown to induce neurite retraction (Pugh and Berg, 1994). The retraction required the presence of external calcium and was selectively blocked by αBTX. Given that activation of α7 nAChRs on ciliary ganglia has been shown to elevate levels of intracellular calcium (Vijayaraghavan *et al.*, 1992), these results suggest that α7-nAChRs may play a role in regulating and perhaps stabilizing synapse formation mediated by calcium second messenger pathways.

1.7 Aim of the project

At the beginning of this project there were very few examples of the successful heterologous expression of neuronal nAChR subtypes in mammalian cell lines. The roles for α7-containing receptors in defined pre- and post-synaptic roles is only beginning to emerge, but their high calcium permeability and their ability to form functional homo-oligomeric channels in *Xenopus* oocytes, makes them an attractive model for study. The α7 homo-oligomer provided an ideal system for mutageneisis experiments which examined the contribution of conserved residues within the M2 domain and has also been used to demonstrate the functional role of entire protein domains via the generation of an α7/5-HT_3 chimera, which exhibits nicotinic pharmacology but 5-HT_3 channel characteristics (Eiselé *et al.*, 1993).

The aim of this project was to examine the properties of cloned nAChR subtypes expressed in mammalian cells, with particular focus on the homo-oligomeric α7 and

α8 αBTX-binding receptors. Mammalian cells could theoretically provide a more native environment for nAChR expression (compared with amphibian oocytes) and stable cell lines would provide an abundant source of recombinant nAChRs for biochemical and electrophysiological analysis. Site-directed mutagenesis experiments would be used to explore the structure-function relationships of individual residues or entire protein domains and further characterize the role of the neuronal αBTX-binding receptors.

Materials and Methods

2.0 Materials and methods

All biochemicals were obtained from BDH and all enzymes and reaction buffers were purchased from Promega, unless specified otherwise. All tissue culture media and additives were obtained from GibcoBRL unless otherwise stated.

2.1 Plasmid Constructs and Subcloning

2.1.1 Competent cells

Plasmid constructs were transformed into chemocompetent MC1061, JM109 or HB101 *E. Coli* cells (Invitrogen). In the case of subcloning strategies involving digestion with restriction enzymes blocked by overlapping *dcm* or *dam* methylation, the *dcm*$^-$/*dam*$^-$ *E. Coli* strain GM2163 was used (Dr. Ralf Schoepfer, University College London).

Competent cells were generated according to the suppliers instructions. From a stab, cells were streaked onto SOB agar plates (tryptone 20g/L, yeast extract 5g/L, NaCl 0.5g/L, 2.5mM KCl, 10mM $MgCl_2$, agar 15g/L). A sample of cells were scraped from the plate and used to innoculate 500ml SOB media. The culture was incubated at 37°C in a shaking incubator at 200rpm until the $O.D._{550}$ was 0.50-0.55. Cells were centrifuged in a Beckman J2-M1 centrifuge at 2500rpm using a JA-14 or JA-10 rotor for 15 minutes at 4°C. The pellet was resuspended in 40ml ice-cold RF1 [100mM RbCl, 50mM $MnCl_2.4H_20$, 30mM potassium acetate, 10mM $CaCl_2.2H_20$, 15%(w/v) glycerol, pH adjusted to 5.8 with 1M acetic acid, filter sterilized (0.22μm)] and incubated on ice for 15 minutes. For the HB101 strain, cells were held on ice for 2 hours. The cells were pelleted by centrifugation at 2500rpm for 9 minutes. The pellet was resuspended in 7ml ice-cold RF2 [10mM RbCl, 10mM MOPS (3-*N* -morpholino propanesulphonic acid), 75mM $CaCl_2.2H_20$, 15% (w/v) glycerol, pH adjusted to 6.8

with 1M NaOH, filter sterilised (0.22μm)] and incubated on ice for 15 minutes. Aliquots of competent cells were snap frozen in a dry ice/ethanol bath and stored at -70°C.

2.1.2 Restriction digests

Typically 2-3μg of supercoiled plasmid DNA was digested with 5-10 Units of enzyme in a 30μl reaction volume for 1 hour, usually at 37°C (certain enzymes require incubation at 25°C or 55°C for optimal activity). For double digests where the diluent buffers were incompatible, plasmid DNA was digested with the first enzyme for 1 hour in a 20μl reaction volume. The reaction mix was heat inactivated at 65°C for 10 minutes where appropriate, diluted to 80μl in the preferred digestion buffer and incubated with the second enzyme for a further 1 hour.

2.1.3 Dephosphorylation

For plasmid DNA digested with a single restriction enzyme, 5'-phosphate groups were removed using calf intestinal alkaline phosphatase (CIAP) to prevent re-ligation of the vector backbone. The 2-3μg digested plasmid DNA was diluted 3 fold in CIAP buffer and incubated with 0.2U CIAP for 15-20 minutes at 37°C. The reaction was stopped by the addition of 5mM EDTA (ethylenediaminetetra-acetic acid) and heat inactivated by incubation for 15 minutes at 75°C.

2.1.4 Polymerase chain reaction (PCR)

Polymerase chain reaction (PCR) thermocycling was performed in a Hybaid Omnigene Temperature Cycler. Typically reactions would contain 10-20ng plasmid DNA, 100-125μM dNTPs, 0.25μM forward and reverse primers and 0.3-0.5U *Taq* polymerase. When PCR products were required for subcloning experiments, cloned *Pfu* polymerase (Stratagene) was used. *Pfu* polymerase possesses both 5' - 3' DNA

polymerase, and 3' - 5' exonuclease proofreading activity, which results in a 12-fold increase in fidelity of DNA synthesis compared with Taq DNA polymerase.

2.1.5 Agarose gel electrophoresis and DNA purification

Digested plasmids, PCR products or excised inserts were separated according to molecular weight by electrophoresis through a 0.8% - 2% agarose gel (Gibco BRL). If DNA segments were required for subsequent purification, low melting point agarose was used. DNA bands were removed using a sterile scalpel and transferred to Eppendorf tubes. DNA fragments were extracted from agarose gel segments using Wizard™ DNA clean-up columns (Promega) according to the manufacturers instructions. The agarose gel segments are dissolved in 1ml of a buffered 6M guanidine thiocyanate solution containing Wizard™ DNA-binding resin. The resin is transferred to a 2ml luer syringe attached to a mini-column. The plunger is used to force the resin into the column which is then washed in a similar manner with 2 mls of 80% isopropanol. The columns are briefly spun in a bench-top microfuge to remove excess isopropanol. Bound DNA fragments are eluted in 50µl sterile, pre-warmed (~65°C), milli-Q (MQ) water or 10mM Tris-base pH 8.0. Eluted DNA fragments were spun briefly (2-3 minutes) in a vacuum-centrifuge (speedi-vac) to remove any residual isopropanol which may interfere with subsequent ligation steps. A 2.5µl sample was run on an agarose gel to determine the yield using 1µg *Hind*III digested Lambda DNA as standards (Promega).

2.1.6 Ligations and transformations

Typically, ligations contained a molar ratio of vector:insert of 1:3 which proved to be the most successful. Background religated vector was always determined with a control ligation not containing insert. Fresh ATP (1mM) was added to the ligation mixture (typically 10µl) prior to incubation with 0.5U T4 DNA ligase at 16°C overnight. 1-2 µl of the ligation mixture or ~10-20ng plasmid DNA was used in

transformations containing 50µl aliquots of competent cells. The DNA and competent cells were gently mixed and held on ice for 20-30 minutes. The cells were subjected to heat shock at 42°C for 90 seconds and allowed to recover for a few minutes on ice. 600µl of SOC (tryptone 20g/L, yeast extract 5g/L, NaCl 0.5g/L, 2.5mM KCl, 10mM $MgCl_2$, 20mM glucose) was added and cells were gently shaken at 37°C for 40-45 minutes to allow expression of the antibiotic resistance gene. Aliquots of this mixture were plated onto LB-agar plates containing inhibitory concentrations of the appropriate antibiotic (50µg/ml ampicillin, 12.5µg/ml tetracycline, 50µg/ml kanamycin, 25µg/ml Zeocin).

Individual colonies were picked and screened for those containing vector plus insert. PCR techniques were performed directly on individual bacterial colonies using primers complementary to T7 or SP6 sites either side of the vector multiple-cloning cassette. A standard PCR protocol was used with an additional first cycle of 95°C for 5 minutes to help lyse the bacterial cells and inactivate nucleases. Alternatively, minature preparations of plasmid DNA were isolated by alkali lysis (Sambrook *et al.*, 1989) of 1ml bacterial cultures grown in Luria-Bettani medium [LB: tryptone 10 g/L, yeast extract 5 g/L, NaCl 10g/L, pH ~7.0 with NaOH). Briefly, bacterial pellets were resuspended in 100µl Solution I [50mM glucose, 25mM Tris/Cl pH 8.0, 10mM EDTA pH 8.0], lysed by the addition of 200µl Solution II [0.2M NaOH, 1% SDS] and precipitation of chromosomal DNA induced with 150µl Solution III [100ml: 60ml 5M potassium acetate, 11.5 ml glacial acetic acid, 28.5 ml water. The final solution is 3M with respect to potassium and 5M with respect to acetate concentration]. Samples were phenol/chloroform (1:1, pH 8.0) extracted and ethanol precipitated (70% final concentration). Samples were centrifuged for 10 minutes at full speed in a benchtop microfuge. DNA pellets were washed once with 250µl 70% ethanol, air-dried and resuspended in 30µl milli-Q water containing 10µg/ml RNAase A (DNAase-free, Sigma). Positive clones containing plasmids of increased size were identified by agarose gel electrophoresis.

Individual positive clones were used to innoculate LB cultures for plasmid purification using Qiagen™ DNA purification columns, which also employ alkali lysis isolation of plasmid DNA followed by a further purification step using Qiagen™ DNA-binding resin. DNA bound to the resin is washed twice with wash buffer [1.0M NaCl, 50mM MOPS, 15% v/v ethanol, pH 7.0) and eluted in elution buffer [1.25M NaCl, 50mM Tris-Cl, 15% v/v ethanol, pH 8.5]. Plasmid DNA is precipitated with 70% isopropanol at room temperature, washed once with 70% ethanol and resuspended in 10mM Tris-Cl pH 8.0. DNA concentration and purity is obtained by reading at E_{260} and E_{280} in a Beckman DU-650 Spectrophotometer. An E_{260} of 1 is equal to approximately 50 µg/ml double stranded DNA. A ratio of E_{260}:E_{280} of ~1.8-2.0 is a good indication that the DNA preparation is pure. A ratio significantly less than 1.8 indicates protein contamination in the DNA preparation. Plasmid constructs were then analysed by restriction digestion and both ends of the cDNA fragments were verified by nucleotide sequencing (see Section 2.3).

2.1.7 Plasmid constructs

A summary of the properties of all plasmid expression vectors used in this project are detailed in Chapter 3, Figure 3.0.1. In addition, a summary of all subcloned constructs is presented in Chapter 3, Figure 3.1.1. pcDNA3neo, pZeoSV2(+) and pCMV-βgal were obtained from Invitrogen. pMSG and pSVK3 were both obtained from Pharmacia. pRmHa3 was provided by Dr. Thomas Bunch, University of Arizona and is a modification of the original plasmid pRmHa1 (Bunch *et al.*, 1988). pCOHygro (van der Straten *et al.*, 1989) was supplied by Dr. Martin Rosenberg, SmithKline Beecham Pharmaceuticals, Philadelphia.

The rat α7 cDNA (Seguela *et al.*, 1993) in the *Eco*RV site of the mammalian expression vector pcDNA1neo (Invitrogen), was generously provided by Dr. Jim Patrick, Baylor College of Medicine, Houston. The rat α7 cDNA was excised from pcDNA1neo and subcloned into the *Xho*I / *Spe*I sites of pMSG, the *Kpn*I / *Apa*I sites

of pSVK3 and the *Kpn*I / *Sac*I sites of pRmHa3. The chick α7 cDNA (Couturier *et al.*, 1990a) in the mammalian expression vector pMT3 (Swick *et al.*, 1992), was a gift from Dr. Marc Ballivet, University of Geneva. Chick α7 cDNA was excised from pMT3 with *Sma*I(5') and *Xho*I(3') and directionally subcloned into the *Eco*RV(5') and *Xho*I(3') sites of pcDNA3neo. The human α7 cDNA was generously provided by Dr. Jon Lindstrom, University of Pennsylvania, cloned into the *Bgl*II site of the oocyte expression vector, pMXT (Peng *et al.*, 1994b). The full length human α7 cDNA was excised with *Bgl*II and subcloned into pcDNA3neo.

The mouse $5HT_3$ cDNA in the mammalian expression vector pCDM6x1 (Maricq *et al.*, 1991) was generously provided by Dr David Julius, University of California. The $5HT_3$ gene was excised from pCDM6 with *Hind*III(5') and *Not*I(3') and subcloned into the *Hind*III and *Not*I sites of pZeoSV2(+). The $5HT_3$ cDNA was excised with *Xba*I(5') / *Not*I(3') and subcloned into pRmHa3 *Kpn*I(5') / *Not*I(3') using an 8bp (base pairs) linker oligo: 5' - CTAGGTAC - 3'.

The five rat muscle nAChR subunits (α1, β1, γ, ε and δ) in the oocyte expression vector pSPOoD, a derivative of SP64 (Witzemann *et al.*, 1990), were kindly provided by Dr Viet Witzemenn, Max-Plank-Institut für Medizinische Forschung, Heidelberg. α1, δ and ε were excised from pSPOoD using *Xho*I and subcloned into dephosphorylated *Xho*I digested pcDNA3neo. β1 was excised using *Hind*III(5') and *Xho*I(3') and directionally subcloned into the same sites of pcDNA3. γ could not be excised from the vector and so was amplifed using PCR with two specific primers:

γ-Forward Primer: 5'-ACTGGGCAGAATTCAGGCACCATGCACGGG
*Eco*RI

γ-Reverse Primer: 3'-TACAGCTCTAGAAACAGCATGACCCACATG
*Xba*I

PCR conditions utilised were 95°C denaturation for 30 seconds, 55°C annealing for 30 seconds, 72°C extension for 2.5 minutes. This was repeated for 30 cycles. DNA was precipitated by the addition of 1/10th volume of 3M sodium acetate (pH5.2) and 2 volumes of ethanol. Samples were spun at full speed for 10 minutes, washed with 70% ethanol and resuspended in restriction enzyme digestion buffer. The digested PCR product was gel purifed and subcloned into the *Eco*RI(5')/*Xba*I(3') sites of pcDNA3neo. The rat muscle α1, β, δ and ε subunits were also subcloned into pMSG, pRmHa3 and pSVK3 (for details of the cloning strategies please refer to Chapter 3, Figure 3.1.1).

The chick α8 gene (Schoepfer *et al.*, 1990) was kindly donated by Dr. Jon Lindstrom, cloned into the *Eco*RI site of pBluescript SK(-) (Stratagene). Chick α8 cDNA was excised from pBluescript using *Eco*RI and subcloned into the *Eco*RI site of pcDNA3neo. The rat α9 cDNA (Elgoyhen *et al.*, 1994) was provided by Dr. Belen Elgoyhen, Instituto de Investigaciones Farmacologicas, Buenos Aires, in the *Eco*RI site of the bluescript vector pBS(+). α9 was excised from pBS(+) with *Eco*RI and subcloned into the *Eco*RI site of pcDNA3neo. In addition, α9 was excised from pBS(+) and subcloned into the *Xba*I / *Apa*I sites of pSVK3 and *Kpn*I / *Sac*I sites of pRmHa3.

2.1.8 Introduction of the 'FLAG-epitope' into the intracellular loop region of the α7 subunit.

A unique 'FLAG-epitope' was introduced within the presumed intracellular loop region of the α7 cDNA. The FLAG-epitope consists of an 8 amino acid FLAG-tag sequence which was introduced by site-directed mutagenesis of the α7 cDNA between the M3 and M4 domains at a unique *Stu*I site at position 1173bp (Where A in the first ATG is denoted as 1). The FLAG-tag octopeptide is: *N - Asp Tyr Lys Asp Asp Asp Asp Lys - C.*

Two oligos were generated;

α7-FLAG *Stu*I(+): 5' - CGACTACAAGGACGACGATGACAAGGG - 3'

α7-FLAG *Stu*I(-): 5' - CCCTTGTCATCGTCGTCCTTGTAGTCG - 3'

These were annealed and subcloned into pRmHa3-α7 cut with *Stu*I. pRmHa3 was used in this mutagnesis as it did not contain an *Stu*I site. The presence and correct orientation of the FLAG-tag was verified by sequencing. The full length FLAG-tagged α7 cDNA construct was then excised from pRmHa3 using *Kpn*I(5') and *Not*I(3') and subcloned into the same sites of pcDNA3neo.

2.2 Chimeric Constructs

Various cDNA constructs were generated containing portions of the nAChR α7 subunit and the serotonin $5HT_3$ subunit to create chimeric receptor constructs. PCR techniques were utilised in the construction of these chimeras and a standard protocol was employed; 30 second 95°C denaturation, 30 second 55°C annealing and 75 second 72°C extension phase for 30 cycles. Annealing temperatures of mis-matched primers were optimized and altered if necessary. To enable restriction digestion of the PCR products, the fragments were ethanol precipitated by the addition of 1/10th volume 3M sodium acetate (pH 5.2) and 2 volumes of ethanol. Samples were cooled on ice, spun for 10 minutes at 13000g in a microcentrifuge, washed with 70% ethanol and resuspended in sterile milli-Q water. Where possible, DNA fragments were isolated from restriction digestion of plasmid DNA. All cDNA fragments were gel purified using Wizard™ columns (Promega).

In all cases, the correct orientation and fidelity of the constructs were verified by restriction digest analysis and the ends and the join(s) of the α7/$5HT_3$ chimeric constructs verified by sequencing. For a schematic diagram of the construction of the various chimeric subunits, see Results Section, Chapter 6, Figure 6.1.1.

2.2.1 $\alpha7^{(V201)}/5HT_3$ and $\alpha8^{(I201)}/5HT_3$

Chimeric subunit cDNAs were constructed containing the *N*-terminal portion of the rat α7 or chick α8 nAChR subunits up to the first predicted transmembrane domain, and continuing with the *C*-terminus of the $5HT_3$ receptor subunit, similar to that described previously (Eiselé *et al.*, 1993). Using PCR techniques, a *Bcl*I site was introduced by silent mutation into the rat α7 and chick α8 cDNAs at the corresponding Valine^{201} and Isoleucine^{201} residues in the mature proteins (α7 amino-acid numbering according to Couturier *et al.*, 1990), respectively.

OL 117 (-): 5' - GCG CAT GAT CAC TGT GTA GGT GAC ATC TGG - 3'
($\alpha7^{V201}$) *Bcl*I

OL 216 (-): 5' - TCG TCG CAT GAT CAT GGT GTA TGA GAG - 3'
($\alpha8^{I201}$) *Bcl*I

PCR thermocycling was performed using pcDNA1neo-α7 or pcDNA3neo-α8 as templates with the T7(+) and OL-117(-) or OL-216(-) primers. The *N*-terminal α7 and α8 fragments were ethanol precipitated, digested with *Hind*III(5') and *Bcl*I(3') and cloned into the same sites of pZeoSV2(+) to generate pZeoSV-$\alpha7^{(V201)}$ and pZeoSV-$\alpha8^{(I201)}$.

A *Bcl*I site is situated at the aligned Valine^{216} residue (according to numbering by Maricq *et al.*, 1993) in the mouse $5HT_3$ gene and the entire *C*-terminal portion of $5HT_3$ can be isolated by digesting pRmHa3-$5HT_3$ with *Bcl*I, which also cleaves in the 3' untranslated region of the $5HT_3$ cDNA (pRmHa3 contains no additional *Bcl*I sites). The *Bcl*I *C*-terminal fragment of the $5HT_3$ gene was subcloned into the *Bcl*I sites of pZeoSV-$\alpha7^{(V201)}$ and pZeoSV-$\alpha8^{(I201)}$ to generate pZeoSV-$\alpha7^{(V201)}/5HT_3$ and pZeoSV-$\alpha8^{(I201)}/5HT_3$. The $\alpha7^{(V201)}/5HT_3$ chimera was excised from pZeoSV2 with *Hind*III(5') and *Sca*I(3') and subcloned into the *Hind*III(5') / *Eco*RV(3') sites of pcDNA3neo.

2.2.2 $\alpha 7^{(S235)}/5HT_3$

A chimeric construct was made which encoded for α7 up to the loop between putative transmembrane domains 1 and 2 (to Serine^{235}), and continued with the *C*-terminal domain of $5HT_3$ (from Glycine^{252}). A silent mutation generating a *Bsp*EI site was introduced between Ser^{235} and Gly^{236} in the α7 subunit and at the homologous Ser^{251} and Gly ^{252} residues in the $5HT_3$ protein. Two oligos were designed, one to amplify the *N*-terminus of α7 (OL-174) and the other to amplify the *C*-terminus of $5HT_3$ (OL-175):

OL 174 (-): 5' - CTC TCC GGA GTC TGC AGG CAG CAA GAA TAC - 3'
($\alpha 7^{S235}$) *Bsp*EI

OL 175 (+): 5' - GAC TCC GGA GAG AGA GTC TCT TTC AAG ATC - 3'
($5HT_3^{G252}$) *Bsp*EI

This chimera was generated in 2 steps. Firstly, the *N*-terminus of α7 was amplified from pcDNA1neo-α7 template with T7(+) / OL-174(-). The PCR product was precipitated, digested with *Bam*HI(5') and subcloned into pcDNA3neo digested with *Bam*HI(5') / *Eco*RV(3') (*Pfu* polymerase leaves the PCR product blunt-ended) to generate pcDNA3-$\alpha 7^{(S235)}$. pcDNA3-$\alpha 7^{(S235)}$ was digested with *Bsp*EI (which cuts 5' to the *Eco*RV site) and *Not*I(3'). Secondly, the *C*-terminus of $5HT_3$ was amplified with OL-175(+) / SP6(-) using pZeoSV2-$5HT_3$ as template and a 50°C annealing temperature. The PCR product was digested with *Bsp*EI and *Not*I and subcloned into digested pcDNA3-$\alpha 7^{(S235)}$ to generate pcDNA3-$\alpha 7^{(S235)}/5HT_3$.

2.2.3 $\alpha 7^{(D265)}/5HT_3$

A chimeric gene construct was generated which encoded the *N*-terminal portion of α7 up to the small loop between putative transmembrane domains 2 and 3 (to Aspartate^{265}), and continued with the *C*-terminus of $5HT_3$ (from Glycine^{280}). A *Kpn*I restricion enzyme site at Glycine^{280} of $5HT_3$ was utilised for the mutagenesis.

Digestion of pZeoSV2-$5HT_3$ with *Hind*III and *Kpn*I effectively removes the portion encoding the *N*-terminus of the $5HT_3$ receptor.

A reverse priming oligo (OL-169) was designed to amplify the *N*-terminal encoding portion of pcDNA1neo-α7 and introduce a 3' *Kpn*I site. A PCR product generated with T7(+) and OL-169(-) was ethanol precipitated, digested with *Hind*III(5') and *Kpn*I(3') and subcloned into pZeoSV-$5HT_3$ to create pZeoSV-$\alpha7^{(D265)}/5HT_3$.

OL 169 (-): 5' - GGG GGT ACC ATC AGA TGT TGC TGG CAT GAT CTC - 3'
($\alpha7^{D265}$) *Kpn*I

2.2.4 $\alpha7^{(G301)}/5HT_3$

This chimera contains the entire *N*-terminus of α7 including the first 3 transmembrane domains (to Glycine^{301}) and continues with the *C*-terminal portion of $5HT_3$ (from Arginine^{316}). An *Eae*I site at the beginning of the large third cytoplasimc loop of $5HT_3$ was exploited for this mutagenesis. Digestion of pRmHa3-$5HT_3$ with *Eae*I and *Bcl*I yields the ~1250bp *C*-terminal segment of the $5HT_3$ cDNA. A reverse priming oligo (OL-121) was designed to amplify the *N*-terminus of α7 generating a compatible *Bsp*120I site by silent mutagenesis.

OL 121 (-): 5' - GGC ATT TTG GGC CCA TCA GGG TCA TGG TGG - 3'
($\alpha7^{G301}$) *Bsp*120I

Using pcDNA1neo-α7 as template, a PCR product generated with oligos T7(+) and OL121(-) was obtained with a 45°C annealing step. The PCR product was ethanol precipitated, digested with *Hind*III(5') and *Bsp*120I(3') and gel purified. A three component ligation containing pcDNA3neo digested with *Hind*III (5')/ *Bam*HI(3'), the digested *N*-terminal α7 fragment and the *C*-terminal $5HT_3$ cDNA fragment was successful in creating the pcDNA3-$\alpha7^{(G301)}/5HT_3$ chimera.

2.2.5 Two transmembrane chimera (2TM)

A chimera was generated containing predominantly full length α7 cDNA except for the first two transmembrane domains, and connecting short loop, of the $5HT_3$ subunit. The pZeoSV-$\alpha7^{(V201)}/5HT_3$ chimera was used to construct the 2 transmembrane chimera. Digestion of pZeoSV-$\alpha7^{(V201)}/5HT_3$ with *Kpn*I (at Gly^{280} in $5HT_3$) and *Not*I removes the *C*-terminal portion of $5HT_3$, leaving behind the 2 transmembrane domains. An oligo was designed to amplify the *C*-terminal encoding portion of α7, creating a compatible *Kpn*I site at the 5' end (OL-170).

OL170 (+): 5' - GAT GGT ACC CCC TTG ATA GCA CAA TAC TTC GCC - 3'
($\alpha7^{S266}$) *Kpn*I

Using pcDNA1neo-α7 as template, oligos 170(+) and SP6(-) were used to generate the 1080bp band encoding the *C*-terminal α7 domain. The PCR product was precipitated, digested with *Kpn*I(5') and *Not*I(3'), gel purified and subcloned into *Kpn*I and *Not*I digested pZeoSV-$\alpha7^{(V201)}/5HT_3$.

2.2.6 Three transmembrane chimera (3TM)

This chimera, containing predominantly α7 except for the first three putative transmembrane domains of $5HT_3$ (and short connecting loops), was generated in 2 steps. The first step amplified the *N*-terminal encoding cDNA segment of α7 containing the three $5HT_3$ transmembrane sections from pZeoSV-$\alpha7^{(V201)}/5HT_3$ using a reverse priming oligo (OL-178) to silently mutate the *Eae*I site at Arg^{316} in the $5HT_3$ gene to a less frequent cutter, *Eag*I.

OL178 (-): 5' - GGT ACC GGC CGC TGT AGG TCC TG - 3'
*Eag*I

The T7/OL-178 PCR product was digested with *Eco*RI('5') and *Eag*I(3') and subcloned into pZeoSV2 digested with *Eco*RI/*Not*I. In this case, the *Not*I site is

regenerated in the resulting pZeoSV-α7/5HT$_3$$^{(R316)}$. The second step amplified the *C*-terminal portion of α7 creating a compatible *Bsp*120I site at the aligned Gly^{301} residue of the α7 cDNA, with the forward priming oligo, OL-201.

OL 201 (+): 5' - GAT GGT GGG CCC ATG CCT AAG TGG ACC - 3'
(α7^{G301}) *Bsp*120I

The *C*-terminal region of α7 generated by PCR was digested with *Bsp*120I and subcloned into *Not*I digested pZeoSV-α7/5HT$_3$$^{(R316)}$.

2.3 Sequencing

For pcDNA1neo and pcDNA3neo, the T7 and SP6 priming sites were used to sequence the forward(+) and reverse(-) directions, respectively. For pZeoSV2(+), the forward priming site was T7 and reverse priming site, pcDNA3.1/Bgh (near to the bovine growth hormone polyadenylation site). For pRmHa3 a forward primer was designed to the metallothionein promoter region (MT) and a reverse primer designed to the ADH (alcohol dehydrogenase) polyadenylation site. For the sequencing of α7/5HT$_3$ chimeric constructs, an internal primer was designed to positions 618bp - 631bp within the α7 gene (α7-INT). The oligos used in all cases were:

T7 (+): 5' - TAA TAC GAC TCA CTA TAG GG - 3'

SP6 (-): 5' - TCT AGC ATT TAG GTG ACA CTA TAG - 3'

BGH (-): 5' - CAA CTA GAA GGC ACA GTC GAG G - 3'

MT (+): 5' - CAA TGT GCA TCA GTT GTG GTC AGC - 3'

ADH (-): 5' - AGG AGA AGA ATG TGA GTG TGC ATC - 3'

α7-INT(+): 5' - GAG AAG TTC TAT GAG TGC TGC - 3'

The four rat muscle nAChR receptor subunits (α1, β1, γ, δ) in pcDNA3neo were verified by dideoxy nucleotide (ddNTP) sequencing using the Sequenase^{TM}Version 2.0 DNA Dideoxy Sequencing Kit (Amersham) strictly according to the

manufacturers instructions. [α-^{35}S]-dATP (1000-1500 Ci/mmol, Amersham) is included in the reactions for autoradiographic detection of the sequence. Briefly, double stranded DNA templates (3-5μg for plasmid DNA) are denatured at 95°C for 2 minutes and cooled briefly on ice. 1pmol primer is added to the denatured templates and annealed by heating to 65°C followed by slow cooling to less than 35°C over 15-25 minutes, and then chilled on ice. T7 DNA polymerase and dNTPs (0.2μM final concentration each of dCTP, dGTP, dTTP plus 1-5μCi [α-^{35}S]-dATP) are added to the annealed DNA mixture and incubated at room temperature for 2-5 minutes. Dideoxy nucleotides (ddNTPs) are then added to the polymerase reaction in the ratio ddNTP:dNTP of 1:10 and incubated at 37°C for 5 minutes. The reactions are stopped by the addition of formamide (40% final concentration) and EDTA (8mM final concentration). Labelled DNA fragments were resolved using a 6% polyacrylamide gel (19:1 acrylamide/bis-acrylamide) containing 7M urea and 1X TBE (89mM Tris-base, 89mM Boric Acid, 2mM EDTA, ~pH 8.3).

The remaining constructs were sequenced using a fluorescent Taq DyeDeoxy™ Terminator Cycle Sequencing Kit (Perkin Elmer Applied Biosystems) and resolved using an ABI PRISM 373, and subsequently Model 377, DNA Sequencer. All reactions were performed strictly according to the manufacturers instructions. Plasmid constructs were sequenced using dye-terminator cycle sequencing. Each of the dideoxy terminator nucleotides is coupled to a different fluorescent dye and four sequencing reactions are performed simultaneously in one reaction. Fluorescent cycle sequencing is performed using ~0.7-1.0μg template plasmid DNA and 3.2pmol primer. A pre-made labelling mixture containing FS. Amplitaq DNA™ polymerase, unlabelled dNTPs and dye-labelled ddNTP terminators (Applied Biosystems), is added. FS. Amplitaq DNA™ polymerase has no 5' - 3' nuclease activity and has a drastically reduced discrimination for dideoxy nucleotides. Cycle sequencing is performed using a 30 second 96°C denaturation, 15 second 50°C annealing and 240 second 60°C extension phase for 25 cycles. The DNA fragments are

phenol/chloroform (1:1, pH 8.0) extracted, chloroform extracted and ethanol precipitated to remove unincorporated fluorescent dye ddNTPs. DNA pellets are washed with 250µl 70% ethanol, air-dried and resuspended in loading buffer containing deionized formamide plus 25mM EDTA and blue dextran (50mg/ml) in the ratio 5:1. Fluorescent DNA fragments are separated using a 4% polyacrylamide gel (19:1 acrylamide/bis-acrylamide) (Amresco) containing 6M urea and 1X TBE (Bio-Whittaker).

2.4 Cell lines and transfections

Mammalian cell lines were obtained from either the European Collection of Animal Cell Cultures (monkey kidney, COS7; chinese hamster ovary, CHO; mouse neuroblastoma/rat brain glioma hybrid, NG108; mouse neuroblastoma, NIE 115; mouse neuroblastoma, Neuro 2A; rat adrenal phaeochromocytoma, PC12) or the American Type Culture Collection (human embryonic kidney, HEK293; rat pituitary, GH_4C_1). Human neuroblastoma cells (SH-SY5Y), and the mouse neuroblastoma / chinese hamster embryonic brain cell hybrid (NCB20), were obtained from Yvonne Vallis, University College London. A stably transfected mouse fibroblast NIH 3T3 cell line (B23ε), which expresses the cloned mouse muscle nAChR subunits (α1, β1, δ and ε), was provided by Dr. Toni Claudio, Yale University (Green and Claudio, 1993). Schneider's *Drosophila* S2 cells were obtained from Dr. Thomas Bunch, University of Arizona.

Rat pituitary GH_4C_1 cells were cultured in Hams Nutrient F10 Mixture supplemented with 10% heat inactivated foetal calf serum (FCS) (Sigma) plus 5% heat inactivated horse serum (HS). Rat pheochromocytoma PC12 cells and human neuroblastoma SH-SY5Y cells were maintained in Dulbecco's modified Eagle's medium (DMEM) containing 10% FCS and 5% horse serum. All other mammalian cell lines were grown in DMEM containing 10% FCS. Mammalian cell lines were maintained in a

humidified incubator containing 5% CO_2 at 37°C. *Drosophila* S2 cells were grown in Shields and Sang M3 medium (Sigma) containing 12.5% heat inactivated FCS and 2 g/L yeast extract. *Drosophila* S2 cells were cultured in a non-humidified incubator at 25°C. All cell culture media contained penicillin (100U/ml) and Streptomycin (100µg/ml).

2.4.1 Transient transfection

The day before transfection the cells are trypsinised and replated to 50-70% confluence. Cells were transfected by either a modified calcium phosphate co-precipitation method (Chen and Okayama, 1987) or by LIPOFECTAMINE™ transfection reagent (GibcoBRL). For most cell lines, transfection protocols were optimized using an *E. Coli* β-galactosidase (βgal) reporter construct (pCMV-βgal). Cells were tranfected with pCMV-βgal under different conditions. 24-36 hours following transfection cells were rinsed once with PBS and then fixed using a mixture of 2% formaldehyde plus 0.4% glutaraldehyde (both from Sigma) in PBS for 5-10 minutes at room temperature. The cells were rinsed two or three times with PBS before incubation with a β-galactoside substrate mixture [2mM $MgCl_2$, 1.6mg/ml potassium ferricyanide, 2.1mg/ml potassium ferrocyanide, 0.5mg/ml *o*-nitrophenyl-β-D-galactopyranoside (ONPG, Novabiochem) dissolved in 5-10µl dimethylsulphoxide (DMSO, Sigma) made up in PBS]. Cells were incubated at 37°C for 30 minutes - 3 hours to allow the development of the blue product.

The enzymatic reaction rate is rapidly increased at 37°C and can be left for longer periods at room temperature. It is best to monitor the cells every 15 minutes until the blue colour is just visible. Once the blue product can be detected, the cells are left for a further 15 minutes and then counted. For the most accurate estimation of transfection efficiency, it is best not to allow overdevelopment of the blue product as it becomes difficult to discern untransfected cells amongst a group of transfected

cells. In addition, most cell types express very low levels of β-galactosidase activity and may eventually turn blue.

HEK293 cells were transfected by a modified calcium phosphate-DNA coprecipitation protocol as described previously (Chen and Okayama, 1987). Briefly, for 10 mls of culture media, 0.5 ml of 0.25M $CaCl_2$ is added to 20μg supercoiled plasmid DNA. After gentle mixing, 0.5ml 2X BES [50mM *N,N*-bis (2-hydroxyethyl)-2-aminoethanesulfonic acid, 280mM NaCl, 1.5mM $Na_2HPO_4.2H_2O$, pH 6.96 with 1M NaOH] is gently added and the mixture incubated for 10-15 minutes at room temperature. 1ml of the $CaCl_2$/DNA/BES-buffered saline solution is added drop-wise to dishes of cells containing 10mls culture medium. The cultures were incubated for 7-16 hours at 37°C with 3% CO_2, washed once with PBS and fresh media added.

For calcium phosphate transfection protocols, it was found that the ratio of $CaCl_2$/DNA/BES-buffered saline solution to culture media, and the amount of DNA in this mixture, has a profound affect on the type of DNA precipitate. The surface area: volume ratio is also important in $C0_2$ gas exchange which effects pH and leads to the formation of the precipitate. A fine-medium precipitate results in the highest transfection efficiencies and is also best for the welfare of the cells. Too much acidity leads to the formation of a very coarse precipiate which has an adverse affect on the cells. A ratio of $CaCl_2$/DNA/BES mixture to culture media of 1:10 proved the most effective in generating a fine-medium precipitate in an incubator regulated to 3% CO_2 content. The volumes of culture media which provided the highest transfection efficiencies were: 6 mls of culture medium per 10 cm dish; 1.0-1.5 mls of culture medium per 6-well; and 1.5-2.0 mls of culture media per 6 cm dish.

CHO, COS7, GH_4C_1 and all neuronal cell lines were transfected according to the manufacturers instructions using LIPOFECTAMINE™ Reagent (GibcoBRL) (unless

otherwise stated). The amount of DNA required for optimal transfection was determined using the pCMV-βgal reporter construct. It was found that a ratio of DNA (μg): Lipofectamine (μl) of 1:5-1:6 using 1.5-1.8 ug DNA per 1ml of transfection mixture resulted in the highest transfection efficiencies. Cells were routinely transfected for 6-7 hours (sometimes overnight) in serum-free OPTIMEM™ then complete media was added and the cultures left overnight. In the morning the cells were rinsed once with PBS and fresh media added.

For SH-SY5Y cells, in 1-well of a six-well plate, 1.5μg DNA combined with 7.5μl of lipofectamine in a final volume of 1.0ml Optimem™ generated the highest transfection efficiencies. For GH_4C_1 cells, in 1-well of a six-well plate, 1.8μg DNA combined with 10.8μl lipofectamine in a final volume of 1.0ml Optimem™ produced the most efficient transfection.

Cells transfected with contructs under the control of a CMV-promoter (i.e. pcDNA1neo, pcDNA3neo, pCDM6x1) were usually transfected for 7-8 hours and assayed ~28 hours following transfection. In some instances where a calcium-phosphate transfection protocol was employed, cells were transfected overnight and assayed 40 hours post transfection. Cells for metabolic labelling experiments were transfected overnight and labelled the following morning. Cells transfected with the pZeoSV2(+) vector were transfected overnight and the following morning 5mM sodium butyrate in fresh media was added for 24 hours to enhance expression of the cloned gene.

2.4.2 Stable transfection

In most cases the same transfection procedure as above was used to generate stable cell lines for the various cell types. If necessary, co-transfection of a plasmid containing the gene for neomycin resistance (which confers Geneticin™G418

resistance) was included as a selectable marker at 1/10th the concentration of the plasmid(s) of interest. After 48 hours or when the cells reached confluence, the cultures were trypsinized and split 1:5-1:12 into culture medium containing 0.8-1.0 mg/ml Geneticin G418 Sulphate™ (G418) (GibcoBRL). G418 is an aminoglycoside related to gentamycin and blocks protein synthesis. Dividing cells are more susceptible to G418 which is why cells are plated at lower density. Media containing fresh G418 is replaced twice a week. Clones were visible after 14 days in selection and were subsequently picked (typically after 21 days in selection) using filter squares pre-wet in media. Clones were gradually expanded into clonal cell lines.

For stable transfection of the*Drosophila* S2 cell line, S2 cells are transfected in suspension by a modified calcium phosphate-DNA coprecipitation (Chen and Okayama, 1987). 0.5ml of 0.25M $CaCl_2$ is added to 20μg supercoiled plasmid DNA (containing 1/10th amount of pCOHygro to provide a selectable marker for stable transformants). After gentle mixing, 0.5ml 2X HBS [50mM HEPES (*N*-2-hydroxyethylpiperazine-*N*-2-ethanesulphonic acid), 280mM NaCl, 10mM KCl, 1.5mM $Na_2HPO_4.2H_2O$, 12mM dextrose, pH 7.05 with 1M NaOH], is gently added and the mixture incubated for 10 minutes at room temperature. S2 cells are pelleted by centrifugation at 300g and resupended in 1ml $CaCl_2$/DNA/HBS-buffered saline solution. Cells are left for 10 minutes at room temperature and 9 mls of complete M3 media is added. Cells are transfected for 7-8 hours in a non-humidied incubator at 25°C and then the transfection mixture is carefully aspirated, and fresh media replaced overnight. Polyclonal stable cell lines were generated by growth in Shang and Shields M3 medium containing 300μg/ml hygromycin, a potent inhibitor of protein synthesis.

2.5 Antibodies

A summary of all antibodies used in this project is presented in Chapter 4.0, Figure 4.1.2. Monclonal antibodies (mAbs) mAb319 and mAb308 (Schoepfer *et al.*, 1990) were kindly provided by Dr. Jon Lindstrom, University of Pennsylvania. Both mAb319 and mAb308 were raised against bacterial fusion proteins and recognise linear epitopes within the α7 and α8 large cytoplasmic loops, respectively (McLane *et al.*, 1992). mAb306 (Schoepfer *et al.*, 1990) was raised against a mixture purified native and denatured chick and rat α7 and also recognises a linear epitope mapped to within the large cytplasmic loop of α7 (McLane *et al.*, 1992). mAb306 was obtained from Research Biochemicals International (RBI). mAbOAR1a, mAbOAR5a, and mAbOAR11b raised against native chick α7-containing receptors, were generously donated by Dr. Heinrick Betz, Max-Planck-Institut für Hirnforschung, Frankfurt and recognise conformational extracellular epitopes (Betz and Pfeiffer, 1984). mAb305, raised against purified native and denatured chick α8-containing receptors (Schoepfer *et al.*, 1990) recognises an extracellular conformational epitope of native α8 (McLane *et al.*, 1992), and was obtaned from RBI.

A polyclonal antiserum, raised against a fusion protein containing the intracellular loop region of the mouse $5HT_3$ receptor subunit (Turton *et al.*, 1993) was provided by Dr. Ruth McKernan, Merck Sharp and Dohme Research Laboratories, Harlow. mAbFLAG-M2, which recognises the FLAG epitope octopeptide (Asp-Tyr-Lys-Asp-Asp-Asp-Asp-Lys) (Hopp *et al.*, 1988), was obtained from IBI. A monoclonal antibody which recognises the endoplasmic reticulum lumenal chaperone protein BiP was donated by Dr. Steve Moss, LMP, University College London, and was obtained from Bioaffinity Reagents Incorporated. Rhodamine-conjugated goat anti-rat IgG and goat anti-mouse IgG were obtained from Pierce. Fluorescein-conjugated goat anti-rat and goat anti-rabbit IgG, were both obtained from Calbiochem.

2.6 Metabolic Labelling and Immunoprecipitation

Stable cell lines were trypsinized, washed and replated to 80-90% confluence the evening before the experiment. Cells for transient transfection were trypsinised the previous day to approximately ~70% confluence and were transfected overnight (see Section 2.4.1). To starve cells of methionine confluent 10cm dishes of cells were washed twice with, and bathed for 15 minutes in, L-methionine (Met) and L-cysteine (Cys) free media (Sigma). The cells were then labelled with 250μCi [^{35}S] "Pro-mix" (Amersham) in 3.0mls of Met/Cys-free medium for 3 hours (Pro-mix contains a mixture of [^{35}S]-Met and [^{35}S]-Cys). The labelling was stopped by the addition of 8mls of complete DMEM which contains 30mg/L methionine, 48mg/L cysteine and 10% FCS and chased for 3 hours. Cells were washed three times with phosphate buffered saline (PBS) (Dulbecco's A), scraped from the plates into 1ml of ice-cold lysis buffer (LB) containing protease inhibitors (Sigma) [LB; 150mM NaCl, 50mM Tris/Cl pH 8.0, 5mM EDTA, 1% Triton X-100, 0.2mM phenylmethylsulfonyl fluoride (PMSF), 2mM *N*-ethylmaleimide (NEM) and 10ug/ml each of leupeptin, apoprotinin and pepstatin] and solubilised either for 2 hours or overnight at 4°C. All subsequent steps were performed at 4°C.

Any non-solubilized material was pelleted by centrifugation at 14000g for 15 minutes. The cell lysate was pre-cleared by a 30 minute incubation with 30μl pre-washed Protein G-agarose in a 1:1 mixture with fresh lysis buffer (LB). The samples were spun briefly and the supernatant transferred to a fresh tube. Antibodies (usually 0.5μl of a 2mg/ml solution) were added to the cell lysate and incubated either for 3 hours or overnight. The antibody-receptor complex was immunoprecipitated for 3 hours with 40μl Protein G-sepharose (Calbiochem) (1:1 with LB). The samples were washed twice with 1ml LB containing 1M NaCl, washed once with LB containing 500mM NaCl and washed twice with LB containing 150mM NaCl by brief centrifugation (30 seconds) and resuspension.

The pellets of protein G-sepharose were resuspended in SDS-loading dye [50mM Tris/Cl pH 6.8, 100mM dithiothreitol (DTT), 2% sodium dodecyl sulphate (SDS), 0.2% bromophenol blue, 10% glycerol] and separated on a SDS polyacrylamide gel (Amresco) with a 5% stacking gel and 7.5% resolving gel. Electrophoresis was stopped when the dye front reached the bottom of the gel. The gel was fixed for 30 minutes in 30% methanol, 10% glacial acetic acid and rinsed briefly in distilled water before a 30 minute incubation in Amplify solution (Amersham). The gel was dried and exposed to Kodak XRP film at -80°C with intensifying screens.

2.6.1 Endoglycosidase treatment

HEK293 cells transiently transfected overnight with pcDNA1neo-α7 were metabolically labelled and immunoprecipitated with mAb319 and Protein G-Sepharose, as described in Section 2.6. The washed Sepharose pellets were resuspended in 100µl of the appropriate digestion buffer (endoglycosidase H: 0.1M sodium acetate pH 5.5; endoglycosidase F: 0.1M sodium phosphate pH 7.1, 30mM EDTA, 1% Triton X-100, 0.1% SDS, 1% 2-β-mercaptoethanol). Endoglycosidase H (3×10^{-3} Units) and endogylcosidase F (20×10^{-3} Units) (both from Boehringer Mannheim) were added to the 100µl reaction volumes and the samples incubated overnight at room temperature. The sepharose pellets were washed once with 1ml of lysis buffer, resuspended in SDS-loading dye containing 1% 2-β-mercaptoethanol and separated by SDS-polyacrylamide gel electrophoresis (please refer to Section 2.6). The gel was fixed for 30 minutes in 30% methanol, 10% glacial acetic acid and rinsed briefly in distilled water before a 30 minute incubation in Amplify solution (Amersham). The gel was dried and exposed to Kodak X-Omat Blue film at -80°C with intensifying screens.

2.7 Radioligand Binding

2.7.1 Iodinated α-bungarotoxin(αBTX) binding

i) Crude membrane preparation

To determine total [^{125}I]-αBTX-binding to cell membranes, cells were washed once with PBS then scraped into cold PBS and pelleted by centrifugation at 14 000g for 20 minutes in a benchtop microfuge at 4°C. The cell pellet was resuspended in ice-cold 10mM potassium phosphate buffer (pH7.4) or Hanks Buffered Saline Solution (HBSS) containing 10ug/ml each of leupeptin, apoprotinin and pepstatin. The crude membrane preparation was taken up 5 times through a 23 gauge needle and vortexed into a uniform suspension.

In Chapter 3.0, Section 3.1, crude membranes were incubated with 10nM [^{125}I]-αBTX of specific activity >200 Ci/mmol (Amersham) in the presence or absence of 10mM carbamylcholine to determine non-specific binding. Samples were incubated in Eppendorf tubes for 2 hours at 4°C. Samples were washed 3 times with 1 ml PBS by brief centrifugation and resuspension. Bound [^{125}I]-αBTX was determined by counting the Eppendorf tubes in a Wallac 1261 gamma counter.

For the remaining Results sections of this project, membranes were incubated for 2 hours at 4°C with 1-2nM [^{125}I]-αBTX of specific activity >200 Ci/mmol (Amersham) with a final concentration of 0.5% bovine serum albumin (BSA). The presence of BSA reduced the non-specific binding of [^{125}I]-αBTX to the glass fibre filter. This was usually added with the [^{125}I]-αBTX to enable simple protein assays of the cell samples. Non-specific binding was determined by the addition to duplicate or triplicate tubes of: 100μM methyllycaconitine (MLA, Research Biochemicals International) for samples transfected with α7, or 500mM carbamylcholine plus 500mM nicotine (both from Sigma) for samples transfected

with α8 or the muscle nAChR. Samples were harvested using a Brandel Harvester (Model M-36, Semat, U.K.) onto GF-A glass-fibre filters pre-soaked for 2 hours in 0.5% polyethylenimine (PEI) (Sigma) with five or six 3ml washes of ice-cold 10mM phosphate buffer. Filters were counted in a Wallac 1261 gamma counter. Typically, the glass fibre filters would collect ~0.1-0.3% of the [^{125}I]-αBTX counts included in the assay irrespective of the presence of cellular material.

For saturation binding studies of the clonal SH-SY5Y-α7#7 cell line, increasing concentrations of [^{125}I]-αBTX were used (2pM-6nM). Curves for equilibrium binding were fitted by equally weighted least squares (CVFIT program, David Colquhoun, University College London). The calculated Hill coefficients did not differ significantly from 1, so data were refitted using the Hill-Langmuir equation (with n_H=1) in order to estimate the equilibrium constants for αBTX-binding.

ii) Intact cell suspension

To determine [^{125}I]-αBTX-binding to cell surface membranes, cells were rinsed twice with pre-warmed Hanks Buffered Saline Solution (HBSS) and gently scraped or titurated from the culture dish into 1ml HBSS. HBSS was found to be more osmotically balanced than standard PBS (Dulbecco's A) which proved more effective at keeping the cells intact over longer periods. Prior to addition to the assay tubes, the cells were gently separated into a single-cell suspension by pipetting 3 times with a 1ml pipette tip. Intact cells were incubated with 1-2nM [^{125}I]-αBTX in HBSS containing 0.5% BSA for either 1 hour at 37°C, or at room temperature for 1.5-2.0 hours. Non-specific binding was determined by the addition to duplicate or triplicate tubes of: 100μM MLA for samples transfected with α7, or 500mM carbamylcholine plus 500mM nicotine for samples transfected with α8 or the muscle nAChR. The harvesting and washing of the samples was performed as described in Section 2.7.1(i).

iii) Cell monlayers

Intact cells were labelled with 5-20 nM [^{125}I]-αBTX in their usual culture media for 1 hour at 37°C. Cells were rinsed four times with PBS or HBSS and solubilized in lysis buffer containing protease inhibitors for 1-2 hours on ice. Samples were centrifuged at full speed in a benchtop microfuge for 10 minutes to pellet any unsolubilised material. The supernatant was transferred to a fresh tube and subsequently used for sucrose gradient centrifugation or immunoprecipitation of bound [^{125}I]-αBTX.

2.7.2 Tritiated radioligand binding

i) [^{3}H]-epibatidine

[^{3}H]-Epibatidine binding was performed with cell homogenates. Crude membrane suspensions were prepared as for the [^{125}I]-αBTX binding assay (see Section 2.7.1*i*). Membranes were incubated for 2 hours on ice with 3nM [^{3}H]-epibatidine of specific activity 53 Ci/mmol (Amersham) in HBSS containing 10ug/ml each of leupeptin, apoprotinin and pepstatin. Non-specific binding was determined by the addition of 500μM nicotine and 500μM carbamylcholine (both from Sigma) to duplicate or triplicate samples. Samples were harvested using a Brandel Harvester onto GF-B glass fibre filters pre-soaked for 2 hours in 0.5% PEI and washed four times with ~3mls cold potassium phosphate buffer (pH 7.4). The filters were plucked from the filter sheets and transferred to scintillation vials. 5mls of 'Ready Safe' liquid scintillation cocktail (Beckman) was added to the vials and shaken overnight. Samples were counted in a Beckman LS 6500 Scintillation Counter.

For saturation binding studies of the GH_4C_1-α8 transfected cells, increasing concentrations of [^{3}H]-Epibatidine were used (5pM-10nM). Curves for equilibrium binding were fitted by equally weighted least squares (CVFIT program, David Colquhoun, University College London).

ii) [^{3}H]-GR65630

The binding of the specific 5-HT_3 antagonist, GR65630, was performed on cell homogenates as above. Membranes were incubated for 2 hours at 4°C with 1nM [^{3}H]-GR65630 (specific activity 61.4 Ci/mmol, NEN) in the presence or absence of 100μM 5-hydroxytryptamine (Sigma) to determine non-specific binding. Samples were harvested using a Brandel Harvester onto GF-B glass fibre filters pre-soaked for 2 hours in 0.5% PEI and washed four times with ~3mls cold 10mM potassium phosphate buffer (pH 7.4).

2.8 Sucrose Gradient Sedimentation

Both surface and total receptor populations were analysed using sucrose gradient density centrifugation. For stable cell lines, the day before the experiment cells were trypsinized, washed and replated at a density of 5-6 x 10^6 cells / 10cm dish. In the case of transiently transfected cells, samples were assayed ~28 hours or ~40 hours after transfection (see transfection protocols). Monolayers were washed twice with PBS, then scraped into 2mls ice-cold PBS and centrifuged at 300g for 5 minutes.

For determination of the sedimentation profile of surface receptors, intact cells were first labelled with αBTX by incubation with 5nM [^{125}I]-αBTX (for α7-containing receptors) or 20nM [^{125}I]-αBTX (for α8-containing receptors) in their usual culture media for 1 hour at 37°C. Monolayers were washed three times with 8 mls cold PBS, scraped or triturated into a further 10mls PBS and transferred to a 15ml Falcon tube. Cells were pelleted at 300g for 5 minutes.

In both cases, cell pellets were solubilized for 1-2 hours in 300μl lysis buffer containing protease inhibitors (see Section 2.6, Immunoprecipitation protocol). The samples were spun at 14000g for 15 minutes to pellet any non-solubilized material

and 250µl of the supernatant was gently layered onto a 5ml, 5%-20% linear sucrose gradient prepared in lysis buffer. Gradients were centrifuged in a Beckman XL-80 Ultracentrifuge using a SW-55 Ti swing out rotor at 4°C, 40 000rpm to $\omega^2 t = 9.00 \times 10^{11}$ rad^2/s (approximately 14 hours). Sixteen fractions of 320µl were taken from the top of the gradient. Samples labelled with [^{125}I]-αBTX were analysed in a γ-counter. Fractions from gradients with samples not pre-labelled with [^{125}I]-αBTX were then subjected to further radioligand binding studies or immunoprecipitation experiments.

2.9 Immunofluorescent Microscopy

Cells were trypsinized, washed and plated onto glass coverslips coated with poly-L-lysine. [Coverslips were sterilised with 70% ethanol, washed and incubated with a 1 mg/ml poly-L-lysine (Sigma) solution for at least 1 hour. The coverslips were washed 3 times with sterile MQ water and stored dry.] Cells were transiently transfected on the coverslips and assayed for expression 28-30 hours following transfection. Stable cell lines were left 24-48 hours after trypsinization and replating onto coverslips before immunofluorescent studies. For all immunoflurescent experiments antibodies (and rhodamine αBTX) were diluted in PBS or HBSS containing 2% BSA. Cells were examined with a Zeiss Axiophot microscope using a Plan-Apochromat 100X 1.4 oil-immersion objective. For coverslips analysed by immunofluorescent confocal laser miscroscopy, cells were examined using a Nikon Optiphot-2 microscope using a PlanApo 100X 1.4 oil-immersion objective and a Bio-Rad MRC 1024 laser scanning confocal imaging with Lasersharp 2.1 software.

Dilutions of the following antibodies were used:
mAb319 at 5mg/ml @1:350. mAb305 at 5mg/ml @1:300. mAb308 at 5mg/ml @1:250. mAb306 at 5mg/ml @1:250. mAbOAR1a (hybridoma supernatant) @1:50. mAbOAR5a (hybridoma supernatant) @1:100. mAbOAR11b (hybridoma supernatant) @1:80. Polyclonal anti-5HT$_3$ sera @1:250. Rhodamine-conjugated

goat anti-rat IgG or goat anti-mouse IgG, both at 1.5mg/ml (Pierce) @1:250. Fluorescein-conjugated goat anti-rat or goat anti-rabbit IgG, both at 1mg/ml (Calbiochem) @1:250.

2.9.1 Rhodamine α-bungarotoxin binding (Rd-αBTX)

Coverslips were washed once with HBSS and blocked for 10 minutes in HBSS containing 2% BSA. Cells were incubated with 200nM Rd-αBTX (Molecular Probes) for 1-2 hours at room temperature in a humidified chamber, washed 4 times with PBS and then fixed for 10 minutes in a 3% paraformaldehyde (PFA) solution. [3g paraformaldehyde was dissolved in 100ml PBS with gentle heating to 55°C, a few drops of 2M NaOH was added to aid solubilisation. The solution was allowed to cool and then filtered through Whatman 3M paper. The 3% PFA was stored in frozen aliquots at -20°C.] Following fixation, coverslips were washed 3 times in PBS. Excess PBS was drained to one edge and carefully blotted with tissue. Coverslips were mounted in FluorSave™ (Calbiochem) mounting fluid.

2.9.2 Immunofluorescent staining of surface receptors

Coverslips were washed once with HBSS, blocked for 10 minutes in HBSS containing 2% BSA and incubated with primary antibody in a humidified chamber for 1-2 hours at room temperature. Samples were washed 4 times in PBS and fixed for 10 minutes in a 3% paraformaldehyde solution followed by 3 more washes. Coverslips were blocked again in HBSS + 2% BSA for several minutes and then incubated with an appropriate secondary antibody for 1-2 hours. Coverslips were washed 4 times and mounted.

2.9.3 Immunofluorescent staining of permeabilised cells

Coverslips were washed once in PBS, fixed and permeabilised for 10 minutes in 3% paraformaldehyde containing 0.1% saponin (Sigma) and washed three times in PBS.

Samples were blocked for 10 minutes by incubation in PBS containing 2% BSA and incubated for 1-2 hours at room temperature with primary antibody. The coverslips were washed three times, blocked with PBS + 2% BSA for several minutes before incubation with a suitable secondary antibody for 1 hour. The coverslips were washed 4 times with PBS and mounted.

2.9.4 Double-label immunofluorescent microscopy

Surface αBTX-binding receptors on intact cells are first labelled with Rd-αBTX (see 2.9.1). Unbound Rd-αBTX is removed by washing and the cells are fixed and permeabilized. The protocol for immunofluorescent staining of permeabilised cells (see 2.9.3) is then followed using a fluoroscein-conjugated (fluoroscein isothiocyanate, FITC) secondary antibody. Rhodamine fluorescence indicates receptor populations expressed exclusively at the cell surface and FITC fluorescence reveals intracellular pools of receptor protein (instances where the second antibody recognises an intracellular epitope, FITC fluorescence reveals total cell protein populations as surface receptors and intracellular receptors can be identified).

2.10 Intracellular Calcium Measurement

Cell monolayers were washed in HBSS and gently scraped or titurated from the plate into 5ml HBSS. 4μM Fura-2 acetoxymethyl ester (Fura-2) (Molecular Probes) was added and the cells were incubated for 30-45 minutes at 25°C in the dark. After loading, the cells were pelleted, washed twice with HBSS and then resuspended by gently pipetting in 6 ml of a high calcium buffer osmotically balanced with sucrose (~280-300 mOs) [75mM $CaCl_2$, 35mM Sucrose, 25mM *N*-2-hydroxyethylpiperazine-*N*-2-ethanesulphonic acid (HEPES), pH adjusted to 7.4 with KOH]. Intracellular Ca^{2+} recordings were performed within 30 minutes of loading. Ratiometric intracellular Ca^{2+} measurements were performed using a Perkin-Elmer LS-50B

Luminescence Spectrometer fitted with a stirred cuvette holder and fast filter accessory. The excitation wavelength was alternated rapidly between 340 and 380nm. Emitted fluorescence was detected at 510nm. A 340nm/380nm ratio was calculated every 40ms. Each data point is the average over four ratio data points. Agonists were added directly to the cuvette by micropipette.

Functional responses were generated by the application of 10μM DMPP (1,1-dimethyl-4-phenylpiperazinium iodide) for HEK293 cells transiently transfected with the rat muscle α, β, γ and δ subunits; and 1mM CPBG (1-*m*-chlorophenyl biguanide) for HEK293 cells transiently transfected with the $5HT_3$ subunit. Successful Fura-2 loading of untransfected control cells and cells which did not exhibit functional responses, was achieved by the addition of 0.01% Triton X-100 to permeabilise the cells and saturate all intracellular Fura-2.

Results

3.0 Expression of the rat neuronal nAChR α7 subunit in cultured cell lines.

One of the main aims of this project was to examine the properties of the rat neuronal nicotinic α7 homo-oligomer expressed in cultured mammalian cell lines. The rat nAChR α7 cDNA was obtained from Dr. Jim Patrick in the plasmid construct pcDNA1neo-α7 (Seguela *et al.*, 1993). This plasmid construct contains the full length α7 cDNA cloned downstream of a powerful, constitutively active, cytomegalovirus (CMV) promoter for effective transient expression of the protein of interest (for a summary of plasmid expression vectors, see Figure 3.0.1). The pcDNA1neo-α7 constuct has been used previously for the successful functional expression of rat α7 nAChRs following nuclear injection into *Xenopus* oocytes (Seguela *et al.*, 1993). Upon injection of pcDNA1neo-α7 into oocytes, α7 subunits readily formed functional ion channels which respond to ACh producing rapidly desensitising inward currents blocked by nanomolar concentrations of the nicotinic antagonist α-bungarotoxin (α-BTX).

To enable stable expression of the rat α7 nAChR subunit in a mammalian cell line, the rat α7 cDNA was subcloned into the plasmid expression vector pMSG (Pharmacia) (the rat muscle nAChR α, β, δ and ε subunits were also subcloned into pMSG, for a summary of all subcloned constructs please refer to Figure 3.1.1). pMSG utilizes a glucocorticoid inducible promoter present in the mouse mammary tumour virus long terminal repeat (MMTV LTR, please refer to Figure 3.0.1). The pMSG plasmid expresses the guanine-xanthine phosphoribosyl-transferase (gpt) gene which provides a marker for stable selection of transfected eucaryotic cells. Gpt is involved in the purine nucleotide biosynthesis salvage pathway and permits the reutilization of purine bases. Cells expressing gpt can survive incubation with drugs which block *de novo* nucleotide biosynthesis such as mycophenolic acid (which inhibits inosine monophosphate dehydrogensase, required for the synthesis of purine

Figure 3.0.1. Summary of mammalian and insect expression vectors.

Expression Vector	Promoter	Inducible/ Constitutive	Polyadenylation Signal	Procaryotic Selection	Eucaryotic Selection
Mammalian					
pcDNA1neo	Cytomegalovirus	Constitutive	SV40	kanamycin *SupF (amp/tet)	neomycin (G418)
pcDNA3neo	Cytomegalovirus	Constitutive	Bgh	kanamycin ampicillin	neomycin (G418)
pZeoSV2(+)	SV40	Constitutive	SV40	zeocin	zeocin
pSVK3	SV40 (early)	Constitutive	SV40	ampicillin	-
pMSG	MMTV LTR	Inducible	SV40	ampicillin	gpt
pCDM6x1	Cytomegalovirus	Constitutive	SV40	*SupF (amp/tet)	-
pMT3	Adenovirus	Constitutive	SV40	ampicillin	-
pCMV-βgal	Cytomegolovirus	Constitutive	Bgh	ampicillin	neomycin (G418)
Insect					
pRmHa3	Metallothionein	Inducible	ADH	ampicillin	-
pHygro	Copia LTR	Constitutive	SV40	ampicillin	hygromycin

Abbreviations: SV40, Simian virus; MMTV LTR, mouse mammary tumour virus long terminal repeat; Bgh, bovine growth hormone; ADH, alcohol dehydrogenase; gpt, guanine-xanthine phosphoribosyl-transferase; Copia LTR, *Drosphila* transposable element copia long terminal repeat.

* SupF: Plasmid constructs expressing SupF transfer RNA require growth in a bacterial strain containing the P3 episome such as MC1061. The P3 episome contains ampicillin (amp) and tetracycline(tet) selectable markers which contain amber mutations and are corrected by the SupF transfer RNA.

nucleotides) and aminopterin (which inhibits dihydrofolate reductase, essential for synthesis of pyrimidine nucleotides). A derivative of pMSG, pMSGneo, has been used previously to sucessfully generate a mouse L-cell line stably expressing the chick α4β2 nAChR, the M10 cell line (Whiting *et al.*, 1991a). pMSGneo contains the neomycin resistance gene which allows cells containing this marker to survive stable selection in the presence of Geneticin G418 sulphate (G418).

3.1 Stable expression of α7 in mouse L929 cells

Mouse L929 cells were transfected with pMSG-α7 (20μg per 10cm dish) by calcium phosphate transfection for 7 hours (see materials and methods Section 2.4). The cells were washed and left to recover for three days before being trypsinized and split 1:5, 1:8, 1:10 and 1:12 into culture media containing 2μg/ml aminopterin and 25μg/ml mycophenolic acid, and supplemented with 15μg/ml hypoxanthine, 10μg/ml thymidine and 250μg/ml xanthine. Individual clones were visible in L929 cells transfected with pMSG-α7 after 7 days in selection and 29 single clones were picked using pre-wet filter squares between 14-17 days after selection and expanded into clonal cell lines. The remaining clones were pooled to generate a polyclonal population of stably transfected cells. Untransfected L929 cells died after 3-4 days in selection and no live cells could be detected after two weeks.

The polyclonal L929-α7 cell line was used to determine the time course of dexamethasone induction for expression of the α7 nAChR. L929-α7 cells which were ~90% confluent were incubated for 2-7 days with 1μM dexamethasone (the concentration shown to induce maximum expression levels of the α4β2 nAChR in the M10 cell line (Whiting *et al.*, 1991a) and assayed for [^{125}]-αBTX-binding sites. Crude membrane preparations (see materials and methods Section 2.7.1*i)* were incubated with 10nM [^{125}]-αBTX for 2 hours at 4°C in the presence or absence of 10mM carbamylcholine to determine non-specific binding. Membranes were washed

Plasmid Construct	Subunit type	Restriction enzyme sites
pcDNA3-α7	chick neuronal nAChR	*Eco*RV (*Sma*I) / *Xho*I
pcDNA3-α7	human neuronal nAChR	*Bam*HI (*Bgl*II)
pcDNA3-α8	chick neuronal nAChR	*Eco*RI
pcDNA3-α9	rat neuronal nAChR	*Eco*RI
pcDNA3-α1	rat muscle nACHR	*Xho*I
pcDNA3-β1	rat muscle nACHR	*Hind*III / *Xho*I
pcDNA3-δ	rat muscle nAChR	*Xho*I
pcDNA3-ε	rat muscle nAChR	*Xho*I
pcDNA3-γ	rat muscle nAChR	*Eco*RI / *Xba*I
pMSG-α7	rat neuronal nAChR	*Xho*I / *Nhe*I (*Spe*I)
pMSG-α1	rat muscle nAChR	*Not*I / *Xba*I
pMSG-β1	rat muscle nAChR	*Not*I / *Xho*I
pMSG-δ	rat muscle nAChR	*Not*I / *Xba*I
pMSG-ε	rat muscle nAChR	*Not*I / *Xba*I
pSVK3-α7	rat neuronal nAChR	*Kpn*I / *Apa*I
pSVK3-α9	rat neuronal nAChR	*Xba*I / *Apa*I
pSVK3-α1	rat muscle nAChR	*Kpn*I / *Apa*I
pSVK3-β1	rat muscle nAChR	*Not*I / *Xba*I
pSVK3-δ	rat muscle nAChR	*Eco*RI / *Xba*I
pSVK3-ε	rat muscle nAChR	*Kpn*I / *Apa*I
pRmHa3-α7	rat neuronal nAChR	*Kpn*I / *Sal*I
pRmHa3-α9	rat neuronal nAChR	*Kpn*I / *Sac*I
pRmHa3-α1	rat muscle nAChR	*Not*I / *Xho*I (*Sal*I)
pRmHa3-β1	rat muscle nAChR	*Kpn*I / *Xho*I (*Sal*I)
pRmHa3-δ	rat muscle nAChR	*Xho*I (*Sal*I)
pRmHa3-ε	rat muscle nAChR	*Xho*I (*Sal*I)
pRmHa3-5HT$_3$	mouse 5HT$_3$ R	*Xba*I (*Kpn*I) / *Not*I

Figure 3.1.1. Summary of subcloned constructs. The table illustrates the subcloning strategies of various neuronal nAChR subunits into each of four plasmid vectors; pcDNA3neo, pMSG, pSVK3 or pRmHa3. If there are two restricion enzyme sites listed, the first denotes the enzyme site located at the 5' end of the multiple cloning site of the vector, and the second denotes the enzyme site at the 3' end. Enzymes listed in parenthesis correspond to the restriction enzyme site used to excise the cDNA insert. cDNA inserts with compatible blunt or cohesive ends were then subcloned into digested plasmid DNA. In these cases, neither restriction enzyme recognition site is regenerated.

three times with 1ml PBS in eppendorf tubes by brief centrifugation and resuspension. No specific binding of [^{125}I]-αBTX could be detected for any time point of induction in the polyclonal L929-α7 cells. Eighteen clonal L929-α7 cell lines survived expansion and were assayed for [^{125}I]-αBTX-binding. Cells were harvested following 5 days of induction with 1μM dexamethasone (this length of induction produces maximal nicotinic radioligand binding in the M10 cell line (Whiting *et al.*, 1991a) and cell membranes were incubated with 10nM [^{125}I]-αBTX in the presence or absence of 10mM carbamylcholine. However, no significant [^{125}I]-αBTX-binding could be detected in any of the eighteen L929-α7 clones.

The absence of specific [^{125}I]-αBTX-binding to the α7-transfected stable L929 cell lines was somewhat surprising since α7 homo-oligomers, when expressed in *Xenopus* oocytes, bind [^{125}I]-αBTX with high affinity; chick α7 K_d=1.6nM (Anand *et al.*, 1993b) and human α7 K_d=0.8nM (Peng *et al.*, 1994b). To check the effectiveness of the [^{125}I]-αBTX binding assay, the rat adrenal phaeochromocytoma cell line (PC12) which expresses endogenous αBTX-binding sites, and a mouse fibroblast 3T3 cell line stably expressing the mouse muscle $\alpha_2\beta\delta\varepsilon$ nAChR (B23ε cell line) (Green and Claudio, 1993) were used as positive controls . Clear specific [^{125}I]-αBTX binding could be detected in membrane preparations from both of these cell lines (data describing [^{125}I]-αBTX binding to the B23ε cell line is presented in Figure 3.3.2; a more detailed account of [^{125}I]-αBTX binding to the rat PC12 cell line is presented in Section 4.1).

PC12 cells and the B23ε cell line were used to optimize the conditions for [^{125}I]-αBTX binding, and adapt the technique for use with an automated Brandel Cell harvester which harvests and washes 36 samples simultaneously onto glass fibre filters. It was determined that lower concentrations of [^{125}I]-αBTX reduced non-specific binding without significantly affecting levels of specific binding to the α7 nAChR expressed in PC12 cells and the muscle nAChR expressed in the B23ε cell

line. Non-specific binding could also be reduced by the addition of 0.5% bovine serum albumin (BSA) to block non-specific protein interactions. Incubation of the glass fibre filter with 0.5% polyethylenemine, presumably to overcome non-specific charge interactions, and by using a glass fibre filter with a larger pore size (GF-A = 1.6μm compared with GF-B =1.0μm) also reduced non-specific binding levels.

Due to the absence of specific [^{125}]-αBTX binding in L929 cells stably transfected with pMSG-α7, an alternative stable expression vector, pSVK3, was used (see Figure 3.0.1). pSVK3 utilizes a simian virus SV40 early promoter that is constitutively active although expression of cloned gene products can be enhanced by the addition of sodium butyrate to the culture media (Sine and Claudio, 1991b) . A similar vector (pSV2) was used to generate the B23ε cell line stably transfected with the mouse muscle nAChR ($\alpha_2\beta\delta\varepsilon$) which expresses very high levels of [^{125}]-αBTX binding sites (Sine and Claudio, 1991b; Green and Claudio, 1993). The rat neuronal nAChR α7 subunit was subcloned into pSVK3 (Pharmacia) (in addition to the rat neuronal α9 subunit and rat muscle nAChR α, β, δ and ε subunits, see Figure 3.1.1). Mouse L929 cells and mouse fibroblast 3T3 cells in 10 cm dishes were transfected by lipofection for 7 hours with 6μg pSVK3-α7 plus 0.6μg pcDNA3neo (pcDNA3neo was included in the transfection mixture to provide the neomycin resistance gene as a selectable marker) and 36μl lipofectamine in 3.5mls Optimem™ (Gibco). Cells were left to recover for two days and then split 1:5 and 1:10 into culture media containing 0.8mg/ml G418. Untransfected cells died after 3-7 days in G418 selection and no live cells were visible after three weeks.

Cells transfected with pSVK3-α7 and 1/10th the amount of pcDNA3neo survived G418 selection and individual clones were visible after ~10 days in selection. The plates seeded at 1:5 were trypsinized and pooled 21 days following selection to generate polyclonal populations of stably transfected cells. These cells were split 1:3 and when two of these dishes were ~90% confluent they were incubated for 48 hours

with 10mM sodium butyrate to enhance expression of the cloned α7 gene (10mM sodium butyrate has been shown previously to increase surface expression of the mouse muscle nAChR (Sine and Claudio, 1991b). Cells were harvested and crude membrane preparations were assayed for [^{125}I]-αBTX-binding. Samples were incubated with 5nM[^{125}I]-αBTX in the presence or absence of 2.5mM carbamylcholine plus 2.5mM nicotine. No specific binding of [^{125}I]-αBTX could be detected in L929 or 3T3 cells stably transfected with pSVK3-α7.

3.2 Transient expression of α7 in HEK293 and COS7 cells

Since the pcDNA1neo-α7 construct had been used for the successful functional expression of αBTX-sensitive α7 homo-oligomers in *Xenopus* oocytes, this construct was used to transiently express the rat α7 subunit in human embryonic kidney fibroblast cells (HEK293) and the monkey kidney fibroblast cell line (COS7). The HEK293 cell line has been used previously for the successful functional expression of several ligand-gated ion channels (Pritchett *et al.*, 1988; Keinanen *et al.*, 1990; Hargreaves *et al.*, 1994) and COS7 cells have been used to successfully express the mouse muscle nAChR (Gu *et al.*, 1990; Gu *et al.*, 1991). The calcium phosphate transfection of HEK293 cells and COS7 cells was optimized using a β-galactosidase reporter construct under the control of the CMV promoter (pCMV-βgal) (Invitrogen). β-galactosidase catalyzes the hydrolysis of β-galactosides such as ONPG (*o*-nitrophenyl-β-D-galactopyranoside) which is cell permeable and forms a bright blue product. Transfection mixtures containing 20μg pCMV-βgal per 10cm dish routinely achieved the highest transfection efficiencies of both cell lines, with between 30% - 50% of cells turning blue. HEK293 and COS7 cells were transiently transfected by calcium phosphate transfection with pcDNA1neo-α7 (20μg per 10cm dish). However, no detectable specific binding of [^{125}I]-αBTX was observed in HEK293 or COS7 cells transiently transfected with pcDNA1neo-α7.

3.3 Transient expression of the rat muscle nAChR and homo-oligomeric serotonin 5-HT_3 receptor.

Due to the absence of detectable [^{125}I]-αBTX-binding to cell lines transfected with the rat α7 subunit, the rat muscle nAChR was transiently transfected into HEK293 cells to confirm the efficiency of the transfection and [^{125}I]-αBTX-binding techniques. The four rat muscle α, β, γ, and δ nAChR subunits (Witzemann *et al.*, 1990), were subcloned into pcDNA3neo (see Figures 3.0.1 and 3.1.1). pcDNA3neo is a modification of the pcDNA1neo plasmid and also contains the powerful cytomegalovirus promoter for efficient transient expression of cloned genes. The four rat muscle α, β, γ and δ nAChR subunits were transiently transfected into HEK293 cells in the molar ratio of α:β:γ:δ equivalent to 2:1:1:1. In contrast with results obtained following transient transfection of α7, high levels of surface [^{125}I]-αBTX-binding sites were detected in HEK293 cells transfected with the rat muscle receptor (Figure 3.3.1).

Rat muscle nAChRs expressed on the surface of intact HEK293 cells were analyzed by sucrose gradient centrifugation. Transfected cells were labelled with 5nM [^{125}I]-αBTX in their usual culture media for 1 hour at 37°C . The cells were washed, scraped from the dish and solubilized in lysis buffer containing 1% triton X-100. Solubilized samples were sedimented on a 5-20% sucrose gradient and sixteen fractions were carefully removed from the top of the gradient and analysed by γ-counting (Figure 3.3.2A). The peak of bound [^{125}I]-αBTX was typically detected in fractions 9 and 10 of the gradient, corresponding to a sedimentation coefficient of ~9S. A similar peak and ~9S sedimentation profile was obtained following [^{125}I]-αBTX-labelling of cell surface receptors expressed by the previously characterised B23ε cell line which stably expresses the mouse muscle nAChR $\alpha_2\beta\delta\varepsilon$ (Green and Claudio, 1993). Under identical conditions, the nAChR present in electric organ of *Torpedo* was sedimented on a 5-20% sucrose gradient and labelled with [^{125}I]-αBTX

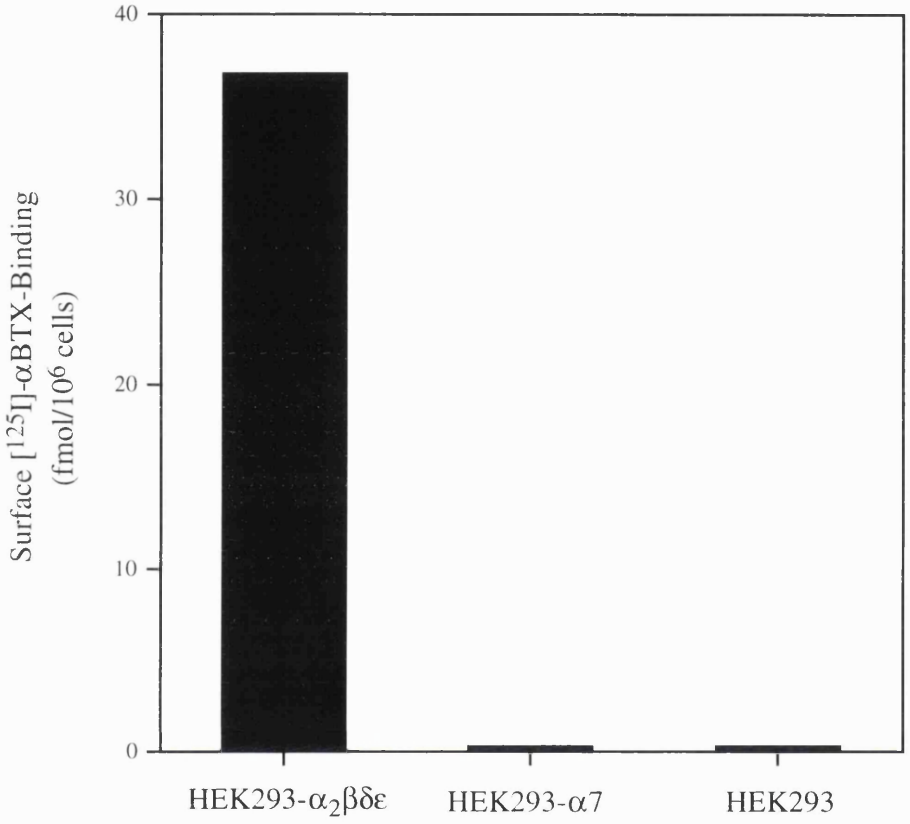

Figure 3.3.1. Specific surface [^{125}I]-αBTX-binding to transiently transfected HEK293 cells. HEK293 cells were transiently transfected with either the rat muscle nAChR subunits α, β, δ, ε in the molar ratio of 2:1:1:1 or the rat α7 subunit. Cells were transfected by calcium phosphate transfection and harvested 28 hours following transfection. Intact cells were incubated with 1nM [^{125}I]-αBTX in HBSS containing 0.5% BSA for 2 hours at room temperature. Samples were harvested onto GF-A glass fibre filters and washed rapidly five times. Non-specific binding, determined by the addition of 500μM nicotine plus 500μM carbamylcholine to triplicate samples, typically represents ~1.4 fmol [^{125}I]-αBTX per filtered sample and has been subtracted.

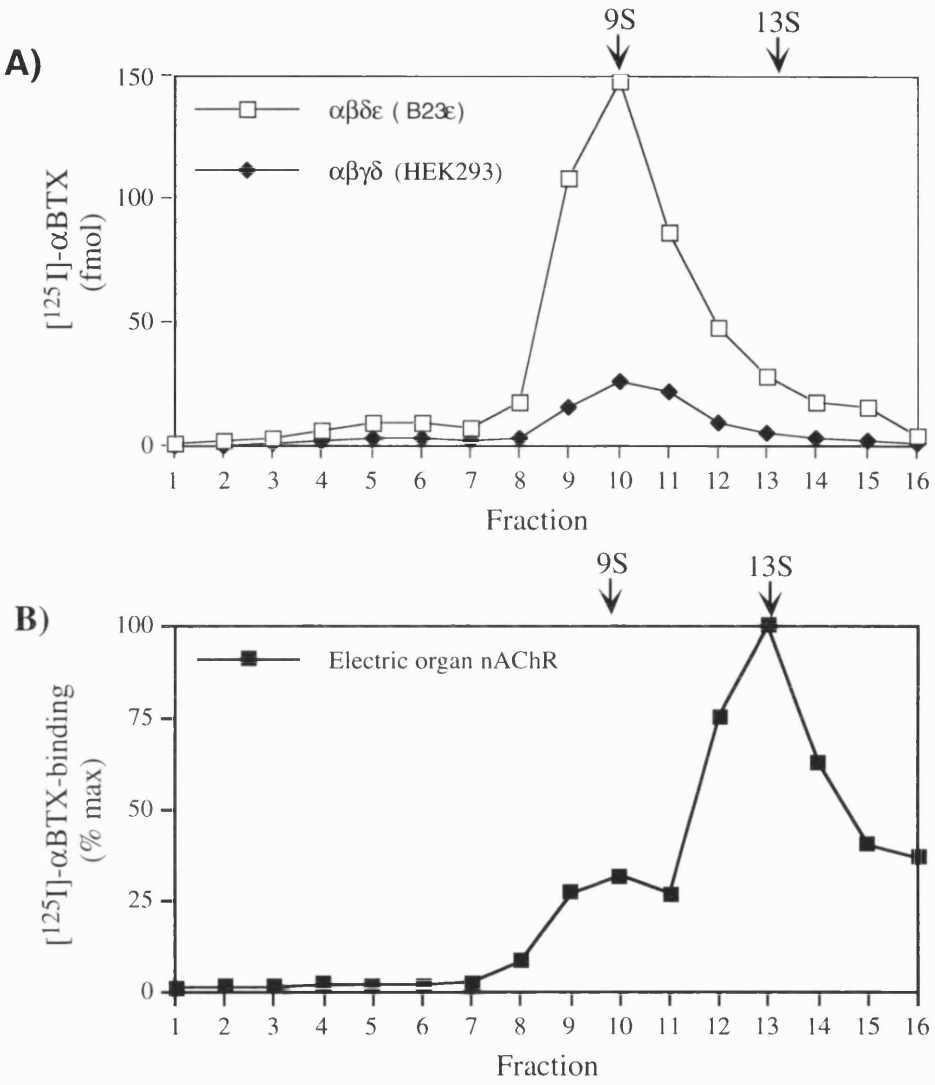

Figure 3.3.2. Sucrose gradient sedimentation of rat muscle and electric organ nAChR. **A)** Sucrose gradient profile of [^{125}I]-αBTX binding to the mouse muscle nAChR ($\alpha_2\beta\delta\varepsilon$) expressed in the B23ε cell line (Green and Claudio, 1993) and the rat muscle nAChR ($\alpha_2\beta\gamma\delta$) transiently expressed in HEK293 cells. Intact cells were labelled with [^{125}I]-αBTX, washed and solubilized in lysis buffer containing 1% Triton X-100. Soluble cell extracts were separated on a 5-20% sucrose gradient and 16 fractions were taken from the top of the gradient and counted in a γ-counter. Data points represent fmol [^{125}I]-αBTX per fraction for 1 x 10^6 cells loaded onto the gradient. **B)** Sucrose gradient profile of [^{125}I]-αBTX binding to electric organ nAChR of *Torpedo*. A solubilized extract of electric organ was separated by sucrose gradient centrifugation under identical conditions. Sixteen fractions removed from the top of the gradient were assayed for [^{125}I]-αBTX binding. The positions of the two peaks of αBTX-binding indicate the sedimentation coefficients of the pentameric nAChR monomer (9S) and disulphide linked dimer (13S), as shown.

(Figure 3.3.2B). The peaks corresponding to the pentameric monomer (9S) and dimer (13S) nAChR species of electric organ are indicated by arrows.

Since the rat muscle nAChR is a hetero-oligomer, it was necessary to establish whether the absence of [^{125}I]-αBTX-binding to cells transfected with the α7 subunit was due to the absence of specific machinery required for the assembly of homo-oligomeric ion channels. The mouse 5-HT$_3$ gene has been cloned from murine neuroblastoma NCB-20 cells and shows high homology to the nicotinic acetylcholine receptor subunits (Maricq *et al.*, 1991). The 5-HT$_3$ sequence exhibits 27% homology to the *Torpedo* α1 subunit and 30% homology to the neuronal α7 subunit (Uetz *et al.*, 1994). The 5-HT$_3$ gene shows particular homology to the neuronal α7 gene in the second putative hydrophobic transmembrane domain (Maricq *et al.*, 1991; Uetz *et al.*, 1994) and also forms a cation-conducting homo-oligomeric channel when expressed in *Xenopus* oocytes (Maricq *et al.*, 1991) and in HEK293 cells (Hargreaves *et al.*, 1994). Transient transfection of cloned 5-HT$_3$ under the control of a CMV promoter in the plasmid vector pCDM6 (pCDM6-5HT$_3$), resulted in the appearance of high-affinity ^{3}H-GR65630 binding sites (Figure 3.3.3A). Cell membranes were incubated with 1nM [^{3}H]-GR65630 in the presence or absence of 100μM 5-hydroxytryptamine to determine non-specific binding. GR65630 is a specific 5-HT$_3$ antagonist which has been shown to bind with high affinity to native and recombinant mouse 5-HT$_3$ receptors (K_d~0.2 nM) (Lummis and Martin, 1991; Green *et al.*, 1995).

Sucrose gradient sedimentation of HEK293 cells transiently transfected with pCDM6-5HT$_3$ were solubilized and sedimented on a 5%-20% sucrose gradient (Figure 3.3.3B). Sixteen fractions carefully removed from the top of the gradient were subjected to [^{3}H]-GR65630 radioligand binding. Gradient fractions were incubated with 1nM [^{3}H]-GR65630 for 2 hours at 4^{o}C. Samples were harvested using a Brandell harvester, washed four times, and filters were counted in a scintillation counter. A peak of [^{3}H]-GR65630 binding was observed in fraction 11 indicating

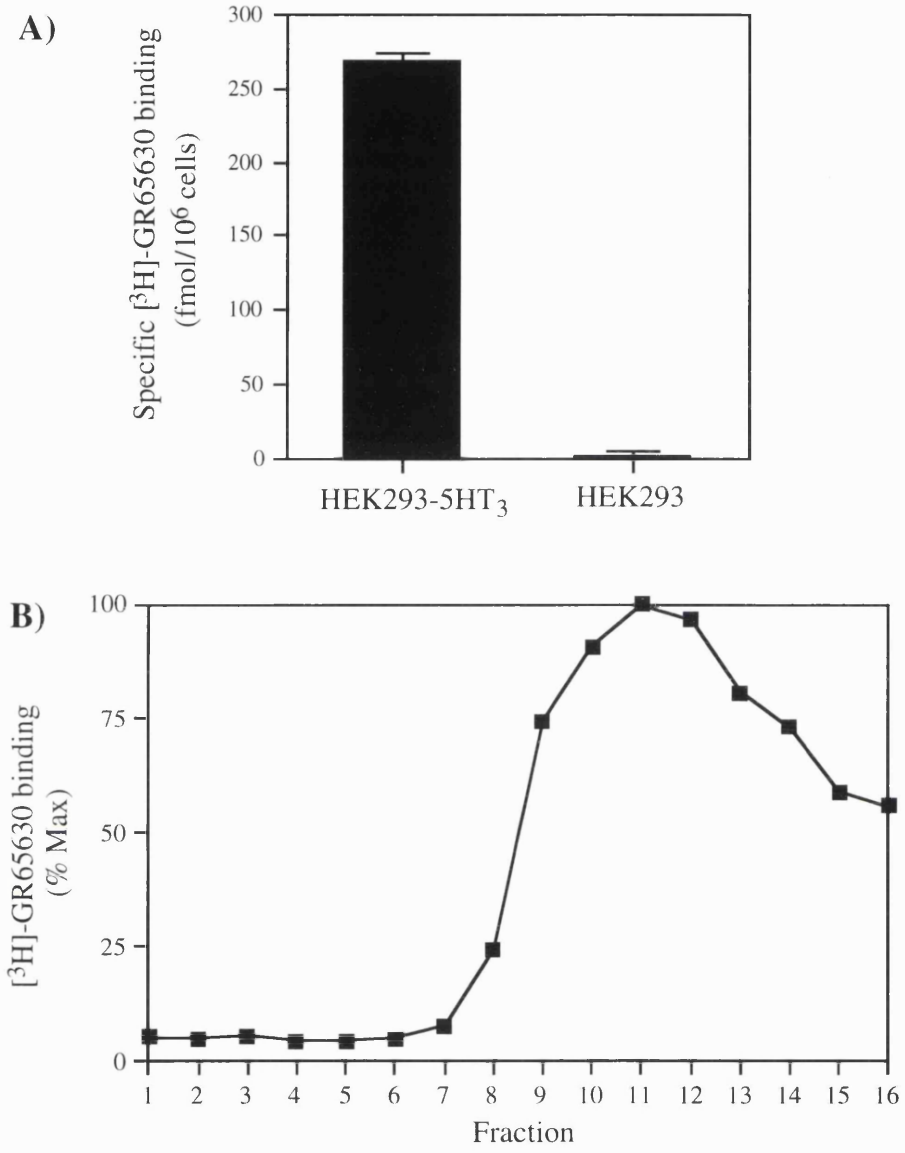

Figure 3.3.3. Specific [^{3}H]-GR65630 binding to HEK293 cells transiently transfected with the 5-HT$_3$ subunit. HEK293 cells were transiently transfected with pCDM6-5HT$_3$ using a standard calcium phosphate protocol and harvested ~30 hours following transfection. **A)** Cell membranes were incubated with 1nM [^{3}H]-GR65630 for 2 hours at 4^{o}C. Samples were harvested onto GF-B glass fibre filters and washed rapidly four times. Data points represent means of triplicate samples and non-specific binding determined by the addition of 100µM 5-hydroxytryptamine (5-HT) has been subtracted (typically 10-12 fmol [^{3}H]-GR65630 per filter sample). **B)** Solubilized cell samples were separated on a 5-20% sucrose gradient. 16 fractions were removed from the top of the gradient and incubated with 1nM [^{3}H]-GR65630 for 2 hours at 4^{o}C. Samples were harvested onto GF-B glass fibre filters and washed rapidly four times.

that the 5-HT_3 subunit efficiently oligomerizes into a complex which sediments with a similar buoyant density to that of the muscle nAChR. Given that the estimated molecular weight of the mouse 5-HT_3 subunit is ~56 kDa (Maricq *et al.*, 1991), the peak of [^{3}H]-GR65630 binding probably corresponds to the position of a pentameric 5-HT_3 receptor.

3.4 Functional expression of the rat muscle nAChR and homo-oligomeric serotonin 5-HT_3 receptor in HEK293 cells.

Fluorimetry experiments using the calcium-sensitive dye Fura-2 was used to determine whether the rat muscle nAChR and homo-oligomeric 5-HT_3 receptor transiently expressed in HEK293 cells were functional. The muscle nAChR is permeable to calcium with a permeability ratio P_{Ca}:P_{Na} of ~0.2 for skeletal muscle (Decker and Dani, 1990). The 5-HT_3 receptor is also permeable to calcium although high concentrations of calcium can attenuate 5-HT_3 function (Maricq *et al.*, 1991; Hargreaves *et al.*, 1994). Transiently transfected HEK293 cells were loaded with 4μM Fura-2 acetoxymethyl ester (Fura-2) (Molecular Probes), a cell-permeable ester of Fura 2, in Hank's buffered saline solution (HBSS). After loading, cells were washed and resuspended in a HEPES buffer containing high calcium and lacking in sodium ions. This buffer has been previously used to detect functional responses of the 5-HT_3 homo-oligomer expressed in HEK293 cells (Hargreaves *et al.*, 1994) and maximizes calcium entry into the cell following agonist-induced opening of the ion channel. Approximately 1 x 10^6 cells resuspended in 1 ml of '"high calcium" buffer are transferred to a stirred cuvette. Agonists are added directly to the cuvette with a micropipette . Intracellular calcium levels are calculated by quantitative ratiometric fluorescent measurements taken every 40ms. The excitation wavelength is alternated rapidly between 340nm and 380nm and emitted fluorescence is detected at 510nm. When Fura-2 binds free intracellular calcium, the fluorescence detected at 340nm increases and the fluorescence at 380nm decreases. Functional responses are

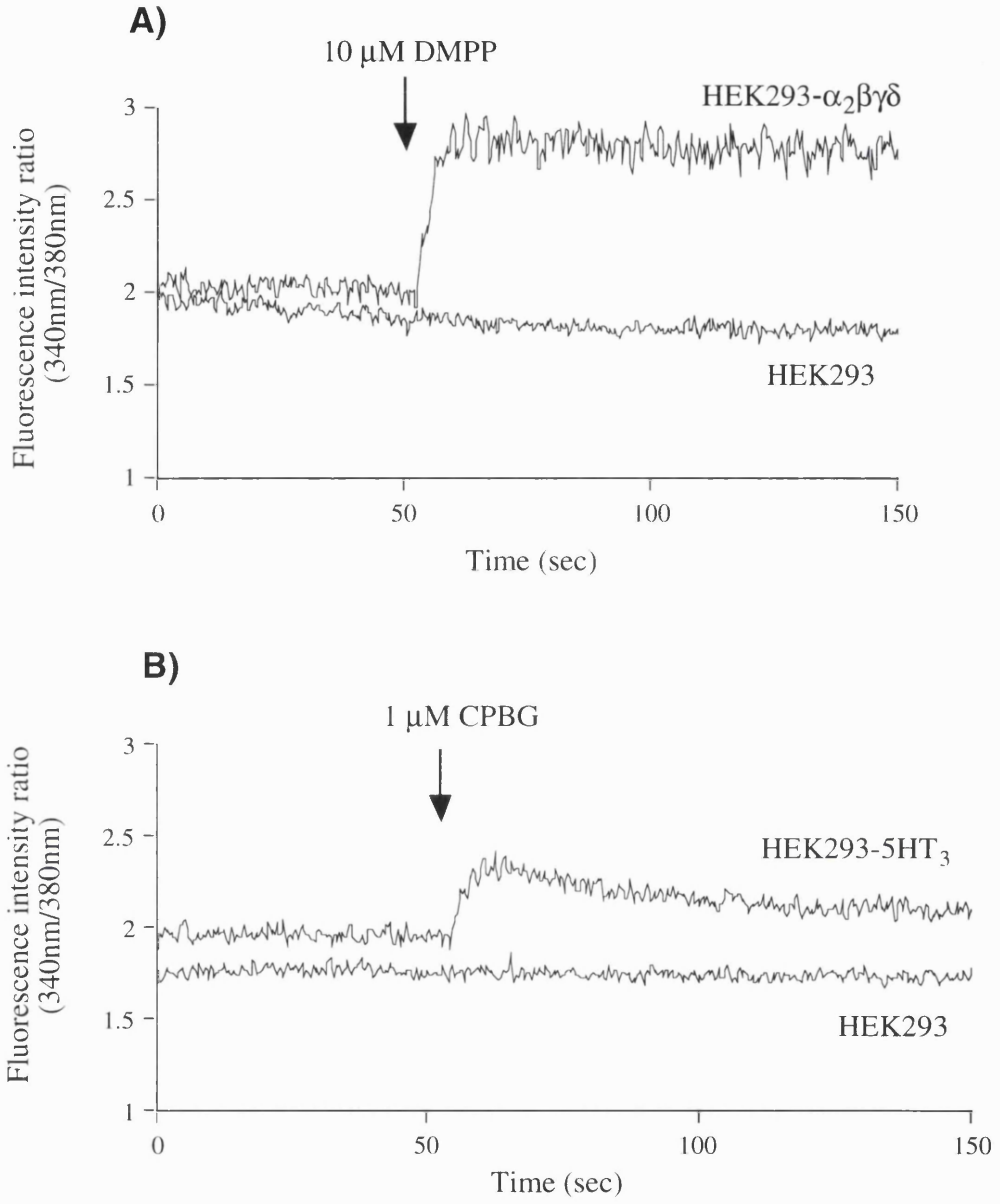

Figure 3.4.1. Functional expression of the muscle nAChR and the $5HT_3$ serotonin receptor in transiently transfected HEK293 cells. Tranfected cells were loaded with the calcium sensitive dye, Fura 2-AM. Approximately 1 x 10^6 cells were examined for an agonist induced influx of calcium, shown by quantitative ratiometric fluorescence measurement. Increases in intracellular calcium is observed as a sharp rise in the measured 340nm/380nm ratio. **A)** Functional response generated by HEK293 cells transfected with rat muscle nAChR α, β, γ and δ subunits following the application of 10 μM 1,1-dimethyl-4-phenylpiperazinium (DMPP). **B)** Elevations in intracellular calcium levels of HEK293 cells transfected with the serotonin $5HT_3$ receptor in response to 1μM 1-(*m*-chlorophenyl)biguanide (CPBG).

observed as a rapid increase in the 340/380nm ratio following the application of specific agonists and signifies calcium entry into the cell (Figure 3.4.1). Both the 5-HT_3 receptor and rat muscle nAChR were shown to form functional ion channels when transiently expressed in HEK293 cells (Figure 3.4.1). Clear elevations in intracellular calcium were observed upon application of the nicotinic agonistDMPP (1,1-dimethyl-4-phenylpiperazinium iodide) (10μM) to HEK293 cells transiently transfected with the rat muscle α, β, γ and δ (Figure 3.4.1A) subunits. Similarly 1μM CPBG (1-*m*-chlorophenyl biguanide), a specific 5-HT_3 receptor agonist, induced calcium influx in HEK293 cells transiently transfected with the 5-HT_3 subunit (Figure 3.4.1B) but not from untransfected cells. However, the addition of increasing concentrations of nicotinic agonists such as DMPP, nicotine or epibatidine (up to 5mM) failed to produced any functional responses from HEK293 cells transfected with α7, or from untransfected cells.

3.5 Expression of α7 in an insect cell line

At this time, other work in our laboratory involved the expression of mammalian and *Drosophila* nAChRs using an insect expression vector (pRmHa3) in a *Drosophila* Schneider S2 cell line (see Figure 3.0.1), both obtained from Dr. Thomas Bunch, University of Arizona. pRmHa3 (Bunch *et al.*, 1988) contains a strictly regulated metallothionein promoter which can be induced by the addition of heavy metal ions (6μM $CuSO_4$) to the culture media. *Drosophila* S2 cells stably transfected with neuronal nicotinic subunits, plus a selectable marker plasmid containing the gene encoding hygromycin resistance (pCOHygro, van der Straten *et al.*, 1989), were producing very high levels of nicotinic radioligand binding. Since amphibian oocytes are incubated at 18°C and mammalian cells are cultured at at 37°C, it was possible that the formation of αBTX-binding α7 nAChRs was temperature dependent. This proposal was investigated by expressing the α7 cDNA in *Drosophila* S2 cells, which are cultured at 25°C.

The rat neuronal α7 nAChR subunit and the mouse serotonin 5-HT_3 subunit were subcloned into the insect expression vector, pRmHa3 (the rat neuronal α9 and rat muscle α, β, δ and ε subunits were also subcloned into pRmHa3, see Figure 3.1.1). *Drosophila* S2 cells were transfected with either the α7 or 5-HT_3 subunits in addition to 1/10th the amount of pHygro using a calcium phosphate transfection protocol. Polyclonal populations of stably transfected cells were obtained following selection with 300μg/ml hygromycin. Polyclonal cell lines were induced for 24 hours with 6 μM $CuSO_4$ and radioligand binding performed on crude membrane preparations. Clear specific binding of [^{3}H]-GR65630 could be detected in the polyclonal S2-5HT_3 cell line (approximately 50 fmol/10^6 cells) but no specific [^{125}I]-αBTX (1-10 nM) or [^{3}H]-epibatidine (0.5-15 nM) binding could be detected with the polyclonal S2-α7 cell line.

3.6 Summary

Both stable and transient expression of the rat neuronal α7 nAChR subunit using a variety of expression systems failed to generate a cell line which expresses an α7 nAChR able to bind αBTX. This result is difficult to interpret since α7 readily forms functional homo-oligomeric channels which bind [^{125}I]-αBTX with high affinity when expressed in *Xenopus* oocytes. Several cultured cell lines transfected with the α7 cDNA are apparently unable to generate α7 nAChRs able to bind [^{125}I]-αBTX, but are capable of generating high levels of specific radioligand binding following transfection of the hetero-oligomeric rat muscle receptor or the homo-oligomeric serotonin 5-HT_3 receptor. Furthermore, the rat muscle nAChR and homo-oligomeric 5-HT_3 receptor transiently expressed in HEK293 cells were shown by fluorimetry experiments with the calcium-sensitive dye, Fura 2, to form functional ion channels permeable to calcium. No functional responses to nicotinic agonists could be detected in HEK293 cells transiently transfected with α7.

4.0 Cell-specific folding and assembly of the rat neuronal nAChR α7 subunit

4.1 Cell-specific folding of α7 determined by αBTX binding

The expression of the α7 subunit using a variety of expression vectors in several different cell lines indicates that α7 may not readily form homo-oligomeric nAChRs which bind αBTX in the cell lines tested. The reason for the absence of specific [^{125}I]-αBTX-binding to cell lines transfected with the α7 subunit is unclear. It is possible that oocytes are somehow permissive for α7 expression and the cell lines tested are not. In order to make this assumption it is necessary to verify the presence of α7 protein of the predicted size in cell lines which fail to generate [^{125}I]-αBTX-binding sites. The fate of the rat α7 nAChR subunit expressed in a variety of mammalian cells lines was examined by transient expression using the plasmid construct, pcDNA1neo-α7.

A panel of mammalian cell lines were transfected with pcDNA1neo-α7 that are not thought to express the α7 protein endogenously. Three epithelial cell lines (CHO, COS-7, HEK293) and four neuronal cell lines (NIE-115, NCB20, N2A, NG108-15), which did not possess specific [^{125}I]-α-BTX-binding sites, were examined (see Figure 4.1.1). For each cell line, two plates of cells were transfected overnight with pcDNA1neo-α7 using a lipofectamine transfection protocol (see materials and methods, Section 2.4). The following morning one plate of transfected cells was used in metabolic labelling experiments and the duplicate plate left for a further 24 hours and assayed for [^{125}I]-αBTX binding. Efficient expression of the α7 subunit protein in all cell lines was confirmed by metabolic labelling and immunoprecipitation with the monoclonal antibody mAb319 (for a summary of all antibodies used in this Section, see Figure 4.1.2). mAb319 was raised against a bacterially expressed fusion protein encoding the intracellular loop region of the chick α7 subunit and has been

Figure 4.1.1. The cell-specific binding of [^{125}I]-αBTX in mammalian cell lines transfected with the rat α7 nAChR subunit constructs.

Cell Line	Cell Type	Transfected with α7-pcDNA1			Transfected with α7FLAG-pcDNA3	
		Endogenous αBTX binding	α7 protein detected by mAb319 immptn.	[^{125}I]-αBTX Binding	Protein detected by mAbFLAG fluorescence	[^{125}I]-αBTX Binding
CHO	Hamster ovary	-	+++	-		
COS7	Monkey Kidney	-	+++	-		
HEK293	Human Kidney	-	+++	-	+++	-
NIE-115	Mouse neuroblastoma	-	++	-		
NCB20	Mouse Neuroblastoma/ hamster brain hybrid	-	++	-		
Neuro 2A	Mouse neuroblastoma	-	+++	-		
NG108-15	Mouse neuroblastoma/ rat glioma hybrid	-	+++	-		
PC12	Rat adrenal phaeo-chromocytoma	+		+++	+++	+++
SH-SY5Y	Human neuroblastoma	+	+++	+++	+++	+++

Immptn.; Immunoprecipitation

Figure 4.1.2. Properties of monoclonal and polyclonal antibodies used in this study.

Name	Species Immunized	Antigen	Isotype	Specificity
α7-specific				
mAb319[A]	Rat	Bacterial-fusion protein of chick α7 (amino acids 327-412)	IgG	Intracellular loop region of α7. Mapped to amino acid residues 365-384[B].
mAb306[A]	Mouse	Purified native and denatured chick and rat brain αBTX-binding receptor	IgG_1	Intracellular loop region of α7. Mapped to amino acid residues 380-400[B].
mAbOAR1a[C]	Mouse	Purified native αBTX-binding receptor of the chick optic lobe	IgG_1	Extracellular conformational epitope.
mAbOAR5a[C]	Mouse	Purified native αBTX-binding receptor of the chick optic lobe	IgG_1	Extracellular conformational epitope.
mAbOAR11b[C]	Mouse	Purified native αBTX-binding receptor of the chick optic lobe	IgG_1	Extracellular conformational epitope.
α8-specific				
mAb308[A]	Rat	Bacterial fusion protein of chick α8 (amino acids 293-435)	IgG_{2B}	Intracellular loop region of α8. Mapped to amino acid residues 323-342[B].
mAb305[A]	Rat	Purified native and denatured chick and rat brain αBTX-binding receptor	IgG_{2C}	Extracellular epitope of α8, absolutely conformationally dependent[B].
$5HT_3$-specific				
α-5HT3 sera[D]	Rabbit	Bacterial fusion protein containing the intracellular loop of $5HT_3$	IgG	Intracellular loop region of $5HT_3$.

[A] Schoepfer *et al*, 1990; [B] McLane *et al*, 1992; [C] Betz *et al*, 1984; [D] Turton *et al*, 1993.

used successfully for the immunoprecipitation of native α7 protein from chick and rat (Schoepfer *et al.*, 1990; Dominguez Del Toro *et al.*, 1994). Cells were metabolically labelled using a mixture of [^{35}S]-methionine and [^{35}S]-cysteine in serum-free culture media (lacking unlabelled methionine and cysteine). The cells were washed, and solubilized in lysis buffer containing 1% Triton X-100. Radiolabelled α7 protein was immunoprecipitated by incubation with mAb319 followed by Protein-G sepharose. A specific immunoprecipitated band of apparent molecular weight ~58 kDa was detected following SDS polyacrylamide gel electrophoresis (SDS-PAGE) of labelled samples from all α7- transfected cell lines, but not from untransfected cells (Figure 4.1.3). This apparent molecular weight is in close agreement with the estimated molecular weight of the α7 subunit immunoprecipitated from rat brain (~59 kDa) (Dominguez Del Toro *et al.*, 1994) and chick brain (~57 kDa) (Gotti *et al.*, 1992).

The difference in intensities of the immunoprecipitated α7 protein bands indicates, to some extent, the difference in transfection efficiency between the cell lines. Control transfections using the β-galactosidase reporter construct pCMV-βGal demonstrates that CHO, COS-7, HEK293, N2A and NG108 cell lines transfect with high efficiency (routinely at least 30-40% transfection efficiency), whereas NIE-115 and NCB20 cells exhibit lower transfection efficiencies (usually around 15-20% efficiency).

Each duplicate plate of transfected cells was harvested around 40 hours after transfection and cell membranes were incubated with 2.5nM [^{125}I]-αBTX in the presence or absence of 100μM methyllycaconitine (a potent antagonist of the α7 nAChR) to determine non-specific binding. Remarkably, despite the high levels of expression of α7 protein detected by immunoprecipitation with mAb319 from each of the transfected cell lines, no specific binding of the nicotinic antagonist [^{125}I]-αBTX could be detected in cells from duplicate plates (see Figure 4.1.1). These results would suggest that although these cell lines are synthesizing high levels of α7 subunit

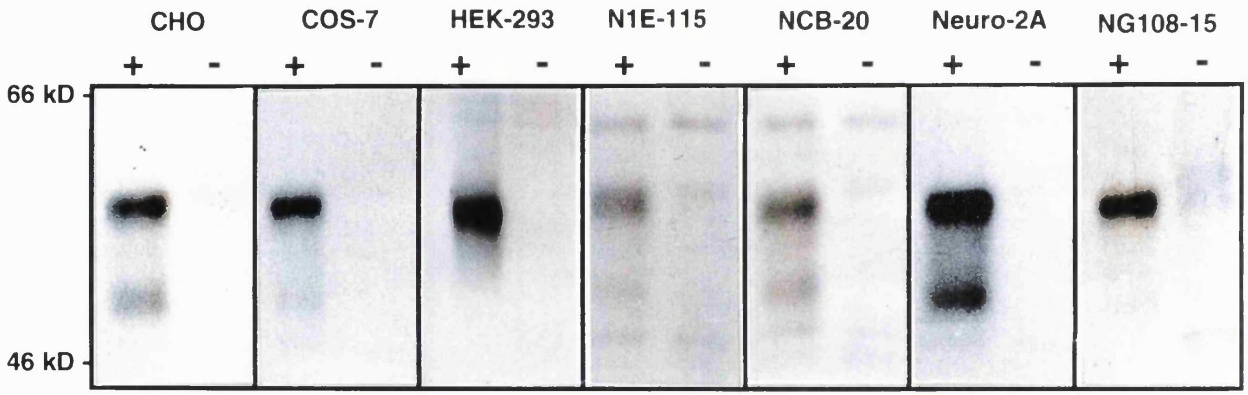

Figure 4.1.3. Immunoprecipitation of the α7 subunit with mAb319, an antibody which recognizes a linear epitope within the cytoplasmic loop region of α7. A panel of seven mammalian cell lines were transiently transfected with the pcDNA1neo-α7 construct by lipofection. Cells were metabolically labelled using a mixture of [^{35}S]-methionine and [^{35}S]-cysteine contained in serum-free DMEM for three hours and then incubated with complete DMEM for a further two hours. Cells were washed, solubilized and immunoprecipiated with mAb319 followed by protein-G sepharose. Sepharose pellets were washed and the immunoprecipitated protein samples were analyzed by SDS-PAGE. The gel was fixed, dried and exposed to X-ray film for 6-24 hours. A protein band of ~58 kDa, corresponding to the α7 subunit, was detected in α7-transfected cell lines (lanes marked +) but not in untransfected controls (lanes marked -). A lower molecular weight band of ~50 kDa, occasionally seen in some cell lines, is thought to be a proteolytic degradation product or a differently glycosylated α7 subunit species.

protein, it does not appear to be folded into a conformation which is able to bind α-bungarotoxin.

Several cultured mammalian neuronal cell lines known to express nicotinic AChR subunits have been shown to express α7 subunit mRNA and also possess αBTX-binding sites (Rogers *et al.*, 1992; Lukas *et al.*, 1993; Henderson *et al.*, 1994; Peng *et al.*, 1994a) (Figure 4.1.1). Isolates of two of these cell lines, the rat adrenal phaeochromocytoma (PC12) and the human neuroblastoma (SH-SY5Y) cell lines were shown in our laboratory to express only low levels of surface [^{125}I]-αBTX binding sites, approximately 20-40 fmol/mg membrane protein. Both cell lines were transfected with the rat pcDNA1neo-α7 construct and due to the low transfection efficiency of these cell lines, stably transfected cells were obtained through selection with G418. Polyclonal populations of cells stably transfected with pcDNA1neo-α7 were then subjected to radioligand binding analysis.

Both PC12 and SH-SY5Y polyclonal stable cell lines transfected with α7-pcDNA1neo exhibited marked elevations in the levels of surface [^{125}I]-αBTX-binding sites. In both cell lines there was a 7- to 10-fold increase in surface [^{125}I]-αBTX-binding compared with untransfected cells (Figure 4.1.4). Polyclonal stable cell lines of PC-12 and SH-SY5Y cells mock transfected with the pcDNA3neo plasmid vector were also generated, but showed no elevation in αBTX binding. Increases in surface [^{125}I]-αBTX-binding (typically between 0.5 - 1 fold increase) could also be detected in SH-SY5Y cells transiently transfected with the pcDNA1neo-α7 construct, compared with untransfected cells.

Twelve clonal SH-SY5Y cell lines stably transfected with pcDNA1neo-α7 were isolated and screened for [^{125}I]-αBTX-binding. A clonal cell line was obtained which expressed a ~20-fold increase in specific [^{125}I]-αBTX-binding over untransfected cells and was used for further studies (SH-SY5Y-α7#7). Saturation

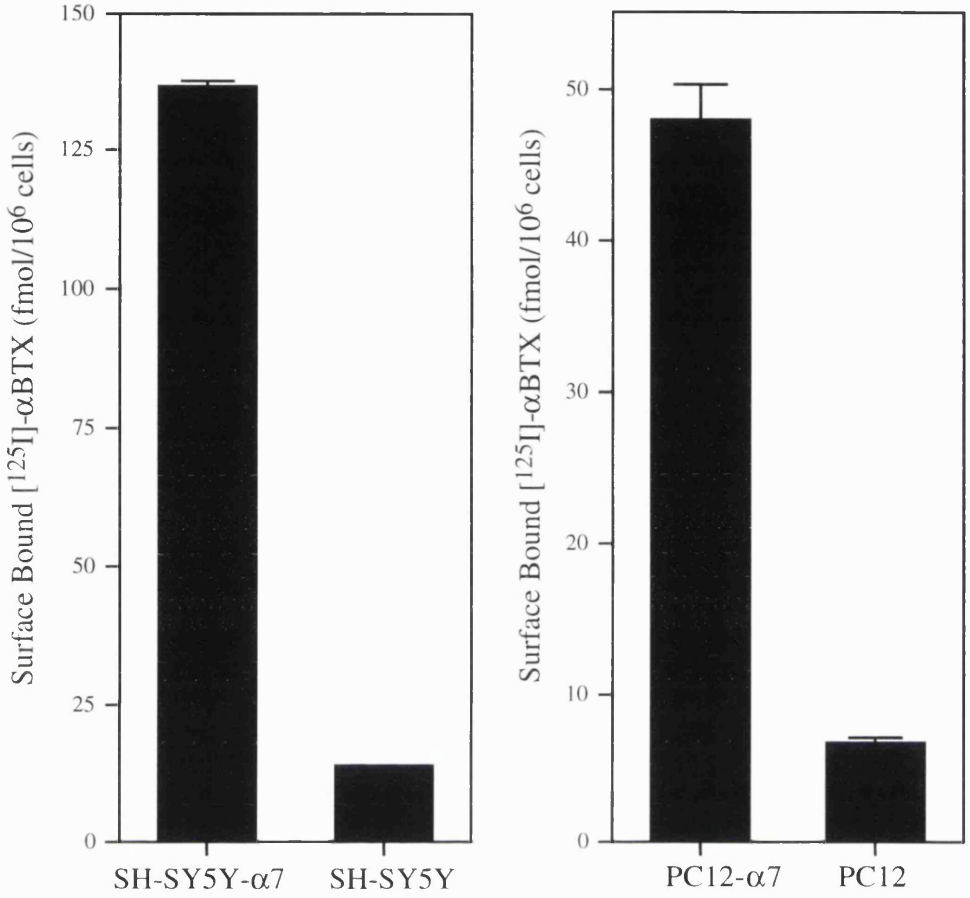

Figure 4.1.4. Specific surface [^{125}I]-αBTX-binding to untransfected and α7-transfected SH-SY5Y and PC12 cell lines. SH-SY5Y and PC12 cells were transfected with pcDNA1neo-α7 and subjected to selection with 1 mg/ml G418. Cells surviving selection were pooled to generate polyclonal populations of stably transfected cells. Intact cells were labelled with 1nM [^{125}I]-αBTX in HBSS containing 0.5% BSA. Samples were harvested into GF-A glass fibre filters and washed rapidly five times. Data points were obtained from the mean of triplicate samples. Non-specific binding was determined by the addition of 50μM methyllycaconitine (MLA) and has been subtracted (and typically represents 1.2-1.5 fmol [^{125}I]-αBTX per filtered sample). **A)** Surface [^{125}I]-αBTX-binding to polyclonal SH-SY5Y-α7 cells and untransfected SH-SY5Y controls. **B)** Surface [^{125}I]-αBTX-binding to polyclonal PC12-α7 cells and untransfected PC12 controls.

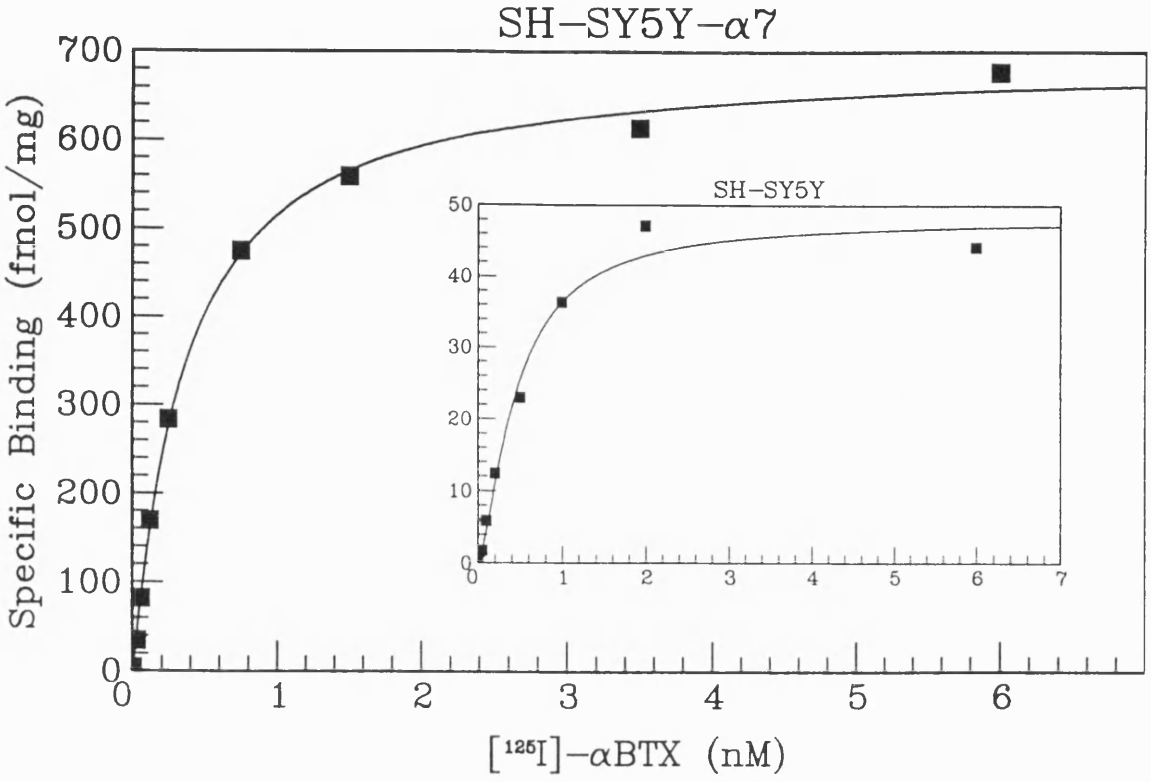

Figure 4.1.5. Saturation binding of [^{125}I]-αBTX to the transfected clonal SH-SY5Y-α7#7 cell line and to untransfected SH-SY5Y cells. Specific binding of [^{125}I]-αBTX to cell membrane preparations from SH-SY5Y-α7#7 (**main figure**) and to untransfected SHSY5Ycells (**inset**) is shown. Non-specific binding, determined by the addition of 100μM methyllycaconitine, has been subtracted. Data points are the average of duplicate samples and the data are typical of three separate determinations that gave mean K_D values of 0.7 ± 0.1nM and 0.6 ± 0.3 nM for the transfected and untransfected SH-SY5Y cell lines, respectively. Maximum specific binding (B_{max}) values were 738 ± 35 fmol/mg of membrane protein for transfected SH-SY5Y-α7#7 cells and 45±9 fmol/mg of membrane protein for untransfected SH-SY5Y cells. The calculated Hill coefficients were ~ 1.1.

binding to membrane preparations of SH-SY5Y-α7#7 and untransfected SH-SY5Y cells (Figure 4.1.5) revealed that both cell lines bound [^{125}I]-αBTX with high affinity (K_d = 0.7 ± 0.1 nM for the clonal SH-SY5Y-α7#7 cell line, and K_d = 0.6 ± 0.3 nM for untransfected SH-SY5Y cells) in good agreement with the estimated affinity of [^{125}I]-αBTX for the human α7 receptor expressed endogenously in SHSY5Y cells, K_d = 1.06 nM (Peng *et al.*, 1994b). The mean B_{max} from three determinations for [^{125}I]-αBTX-binding to SH-SY5Y-α7#7 cells was 738 ± 35 fmol/mg protein and 45 ± 9 fmol/mg protein for untransfected cells (Figure 4.1.5). For both cells lines, analysis of the saturation binding data calculated the Hill coefficient to be 1.1 which does not indicate co-operative binding of [^{125}I]-αBTX to the α7 nAChR. This correlates with results generated from functional analysis of SH-SY5Y cells which state the average Hill coefficient for all ligands tested to be n_H = 0.91 ± 0.13 (range 0.46-1.1) (Peng *et al.*, 1994b).

4.2 Misfolding of α7 confirmed by conformation-dependent antibodies.

The absence of αBTX-binding in several mammalian cell lines shown to express high levels of α7 protein implies that α7 is misfolded. This proposal was supported by evidence from monoclonal antibodies raised against native α7 receptor and which recognise conformational extracellular epitopes. mAbOAR1, mABOAR5a and mAbOAR11b were raised against native α7 receptor protein purified from the chick optic lobe (see Table 4.1.2) (Betz and Pfeiffer, 1984). These three antibodies have been shown to bind to the extracellular domain of the α7 receptor and have also been shown to cross-react with the native rat αBTX-binding receptor expressed in PC12 cells (Betz and Pfeiffer, 1984).

HEK293 cells transiently transfected with pcDNA1neo-α7 and the stably transfected SH-SY5Y-α7#7 cell line were metabolically labelled, solubilized and immunoprecipitated with either mAb319 which recognises a linear intracellular

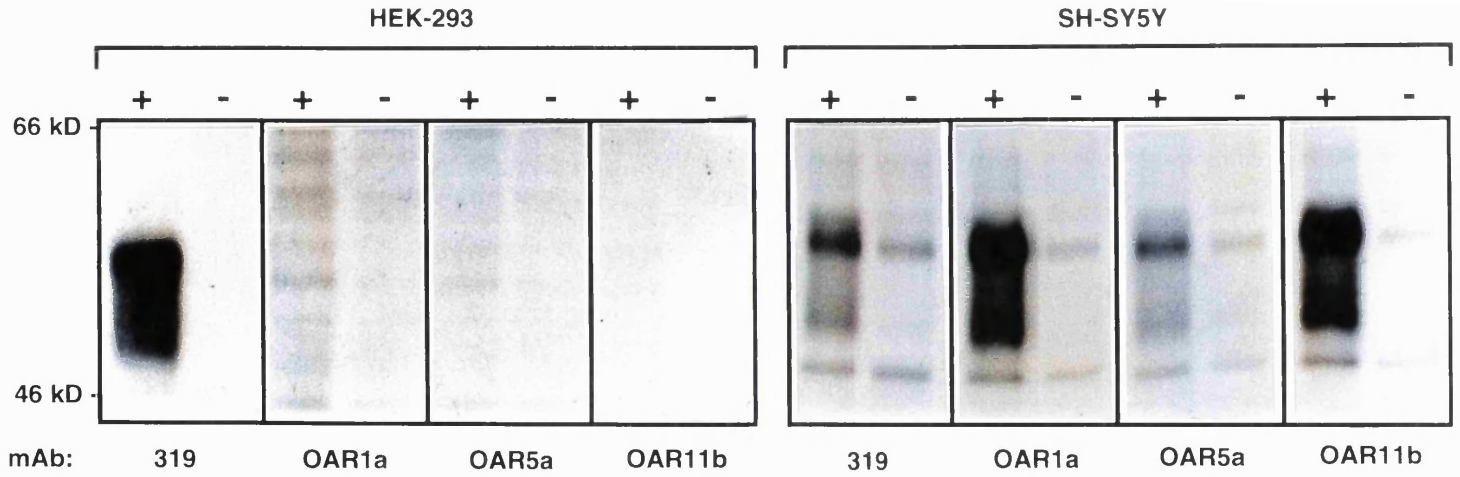

Figure 4.2.1. Immunoprecipitation of the α7 subunit with mAbs 319, OAR1a, OAR5a and OAR11b. Transiently transfected HEK293-α7 cells and the clonal SH-SY5Y-α7#7 stable cell line were metabolically labelled using a mixture of [^{35}S]-methionine and [^{35}S]-cysteine. Cells were washed, solubilized and immunoprecipiated with each of the four monoclonal antibodies followed by protein-G sepharose. Immunoprecipitated protein samples were analyzed by SDS-PAGE and autoradiography. Cell samples transfected with α7 are marked (+), untransfected cells are marked (-). Despite being able to detect the ~58 kDa α7 protein in transfected HEK293 cells with mAb319, the α7 subunit could not be immunoprecipiated from this cell line by three mAbs that recognize conformation-dependent epitopes on α7 (OAR1a, OAR5a and OAR11b). In contrast, all four antibodies were able to immunoprecipitate α7 from the SH-SY5Y-α7#7 stable cell line. A~58 kDa was also detected in untransfected SH-SY5Y cells and presumably corresponds to α7 protein expressed endogenously in this cell line. A lower molecular weight band of ~50 kDa is thought to be a proteolytic degradation product or a differently glycosylated α7 subunit species.

epitope of the α7 subunit, or with each of the three mAbOAR1, mAbOAR5a or mAbOAR11b antibodies which recognise conformational epitopes within the extracellular domain of the α7 receptor (Figure 4.2.1). mAb319 readily immunoprecipitated a ~58 kDa protein band corresponding to the α7 subunit from transfected HEK293-α7 cells, but not from untransfected controls. In contrast, the three antibodies which recognise conformational extracellular epitopes were unable to immunoprecipitate metabolically labelled α7 protein from identical solubilized samples of transfected HEK293-α7 cells. However, all four antibodies were able to immunoprecipitate α7 protein expressed in SHSY5Y-α7#7 and untransfected SHSY5Y cells (Figure 4.2.1).

The failure of the three antibodies which recognise the extracellular domain of native α7 nAChR to immunoprecipitate α7 protein expressed in transiently transfected HEK293-α7 cells demonstrates that the α7 protein expressed in HEK293 cells is incorrectly folded. Although immunoprecipitation with mAb319 confirms the presence of high levels of α7 protein expressed HEK293-α7 cells, it is not folded into a conformation required for αBTX-binding and nor does it form the recognition epitopes for several monoclonal antibodies which recognise the extracellular domain of correctly folded native α7 receptor.

Immunofluorescent microscopy of transfected cell lines supports the proposal that α7 misfolds in transfected HEK293-α7 cells and is not recognized by conformation-dependent antibodies. Surface staining of SH-SY5Y-α7#7 cells with mAbOAR1, mABOAR5a or mAbOAR11b followed by a rhodamine-conjugated secondary antibody reveals a very bright specific immunofluorescent staining pattern (Figure 4.2.2A). This immunofluorescent staining pattern was not detected in untransfected SH-SY5Y cells stained under identical conditions (Figure 4.2.2B). The absence of positive staining with mAbOAR1, mABOAR5a or mAbOAR11b in untransfected SH-SY5Y cells (despite endogenous α7 expression) indicates limitations in the

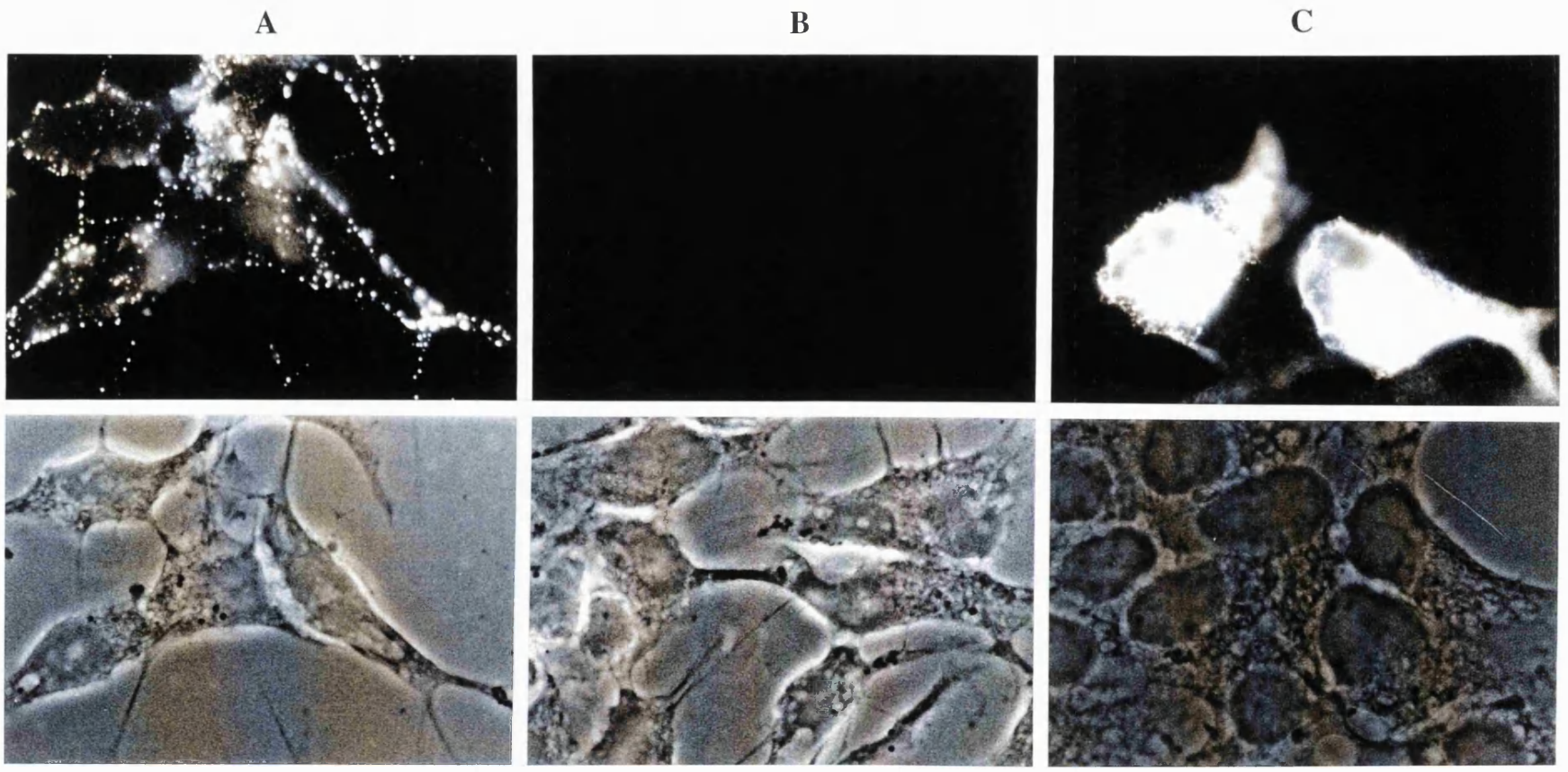

Figure 4.2.2. Immunofluorescent staining of the α7 subunit in transfected cell lines. Bright surface staining of α7 nAChRs expressed on intact cells can be seen in SH-SY5Y-α7#7 stably transfected cells (**A**) but not in untransfected SH-SY5Y cells (**B**) by labelling with mAbOAR11b, which recognizes a conformation-dependent extracellular epitope of α7, followed by a rhodamine-conjugated secondary antibody. No staining with mAbOAR11b could be detected in HEK293 cells transiently transfected with α7 (data not shown). However, bright intracellular staining could be detected in transfected HEK293-α7 cells by labelling with mAb319, which recognizes a linear epitope of α7, followed by a fluorescein-conjugated secondary antibody (**C**).

sensitivity of immunofluorescent techniques and also demonstrates the significant upregulation of surface α7 nAChRs in the stably transfected SH-SY5Y-α7#7 cell line. The staining pattern observed when live SH-SY5Y-α7#7 cells are incubated with mAbOAR1, 5a or 11b (followed by washing, fixation and incubation with a rhodamine-conjugated secondary antibody) has a clustered appearance. This clustered staining pattern is probably due to antibody cross-linking of surface nAChRs and closely resembles the microclustered staining pattern observed when live mouse L-cells stably expressing the *Torpedo* nAChR are labelled with mAb35 (which recognises *Torpedo* α 1), followed by a fluorescein-conjugated secondary antibody (Hartman *et al.*, 1991).

No specific staining of transfected HEK293-α7 cells could be detected following surface or intracellular staining with mAbOAR1, mABOAR5a or mAbOAR11b (data not shown) despite observing strong intracellular staining of α7 protein with mAb319 on a duplicate coverslip (Figure 4.2.2C).

4.3 Analysis of α7 oligomerization in transfected cell lines by sucrose gradient centrifugation.

The α7 nAChRs expressed at the cell surface of transfected SH-SY5Y-α7#7 and PC12-α7 cells were analyzed by sucrose gradient centrifugation (Figure 4.3.1). Cell surface receptors of intact SH-SY5Y-α7#7 and PC12-α7 cells were labelled with [^{125}I]-αBTX, washed and solubilized. Soluble cell extracts containing [^{125}I]-αBTX-labelled α7 nAChRs were sedimented on a 5%-20% sucrose gradient under identical conditions used previously to resolve the pentameric muscle-type and electric organ nAChRs (see Figure 3.3.2). Sixteen fractions were carefully removed from the top of each gradient and analysed by γ-counting. For both the SHSY5Y-α7#7 and PC12-α7 cell lines, a significant upregulation of bound [^{125}I]-αBTX is detected in the peak fractions of α7-transfected cell lines compared with untransfected controls (see

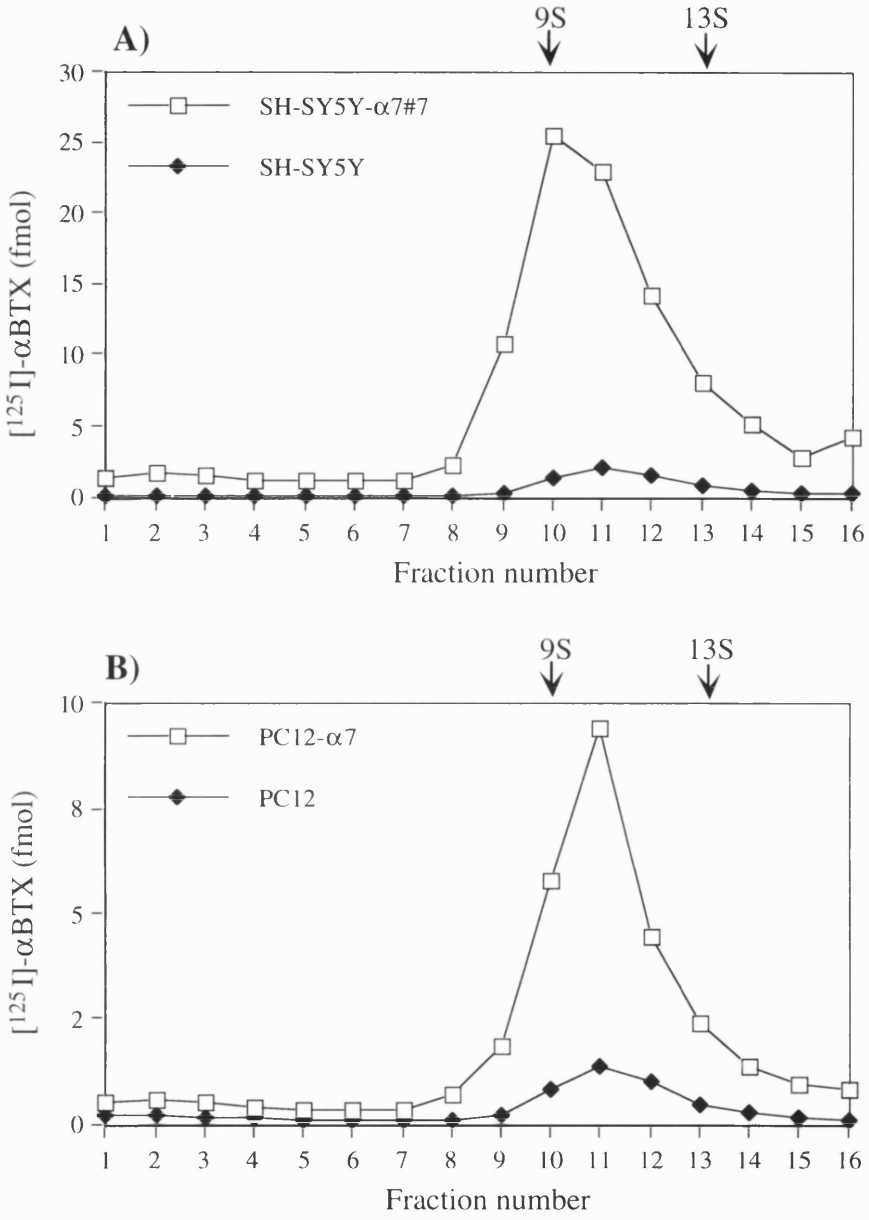

Figure 4.3.1. Sucrose gradient sedimentation of [^{125}I]-αBTX binding to untransfected and transfected SH-SH5Y-α7#7 and PC12-α7 cell lines. Intact cells were labelled with 5nM [^{125}I]-αBTX and washed to remove unbound toxin. Cells were solubilized in lysis buffer containing 1% triton X-100, and soluble extracts were gently layered onto a linear 5%-20% sucrose gradient. Following centrifugation, 16 fractions of 320µl were collected from the top of the gradient and counted in a γ-counter. **A)** Sucrose gradient profile of [^{125}I]-αBTX binding to SH-SH5Y-α7#7 and untransfected SH-SY5Y cells. **B)** Sucrose gradient profile of [^{125}I]-αBTX binding to PC12-α7 and untransfected PC12 cells. Data points represent fmol [^{125}I]-αBTX bound in each fraction per 1 x 10^6 cells loaded onto the gradient. The positions of the electric organ nAChR pentameric monomer (9S) and dimer (13S) are shown.

Figure 4.3.1). The muscle and electric organ nAChR labelled with [^{125}I]-αBTX typically sediments in fraction 10 of a 5%-20% sucrose gradient and is known to sediment with a buoyant density of 9S (Reynolds and Karlin, 1978; Sine and Claudio, 1991b). For transfected and untransfected PC12 and SH-SY5Y cell lines, the peak of bound [^{125}I]-αBTX was reproducibly detected in fractions 10 and 11 of the gradient which corresponds to a sedimentation coefficient slightly greater than 9S. These results are in close agreement with the 10S sedimentation coefficient obtained for native chick brain α7 nAChRs, and the chick α7 homo-oligomer expressed in *Xenopus* oocytes (Anand *et al.*, 1993b).

The α7 nAChR appears to have a slightly greater buoyant density compared with the muscle receptor (M_r~260kDa) which is possibly due to the binding of additional αBTX molecules (M_r~8.9kDa) and/or due to the larger size of the α7 subunit, estimated to be ~58 kDa. The sucrose gradient profiles describe a sharp peak of [^{125}I]-αBTX-binding at a position in the gradient corresponding to the location of the pentameric nAChR, which suggests that [^{125}I]-αBTX binds only to fully assembled receptor and not to individual subunits or assembly intermediates, consistent with reports from α7 expressed in *Xenopus* oocytes (Anand *et al.*, 1993b).

Due to the absence of αBTX-binding to α7-transfected HEK293 cells, it was necessary to study the oligomerization of α7 subunits in this cell line by analysis of the distribution of metabolically labelled α7 protein. To compare the sucrose gradient profiles of the α7 subunit expressed in HEK293 cells and in SHSY5Y-α7#7 cells, transfected cells were metabolically labelled and solubilized extracts separated on a 5%-20% sucrose gradient as before. Following centrifugation, α7 protein was immunoprecipitated from gradient fractions with mAb319 and protein-G sepharose.

The sixteen immunoprecipitated samples were separated by SDS-PAGE and the sedimentation profile generated by plotting the relative intensities of the radiolabelled

Figure 4.3.2. Sucrose gradient centrifugation profiles of immunoprecipitated α7 protein from stably transfected SH-SY5Y-α7#7 (**A**) and transiently transfected HEK293-α7 (**B**) cells. Cells were metabolically labelled, solubilized in lysis buffer containing 1% Triton X-100, and sedimented by sucrose gradient centrifugation. Sixteen fractions of 320μl were collected from the top of the gradient. The α7 subunit was immunoprecipiated from individual gradient fractions with mAb319 followed by protein-G-sepharose. Sepharose pellets were washed and immunoprecipitated protein samples were analyzed by SDS-PAGE. The intensity of the ~58 kDa protein was determined by scanning laser densitometry. The profile of α7 distribution in the gradient fractions is plotted as a percentage of the maximum band intensity.

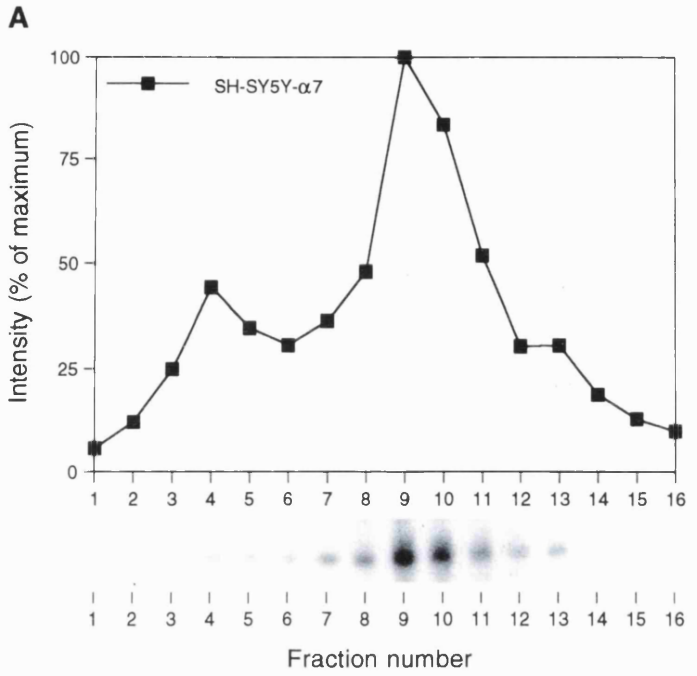
A
SH-SY5Y-α7
Intensity (% of maximum)
100
75
50
25
0
1 2 3 4 5 6 7 8 9 10 11 12 13 14 15 16
Fraction number

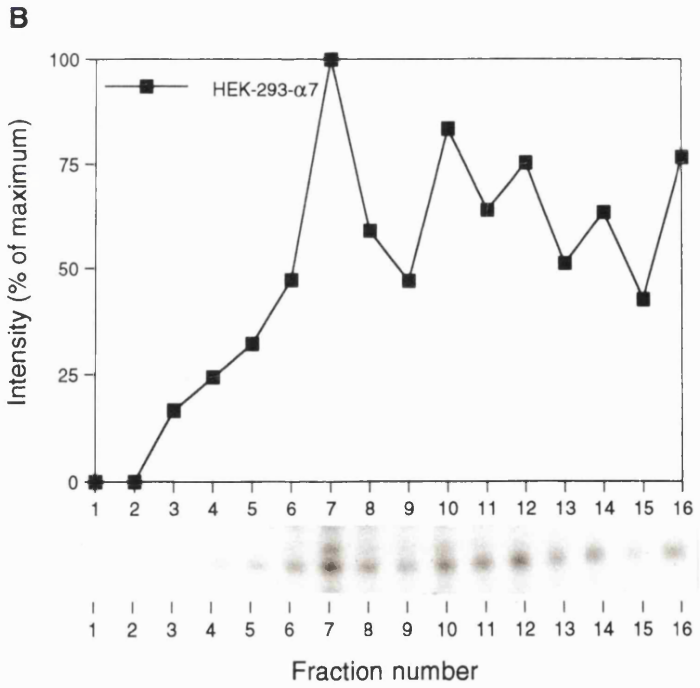
B
HEK-293-α7
Intensity (% of maximum)
100
75
50
25
0
1 2 3 4 5 6 7 8 9 10 11 12 13 14 15 16
Fraction number

α7 protein bands determined by densitometric analysis (Figure 4.3.2). Immunoprecipitation of labelled α7 protein from SHSY5Y-α7#7 cells revealed that the major peak of α7 protein co-migrated with the previously observed ~10S peak of [^{125}I]-αBTX-binding in this cell line (Figures 4.3.2A and see also Figure 4.3.1A). In addition a minor, shallow peak, of α7 protein could be detected in fraction 4 of the gradient which presumably corresponds to unassembled or partially assembled α7 subunits which do not bind αBTX with high affinity.

In contrast, immunoprecipitation results from a duplicate sucrose gradient containing solubilized extract of transfected HEK293-α7 cells revealed that the α7 protein in this cell line was broadly distributed throughout the entire gradient and probably represents a mixture of assembled or aggregated subunit complexes of varying sizes (Figure 4.3.2B). Gradient profiles of α7 expressed in HEK293 cells were repeated several times with some experiments producing high levels of large molecular weight α7 protein complexes sedimenting in the lowest fractions near the bottom of the gradient. The absence of a large peak of unassembled α7 protein indicates that the α7 subunit does form complexes with other α7 subunits in HEK293 cells. However, the high molecular weight complexes observed in most gradients suggest that α7 may form non-specific aggregates in this cell line, perhaps as a result of incorrect folding.

4.4 Discrimination between endogenous α7 and recombinant α7 expressed in transfected PC12 and SH-SY5Y cells.

Despite the upregulation of [^{125}I]-αBTX-binding in polyclonal and clonal PC12 and SHSY5Y cell lines transfected with α7 (and the absence of any such upregulation in mock transfected cells), it was important to discriminate between endogenous α7 expression levels and αBTX-binding generated by expression of recombinant rat α7. To distinguish between these two species of α7 nAChR in transfected neuronal cell lines, an "epitope-tag" was introduced into the recombinant rat α7 gene by site-

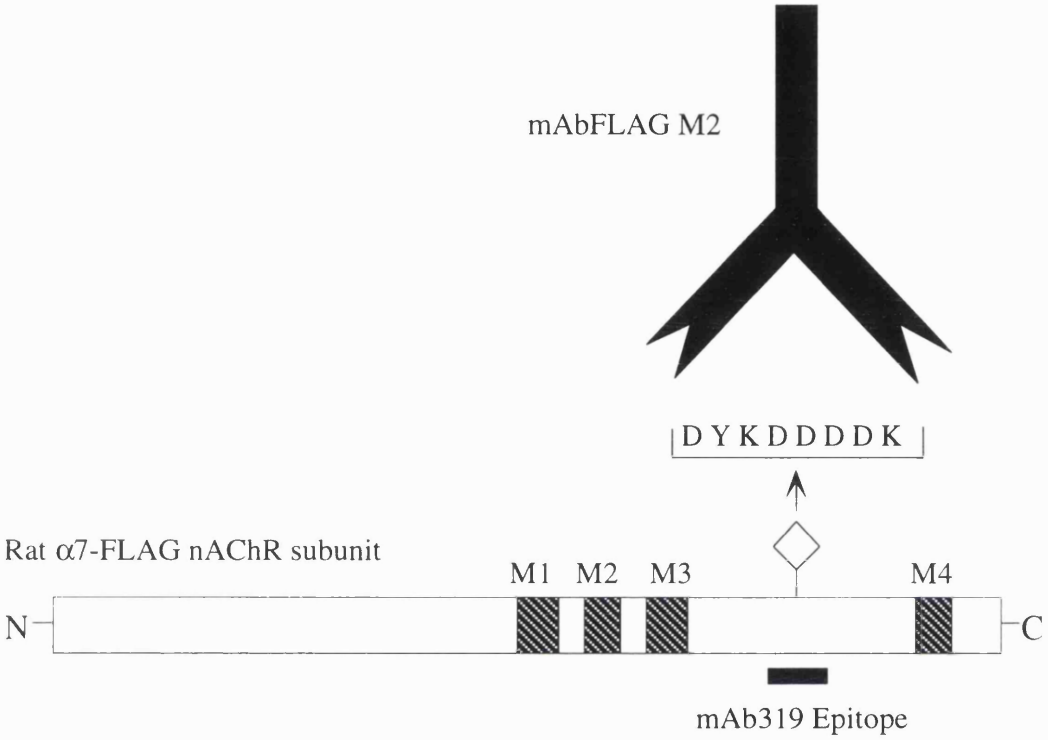

FIGURE 4.4.1. Schematic diagram of the rat α7-FLAG nAChR subunit construct. An eight amino acid epitope tag, the FLAG-tag octopeptide, was introduced by site-directed mutagenesis into the cytoplasmic loop region of the α7 cDNA between transmembrane domains M3 and M4 at a restriction enzyme *Stu*I site. The eight amino acid epitope (Asp-Tyr-Lys-Asp-Asp-Asp-Asp-Lys) is recognised by the monoclonal antibody mAbFLAG M2. The FLAG-tag sequence is inserted within the region identified as forming the recognition epitope for mAb319 (McLane *et al.*, 1992).

directed mutagenesis (Figure 4.4.1). An eight amino acid epitope tag sequence (D-Y-K-D-D-D-D-K), known as the "FLAG-tag", was inserted into the presumed intracellular loop domain of α7 between transmembrane domains M3 and M4. This FLAG-tag sequence forms an epitope recognised by the monoclonal antibody mAbFLAG (Hopp *et al.*, 1988). The recognition site for mAb319 has been mapped to a 20 amino acid segment (amino acids 365-384) within the α7 subunit (McLane *et al.*, 1992). The site at which the FLAG-tag sequence was inserted was within this region and it was predicted that in the process of generating a unique epitope in the α7-FLAG construct, the recognition site for mAb319 would be disrupted.

The pcDNA3-α7FLAG construct was transfected into PC12 and SHSY5Y cells which were then subjected to selection with G418 to generate the polyclonal stable cell lines PC12-α7FLAG and SHSY5Y-α7FLAG, respectively. In accordance with results generated with pcDNA1neo-α7, a significant 8-10 fold upregulation in surface [^{125}I]-αBTX-binding sites was observed in PC12-α7FLAG and SHSY5Y-α7FLAG cell lines compared with untransfected controls (see Figures 4.4.2 and 4.4.3). Sucrose gradient sedimentation of solubilized extracts from both polyclonal cell lines revealed a peak of bound [^{125}I]-αBTX in fractions 10 and 11 (Figure 4.4.2). This peak corresponds to a sedimentation coefficient of ~10S, similar to that of the muscle nAChR and the peak observed in the PC12-α7 and the SHSY5Y-α7#7 stable cell lines (see Figures 3.3.2A and 4.3.1A).

To demonstrate unambiguously that the increase in surface [^{125}I]-αBTX-binding was due to transfected α7FLAG rather than an upregulation of the endogenous α7 subunit, cell surface receptors of intact PC12-α7FLAG and SHSY5Y-α7FLAG cells were labelled with [^{125}I]-αBTX, solubilized and immunoprecipitated with mAb319, mAbFLAG or a mixture of the two antibodies (Figure 4.4.3). A similar low level of [^{125}I]-αBTX was immunoprecipitated by mAb319 from the α7FLAG polyclonal cell lines and from untransfected controls. The amount of bound toxin

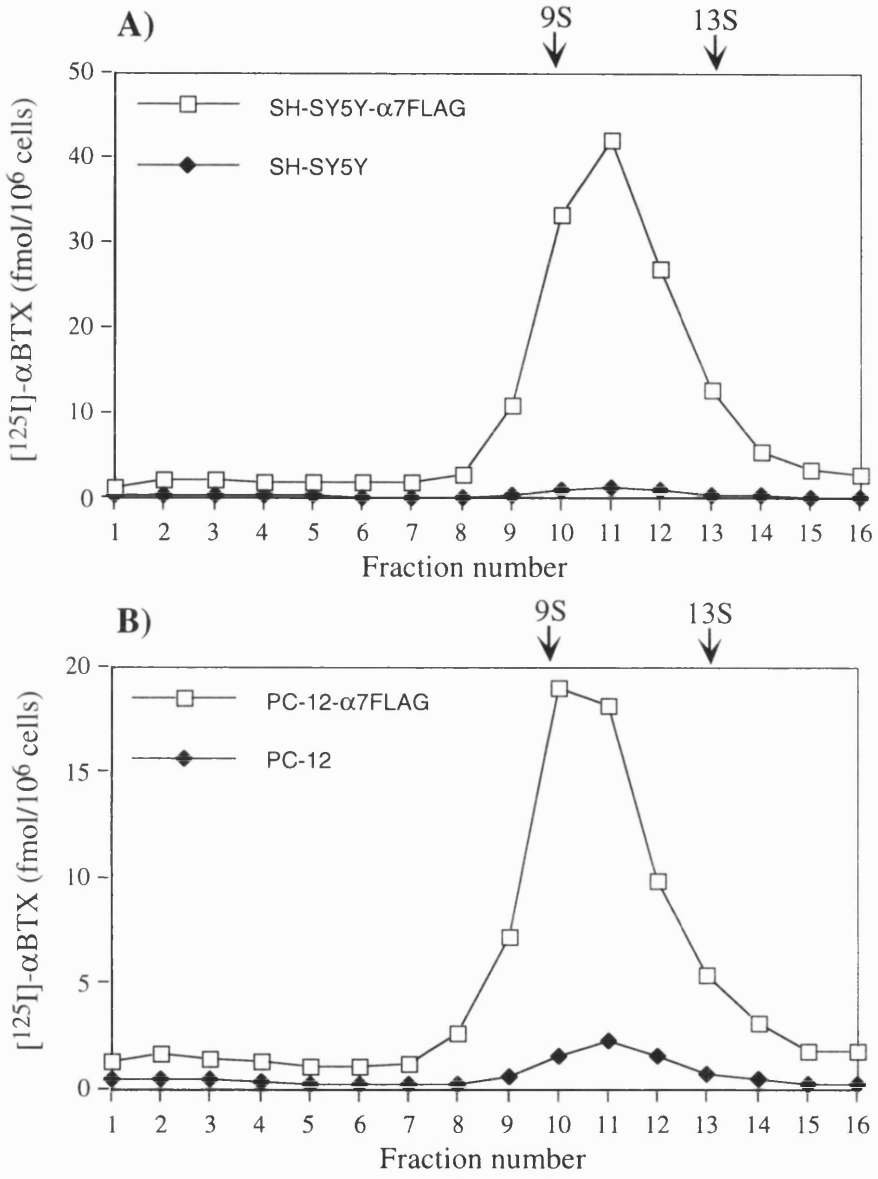

Figure 4.4.2. Sucrose gradient sedimentation of surface [^{125}I]-αBTX-binding to the stably transfected SH-SY5Y-α7FLAG and PC12-α7FLAG polyclonal cell lines. Intact cells were labelled with [^{125}I]-αBTX, washed to remove unbound toxin, and solubilized in lysis buffer containing 1% Triton X-100. Soluble cell extracts were layered onto a linear 5%-20% sucrose gradient. Following centrifugation, sixteen fractions were collected from the top of the gradient and counted in a γ-counter. **A)** Sucrose gradient profile of [^{125}I]-αBTX-binding to SH-SY5Y-α7FLAG and mock transfected SH-SY5Y-pcDNA3 polyclonal cell lines. **B)** Sucrose gradient profile of [^{125}I]-αBTX-binding to PC12-α7FLAG and mock transfected PC12-pcDNA3 polyclonal cell lines. The positions of the electric organ nAChR pentameric monomer (9S) and dimer (13S) are shown.

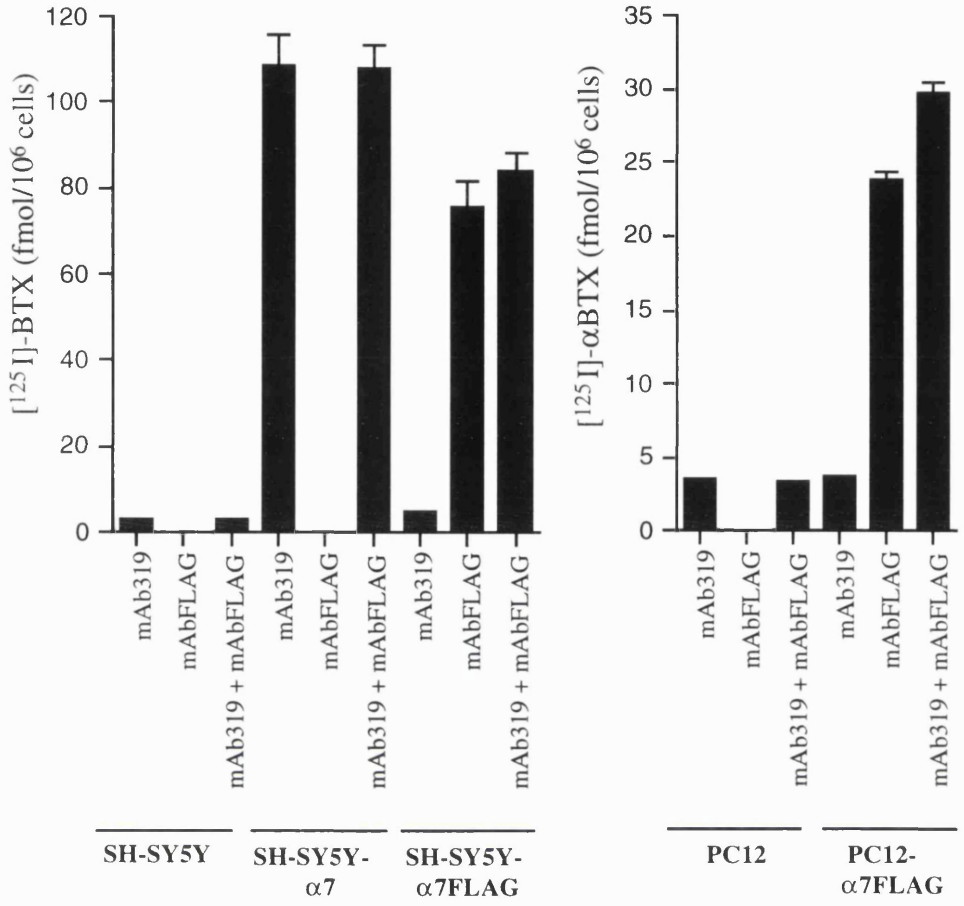

Figure 4.4.3. Immunoprecipitation of surface bound [^{125}I]-αBTX from untransfected and transfected SH-SY5Y and PC12 cell lines with monoclonal antibodies, mAb319 and mAbFLAG-M2. **A)** Immunoprecipitation of surface bound [^{125}I]-αBTX from untransfected SH-SY5Y cells, the polyclonal SH-SY5Y-α7FLAG cell line, or from the clonal SH-SY5Yα7#7 cell line. **B)** Immunoprecipitation of surface bound [^{125}I]-αBTX from the polyclonal PC12-α7FLAG cell line and untransfected PC-12 cells. Intact cells were labelled with [^{125}I]-αBTX, washed and solubilized in lysis buffer containing 1% Triton X-100. Soluble extracts were then incubated with mAb319, mAbFLAG M2 or a combination of both antibodies. Protein-G sepharose was used to pellet solubilized nAChR coupled to antibody. To determine levels of bound [^{125}I]-αBTX, washed protein-G sepharose pellets were counted in a γ-counter. Data points are the mean of triplicate samples. The data shown are from a single experiment which has been repeated three times.

immunoprecipitated by mAb319 establishes endogenous α7 expression levels in the untransfected PC12 and SH-SY5Y cell lines and also confirms the disruption of the mAb319 epitope in the α7FLAG construct (since mAb319 is unable to immunoprecipitate the increased levels of [^{125}I]-αBTX-binding in the α7FLAG cell lines). In contrast, the mAbFLAG antibody was able to immunoprecipitate 8-10 fold higher levels of [^{125}I]-αBTX from PC12-α7FLAG and SHSY5Y-α7FLAG cell lines indicating that the α7FLAG subunit efficiently forms a receptor exported to the cell surface and is able to bind [^{125}I]-αBTX. mAbFLAG failed to precipitate any [^{125}I]-αBTX-binding from untransfected PC12 and SHSY5Y cells and so does not recognise endogenous SH-SY5Y human α7 expression. The mixture of mAb319 and mAbFLAG represents the total population of αBTX-binding receptors in the cell lines and correlates with levels individually precipitated by the two antibodies.

Transient transfection of pcDNA3-α7FLAG into HEK293 once again failed to produce detectable specific [^{125}I]-αBTX-binding. Immunofluorescent confocal laser microscopy was used to examine the cellular distribution of α7 protein in transfected HEK293 cells. Both the pcDNA1neo-α7 and pcDNA3neo-α7FLAG constructs were used to transiently transfect HEK293 cells. Transfected cells were stained with either mAb319 or mAbFLAG M2 and a suitable rhodamine-conjugated secondary antibody (Figure 4.4.4). Confocal immunofluorescent microscopy revealed a very strong intracellular staining pattern with both monoclonal antibodies confirming efficient α7 or α7FLAG subunit expression in transfected HEK293 cells (Figure 4.4.4 A & B). The specificity of staining is demonstrated by the absence of staining of some cells within the same field. No fluorescent staining could be detected with either antibody in untransfected cells. In addition, the mAbFLAG M2 antibody did not detect wild-type α7 protein expressed in transfected HEK293 cells. The threadlike network of intracellular staining resembles the staining pattern observed following staining of untransfected HEK293 cells with a monoclonal antibody raised against the ER lumenal chaperone, BiP, and indicates that a large amount of α7 protein appears to be

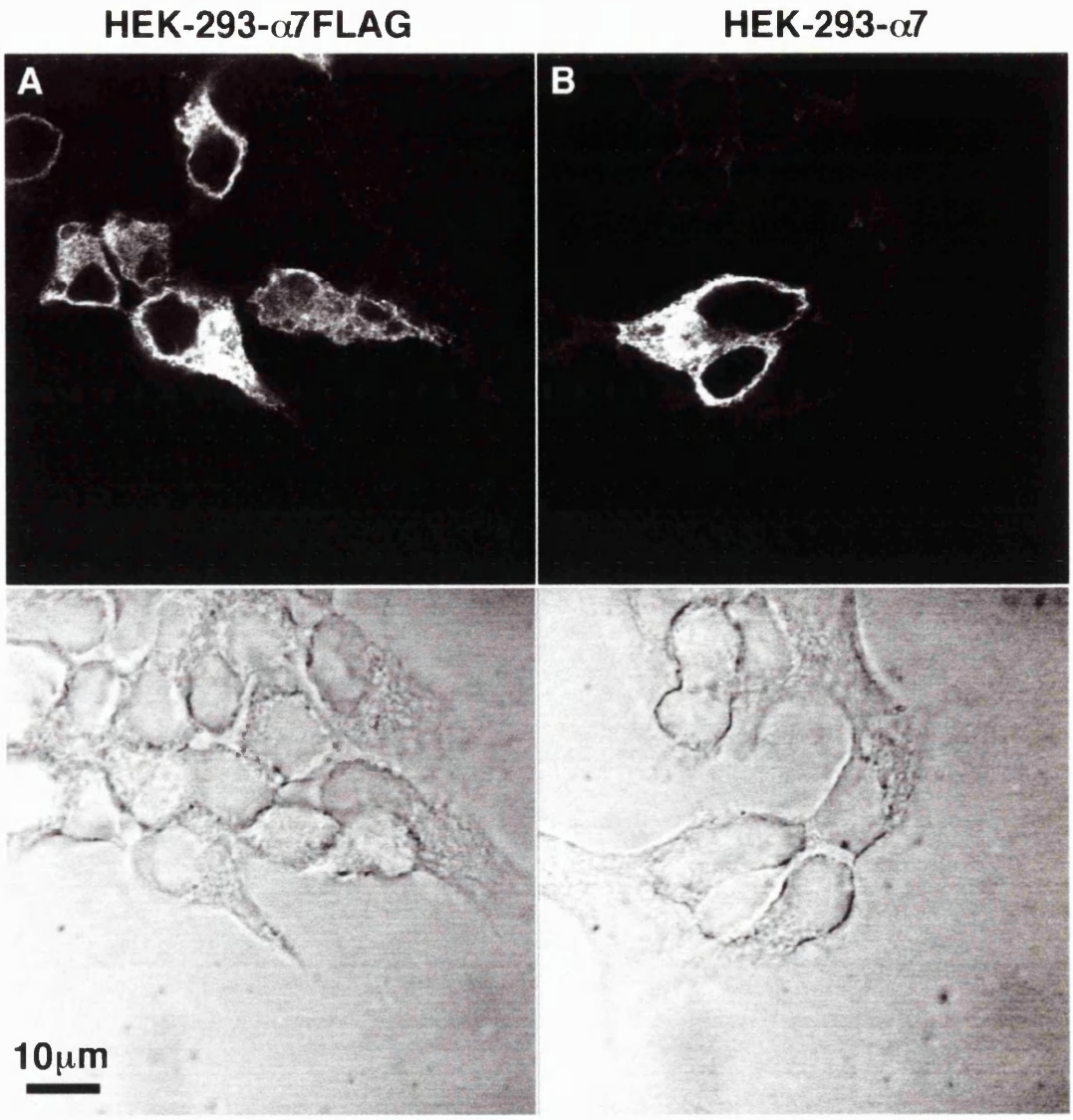

Figure 4.4.4. Intracellular distribution of α7 protein revealed by immunofluorescent staining of permeabilized cells and confocal microscopy. **A)** Strong intracellular staining was seen in HEK293 cells transiently transfected with pcDNA3neo-α7FLAG construct after labelling with mAbFLAG M2 and a rhodamine-conjugated secondary antibody. **B**) A similar strong intracellular staining pattern was detected in HEK293 cells transiently transfected with the pcDNA1neo-α7 construct after labelling with mAb319 and a rhodamine-conjugated secondary antibody. A phase transmission image of the same field of cells is shown (bottom panel).

retained in the endoplasmic reticulum.

4.5 Misfolded α7 is retained in the endoplasmic reticulum.

Evidence that α7 expressed in HEK293 cells is misfolded and does not form surface αBTX-binding sites also indicates that it may be retained in the endoplasmic reticulum (ER). This proposal was supported by evidence from glycosylation analysis using the endoglycosidases H and F. Specific N-endoglycosidases exhibit different specificities for oligosaccharide groups during their maturation pathway through the ER and Golgi apparatus. Endoglycosidase F (Endo F) cleaves simple high mannose and complex N-linked oligosaccharides (Elder and Alexander, 1982). Endoglycosidase H only cleaves N-linked oligosaccharides with simple high-mannose groups (Tarentino *et al.*, 1978). The processing of simple high-mannose groups to Endo H resistant complex oligosaccharides occurs in the Golgi apparatus (Kornfeld and Kornfeld, 1985). Hence, glycosylated protein resistant to cleavage by EndoH are complex glycoproteins that have exited the endoplasmic reticulum and passed into the Golgi.

To examine the glycosylation properties of the α7 subunit expressed in HEK293 cells, transiently transfected HEK293-α7 cells were metabolically labelled, immunoprecipitated and subjected to digestion by EndoH and EndoF (Figure 4.5.1). Undigested α7 protein is detected as a ~58 kDa band and appears to be accompanied by a minor, lower molecular weight species (also see Figures 4.1.3 and 4.2.1) which is probably represents a degradation product or unglycosylated species. The ~58 kDa glycosylated form of α7 is sensitive to digestion by both EndoH and EndoF indicating that at least the majority of, if not all α7 protein, does not exit the endoplasmic reticulum into the Golgi apparatus where oligosaccharide trimming of the mature protein would take place.

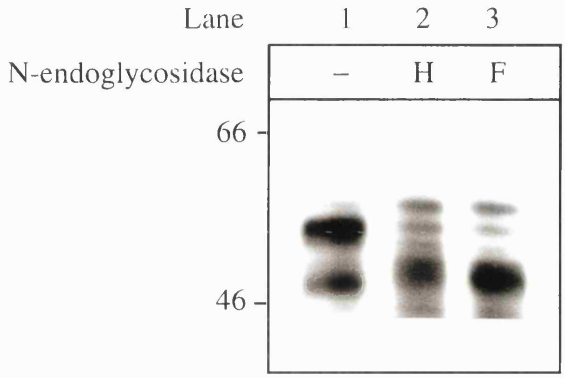

Figure 4.5.1. Glycosylation analysis of the α7 subunit expressed in transfected HEK293 cells. HEK293 cells transiently transfected with pcDNA1neo-α7 were metabolically labelled and solubilized in lysis buffer containing 1% Triton X-100. The α7 subunit was immunoprecipitated with mAb319 followed by protein-G-sepharose. Immunoprecipitated samples were left untreated (Lane 1) or digested overnight with endoglycosidase H (Endo H, Lane 2) or endoglycosidase F (Endo F, Lane 3) and then analyzed by SDS-PAGE and autoradiography. The ~58 kDa protein band corresponding to the glycosylated α7 subunit is sensitive to digestion to both Endo H and Endo F indicating that it does not exit the endoplasmic reticulum.

4.6 Modulation of α7 expression by intracellular cAMP levels

To determine whether intracellular cAMP levels can influence the folding of α7, transfected cells were treated with a cell permeable and hydrolysis-resistant cyclic AMP analogue. Transiently transfected HEK293-α7 cells and the stably transfected SH-SY5Y-α7#7 cell line were treated overnight with 2mM 8-Bromo-cAMP and the phosphatase inhibitor isobutylmethylxanthine (IBMX, 1mM), in order to elevate intracellular cAMP levels. The following morning intact cells were incubated with 1nM [^{125}I]-αBTX in the presence or absence of 50mM methyllycaconitine to determine non-specific binding. An approximate two fold upregulation in surface [^{125}I]-αBTX-binding sites was observed for the SHSY5Y-α7#7 cell line treated with 8-Bromo-cAMP and IBMX compared with untreated cells (Figure 4.6.1). However, transfected HEK293-α7 cells treated with 8-Bromo-cAMP and IBMX did not acquire the ability to bind [^{125}I]-αBTX and no specific binding was detected in either the treated, or untreated transfected HEK293-α7 cells.

The two-fold upregulation of surface [^{125}I]-αBTX-binding sites in SHSY5Y-α7#7 following treatment with 8-Bromo-cAMP is similar to that reported for the *Torpedo* nAChR stably expressed in mouse fibroblasts (Green *et al.*, 1991b; Ross *et al.*, 1991). A two- to three- fold upregulation of surface *Torpedo* nAChRs expressed in mouse fibroblasts was observed following treatments which elevate intracellular cAMP levels.

4.7 The possible role of prolyl isomerase in α7 folding and assembly

It has been reported that the efficient functional expression of homo-oligomeric receptors expressed in *Xenopus* oocytes is dependent on the actions of the peptidyl-prolyl isomerase cyclophilin (Helekar *et al.*, 1994; Helekar and Patrick, 1997). Functional responses in oocytes generated by either the homo-oligomeric α7 nAChR

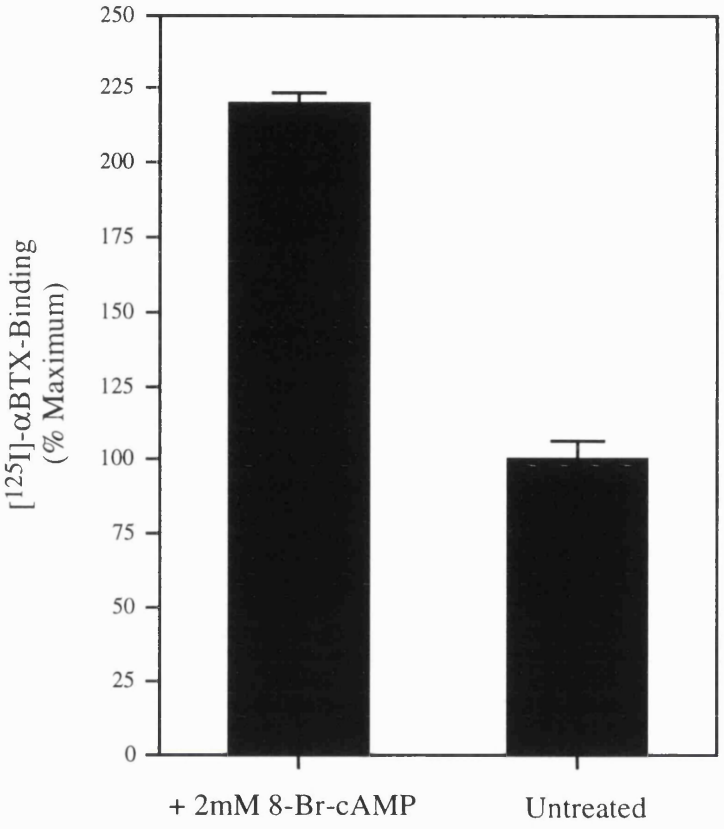

Figure 4.6.1. cAMP-stimulated upregulation in surface [^{125}I]-αBTX-binding sites in SH-SY5Y-α7#7 cells. SH-SY5Y-α7#7 cells were trypsinized and replated at a density of 3 x 10^6 cells per 6 cm plate. Cells were left to adhere and then incubated in the presence or absence of 2mM 8-Br-cyclic AMP plus 1mM isobutylmethylxanthine (IBMX) for 16-20 hours. Treated and untreated cells were gently scraped from the plate and subjected to radioligand binding experiments. Intact cells were incubated with 1 nM [^{125}I]-αBTX in HBSS containing 0.5% BSA. Samples were harvested onto GF-A filters and washed rapidly five times. Non-specific binding, determined by the addition of 50μM methyllycaconitine (MLA), has been subtracted. Data points represent the average of duplicate samples. The data series is generated from the mean of three separate experiments.

or the serotonin $5HT_3$ receptor, but not the hetero-oligomeric muscle receptor, were reduced by treatment with the cyclophilin inhibitor, Cyclosporin A. Functional responses generated by α7 or $5HT_3$ were inhibited by up to 80% following prior incubation of oocytes for 5-7 days with 30μM Cyclosporin A (IC_{50}~4μM) and this inhibition could be reversed by overexpression of the cytoplasmic rat brain cyclophilin. Cyclosporin A was also shown to reduce the production of surface [^{125}I]-αBTX- and anti-peptide α7 antibody-binding sites, following nuclear injection of oocytes with α7cDNA constructs.

To investigate whether overexpression of cyclophilin could alleviate the misfolding of α7 in the HEK293 cell line, ER-specific and cytoplasmic isoforms of cyclophilin were co-transfected with α7. The cytoplasmic isoform of cyclophilin was re-cloned in our laboratory from a rat superior cervical ganglia (SCG) λ-Zap cDNA library (Prof. D. Lipscombe, Brown University, Rhode Island) and a rat cerebellum cDNA library (UK Human Genome Mapping Project, Resource Centre, Cambridge) by PCR using two primers based on published sequences (Danielson *et al.*, 1988). The amplified cytoplasmic cyclophilin cDNAs and the ER-specific cyclophilin cDNA in pMU-6.0 (Hasel *et al.*, 1991), were subcloned into pcDNA3neo. HEK293 cells were transiently transfected with pcDNA1neo-α7 alone, pcDNA1neo-α7 plus pcDNA3neo-cyclophilin (each isoform), or with the four rat muscle α, β, δ, ε subunits. Transfected cells were subjected to [^{125}I]-αBTX-binding experiments. High levels of specific [^{125}I]-αBTX-binding was detected in HEK293 cells transiently transfected with the rat muscle nAChR indicating that the transfection procedure was successful. However, co-transfection of HEK293 cells with either the ER-specific or cytoplasmic isoforms of cyclophilin with α7 failed to produce [^{125}I]-αBTX-binding sites.

In addition, SHSY5Y-α7#7 cells were treated with Cyclosporin A to determine whether a reduction in the number of surface [^{125}I]-αBTX-binding sites would result.

Unfortunately, micromolar concentrations of Cyclosporin A proved toxic to both transfected and untransfected SHSY5Y cells (and other mammalian cell lines tested) and so the influence of Cyclosporin A on levels of surface expressed α7 nAChR could not be accurately estimated.

4.8 Expression of cloned human and chick α7 nAChR subunits

Interestingly, during the course of this research, the successful functional expression of the cloned human α7 nAChR was achieved in HEK293 cells (Gopalakrishnan *et al.*, 1995a). The amino-acid sequences of the human and rat α7 subunits are 94% homologous and it would seem unlikely that this could explain the failure of the rat α7 to form α-BTX-binding sites when expressed in HEK293 cells. Another possible explanation is that there are differences between the two isolates of HEK293 cells used in the two laboratories which affects the efficient folding of the α7 nAChR subunit.

In an attempt to reproduce the results of Gopalakrishnan and colleagues, the human α7 cDNA was obtained from Dr. Jon Lindstrom (Peng *et al.*, 1994b) and subcloned into pcDNA3neo. The chick α7 cDNA (Couturier *et al.*, 1990a) in the mammalian expression vector pMT3 (which utilizes an adenovirus promoter for constitutive expression, see Figure 3.0.1) was obtained from Dr. Marc Ballivet. The rat pcDNA1neo-α7, chick pMT3-α7 and human pcDNA3neo-α7 constructs were each transiently transfected into HEK293 cells in duplicate plates. Following transfection, one plate of transfected cells was metabolically labelled and α7 protein immunoprecipitated with mAb319, and the other plate was assayed for [^{125}I]-αBTX-binding sites following day. High levels of rat and human α7 protein were efficiently immunoprecipitated by mAb319 from transfected HEK293 cells revealing a protein band for each of ~58 kDa (Figure 4.8.1 inset, lanes 1 & 3). A significantly more faint ~58 kDa band corresponding to the chick α7 subunit could also be detected (Figure

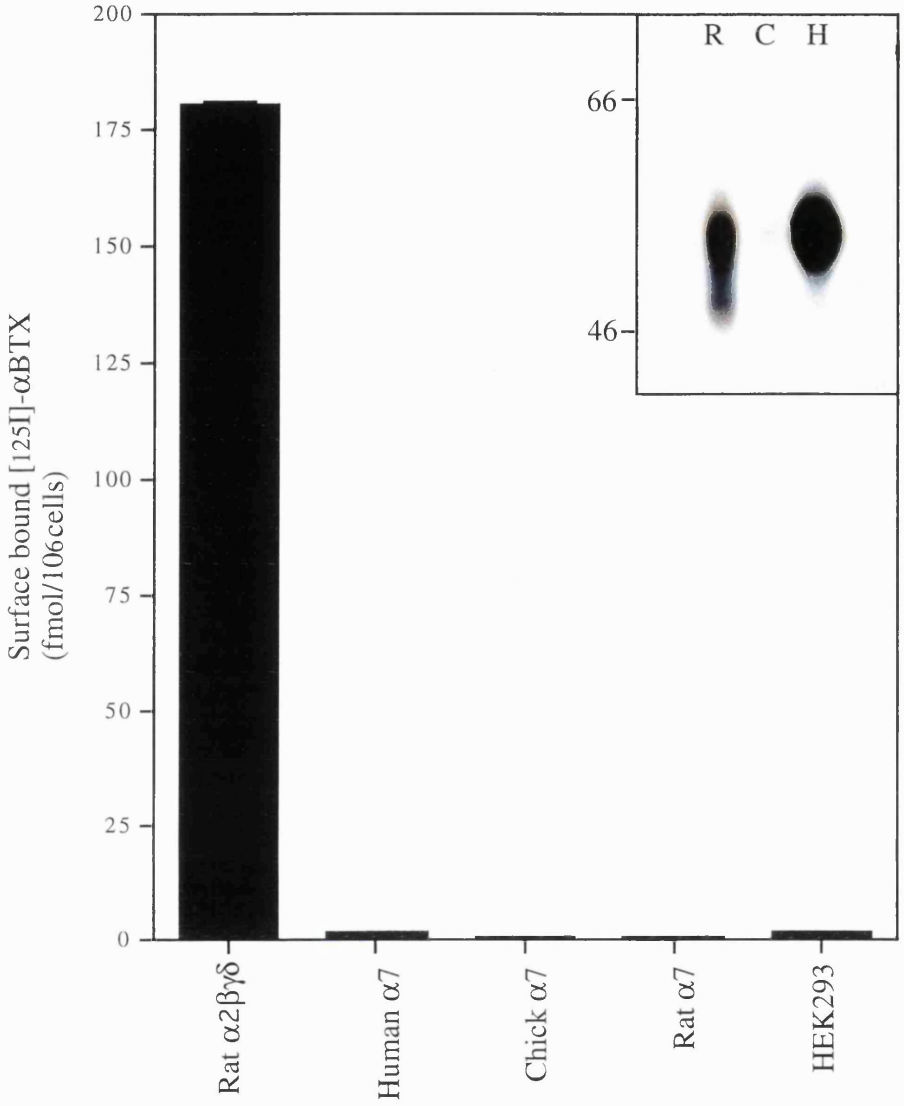

Figure 4.8.1. Specific [^{125}I]-αBTX-binding to transiently transfected HEK293 cells. HEK293 cells were transfected with either the rat muscle nAChR α, β, γ and δ subunits in the molar ratio 2:1:1:1, respectively, or the human, chick or rat neuronal α7 nAChR subunit. Intact cells were incubated with 2nM [^{125}I]-αBTX in HBSS containing 0.5% BSA for 2 hours at room temperature. Samples were harvested onto GF-A glass fibre filters and rapidly washed 5 times. Non-specific binding was determined by the addition of 100mM methyllycaconitine (MLA) to samples containing α7, or 500mM each of carbamylcholine and nicotine for samples transfected with the muscle nAChR. Data points represent specific binding generated from the means of triplicate samples. Non-specific binding has been subtracted and typically represents 3 fmol of [^{125}I]-αBTX-binding per filtered sample. **Inset**: Lanes 1, 2 and 3 correspond to mAb319 immunoprecipitated metabolically labelled protein from duplicate plates of HEK293 cells transfected with the rat, chick and human α7 subunits, respectively.

4.8.1 inset, lane 2). The lower level of immunoprecipitated protein from HEK293 cells transiently transfected with the chick pMT3-α7 construct is probably due to the lower level of expression from the adenovirus promoter compared with the CMV promoter of pcDNA1neo and pcDNA3neo. The rat muscle nAChR receptor (α2βγδ) was co-transfected into an additional plate of HEK293 cells in parallel with the human, chick and rat α7 constructs. High levels of [^{125}I]-αBTX-binding was detected in transfected HEK293-$\alpha_2\beta\gamma\delta$ cells, but no specific surface [^{125}I]-αBTX-binding could be detected in any of the duplicate plates transfected with the rat, chick or human α7 cDNA constructs (Figure 4.8.1).

These results suggest that the successful expression of the human α7 construct reported by Gopalakrishnan and colleagues in HEK293 cells is not due to a species-specific difference between the human and rat isoforms of the α7 subunit. Evidence from these experiments show that the isolate of HEK293 cells used in our laboratory can synthesize high levels of the human α7 subunit following transient transfection, but still fail to produce specific [^{125}I]-αBTX-binding sites. This suggests that there is a difference between the two isolates of HEK293 cells used in the two laboratories.

4.9 Does α7 require other nAChR subunits to form α-BTX-binding sites?

It is still unclear whether native α7 αBTX-binding receptors exist in the mammalian brain as homo-oligomers or are assembled with other, perhaps still unidentified, nAChR subunits. Although α7 forms functional homo-oligomers when expressed in *Xenopus* oocytes in the absence of any other neuronal nAChR subunits, the pharmacological properties of homo-oligomeric α7 receptors closely mimic but are not identical to native α7 receptors (Anand *et al.*, 1993b). Interpretation of results from transfection studies in PC12 and SHSY5Y cells is complicated by the expression of other neuronal nAChR subunits in addition to α7. Northern blotting, RNAase protection assays and immunocytochemistry has revealed that PC12 cells

express α3, α5, α7, β2, β3 and β4 subunits (Rogers *et al.*, 1992; Henderson *et al.*, 1994) and SHSY5Y cells express α3, α5, α7, β2 and β4 subunits (Lukas *et al.*, 1993; Peng *et al.*, 1994a; Puchacz *et al.*, 1994).

To determine whether co-assembly with other nAChR subunits could alleviate the cell-specific misfolding of α7 observed in HEK293 cells, all nicotinic subunits expressed in PC12 and SH-SY5Y cells were tested in multi-subunit transfections of HEK293 cells (all neuronal subunit cDNAs were contained in pcDNA1neo). Significant elevations in [^{3}H]-epibatidine binding was detected following transfection of multi-subunit combinations containing α3 in combination with either β2 or β4, but no specific [^{125}I]-αBTX-binding sites could be detected. However, co-transfection of the four muscle α,β,γ and δ subunits performed as a positive control resulted in the appearance of high levels of surface [^{125}I]-αBTX-binding sites.

There is evidence from immunoprecipitation experiments from chick brain and retina that α7 may co-assemble with α8 *in vivo* (Keyser *et al.*, 1993; Gotti *et al.*, 1994). A mammalian homologue of the chick α8 subunit has yet to be identified, so we investigated whether co-expression of α7 with the chick α8 subunit would lead to the formation of αBTX-binding sites in HEK293 cells. Immunoprecipitation of surface bound [^{125}I]-αBTX with α7-specific antibodies would be used to verify the contribution of the α7 subunit to αBTX-binding receptor subtypes. However, co-expression of α8 with either the rat or chick α7 did not produce specific [^{125}I]-αBTX- or [^{3}H]-Epibatidine-binding sites in HEK293 cells.

4.10 Summary

These results indicate that the ability of oocytes, SH-SY5Y and PC12 cells to correctly fold and assemble the rat neuronal α7 subunit into an oligomeric complex, able to bind αBTX with high affinity, is not a property common to all mammalian

cell lines. Expression of the α7 subunit in a panel of nine mammalian cell lines revealed that in only two cell lines (PC12 and SH-SY5Y) could the recombinant rat α7 subunit fold into a conformation able to bind [^{125}I]-αBTX. Efficient expression of the α7 subunit protein in all transfected cell lines was verified by metabolic labelling and immunoprecipitation experiments with mAb319, an antibody which recognises a linear epitope within the cytoplasmic loop of the α7 subunit. The absence [^{125}I]-αBTX binding in seven transfected cell lines shown to express high levels of α7 subunit protein implies α7 is misfolded in these cell lines. This proposal is supported by evidence from three monoclonal antibodies which recognise conformation-dependent epitopes located within the extracellular domain of the α7 nAChR (mAbOAR1, mAbOAR5a, mAbOAR11b). These three antibodies successfully detected α7 protein in SH-SY5Y-α7#7 cells by both immunoprecipitation and immunofluorescent techniques but failed to recognise α7 protein expressed in transfected HEK293-α7 cells. These data suggest that the ability of the α7 subunit to correctly fold into a conformation able to bind αBTX and conformation-dependent antibodies is critically dependent on the host cell type.

Results presented in this section are described in Cooper and Millar, 1997.

5.0 Cell-specific folding of the chick neuronal nAChR α8 subunit.

5.1 Cell-specific folding of α8 revealed by immunoprecipitation and radioligand binding.

During the investigation of the cell specific folding of the α7 subunit in mammalian cell lines, one experiment examined the possible co-assembly of α7 with the chick α8 subunit since evidence from immunoprecipitation experiments from chick brain and retina imply that α7 and α8 may co-assemble *in vivo* (Keyser *et al.*, 1993; Gotti *et al.*, 1994). The chick α8 subunit has also been shown to form functional homo-oligomeric nicotinic channels sensitive to αBTX when expressed in *Xenopus* oocytes (Gerzanich *et al.*, 1994). Surprisingly, co-transfection of α7 with α8 into HEK293 cells did not result in the appearance of high affinity [^{125}I]-αBTX or [^{3}H]-epibatidine binding sites, indicating that the cell-specific folding of α7 in several mammalian cell lines may also be a property of the homo-oligomeric α8 subunit.

The possible cell-specific misfolding of the chick neuronal nAChR α8 subunit was examined. The chick α8 gene (Schoepfer *et al.*, 1990) was obtained from Dr. Jon Lindstrom and subcloned into pcDNA3neo (please refer to Figure 3.1.1). HEK293 cells were transiently transfected with pcDNA3neo-α8 by calcium phosphate transfection and transfected cells were assayed for nicotinic radioligand binding sites with [^{125}I]-αBTX (up to 20nM) or [^{3}H]-epibatidine (up to 10nM). Non-specific binding was determined by the addition of 500μM nicotine plus 500μM carbamylcholine to triplicate samples. However no specific [^{125}I]-αBTX or [^{3}H]-epibatidine binding to transfected HEK293-α8 cells could be detected.

Metabolic labelling and immunoprecipitation experiments were used to provide evidence for the successful production of α8 subunit protein in transfected HEK293-

α8 cells which failed to produce specific radioligand binding (Figure 5.1.1). Duplicate plates of transfected HEK293-α8 cells were metabolically labelled and immunoprecipitated with either mAb308 or mAb305 (Schoepfer *et al.*, 1990). mAb308 was raised against a bacterially expressed α8 fusion protein and has been shown to specifically recognise a linear epitope within the cytoplasmic loop of the α8 subunit (see Figure 4.1.2) (McLane *et al.*, 1992). Immunoprecipitation with mAb308 and analysis by SDS-PAGE revealed the presence of a single band of approximately ~57 kDa from transfected HEK293-α8 cells, but not from untransfected controls (Figure 5.1.1). This apparent molecular weight correlates well with previous estimations of the molecular weight of native α8 immunoisolated from chick brain (~60 kDa) (Schoepfer *et al.*, 1990), optic lobe (~57 kDa) (Gotti *et al.*, 1993; Gotti *et al.*, 1994) and retina (~58 kDa) (Gotti *et al.*, 1997).

mAb305 was raised against purified native and denatured chick brain αBTX-binding receptor, but is strictly conformation dependent and fails to recognise denatured protein (McLane *et al.*, 1992). In contrast to results obtained with mAb308, mAb305 was unable immunoprecipitate α8 protein from a duplicate sample of metabolically labelled, solubilized HEK293-α8 cells (Figure 5.1.1A). The α8 subunit expressed in transfected HEK293 cells is not folded into a conformation which forms radioligand binding sites or an extracellular conformational epitope recognised by mAb305 and closely parallels the cell-specific misfolding observed for the rat α7 subunit. Therefore, the α8 subunit was expressed in SH-SY5Y cells which had been previously shown to correctly fold the recombinant rat α7 subunit. SH-SY5Y cells were transfected with pcDNA3neo-α8 and a polyclonal population of stably transfected cells were obtained through selection with G418. A substantial increase in surface [^{125}I]-αBTX-binding was detected in both transiently and stably transfected SH-SH5Y-α8 cells. A ~30 fold increase in surface [^{125}I]-αBTX-binding was observed in a polyclonal stable SH-SY5Y-α8 cell line compared with

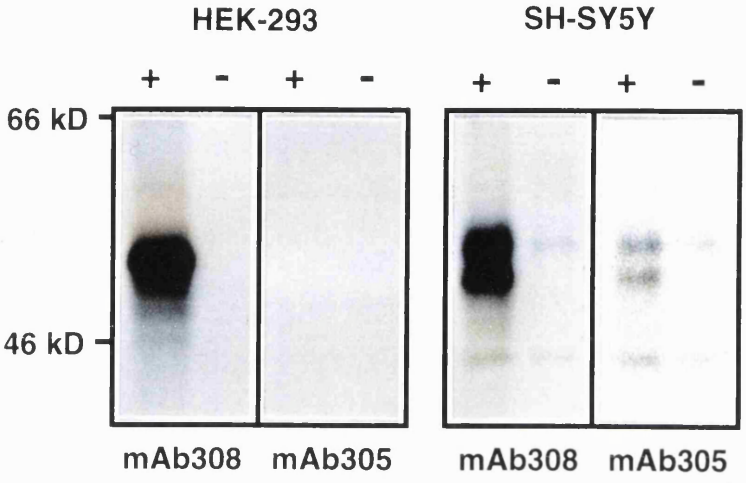

Figure 5.1.1. Immunoprecipitation of the nAChR α8 subunit from transfected HEK293 and SH-SY5Y cell lines. Cells transfected with the pcDNA3neo-α8 construct were metabolically labelled and solubilized in lysis buffer containing 1% Triton X-100. The α8 subunit was immunoprecipitated with either mAb308, which recognizes a linear epitope on α8, or mAb 305, which recognizes a conformation-dependent epitope within the extracellular domain of the α8 nAChR. **A)** A ~57 kDa protein band corresponding to the α8 subunit was immunoprecipitated by mAb308 from transiently transfected HEK293-α8 cells (+) but not from untransfected HEK293 cells (-). However, mAb305 failed to immunoprecipitate α8 protein from transfected HEK293-α8 cells. **B)** Both mAb308 and mAb305 were able to immunoprecipitate α8 protein from a polyclonal SH-SY5Y-α8 cell line (+) but not from untransfected SH-SY5Y cells (-). α8 expressed in SH-SY5Y cells was apparent as two protein bands of ~54 and ~58 kDa and probably represent differently glycosylated species.

untransfected, or mock transfected (plasmid vector not containing the α8 cDNA), controls (Figure 5.1.2).

SH-SY5Y cells are not thought to express the α8 subunit and a mammalian homologue of the chick α8 has yet to be identified. In order to confirm that the upregulation in αBTX-binding was due to expression of the recombinant α8 protein, cell surface receptors of intact polyclonal SH-SH5Y-α8 cells were labelled with [^{125}I]-αBTX and immunoprecipitated with monoclonal antibodies specific for either the α7 subunit (mAb306) or the α8 subunit (mAb308) (Figure 5.1.2 and see the antibody summary in Figure 4.1.2). Using the α7-specific antibody, mAb306, similar low levels of [^{125}I]-αBTX-binding could be immunoprecipitated from both untransfected SH-SY5Y cells and the polyclonal stable SH-SY5Y-α8 cell line. This represents endogenous α7 expression levels and also confirms that the increased abundance of surface [^{125}I]-αBTX-binding receptors in SHSY5Y-α8 cells do not contain α7. In contrast, ~30 times more [^{125}I]-αBTX could be precipitated from SHSY5Y-α8 cells with the α8-specific antibody, mAb308. No [^{125}I]-αBTX could be immunoprecipitated with mAb308 from untransfected SHSY5Y cells, indicating the absence of an α8 nAChR able to bind αBTX in untransfected SH-SY5Y cells.

The α8 subunit expressed in SH-SY5Y cells appears to fold into a conformation able to bind αBTX and is efficiently exported to the cell surface. This indicates that α8 adopts a more native conformation when expressed in SH-SY5Y cells. This suggestion is supported by evidence from the successful immunoprecipitation of metabolically labelled α8 protein from the polyclonal stable SH-SY5Y-α8 cell line and untransfected SH-SY5Y cells with both mAb308 and mAb305 (Figure 5.1.1B). The separation of immunoprecipitated labelled protein by SDS-PAGE reveals the presence of two bands of ~54 and ~58 kDa. The absence of these two bands in untransfected cells indicates that both bands correspond to specific α8 protein bands and probably represent differently glycosylated forms of the α8 subunit. The

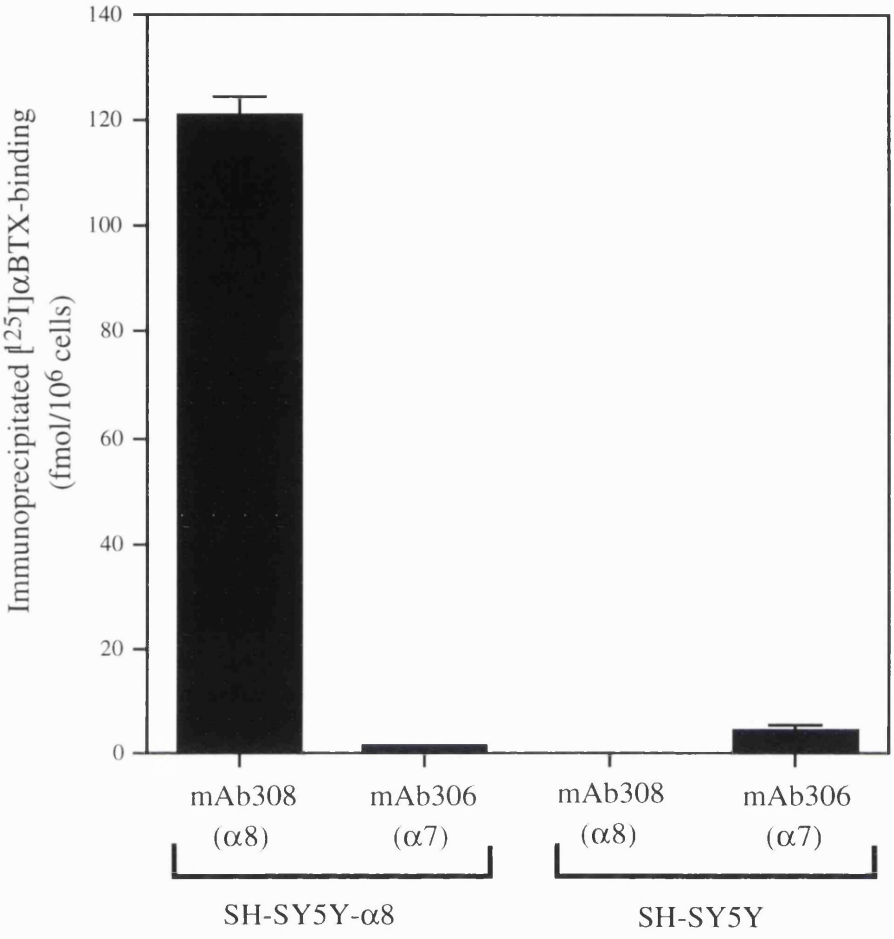

Figure 5.1.2. Immunoprecipitation of surface bound [^{125}]-αBTX from untransfected SH-SY5Y cells and the stably transfected SH-SY5Y-α8 polyclonal cell line with subunit-specific monoclonal antibodies, mAb308 and mAb306. mAb308 is specific for the α8 nAChR subunit, and mAb306 is specific for the α7 nAChR subunit. Intact cell monolayers were labelled with 20nM [^{125}]-αBTX in normal culture media for 1 hour at 37°C. Unbound toxin was removed by washing and cells were solubilized in lysis buffer containing 1% Triton X-100. Soluble cell extracts were divided into 6 aliquots and incubated with either mAb308 or mAb306 followed by protein-G-sepharose. Sepharose pellets coupled to antibody-bound nAChR were washed and levels of bound [^{125}]-αBTX determined by γ-counting. Data points represent the means of triplicate samples.

intensity of the protein band immunoprecipitated by mAb305 is clearly visible but considerably more faint than that obtained with mAb308. This could be due to the strict conformational dependence of mAb305 resulting in the less successful immunoprecipitation of α8 protein following solubilization and high salt washing conditions employed during this procedure. A better example of the efficient recognition of the α8 protein expressed in SH-SY5Y-α8 cells by the conformation-dependent mAb305 is provided by immunofluorescent microscopy presented in Section 5.2.

5.2 Cell specific folding of α8 by immunofluorescent microscopy.

mAb305 was used to detect α8 nAChRs expressed on the extracellular membrane of transiently transfected HEK293-α8 and polyclonal stable SHSY5Y-α8 cells. Intact cells were incubated with mAb305 followed by a rhodamine-conjugated secondary antibody. Immunofluorescent microscopy revealed very bright surface staining of the polyclonal SHSY5Y-α8 cell line (Figure 5.2.1). No specific staining of mAb305 could be detected in untransfected SH-SY5Y cells. The specificity of mAb305 staining is demonstrated by the absence of staining of some SHSY5Y-α8 cells not expressing surface α8 nAChRs within the same microscope field shown in the photograph. Variability in expression of a transfected construct is often observed in polyclonal cell lines and is probably due to differences in the copy number of stably integrated plasmids in different cells. Some cells which do not express α8 subunit protein despite possessing resistance to G418 probably arise due to insertional inactivation of the transfected construct during stable integration into the host cell genome, by disruption of the promoter or inhibition of transcription effected by the site of insertion.

The pattern of immunofluorescent staining of live SHSY5Y-α8 cells with mAb305, resembles the clustered appearance of mAbOAR11b staining of surface α7 nAChR

A)

B)

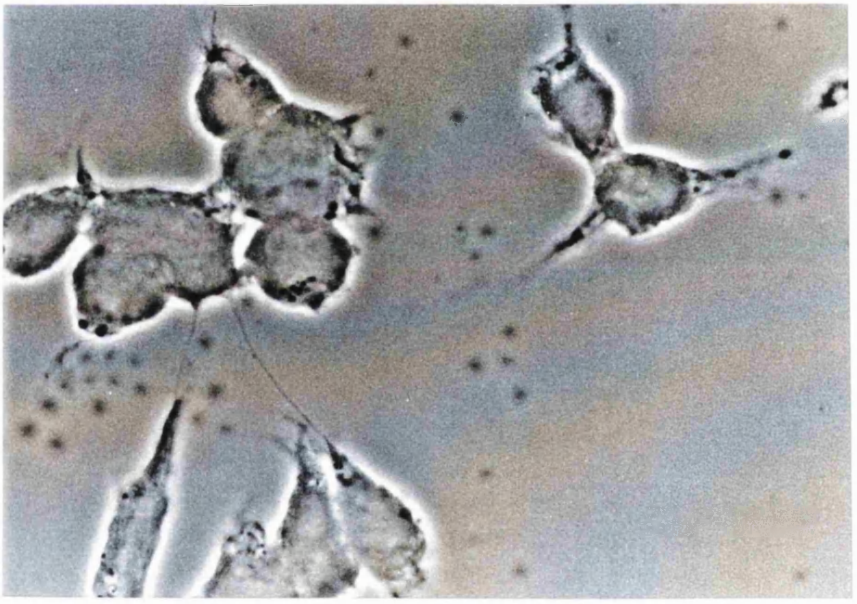

Figure 5.2.1. Immunofluorescent staining of α8 nAChRs expressed on the surface of transfected SH-SY5Y-α8 cells. A polyclonal population of stably transfected SH-SY5Y-α8 cells were labelled with mAb305 which recognizes an extracellular conformational epitope. Live cells were incubated with mAb305 for 1 hour at room temperature in HBSS containing 2% BSA. Unbound antibody was removed by washing. The cells were then fixed and incubated with a rhodamine-conjugated secondary antibody. Clear surface staining in the form of antibody crosslinked microclusters of α8 nAChRs could be seen in SH-SY5Y-α8 cells. The specificity of staining is confirmed by the absence of staining of some cells within the same microscope field. No specific staining with mAb305 could be detected in untransfected SH-SY5Y cells (data not shown).

expressed in SH-SY5Y-α7#7 cells (Figure 4.2.2A) thought to be induced by antibody cross-linking of surface nAChRs. This suggestion is supported by the staining of intact SH-SY5Y-α7#7 or SH-SY5Y-α8 cells with rhodamine-conjugated αBTX which did not reveal such an extensive clustered staining pattern (see Section 5.5, Figure 5.5.1B)

5.3 Cell specific folding of α8 in a rat pituitary GH_4C_1 cell line.

Recently the α7 nAChR subunit has been reported to form functional nicotinic channels which bind [^{125}I]-αBTX in the rat pituitary cell line GH_4C_1, which does not express nicotinic subunits endogenously (Quik *et al.*, 1996; Quik *et al.*, 1997). The α8-pcDNA3neo construct was transiently transfected into GH_4C_1 cells and assayed for radioligand binding. GH_4C_1-α8 cells were shown to express specific [^{3}H]-epibatidine-binding sites and saturation binding analysis of transiently transfected GH_4C_1-α8 cells with [^{3}H]-epibatidine (5 pM-10 nM) revealed that the α8 nAChR binds epibatidine with high affinity with a K_d of 0.24 ± 0.4 nM (from 2 determinations) and a calculated Hill Coefficient of 0.9 ± 0.2 (Figure 5.3.1).

Expression of the α7 subunit in GH_4C_1 cells also resulted in the appearance of high-affinity [^{125}I]-αBTX-binding sites (Figure 5.3.2). The human, chick and rat isoforms of the α7 subunit were transiently transfected into GH_4C_1 cells and formed specific [^{125}I]-αBTX-binding sites (Figure 5.3.2A). Differences in the levels of [^{125}I]-αBTX-binding generated by each isoform of the transfected α7 subunit cDNAs was not investigated further and may be due to the different expression vectors (pcDNA1neo for rat and pcDNA3neo for chick and human) and differences in mRNA transcript levels or stability. Sucrose gradient sedimentation of the rat α7 nAChR expressed in GH_4C_1 cells revealed a peak of surface bound [^{125}I]-αBTX in fraction 11 corresponding to a sedimentation coefficient of ~10S and indicates that the α7

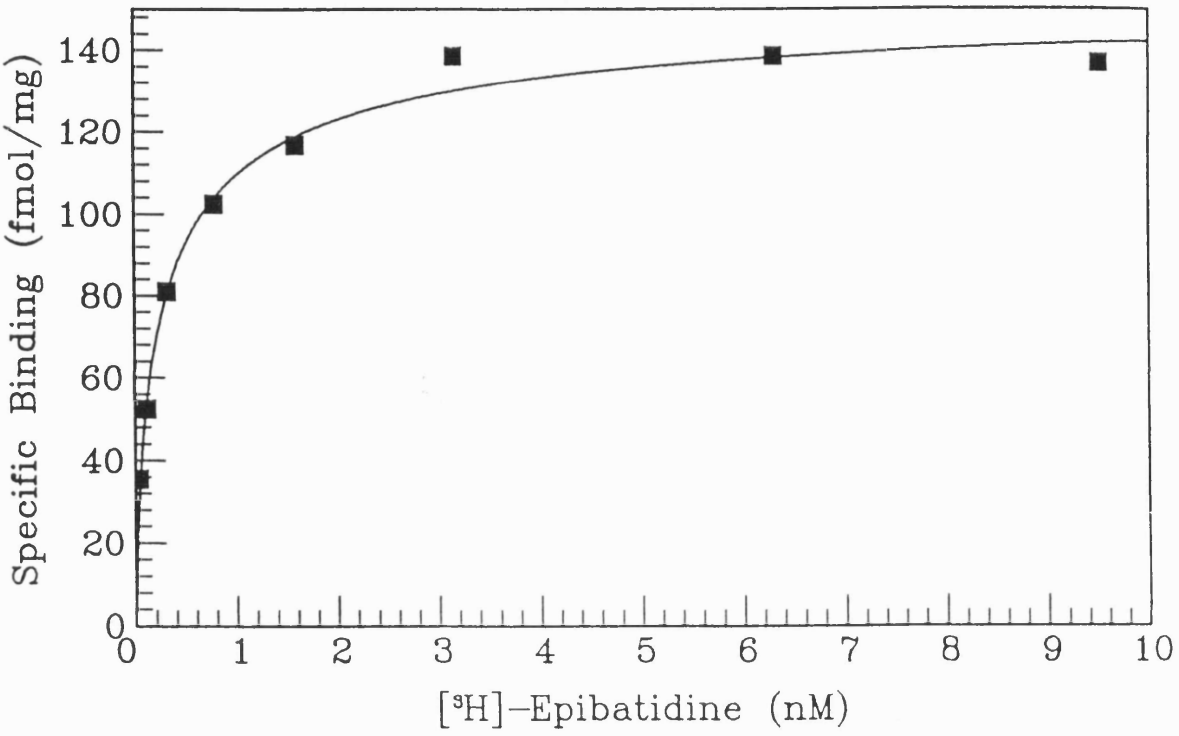

Figure 5.3.1. Saturation binding of [^{3}H]-epibatidine to GH_4C_1 cells transiently transfected with pcDNA3neo-α8. Cell membranes were incubated with increasing concentrations of [^{3}H]-epibatidine (5pM-10nM). Non-specific binding, determined by the addition of 500μM carbamylcholine plus 500μM nicotine to duplicate samples, has been subtracted. Data points represent the average of duplicate samples and the data series are typical of two separate determinations resulting in an average K_d of 0.24nM ± 0.04 with a calculated Hill coefficient of 0.9 ± 0.2. The maximum specific binding (B_{max}) of [^{3}H]-epibatidine to transiently transfected GH_4C_1-α8 cells in this experiment was 153 fmol/mg membrane protein.

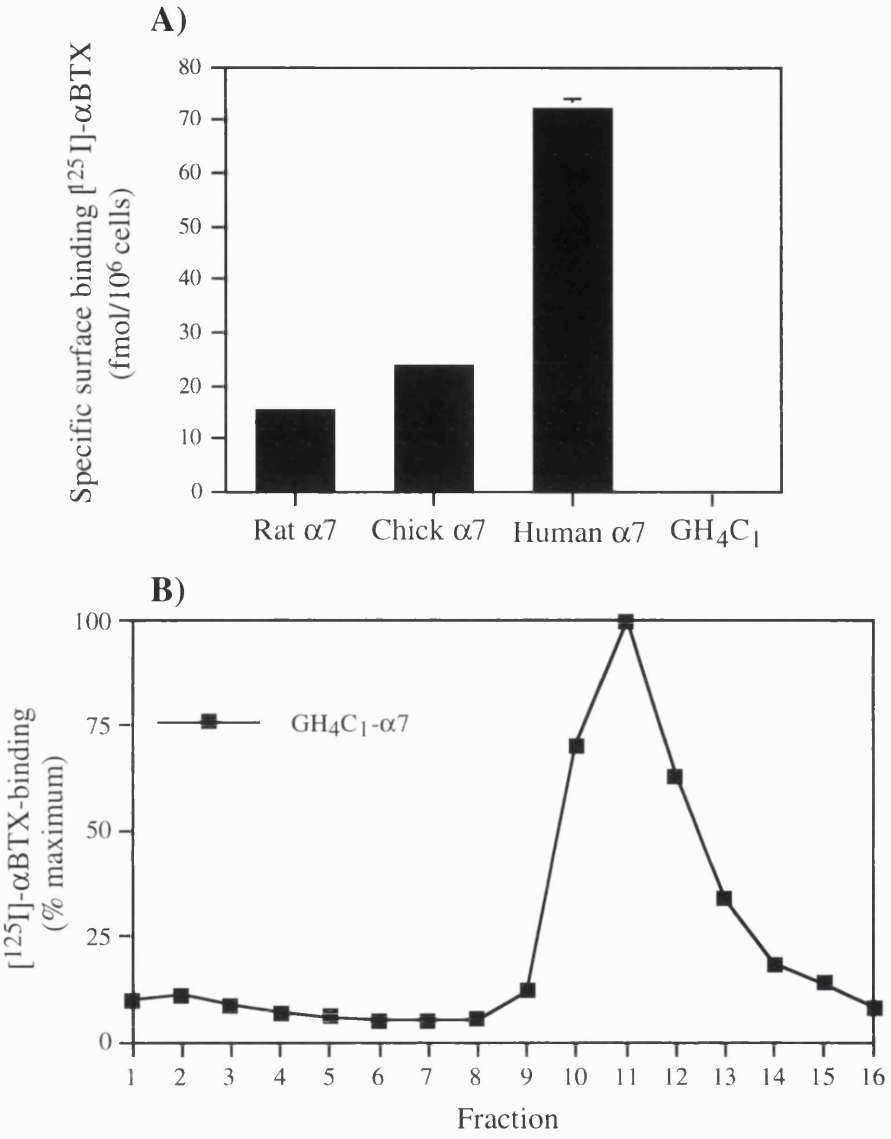

Figure 5.3.2. Surface [^{125}I]-αBTX-binding to GH_4C_1 cells transiently transfected with α7. **A**) GH_4C_1 cells in 6 cm dishes were transiently transfected with rat α7 (pcDNA1neo-α7), chick α7 (pcDNA3neo-α7) or human α7 (pcDNA3neo-α7) constructs by lipofection. Intact cells were incubated with 1nM [^{125}I]-αBTX in HBSS containing 0.5% BSA approximately 30 hours after transfection. Non-specific binding, determined by the addition of 100μM MLA to triplicate samples, typically represents ~1.0 fmol [^{125}I]-αBTX per filtered sample and has been subtracted. **B)** Sucrose gradient centrifugation of GH_4C_1 cells transiently transfected with rat α7. Intact cells were labelled with 5nM [^{125}I]-αBTX, washed and solubilized in lysis buffer containing 1% Triton X-100. Soluble cell extracts were sedimented on a 5-20% linear sucrose gradient. 16 fractions removed from the top of the gradient were assayed for [^{125}I]-αBTX-binding by γ-counting.

subunit forms a pentameric receptor which is readily exported to the plasma membrane in transfected GH_4C_1 cells.

GH_4C_1 cells transfected with pcDNA3neo-α8 were subjected to selection with G418 and 28 individual clones were picked and expanded into clonal cell lines. Tritiated epibatidine binding analysis revealed that only seven of the clonal isolates possessed detectable levels of specific nicotinic radioligand binding. This result is surprising considering that the plasmid construct containing the cloned α8 cDNA also contains the gene encoding G418 resistance and must also be stably integrated. Levels of detectable [^{3}H]-epibatidine binding to the clonal cell lines and a polyclonal population were remarkably low (~20-60 fmol/mg membrane protein) in comparison to expression levels achieved in the SHSY5Y-α8 polyclonal stable cell line (>1pmol/mg membrane protein). The reason for this low level of expression is unclear but because of this, transient expression systems were used for fluorescent microscopy and sucrose gradient analysis.

5.4 Sucrose gradient centrifugation of the α8 nAChR expressed in GH_4C_1 and SH-SY5Y cells.

The sucrose gradient sedimentation profile of the α8 nAChR expressed in transiently transfected GH_4C_1-α8 cells was determined by two methods. Receptors present on the extracellular membrane of transfected cells were analyzed by prior labelling of cell surface receptors on intact cells with [^{125}I]-αBTX. Alternatively, total α8 nAChR populations were examined by [^{3}H]-epibatidine binding following sucrose gradient centrifugation of unlabelled detergent-solubilized cell extracts. The sucrose gradient profile obtained under both conditions revealed a ~10S peak of radioligand binding similar to that observed for the muscle and electric organ nAChR (Figure 5.4.1). This demonstrates that α8 assembles into a oligomeric complex of similar

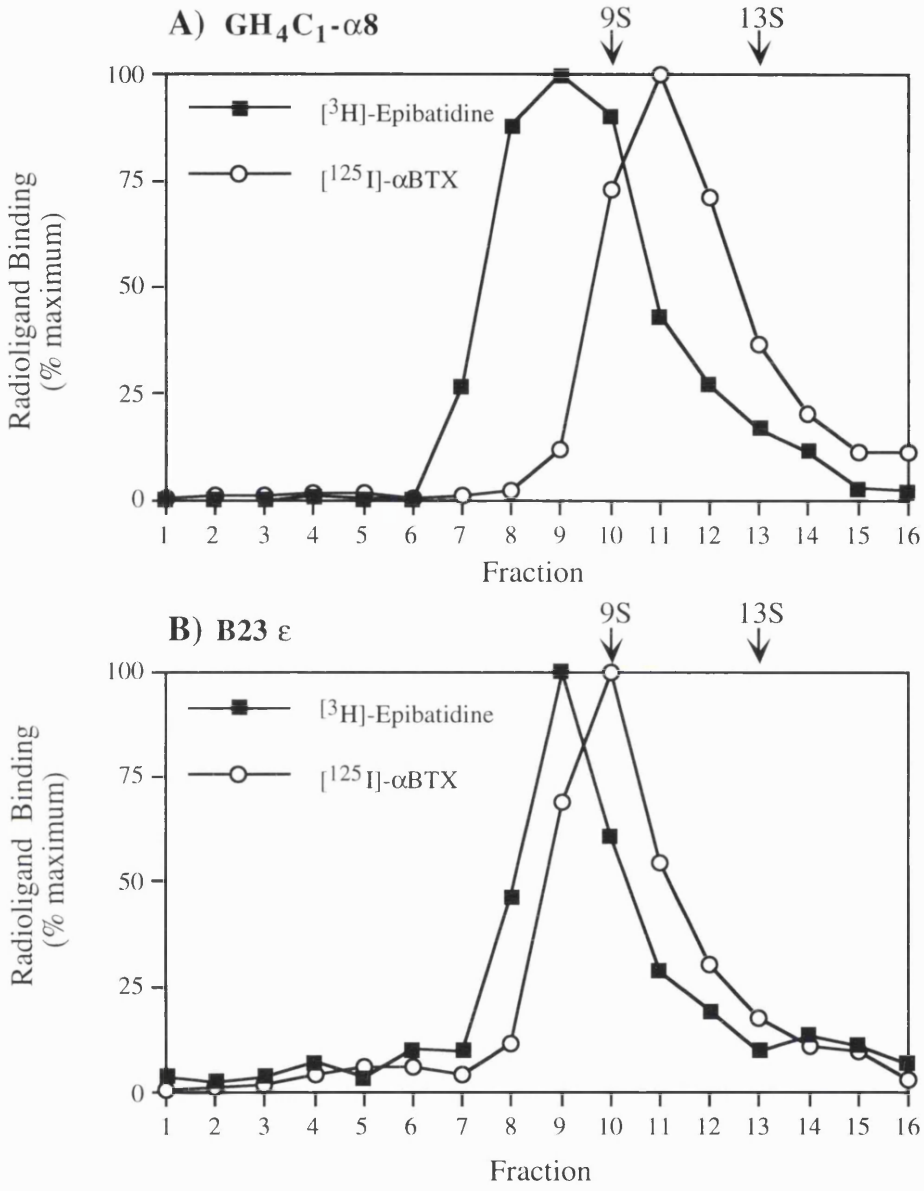

Figure 5.4.1. Sucrose gradient centrifugation of neuronal α8 nAChR and the muscle ($\alpha_2\beta\delta\varepsilon$) nAChR. **A**) The sucrose gradient profile of GH_4C_1 cells transiently transfected with the chick α8 nAChR subunit. **B**) The sucrose gradient profile of the mouse muscle ($\alpha_2\beta\delta\varepsilon$) nAChR stably expressed in the B23ε cell line. All samples were solubilized in lysis buffer containing 1% Triton X-100 and separated on a linear 5%-20% sucrose gradient. For unlabelled samples, individual fractions were taken and assayed for [^{3}H]-epibatidine binding (filled squares). Solubilized samples from intact cells which had been pre-labelled with [^{125}I]-αBTX were counted in a γ-counter (open circles). The data series are typical of one experiment which was repeated at least once, in its entirety, with identical results. The positions of the electric organ pentameric monomer (9S) and disulphide-linked dimer (13S) are shown.

buoyant density to that of the muscle and electric organ receptor and is also likely to be pentameric.

A similar sucrose gradient profile was observed for [^{125}I]-αBTX-labelled cell surface receptors from a polyclonal population of stably transfected SH-SY5Y-α8 cells. The amount of bound [^{125}I]-αBTX in the peak fractions of transfected SH-SY5Y-α8 cells (Figure 5.4.2A) demonstrates an approximate 30-fold upregulation of [^{125}I]-αBTX-binding sites compared to endogenous α7 expression levels in untransfected SH-SY5Y controls (Figure 5.4.2B).

It has been established that when the muscle or electric organ nAChR expressed in mammalian fibroblasts is labelled with [^{125}I]-αBTX, it sediments as a tight peak of 9S (Claudio, 1987; Sine and Claudio, 1991b). Under the conditions used in these sucrose gradients, this 9S sedimentation coefficient correlates to fraction 10 (see Figures 3.3.2 and 5.4.1). A small shift is observed in the peak fraction of bound radioligand when the mouse muscle nAChR is sedimented with and without prior labelling of α-BTX (Figure 5.4.1A). When mouse muscle nAChR is pre-labelled with [^{125}I]-αBTX and sedimented on a 5%-20% sucrose gradient, the peak fraction of bound [^{125}I]-αBTX sediments predominantly in fraction 10. However, when unlabelled receptor is sedimented on an identical sucrose gradient and the fractions are then subjected to radioligand binding, the peak fraction of bound [^{3}H]-epibatidine occurs predominantly in fraction 9.

Interestingly, when unlabelled and [^{125}I]-αBTX-labelled α8 nAChR are sedimented under identical conditions, a similar but more pronounced shift from fraction 9 (unlabelled α8 nAChR) to fraction 11 (αBTX-labelled α8 nAChR) is observed in the peak of bound radioligand (Figure 5.4.1B). This larger shift in the buoyant density of the αBTX-labelled α8 nAChR may be interpreted as evidence that more than two molecules (and possibly five) of αBTX bind to the α8 nAChR. Although the

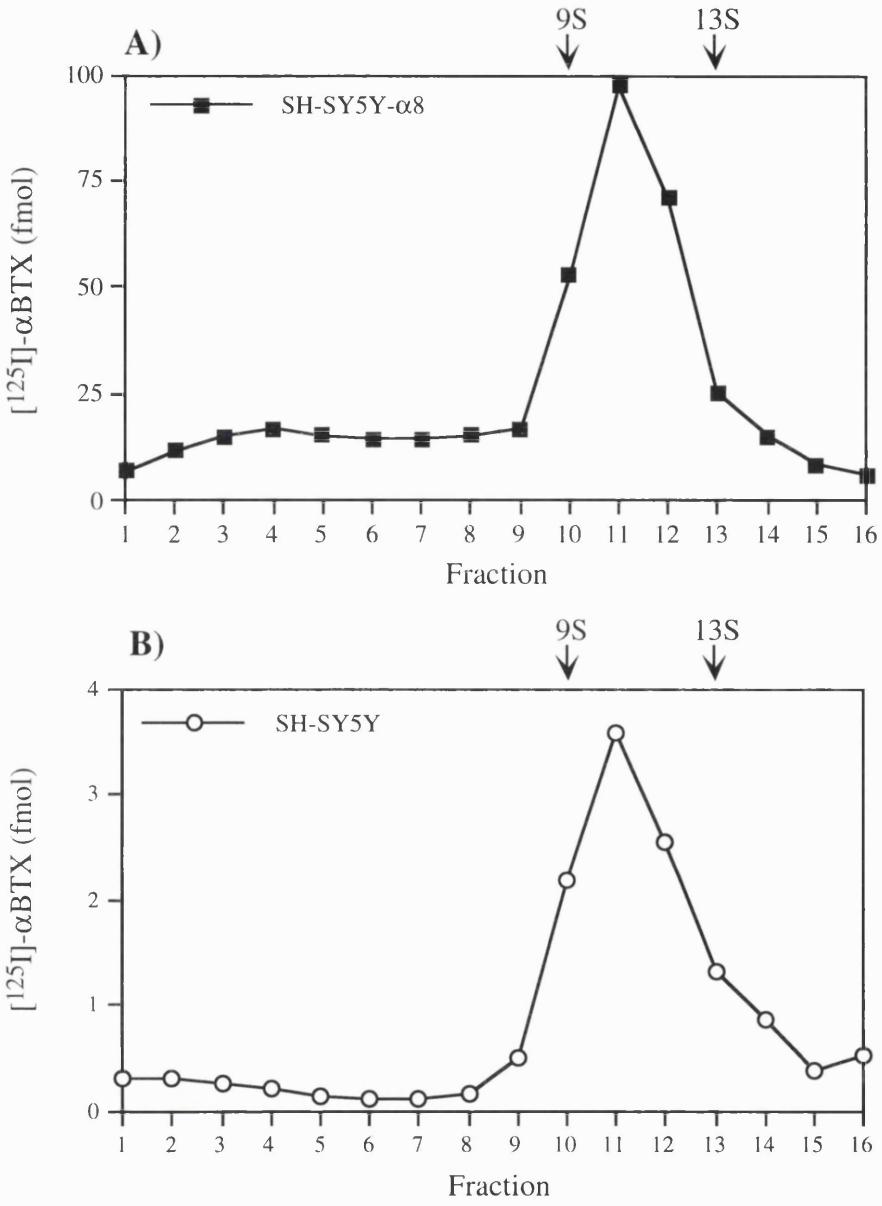

Figure 5.4.2. Sucrose gradient sedimentation of the neuronal α8 nAChR expressed in SH-SY5Y-α8 cells. Intact cells were labelled with 20nM [^{125}I]-αBTX, washed and solubilized in lysis buffer containing 1% Triton X-100. Soluble extracts were layered onto a 5-20% linear sucrose gradient. Sixteen fractions were taken from the top of the gradient and counted in a γ-counter. **A)** Sucrose gradient profile of [^{125}I]-αBTX-binding to a polyclonal population of stably transfected SH-SY5Y-α8 cells. **B)** Sucrose gradient profile of [^{125}I]-αBTX-binding to untransfected SH-SY5Y cells. Data points represent fmol bound [^{125}I]-αBTX per fraction for the equivalent of 1 x 10^6 cells loaded onto the gradient. The positions of the native electric organ nAChR pentameric monomer (9S) and dimer (13S) are shown.

relationship of buoyant density to molecular weight is not linear, each molecule of αBTX bound adds an additional molecular weight of ~8.9kDa.

5.5 Double-label immunofluorescent microscopy of α8 expressed in transfected cell lines.

Immunofluorescent microscopy was used to examine the distribution and conformation of expressed α8 protein in transfected cell lines. Using the combination of two different immunofluorescent labels, it was possible to discern both the population of αBTX-binding α8 receptors at the cell surface and the total population of α8 protein expressed throughout the cell. Firstly, α8 nAChRs expressed at the surface membrane of intact cells were labelled with rhodamine-conjugated αBTX (Rd-αBTX). Unbound Rd-BTX was removed by thorough washing and the cells were then fixed and permeabilized. The total population of α8 subunit protein was then labelled with mAb308, which recognises a linear epitope within the cytoplasmic loop, and a fluorescein-conjugated secondary antibody.

HEK293 cells transiently transfected with the α8 subunit exhibited clear intracellular immunofluorescent staining with mAb308 depicted by bright green fluorescein fluorescence (Figure 5.5.1A, top panel). Routinely, ~40% of cells were labelled with mAb308, which is similar to the estimated transfection efficiency of HEK293 cells determined by transfection experiments with the β-galactosidase reporter construct. The specificity of mAb308 for expressed α8 subunit protein is confirmed by the absence of staining of some cells within the same field, and the absence of staining in untransfected or mock transfected cells (data not shown). While still examining the same field of cells, the filter on the fluorescent microscope was used to switch from conditions which excite the fluorescein fluorophore to conditions which excite the rhodamine fluorophore and correspond to surface α8 nAChRs labelled with Rd-αBTX (middle panel). As was expected from radioligand binding data, no specific

Figure 5.5.1. Double label immunofluorescent microscopy of the α8 nAChR subunit expressed in transfected cell lines with mAb308 and Rd-αBTX. Transiently transfected HEK293-α8 cells (**A**), polyclonal stably transfected SH-SY5Y-α8 cells (**B**) and transiently transfected GH_4C_1-α8 cells (**C** & **D**) are shown. Cell surface receptors on intact cells were labelled with rhodamine-conjugated αBTX (Rd-αBTX, middle panel). Unbound toxin was removed by washing and the cells were fixed and permeabilized. Intracellular α8 protein was then labelled with mAb308 followed by a fluorescein-conjugated secondary antibody (top panel). Phase images of the same fields of cells are also shown (bottom panel).

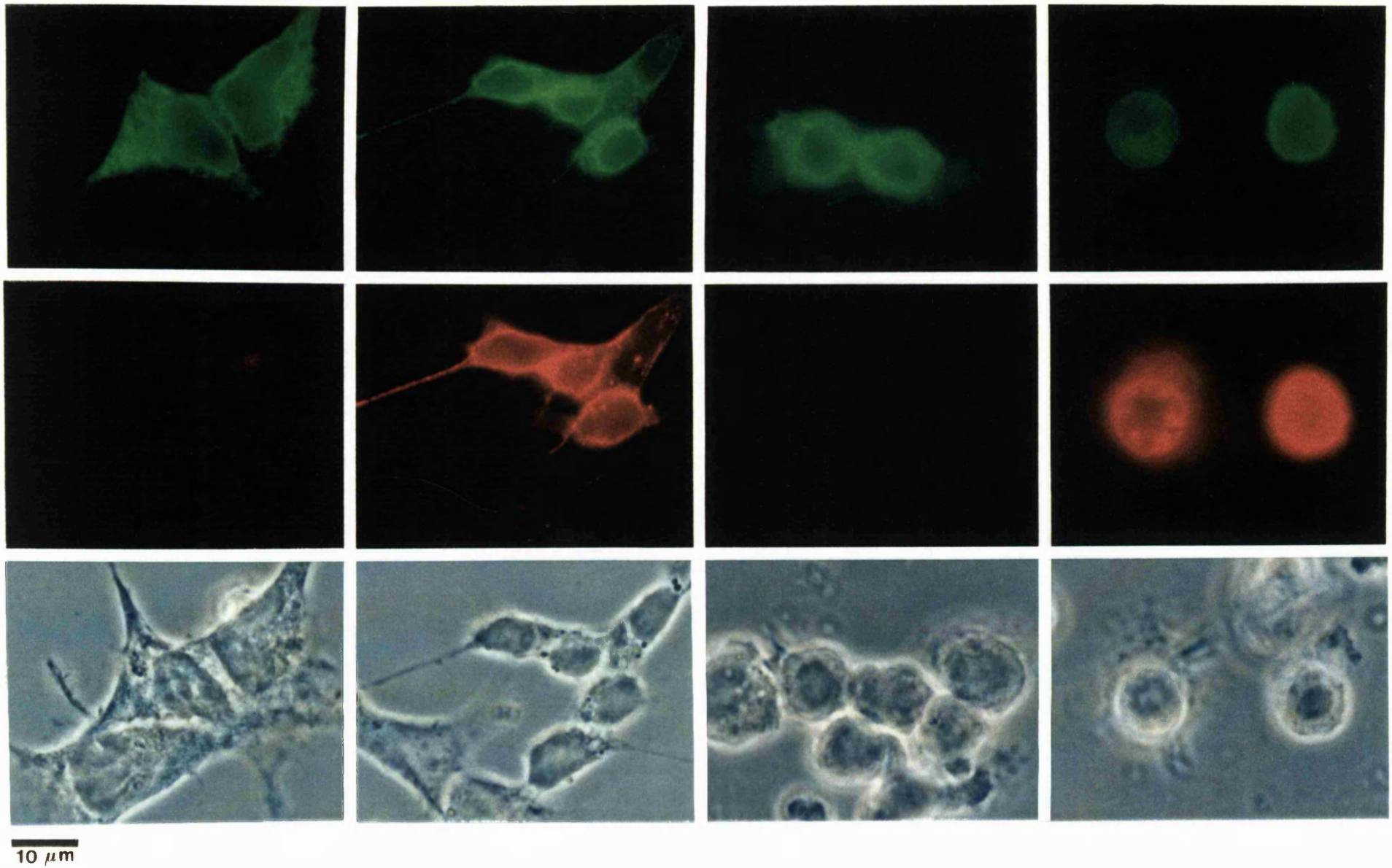
HEK-293-α8
SH-SY5Y-α8
GH4C1-α8
GH4C1-α8
10 μm

Rd-αBTX staining could be detected on the surface of the same transfected HEK293 cells shown to contain intracellular α8 protein (5.5.1A, middle panel).

In contrast, for the stably transfected polyclonal SHSY5Y-α8 cell line, all cells which show bright green intracellular staining with mAb308 and a fluorescein-conjugated secondary antibody (Figure 5.5.1B, top panel), also display intense surface staining with Rd-αBTX (Figure 5.5.1B, middle panel). This suggests that virtually every cell which expresses the α8 subunit also folds and assembles a proportion of α8 protein into a conformation which binds αBTX and is exported to the cell surface. The specificity of staining by both techniques is confirmed by the absence of positive labelling with either Rd-αBTX or mAb308 above background in some cells within the same field. No staining with mAb308 could be detected in untransfected SHSY5Y cells. No staining of Rd-αBTX above background can be detected in untransfected SH-SY5Y cells despite detectable levels of [^{125}I]-αBTX-binding (because of endogenous α7 expression) due to the lower sensitivity of immunofluorescent techniques.

Immunofluorescent staining of transiently transfected GH_4C_1-α8 cells reveals that only a subset of GH_4C_1 cells expressing intracellular α8 protein are able to correctly fold and assemble the α8 subunit into a conformation that is exported to the cell surface and able to bind αBTX. Intracellular staining with mAb308 reveals specific labelling of the α8 subunit in up to 20% of transfected GH_4C_1-α8 cells, but not in untransfected controls (shown by bright green fluorescence, Figure 5.5.1 C & D, top panels). By examining individual fields of double-labelled GH_4C_1-α8 cells brightly stained with mAb308 under conditions which excite Rd-αBTX, it was possible to demonstrate that not all cells which clearly contain an abundance of intracellular α8 protein possessed surface Rd-αBTX binding receptors (Figure 5.5.1 C & D, middle panels). As can be seen in Figure 5.5.1D, both transfected GH_4C_1-α8 cells expressing intracellular α8 protein (as visualised by green mAb308 staining) also

express surface αBTX-binding sites (indicated by red Rd-αBTX staining). However, Figure 5.5.1C demonstrates that within a different field of the same coverslip, two cells with brightly stained intracellular α8 protein, do not exhibit surface Rd-αBTX staining.

5.6 Summary

These results demonstrate that correct folding of the α8 nAChR into a conformation able to bind nicotinic radioligands and conformation-dependent antibodies is cell-type specific. HEK293 cells transiently transfected with the α8 subunit were shown to express high levels of α8 protein determined by metabolic labelling and immunoprecipitation with mAb308, but failed to produce detectable nicotinic radioligand binding. Furthermore, the monoclonal antibody mAb305 which recognizes a conformational epitope within the extracellular domain of the native α8 nAChR failed to recognise the α8 protein expressed in HEK293 cells by immunoprecipitation or immunofluorescent microscopy. In contrast to results with HEK293 cells, the α8 subunit expressed in SH-SY5Y cells readily folds into to conformation able to bind αBTX which is efficiently exported to the plasma membrane and is recognised by the conformation-dependent mAb305. A rat pituitary GH_4C_1 cell line which does not express endogenous nicotinic subunits was also shown to generate specific nicotinic radioligand binding sites following transient transfection with the α8 subunit. However, double-label immunofluorescent microscopy reveals that only a subset of transiently transfected GH_4C_1-α8 cells shown to express intracellular α8 protein are capable of correctly folding the α8 subunit into a conformation able to bind Rd-αBTX.

The results presented in this section are described in Cooper and Millar, 1998.

6.0 Current results and future directions

6.1 Radioligand binding of α7/5-HT$_3$ and α8/5-HT$_3$ chimeras expressed in HEK293 cells.

The previous three chapters have illustrated that the ability of the neuronal α7 and α8 nAChR subunits to fold correctly and acquire the ability to bind radioligands and conformation-dependent antibodies is critically dependent upon the host cell. This property does not seem to be shared by the hetero-oligomeric muscle nAChR or the homo-oligomeric serotonin 5-HT$_3$ receptor. Radioligand binding and functional expression have been obtained for both the muscle nAChR and the 5-HT$_3$ receptor in HEK293 cells which fail to correctly fold the α7 and α8 nAChR subunits.

Previously, the construction of five subunit chimeras which contain portions of the N-terminal region of the α7 receptor and the complementary C-terminal domain of the 5-HT$_3$ receptor has been reported (Eiselé *et al.*, 1993). Interestingly, this report states that four out of the five chimeras yielded [^{125}I]-αBTX-binding sites on expression in HEK293 cells. The fifth chimera lacks part of the N-terminal domain containing residues thought to form part of the ligand binding site of the nAChR (Dennis *et al.*, 1988), including two highly conserved adjacent cysteine residues, and does not form [^{125}I]-αBTX-binding sites in HEK293 cells. The investigators did not report whether wild-type α7 forms [^{125}I]-αBTX-binding sites when expressed in HEK293 cells.

Two chimeric constructs were generated which encoded for α7 or α8 up to a few amino acids before the first putative transmembrane domain (to Valine^{201} for α7 and the aligned Isoleucine^{201} in α8) and continued with *C*-terminal region of the 5-HT$_3$ subunit, including the four putative transmembrane domains and connecting loops (see Figure 6.1.1A and 6.1.1B) (Details of the construction of these and other chimeric constructs used in this chapter are presented in more detail in materials and

Figure 6.1.1. Structure and radioligand binding properties of $\alpha7/5HT_3$ and $\alpha8/5HT_3$ chimeric constructs.

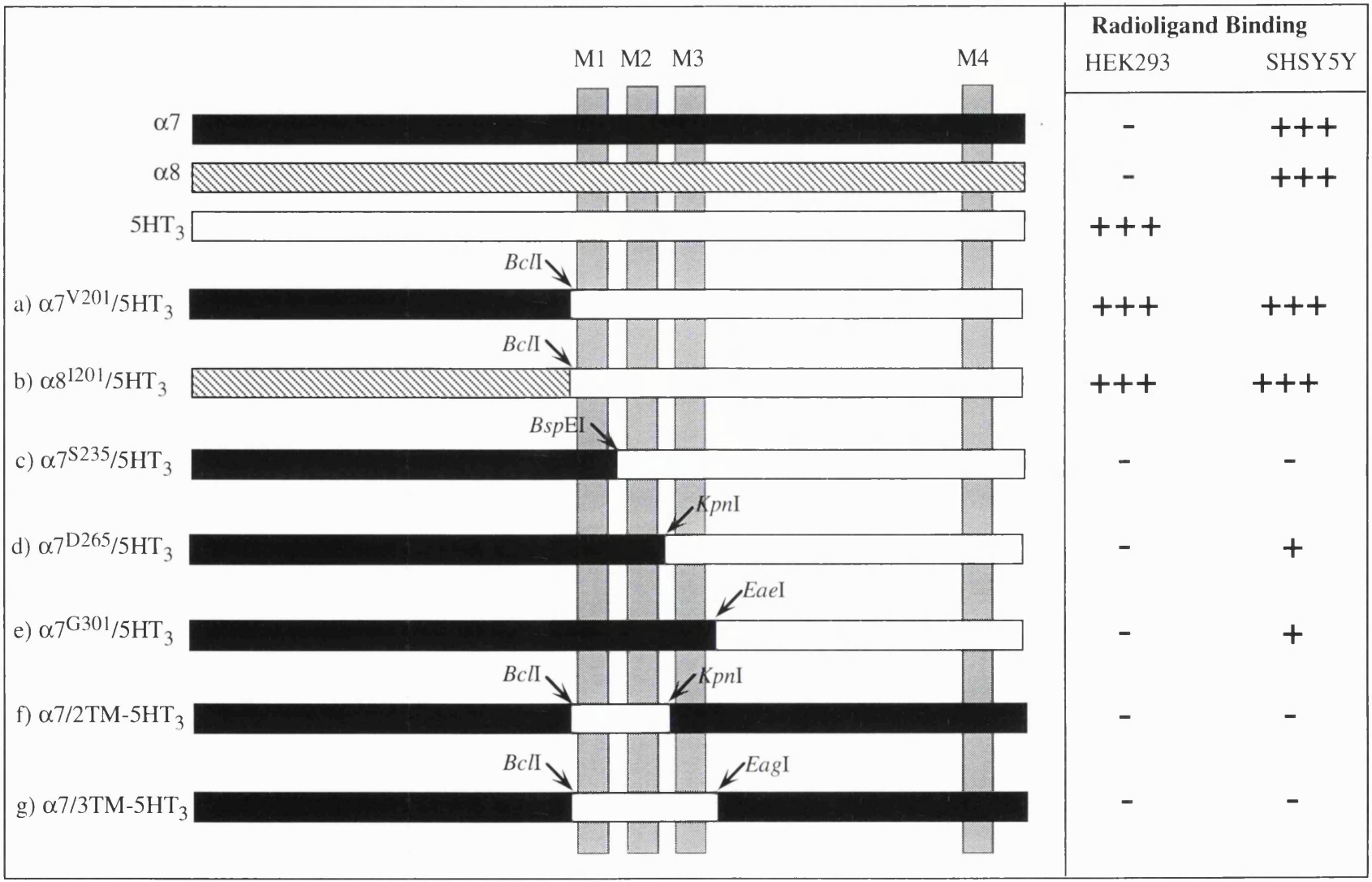

Radioligand Binding	
HEK293	SHSY5Y
-	+++
-	+++
+++	
+++	+++
+++	+++
-	-
-	+
-	+
-	-
-	-

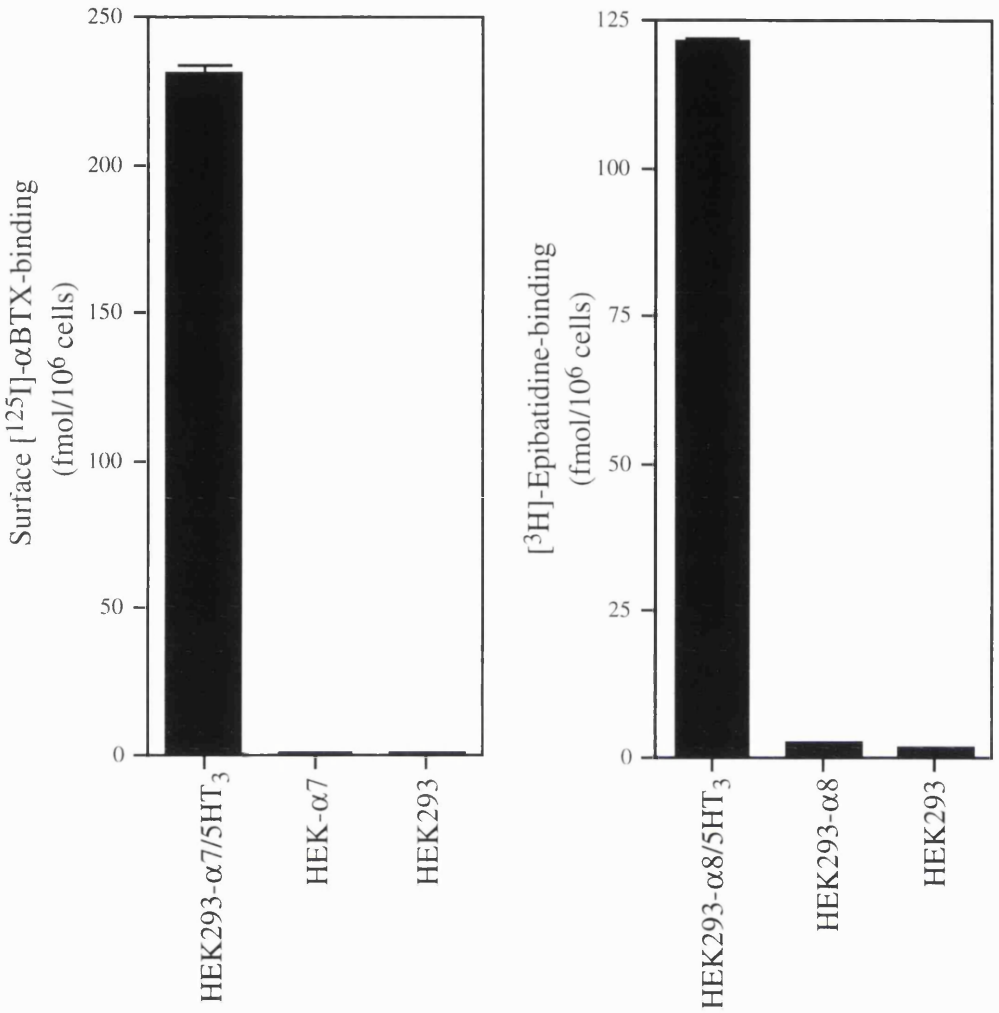

Figure 6.1.2. Radioligand binding to HEK293 cells transiently transfected with $\alpha7^{V201}$/5-HT_3 or $\alpha8^{I201}$/5-HT_3 chimeras. **A)** HEK293 cells were transfected with the $\alpha7^{V201}$/5-HT_3 chimeric construct, the α7 nAChR subunit or mock transfected with pZeoSV2(+). Intact cells were assayed for surface [^{125}I]-αBTX-binding ~40 hours following transfection. Non-specific binding was determined by the addition of 100μM methyllycaconitine (MLA) and has been subtracted. Data points represent the means of triplicate samples. **B)** HEK293 cells were transfected with the $\alpha8^{I201}$/5-HT_3 chimeric construct, the α8 nAChR subunit or mock transfected with pZeoSV2(+). Cells were harvested ~40 hours following transfection and specific [^{3}H]-epibatidine-binding to cell membranes was determined. Non-specific binding was determined by the addition of 500μM carbamylcholine plus 500μM nicotine and has been subtracted. Data points represent the means of triplicate samples.

methods, Section 2.2). These constructs are similar to an α7/5-HT_3 chimera (called V201) described by Eiselé and co-workers who demonstrated that this chimeric subunit formed functional homo-oligomeric channels when expressed in *Xenopus* oocytes which were activated by nicotinic agonists but exhibited channel properties characteristic of the 5-HT_3 receptor.

The $\alpha7^{V201}$/5-HT_3 and $\alpha8^{I201}$/5-HT_3 cDNA constructs were transiently transfected into HEK293 cells and subjected to radioligand binding experiments. In marked contrast to results obtained by expression of α7 or α8 nAChR subunits in HEK293 cells, the $\alpha7^{V201}$/5-HT_3 and $\alpha8^{I201}$/5-HT_3 chimeric subunits produced very high levels of surface [^{125}I]-αBTX- and [^{3}H]-epibatidine-binding sites, respectively (Figure 6.1.2).

6.2 Double-label immunofluorescent microscopy of the α7/5-HT_3 and α8/5-HT_3 chimeras expressed in HEK293 cells.

Double-label immunofluorescent microscopy was performed on HEK293 cells transiently transfected with pZeoSV-$\alpha7^{V201}$/5-HT_3 and pZeoSV-$\alpha8^{I201}$/5-HT_3 chimeras (Figure 6.2.1). Cell surface receptors on intact cells were first labelled with Rd-αBTX. Unbound toxin was removed by washing and the cells were then fixed and permeabilized. Intracellular protein was stained with the polyclonal antibody sera pAb-α5HT_3, raised against a fusion protein containing the intracellular loop region of the 5-HT_3 subunit (Turton *et al.*, 1993), followed by a fluorescein-conjugated secondary antibody. Immunofluorescent microscopy revealed that all cells which showed clear intracellular staining with the polyclonal antibody pAb-α5HT_3 (indicated by bright green fluorescein staining) (Figure 6.2.1, top panel), also possessed very bright surface staining with Rd-αBTX (red fluorescence) (Figure 6.2.1, middle panel). Radioligand binding data and immunofluorescent staining patterns demonstrate that both $\alpha7^{V201}$/5-HT_3 and $\alpha8^{I201}$/5-HT_3 chimeric subunits

Figure 6.2.1. Double label immunofluorescent microscopy of HEK293 cells transiently transfected with $\alpha7^{V201}/5HT_3$ or $\alpha8^{I201}/5HT_3$ chimeras. HEK293 cells were transiently transfected with pZeoSV-$\alpha7^{V201}/5HT_3$ (**A**) or pZeoSV-$\alpha8^{I201}/5HT_3$ (**B**) by lipofection. Cell surface receptors on intact cells were labelled with rhodamine-conjugated αBTX (Rd-αBTX, middle panels). After fixation and permeabilization, cells were labelled with a polyclonal antibody raised against a fusion protein from the intracellular loop region of the 5-HT_3 subunit (pAb-$5HT_3$) followed by a fluorescein-conjugated secondary antibody (top panels). Phase images of the same fields of cells are also shown (bottom panels).

HEK-293
$\alpha 7^{(V201)}$/5-HT_3

HEK-293
$\alpha 8^{(I201)}$/5-HT_3

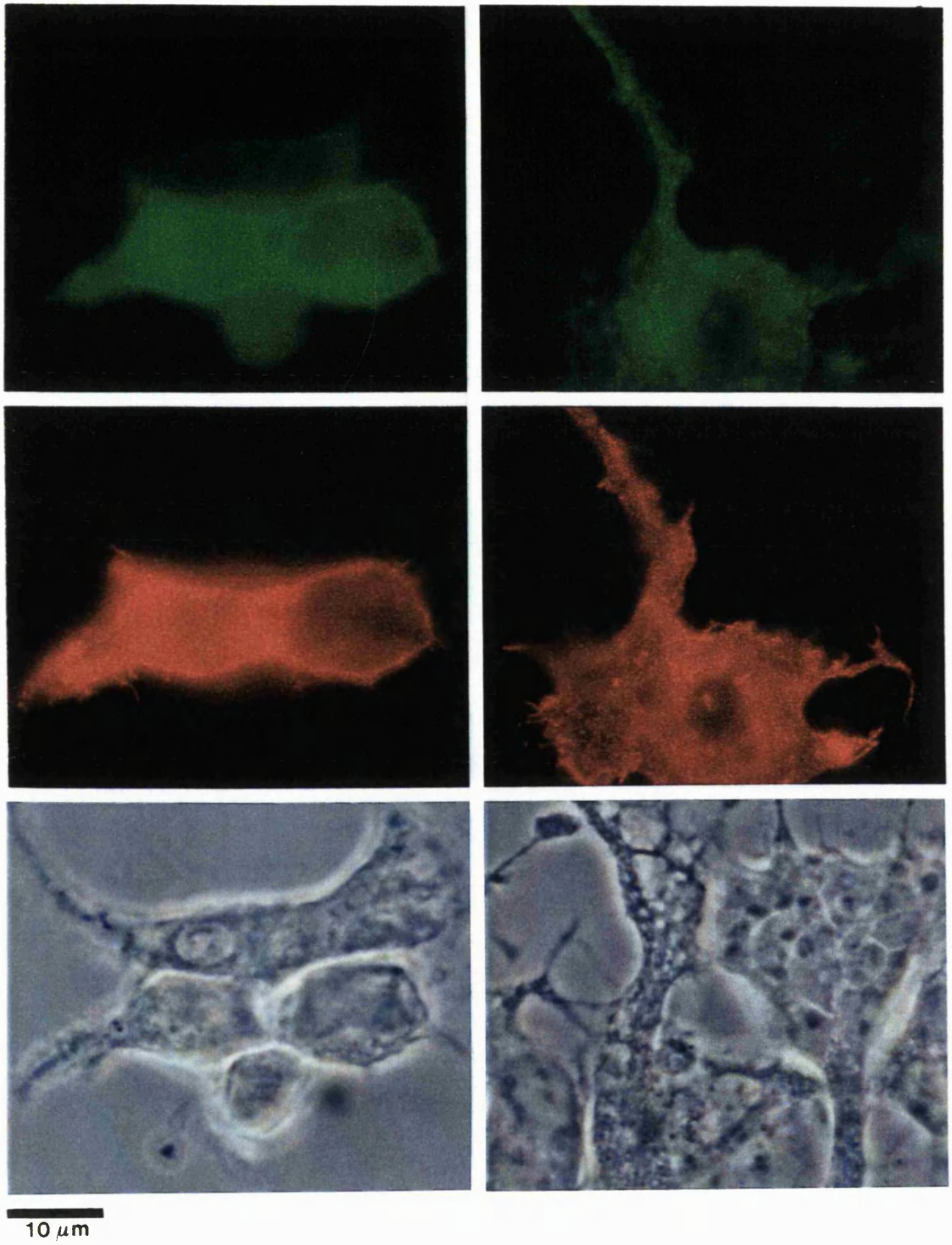

10 μm

readily fold into a conformation able to bind αBTX and that these receptors are efficiently exported to the cell surface. Expression of both the $\alpha7^{V201}$/5-HT_3 and $\alpha8^{I201}$/5-HT_3 chimeric subunits in several cell types has produced no evidence of cell-specific misfolding. This would imply that the *C*-terminal domain of the α7 and α8 subunits, including the putative transmembrane domains and large intracellular loop region, are responsible for inducing the cell-specific misfolding of these subunits in HEK293 cells.

6.3 Construction of a panel of α7/5HT_3 chimeric constructs.

To try and elucidate which regions of the *C*-terminal domain of the α7 and α8 subunits are involved in the apparent cell-specific misfolding phenomenon observed in this study, a panel of α7/5-HT_3 chimeras were generated (see Figure 6.1.1 C-G). Three additional chimeric constructs were generated which encoded for the *N*-terminal region of α7 up to a few residues just before M2 ($\alpha7^{S235}$/5-HT_3; Figure 6.1.1C), before M3 ($\alpha7^{D265}$/5-HT_3;Figure 6.1.1D) and just after M3 ($\alpha7^{G301}$/5-HT_3; Figure 6.1.1E) and continued with the complementary *C*-terminal region of the 5-HT_3 subunit (determined by subunit alignments). Two further chimeras were constructed which predominantly contain sequences encoding for the α7 subunit, but which comprise sequences encoding two transmembrane domains (M1 and M2, α7/2TM-5HT_3; Figure 6.1.1F) or three transmembrane domains (M1, M2 and M3; α7/3TM-5HT_3, Figure 6.1.1G) from the 5-HT_3 subunit.

The chimeric constructs were transiently transfected into both the HEK293 and SH-SY5Y cell lines and assayed for surface [^{125}I]-αBTX-binding sites. By using SH-SY5Y cells, which correctly fold the α7 subunit, this indicates which constructs form

viable chimeric subunits which are capable of forming [^{125}I]-αBTX-binding sites. Expression of viable constructs in HEK293 cells then demonstrates whether these chimeras are also able to bind αBTX in this cell line or whether they exhibit cell-dependent folding, like α7, and fail to form αBTX-binding sites in HEK293 cells.

Two of these constructs, $\alpha7^{D265}$/5-HT$_3$ and $\alpha7^{G301}$/5-HT$_3$, produced specific [^{125}I]-αBTX-binding when transiently expressed in SH-SY5Y cells, although somewhat less efficiently than that observed for the $\alpha7^{V201}$/5-HT$_3$ chimera (Figure 6.1.1). However, transient transfection of HEK293 cells with $\alpha7^{D265}$/5-HT$_3$ and $\alpha7^{G301}$/5-HT$_3$ failed to produce specific [^{125}I]-αBTX-binding. This result indicates that both the $\alpha7^{D265}$/5-HT$_3$ and $\alpha7^{G301}$/5-HT$_3$ chimeras do not contain the regions of the 5-HT$_3$ subunit which alleviate cell-specific misfolding in HEK293 cells, characteristic of the α7 subunit.

Unfortunately the three other chimeras failed to produce specific [^{125}I]-αBTX-binding when expressed in either SH-SY5Y or HEK293 cells. This probably indicates that these constructs do not produce stable chimeric subunit proteins and misfold and/or are degraded in both cell lines. Immunoprecipitation of subunit protein of the predicted size and extensive sequencing of the constructs is required to determine if a mutation has been introduced through PCR. At this time no information can be generated from these constructs and further investigation and the production of additional chimeras will be necessary to determine more precisely which domains of the C-terminal region of α7 are involved in cell type-specific misfolding. However, these data may suggest that to generate a viable chimeric subunit construct containing a minimal amount of the 5-HT$_3$ subunit, it may be necessary to include all four putative transmembrane domains from a single subunit for correct folding of the protein, in any cell line.

6.4 Future Directions

To determine which factor(s) influence the host cell-specific folding of the α7 and α8 nAChR subunits, my current research focuses on expression cloning using a cDNA library generated from the SH-SY5Y cell line. Expression cloning in *Xenopus* oocytes has been used to isolate several ligand-gated ion channels such as the 5-HT_3 receptor from a NCB-20 cDNA library (Maricq *et al.*, 1991) and the ionotrophic ATP receptor from a PC12 cDNA library (Brake *et al.*, 1994). More recently, expression cloning in mammalian HEK293 cells resulted in the identification of the gene encoding the capsaicin ion channel receptor from a dorsal root ganglion cDNA library (Caterina *et al.*, 1997). For this project, pools of cDNA clones will be co-transfected with the pcDNA1neo-α7 construct into HEK293 cells. Transfected cells capable of correctly folding the α7 subunit will be identified by Rd-αBTX immunofluorescent staining. The simplicity of the Rb-αBTX staining and the ability to screen large numbers of cells quickly should be advantageous. Given that the component(s) required to facilitate correct folding the α7 subunit are successfully co-transfected into individual HEK293 cells, and a sufficient amount of correctly folded α7 protein is expressed, this technique could potentially identify factor(s) known to be expressed in the SH-SY5Y cell line which permit the correct folding of the α7 subunit.

Discussion

7.0 Discussion

7.1 The correct folding of the α7 nAChR subunit is host cell-specific

Expression of the neuronal nAChR α7 subunit in *Xenopus* oocytes generates functional ion channels which are characterized by a rapidly densensitizing response which can be blocked by nanomolar concentrations of αBTX (Couturier *et al.*, 1990a; Anand *et al.*, 1993b; Seguela *et al.*, 1993; Peng *et al.*, 1994b; Garcia-Guzman *et al.*, 1995). Although neuronal α7 nAChRs expressed in oocytes bind αBTX with high affinity (Anand *et al.*, 1993b; Peng *et al.*, 1994b), stable transfection of the rat neuronal nAChR α7 subunit into mouse L929 cells, mouse 3T3 cells or *Drosophila* S2 cells, in three different expression vectors (pMSG, pSVK3 and pRmHa3), failed to produce a clonal or polyclonal cell line which exhibits specific [^{125}I]-αBTX-binding sites. The reason for the absence of specific [^{125}I]-αBTX-binding to cell lines stably transfected with the α7 subunit is unclear. One possible explanation would be that problems had arisen due to the subcloning of the a7 cDNA into the plasmids used for stable expression. However, the pcDNA1neo-α7 construct, from which the rat α7 cDNA was subcloned, was able to generate functional homo-oligomeric channels sensitive to αBTX following nuclear injection into *Xenopus* oocytes (Seguela *et al.*, 1993). In addition, the same pcDNA1neo-α7 plasmid preparation used in these experiments was shown to form functional ion channels when transiently expressed in *Xenopus* oocytes (electrophysiological data generated in the laboratory of Prof. D. Colquhoun, Department of Pharmacology, University College London).

To determine the fate of the α7 subunit expressed in cultured cells, the pcDNA1neo-α7 construct was transfected into a panel of 9 mammalian cell lines which were then metabolically labelled to verify the presence of α7 protein, and a duplicate sample assayed for [^{125}I]αBTX-binding. High levels of the α7 subunit in all cell lines could be detected by metabolic labelling and immunoprecipitation with a monoclonal antibody raised against an intracellular linear epitope (mAb319). The apparent

molecular weight of α7 expressed in these cell lines was estimated to be ~58 kDa and is similar to that reported for the α7 subunit immunoprecipitated from rat and chick brain (Gotti *et al.*, 1992; Dominguez Del Toro *et al.*, 1994). However, in only two cell lines (PC12 and SH-SY5Y) could the transfected α7 subunit bind [^{125}I]-αBTX.

The successful overexpression of recombinant α7 nAChRs in SH-SY5Y cells has previously been reported (Puchacz *et al.*, 1994). In agreement with these results, a significant upregulation in surface [^{125}I]-αBTX-binding sites was observed in polyclonal PC12 and SH-SY5Y cell lines stably transfected with the α7 cDNA, compared with levels of endogenous α7 expression in untransfected cells, and a clonal SH-SY5Y-α7#7 cell line which expressed a ~20-fold increase in specific [^{125}I]-αBTX-binding was isolated. Saturation binding analysis demonstrated that the α7 subunit expressed in untransfected and transfected SH-SY5Y cells binds [^{125}I]-αBTX with high affinity (K_d = 0.6 - 0.7 nM), which correlates with previous reports of the estimated affinity of [^{125}I]-αBTX for the human α7 nAChR expressed in SH-SY5Y cells (K_d = ~1 nM) (Peng *et al.*, 1994b). Sucrose gradient sedimentation revealed that the α7 subunit expressed in transfected and untransfected PC12 and SH-SY5Y forms a complex which sediments with a buoyant density similar to that of the muscle receptor, and is likely to be pentameric.

Three monoclonal antibodies which recognise conformation-dependent epitopes within the extracellular domain of the native chick brain α7 nAChR (mAbs OAR1a, OAR5a and OAR11b) (Betz and Pfeiffer, 1984) were able to immunoprecipitate metabolically labelled α7 protein from solubilized α7-transfected and untransfected SH-SY5Y cells. In addition, incubation of intact SH-SY5Y-α7#7 cells with mAb OAR1a, OAR5a or OAR11b followed by a rhodamine-conjugated secondary antibody resulted in the specific immunofluorescent staining of cell surface receptors. Immunoprecipitation of metabolically labelled protein and immunofluorescent staining of transiently transfected HEK293-α7 cells revealed that in contrast to results

obtained with mAb319, none of the three conformation-dependent antibodies could detect α7 protein expressed in transfected HEK293-α7. The absence of [^{125}I]-αBTX-binding and the inability of antibodies which recognize conformational epitopes to detect the α7 subunit expressed in transfected HEK293 cells, indicates that α7 is misfolded. Recent reports demonstrate that in the chick fibroblast QT-6 cell line, the α7 subunit inefficiently folds into a conformation able to bind αBTX, and incorrectly folded α7 protein appears to be quickly degraded (Kassner and Berg, 1997). In addition, the four muscle nAChR subunits when expressed individually in fibroblast cells, misfold and are rapidly degraded (Paulson*et al.*, 1991; Ross *et al.*, 1991) . However, throughout this project, the 58 kDa protein corresponding to the α7 subunit was often detected as a discreet band, even in cell lines which failed to generate αBTX-binding, with little evidence for gross degradation.

Sucrose gradient sedimentation and immunoprecipitation of metabolically labelled transfected SH-SY5Y-α7#7 and HEK293-α7 cells showed that the peak of α7 subunit protein from solubilized SH-SY5Y-α7#7 cells co-migrates with the peak of [^{125}I]-αBTX-binding in this cell line. This suggests that the majority of α7 protein expressed in SH-SY5Y-α7#7 cells assembles into a 9S complex which appears to be the predominant species able to bind αBTX, consistent with other reports (Anand *et al.*, 1993b; Kassner and Berg, 1997). However, the sedimentation profile of the α7 subunit expressed in transfected HEK-293 cells resembles a heterogeneous population of α7 subunit complexes distributed throughout the entire sucrose gradient, often accompanied by high molecular weight aggregates. This suggests that the α7 does not oligomerize efficiently in HEK293 cells and probably forms non-specific protein aggregates. This is similar to what is observed in mouse fibroblasts transfected with single subunits of the *Torpedo* nAChR, which in the absence of other nAChR subunits misfold, and form non-productive protein aggregates (Paulson *et al.*, 1991).

7.2 The α7-FLAG construct demonstrates that recombinant α7 forms αBTX-binding sites in PC12 and SH-SY5Y cells.

Because both PC12 and SH-SY5Y cell lines express the α7 subunit endogenously (Rogers *et al.*, 1991; Lukas *et al.*, 1993; Henderson *et al.*, 1994), it was necessary to distinguish between basal levels of [^{125}I]-αBTX-binding due to endogenous α7 expression and [^{125}I]-αBTX-binding sites generated by recombinant α7. A novel epitope in the form of a "FLAG-tag" octopeptide, specifically recognized by the monoclonal antibody mAbFLAG M2 (Hopp *et al.*, 1988), was introduced by site-directed mutagenesis into the cytoplasmic loop region of the α7 cDNA. PC12 and SH-SY5Y cell lines stably transfected with the α7-FLAG cDNA exhibited an 8-10 fold upregulation in surface [^{125}I]-αBTX-binding sites, similar to that obtained with wild-type α7, compared with untransfected cells. Increased levels in cell surface [^{125}I]-αBTX-binding receptors were immunoprecipitated with mAbFLAG M2 confirming that the upregulation of [^{125}I]-αBTX-binding in α7-transfected PC12 and SH-SY5Y cell lines is due to expression of the recombinant α7 subunit.

7.3 HEK293 cells express functional rat muscle nAChRs and homo-oligomeric 5-HT$_3$ receptors.

Despite the inability of HEK293 cells to correctly fold the α7 subunit, functional cell surface expression of the hetero-oligomeric rat muscle nAChR and the homo-oligomeric serotonin 5-HT$_3$ receptor was obtained in transiently transfected HEK293 cells. Transient transfection of HEK293 cells with the four rat muscle α, β, γ and δ nAChR subunits, or the homo-oligomeric 5-HT$_3$ subunit, resulted in high levels of specific radioligand binding. Both the rat muscle nAChR and the 5-HT$_3$ receptor expressed in HEK293 cells formed complexes which sedimented with a buoyant density of 9-10S, indicating the successful oligomerization and assembly into pentameric complexes. By loading transfected cells with the cell permeable, calcium-

sensitive dye Fura 2-AM, it was possible to demonstrate by fluorimetry experiments that the rat muscle nAChR and the 5-HT_3 receptor expressed in HEK293 cells were functional, and readily produced clear elevations in intracellular calcium levels in response to the application of specific agonists. HEK293 cells appear to possess all of the intracellular machinery required for the correct folding, assembly and export to the plasma membrane for these ligand-gated ion channels and indicates that there is a genuine difference in the assembly pathway of the α7 homo-oligomer not fulfilled by HEK293 cells.

7.4 Isolates of established cultured cell lines differ in their ability to fold the α7 subunit

Gopalkrishnan *et al* (1995) reported the successful functional expression of the human α7 subunit in HEK293 cells while this work was in progress (Gopalakrishnan *et al.*, 1995a). The human and rat isoforms of the α7 nAChR subunit are highly homologous (~94% sequence identity), although species-specific differences in the pharmacological properties of the human and rat α7 homo-oligomers expressed in *Xenopus* oocytes have been documented (Seguela *et al.*, 1993; Peng *et al.*, 1994b). However, by expression of the human α7 subunit in HEK293 cells it was possible to demonstrate that the misfolding of the rat α7 subunit in this cell line was not due to species-specific differences in the cDNA sequence. Efficient translation of transfected rat and human α7 cDNAs was confirmed by metabolic labelling and immunoprecipitation but despite high levels of protein synthesis, no specific surface binding of [^{125}I]-αBTX could be detected in HEK-293 cells transiently transfected with either the rat or human α7 subunit isoforms. These results indicate that there may be differences between the isolates of HEK293 cells used in the two laboratories which affects the folding of the α7 subunit expressed in this cell line. This suggestion is supported by the recent results in our laboratory which demonstrate the correct folding of the rat α7 subunit into a conformation able to bind [^{125}I]-αBTX in an

isolate of HEK293 cells obtained from Dr. Sarah Lummis, Laboratory for Molecular Biology, Cambridge.

The observation that different isolates of HEK293 cells possess different abilities to correctly fold the α7 subunit is paralleled by evidence that different isolates of the rat PC12 cell line, which express endogenous nicotinic subunits including α7, differ in their ability to express αBTX-binding receptors irrespective of levels of endogenous α7 mRNA and protein (Blumenthal *et al.*, 1997). Blumenthal and co-workers demonstrated that the amplitudes of the αBTX-sensitive, rapidly desensitizing ACh-induced current observed in cells from three different PC12 isolates, correlated well with the corresponding levels of [^{125}I]-αBTX-binding sites. In contrast, the levels of [^{125}I]-αBTX-binding sites showed no correlation with levels of α7 mRNA present. Cells with high levels of α7 mRNA and detectable α7 protein were negative for toxin binding. Furthermore, following the transfection and overexpression of recombinant chick α7 cDNA, PC12 cell isolates still differed in their ability to produce [^{125}I]-αBTX-binding sites.

7.5 N-endoglycosidase analysis indicates that the α7 subunit is retained in the endoplasmic reticulum

Treatment with specific N-endoglycosidases indicate that the α7 subunit expressed in HEK293 cells does not exit the endoplasmic reticulum (ER). Misfolded proteins are known to be retained within the endoplasmic reticulum and are often rapidly degraded (Chen *et al.*, 1988; Hurtley *et al.*, 1989; Paulson and Claudio, 1990; Green *et al.*, 1991b). The α7 subunit expressed in transfected HEK293 cells was metabolically labelled, immunoprecipitated, and digested with EndoF (which cleaves simple and complex N-linked oligosaccharides) and with EndoH (which cleaves only simple high-mannose N-linked oligosaccharides). The processing of simple high mannose carbohydrates to complex EndoH-resistant carbohydrate groups occurs in

the Golgi (Kornfeld *et al.*, 1995). The glycosylated form of the α7 subunit was sensitive to digestion with both EndoF and EndoH which indicates that the carbohydrate moieties of α7 have not been modified in the Golgi apparatus suggesting that α7 protein is retained in the endoplasmic reticulum or pre-Golgi compartment. Similar results have been reported with the α7 subunit expressed in COS7 cells, which fails to bind αBTX and is sensitive to digestion with both EndoF and EndoH and so presumably also does not exit the ER (Chen *et al.*, 1998).

Oligomerization studies of the mouse muscle $\alpha_2\beta\delta\varepsilon$ receptor expressed in mouse fibroblasts reveals that unassembled subunits are retained in the ER (Ross *et al.*, 1991). The formation of the αBTX-binding site and the folding and oligomerization of the muscle nAChR, which are the rate limiting steps in nAChR assembly, occurs in the endoplasmic reticulum (Smith *et al.*, 1987; Ross *et al.*, 1991). Following assembly, nAChRs move rapidly into the Golgi and through to the plasma membrane The muscle nAChR expressed in a variant of C2 muscle cells is found to be retained within the ER (Gu *et al.*, 1989). Glycosylation analysis showed that both the δ and γ subunits lack EndoH-resistant oligosaccharides and sub-cellular fractionation revealed that virtually all intracellular nAChR was located within the ER. However, the variant C2 cells were shown to express normal amounts of surface insulin receptor and transferrin receptor. In addition, N-linked glycosylation of endogenous fibronectin and infected influenza virus haemagglutinin protein was examined, both were found to be fully glycosylated and exported to the cell surface with normal kinetics. Interestingly, a small fraction of nAChR was found to be normally glycosylated and exported to the cell surface (Gu *et al.*, 1989). These observations raise the question of whether the defect lies within a mutation of the nAChR or is the result of a defect in another protein required for the correct post-translational modification of the nAChR, but not for the maturation pathways of the majority of cellular proteins. This possibility strongly resembles the phenomenon observed in

this study for the cell-dependent folding of α7, which appears to be due to unidentified factors which influence its folding and assembly.

7.6 Attempts to alleviate the misfolding of α7

cAMP Treatment

It has been reported that treatments which elevate intracellular cAMP increase the efficiency of assembly of the cloned *Torpedo* and mouse muscle nAChR expressed in mouse fibroblast cells by two- to three-fold (Green *et al.*, 1991b; Ross *et al.*, 1991). A similar two-fold upregulation in surface [^{125}I]-αBTX-binding sites was detected in SH-SY5Y-α7#7 cells treated with a cell permeable cAMP analogue (8-bromo-cAMP) and the phosphatase inhibitor IBMX, compared with untreated cells. However, elevations in intracellular cAMP levels was unable to overcome the misfolding of the α7 subunit transiently expressed in HEK293-α7 cells.

The upregulation of cell surface levels of the mouse muscle nAChRs in response to elevations in intracellular cAMP occurs through post-translational mechanisms involving increased assembly efficiency of nAChR subunits and correlates with increased phosphorylation of the γ-subunit (Green *et al.*, 1991b; Green *et al.*, 1991a). Mutagenesis of identified phosphorylation sites revealed that phosphorylation of the γ-subunit was not responsible for the cAMP-stimulated upregulation of surface nAChRs and it was proposed that increased receptor expression was mediated through a separate mechanism which may involve a cellular protein involved in the folding and/or assembly of protein complexes (Jayawickreme *et al.*, 1994). The cAMP-induced upregulation in surface αBTX-binding receptors expressed in the SH-SY5Y-α7#7 cell line may occur through similar post-translational mechanisms although whether it correlates with receptor phosphorylation was not determined.

Expression of the prolyl isomerase, cyclophilin

A role for the peptidyl-prolyl isomerase, cyclophilin, in the efficient functional expression of the homo-oligomeric α7 and 5-HT_3 receptors expressed in *Xenopus* oocytes has recently been established (Helekar *et al.*, 1994; Helekar and Patrick, 1997). Functional responses elicited by either the α7 or 5-HT_3, but not the hetero-oligomeric muscle nAChR were reduced by treatment with Cyclosporin A, which specifically inhibits cyclophilin. This blockade can be reversed by overexpression of a cytoplasmic isoform of rat brain cyclophilin. Co-expression of the cytoplasmic or the ER-specific isoforms of rat brain cyclophilin, with rat α7 in HEK293 cells, did not result in the formation of αBTX-binding sites.

These results, and the successful functional expression of the homo-oligomeric 5-HT_3 subunit in HEK293 cells, do not suggest a requirement for cyclophilin for the correct folding and assembly of α7 receptors able to bind αBTX in HEK293 cells. A similar conclusion was drawn following Cyclosporin A treatment of cultured chick ciliary ganglion neurones and a chick fibroblast QT-6 cell line stably expressing the chick α7 subunit, which had no effect on levels of [^{125}I]-αBTX-binding (Kassner and Berg, 1997).

Does α7 require co-assembly with other nAChR subunits?

Co-expression of α7 with all other cloned neuronal nAChRs expressed in PC12 and SH-SY5Y cells did not produce specific [^{125}I]-αBTX-binding sites in HEK293 cells. No evidence for co-assembly of α7 with other subunits expressed in SHSY5Y cells has been detected using identical solubilization and washing conditions used to co-precipitate pairwise combinations of nAChR subunits expressed heterologously (Lansdell *et al.*, 1997 and unpublished results from our laboratory). Evidence generated from the successful functional expression of homo-oligomeric α7 nAChRs which bind [^{125}I]-αBTX with high affinity in *Xenopus* oocytes (Gerzanich *et al.*, 1994; Peng *et al.*, 1994b), HEK293 cells (Gopalakrishnan *et al.*, 1995a), rat pituitary

GH_4C_1 cells (Quik *et al.*, 1996; Quik *et al.*, 1997) and chick QT-6 cells (Kassner and Berg, 1997) indicates that other subunits are not required for the correct folding and αBTX-binding properties of the α7 nAChR in several heterologous expression systems.

Immunoprecipitation of the αBTX-binding receptor from rat brain, followed by western blotting with a panel of antibodies which recognise all cloned mammalian nAChRs expressed in the brain, indicate that α7 is not assembled with other cloned neuronal nAChR subunits in rat brain (Chen and Patrick, 1997). A panel of 5 antibodies raised against N-terminal fragments of the α5, α7, β2 and β4 subunits were used to probe western blots of αBTX-purified receptors from rat brain (Chen and Patrick, 1997). The antibodies were shown to cross react with N-terminal fragments of all mammalian nAChR subunits identified, excluding α9 (not tested), to picomolar sensitivity. α7 was the only nAChR subunit positively identified from the preparation of native rat brain αBTX-binding receptors.

However, immunopurification of αBTX-binding receptors from chick brain and retina reveals the presence of three protein components, and western blotting with subunit-specific antibodies indicate that α7 and α8 co-assemble *in vivo* (Keyser *et al.*, 1993; Gotti *et al.*, 1994; Gotti *et al.*, 1997). There appear to be at least three classes of αBTX-binding receptor in the chick nervous system and evidence suggests that the predominant chick brain subtype contains α7 subunits while a minor subtype contains both α7 and α8 subunits. In chick retina, the major species of αBTX-binding receptor contains the α8 subunit, but not the α7 subunit. A mammalian homologue of the chick α8 subunit has yet to be identified but co-expression of chick α8 with α7 in HEK293 cells did not permit the correct folding of α7 into a conformation able to bind αBTX in this cell line.

7.7 The correct folding of the α8 subunit is host cell-dependent

Expression of the chick α8 cDNA in HEK293 cells failed to produce specific nicotinic radioligand binding despite detecting high levels of α8 subunit protein by metabolic labelling and immunoprecipitation with a monoclonal antibody which recognizes a linear intracellular epitope (mAb308). In contrast, stable transfection of the α8 subunit into SH-SY5Y cells resulted in a ~30-fold increase in the levels of surface [^{125}I]-αBTX-binding compared with untransfected SH-SY5Y cells. Immunoprecipitation of cell surface receptors pre-labelled with [^{125}I]-αBTX with subunit-specific antibodies demonstrates that the increased levels of [^{125}I]-αBTX-binding is due to expression of the recombinant α8 subunit and that these α8-containing surface [^{125}I]-αBTX-binding receptors do not also contain α7 subunits. The α8 subunit expressed in transfected SH-SY5Y-α8 cells could be detected by immunoprecipitation and by immunofluorescent microscopy with a monoclonal antibody which recognizes a conformational extracellular epitope (mAb 305). However, the conformation-dependent mAb305 was unable to detect α8 protein expressed in transiently transfected HEK293 cells.

The successful expression of α8 and α7 nAChRs able to bind [^{125}I]-αBTX was obtained following transfection of a rat pituitary GH_4C_1 cell line. This cell line had been shown during the course of this research to express functional rat α7 nAChRs which bind [^{125}I]-αBTX with high affinity (Quik *et al.*, 1996; Quik *et al.*, 1997). The α8 nAChR expressed in transiently transfected GH_4C_1-α8 cells binds [^{3}H]-epibatidine with high affinity (K_d ~ 0.24 nM). However, double-label immunofluorescent microscopy demonstrates that only a subset of transiently transfected GH_4C_1 cells shown to express intracellular α8 protein, are able to correctly fold the α8 subunit into a conformation able to bind rhodamine-conjugated αBTX (Rd-αBTX). In contrast, all of the SH-SY5Y-α8 cells examined which were

shown to express intracellular α8 protein, also possess high levels of surface Rd-αBTX-binding sites.

Sucrose gradient sedimentation of the α8 nAChR expressed in the SH-SY5Y-α8 polyclonal stable cell line and in transiently transfected GH_4C_1 cells, indicate that the α8 subunit forms complexes of a similar buoyant density to that of the muscle and electric organ nAChR and is also, presumably, pentameric. Analysis of the mouse muscle nAChR expressed in B23ε cells (Green and Claudio, 1993) and α8 nAChRs expressed in GH_4C_1-α8 cells with and without prior labelling with [^{125}I]-αBTX, suggests that more than two molecules of αBTX bind to the α8 nAChR. This was demonstrated by comparing the peaks of radioligand binding in the sedimentation profiles of receptors pre-labelled with αBTX, with profiles obtained with unlabelled receptors assayed for radioligand binding following centrifugation. A larger shift in the buoyant density was observed when unlabelled and αBTX-labelled α8 nAChRs were sedimented, compared with the shift observed after two molecules of αBTX bind to the muscle nAChR. This was interpreted as an indication that more than two molecules of αBTX bind to the α8 nAChR.

7.8 α7/5-HT$_3$ and α8/5-HT$_3$ chimeras implicate the C-terminus of α7 and α8 in cell-specific folding

Chimeric subunits encoding the N-terminal portion of α7 or α8 (up to the first putative transmembrane domain) and the complementary C-terminal portion of the 5-HT_3 subunit revealed that the C-terminal domains of the α7 and α8 subunits are involved in cell-specific folding. A similar α7/5-HT_3 construct had been previously reported to form [^{125}I]-αBTX-binding sites following transient expression in HEK293 cells (Eiselé *et al.*, 1993). Expression of α7/5-HT_3 and α8/5-HT_3 chimeric subunits in our isolate of HEK293 cells produces high levels of specific nicotinic radioligand binding. Double-label immunofluorescent microscopy demonstrates that

every cell shown to contain intracellular α7/5-HT_3 and α8/5-HT_3 chimeric protein, also possess very high levels of surface Rd-αBTX-binding sites. These observations suggest that the folding of the α7/5-HT_3 and α8/5-HT_3 subunits is not cell specific, and therefore implicates the C-terminal regions of α7 and α8, including the putative transmembrane and large intracellular loop domains, in cell-specific folding.

7.9 Conclusion

The data presented here indicate the correct folding of the neuronal nicotinic AChR α7 and α8 subunits is critically dependent on the host cell type. Cell lines which fail to correctly fold α7 or α8, are capable of correctly folding the rat muscle nAChR and the serotonin 5-HT_3 homo-oligomeric receptor into functional cell surface receptors. These results demonstrate that there are differences in the folding and maturation pathways of the homo-oligomeric α7 and α8 neuronal nAChR subunits which do not exist for the muscle nAChR or the 5-HT_3 receptor. Chimeric α7/5-HT_3 and α8/5-HT_3 subunits are correctly folded, assembled and exported to the plasma membrane in HEK293 cells non-permissive for α7 and α8 folding suggesting that it is C-terminal region of α7 and α8 subunits which mediates the effects of cell specific misfolding.

Different isolates of the same cell line have been shown to differ in their ability to correctly fold the α7 and α8 subunits. Moreover, some cells within the isolate of GH_4C_1 cells cultured in our laboratory are able to correctly fold the α8 subunit while other cells are not. These results imply that extensive propagation of cultured cell lines exerts selective pressures on cell populations which results in different isolates of established cell lines expressing different gene products. Some of these gene products must selectively influence the folding of the α7 and α8 subunits. There have been no reports to date of the successful expression of the α9 subunit in mammalian cells, and I was unable to detect specific radioligand binding to cells

transfected with the α9 cDNA. This may indicate that cell-specific folding may be a property of all nicotinic homo-oligomeric subunits although the factor(s) which mediate this effect remain to be identified. The failure of the α7 and α8 neuronal nAChR subunits to correctly fold in several mammalian cell lines may yet provide a system to identify factors which regulate the folding and assembly of the α-BTX-binding homo-oligomeric receptors. Identification of gene products which facilitate or inhibit the folding of homo-oligomeric proteins may provide insight into possible mechanisms which regulate assembly pathways *in vivo*.

Acknowledgments

I wish to thank Drs. Marc Ballivet, Thomas Bunch, Heinrich Betz, Toni Claudio, David Julius, Jon Lindstrom, Jim Patrick, Ruth McKernan, Steve Moss, Gregor Sutcliff and Viet Witzemann for generously providing some of the antibodies, cDNA clones and cultured cell lines used in this work. I also thank my supervisor, Dr. Neil Millar, for his guidance during this project with its many hurdles, and his critical review of this manuscript. Thank-you to the other members of my laboratory, for listening to my hair-brained schemes, and continually providing helpful advice and suggestions. Finally, thank-you to my parents for their support and encouragement and for providing me with the opportunities to get this far. But mostly thanks to my husband Jason, for helping me stick with it. This work was supported by grants to Dr. Neil Millar from the Wellcome Trust.

References

8.0 References

Abramson, S., Culver, Y. and Taylor, P. (1989). An analogue of lophotoxin reacts covalently with Tyr190 in the α subunit of the nicotinic acetlycholine receptor. *J. Biol. Chem.* **264,** 1266-1267.

Adams, P. R. (1981). Acetylcholine receptor kinetics. *J. Memb. Biol.* **58,** 161-174.

Akabas, M. H. and Karlin, A. (1995). Identification of acetylcholine receptor channel-lining residues in the M1 segment of the α-subunit. *Biochemistry* **34,** 12496-12500.

Akabas, M. H., Stauffer, D. A., Xu, M. and Karlin, A. (1992). Acetylcholine receptor channel structure probed in cysteine-substitution mutants. *Science* **258,** 307-310.

Albuquerque, E. X., Alkondon, M., Pereira, E. F. R., Castro, N. G., Schrattenholz, A., Barbosa, C. T. F., Bonfante-Carbarcas, R., Aracava, Y., Eisenberg, H. M. and Maelicke, A. (1997). Properties of neuronal nicotinic acetylcholine receptors: Pharmacological characterization and modulation of synaptic function. *J. Pharm. Exp. Ther.* **280,** 1117-1136.

Alkondon, M. and Albuquerque, E. (1994). Presence of α-bungarotoxin-sensitive nicotinic acetylcholine receptors in rat olfactory bulb neurons. *Neurosci. Lett.* **176,** 152-156.

Alkondon, M. and Albuquerque, E. X. (1993). Diversity of nicotinic acetylcholine receptors in rat hippocampal neurons: I. pharmacological and functional evidence for distinct structural subtypes. *J. Pharmacol. Exp. Ther.* **265,** 1455-1473.

Alkondon, M., Pereira, E. F. R., Cortes, W. S., Maelicke, A. and Albuquerque, E. X. (1997). Choline is a selective agonist of α7 nicotinic acetylcholine receptors in the rat brain neurons. *Eur. J. Neurosci.* **9,** 2734-2742.

Alkondon, M., Pereira, E. F. R., Wonnacott, S. and Albuquerque, E. X. (1992). Blockade of nicotinic currents in hippocampal neurons defines methyllycaconitine as a potent and specific receptor antagonist. *Mol. Pharmacol.* **41,** 802-808.

Alkondon, M., Reinhardt, S., Lobron, C., Hermsen, B., Maelicke, A. and Albuquerque, E. X. (1994). Diversity of nicotinic acetylcholine receptors in rat hippocampal neurons. II. Rundown and inward rectification of agonist-elicited whole-cell currents and identification of receptor subunits by *in situ* hybridisation. *J. Pharmacol. Exp. Ther.* **271,** 494-506.

Alkondon, M., Rocha, E. S., Maelicke, A. and Albuquerque, E. X. (1996). Diversity of nicotinic acetylcholine receptors in rat brain. V. α-Bungarotoxin-sensitive nicotinic receptors in olfactory bulb neurons and presynaptic modulation of glutamate release. *J. Pharmacol. Exp. Ther.* **278,** 1460-1471.

Amar, M., Thomas, P., Johnson, C., Lunt, G. G. and Wonnacott, S. (1993). Agonist pharmacology of the neuronal α7 nicotinic receptor expressed in Xenopus oocytes. *FEBS Lett.* **327,** 284-288.

Anand, R., Conroy, W. G., Schoepfer, R., Whiting, P. and Lindstrom, J. (1991). Neuronal nicotinic acetylcholine receptors expressed in *Xenopus* oocytes have a pentameric quaternary structure. *J. Biol. Chem.* **266,** 11192-11198.

Anand, R., Peng, X., Ballesta, J. J. and Lindstrom, J. (1993a). Pharmacological characterisation of α-bungarotoxin-sensitive acetylcholine receptors immunoisolated from chick retina: contrasting properties of α7 and α8 subunit-containing subtypes. *Mol. Pharmacol,* **44,** 1046-1050.

Anand, R., Peng, X. and Lindstrom, J. (1993b). Homomeric and native α7 acetylcholine receptors exhibit remarkably similar but non-identical pharmacological properties, suggesting that the native receptor is a heteromeric protein complex. *FEBS Letts* **327,** 241-246.

Anderson, D. J. and Blobel, G. (1981). In vitro synthesis, glycosylation, and membrane insertion of the four subunits of Torpedo acetylcholine receptor. *Proc. Natl. Acad. Sci. USA.* **78,** 5598-5602.

Aracava, Y., Deshpande, S. S., Swanson, K. L., Rapoport, H., Wonnacott, S., Lunt, G. and Albuquerque, E. X. (1987). Nicotinic acetylcholine receptors in cultured

neurons from the hippocampus and the brain stem of the rat characterized by single channel recording. *FEBS Letter* **222,** 63-70.

Ballivet, M., Nef, P., Couturier, S., Rungger, D., Bader, C. R., Bertrand, D. and Cooper, E. (1988). Electrophysiology of a chick neuronal nicotinic acetylcholine receptor expressed in Xenopus oocytes after cDNA injection. *Neuron* **1,** 847-52.

Barnard, E. A., Darlison, M. G. and Seeberg, P. (1987). Molecular biology of the $GABA_A$ receptor: the receptor/channel superfamily. *Trends Neurosci.* **10,** 502-509.

Barnard, E. A., Miledi, R. and Sumikawa, K. (1982). Translation of exogenous messenger RNA coding for nicotinic acetylcholine receptors produces functional receptors in *Xenopus* oocytes. *Proc. R. Soc. Lond. B.* **215,** 241-246.

Belcher, G. and Ryall, R. W. (1977). Substance P and Renshaw cells, a new concept of inhibitory synaptic interactions. *J. Physiol. Lond.* **272,** 105-119.

Benwell, M., Balfour, D. and Anderson, J. (1988). Evidence that tobacco smoking increases the density of (-)-[^{3}H]-nicotine binding sites in human brain. *J. Neurochem.* **50,** 1243-1247.

Bertrand, D., Ballivet, M. and Rungger, D. (1990). Activation and blocking of neuronal nicotinic acetylcholine receptor reconstituted in *Xenopus* oocytes. *Proc Natl Acad Sci U S A* **87,** 1993-7.

Bertrand, D., Devillers-Thiéry, A., Revah, F., Galzi, J.-L., Hussy, N., Mulle, C., Bertrand, S., Ballivet, M. and Changeux, J.-P. (1991). Unconventional pharmacology of a neuronal nicotinic receptor mutated in the channel domain. *Proc. Natl. Acad. Sci. USA* **89,** 1261-1265.

Bertrand, D., Devillers-Thiery, A., Revah, F., Galzi, J. L., Hussy, N., Mulle, C., Bertrand, S., Ballivet, M. and Changeux, J. P. (1992). Unconventional pharmacology of a neuronal nicotinic receptor mutated in the channel domain. *Proc Natl Acad Sci U S A* **89,** 1261-5.

Betz, H., Graham, D. and Rehm, H. (1982). Identification of polypeptides associated with a putative neuronal nicotinic acetylcholine receptor. *J. Biol. Chem.* **257,** 11390-11394.

Betz, H. and Pfeiffer, F. (1984). Monoclonal antibodies against the α-bungarotoxin-binding protein of chick optic lobe. *J. Neurosci.* **4,** 2095-2105.

Blount, P. and Merlie, J. P. (1989). Molecular basis of the two nonequivalent ligand binding sites of the muscle nicotinic acetylcholine receptor. *Neuron* **3,** 349-57.

Blumenthal, E. M., Conroy, W. G., Romano, S. J., Kassner, P. D. and Berg, D. K. (1997). Detection of functional nicotinic receptors blocked by α-bungarotoxin on PC12 cells and dependence of their expression on post-translational events. *J. Biol. Chem.* **15,** 6094-6104.

Boulter, J., Connolly, J., Deneris, E., Goldman, D., Heinemann, S. and Patrick, J. (1987). Functional expression of two neuronal nicotinic acetylcholine receptors from cDNA clones identifies a gene family. *Proc. Natl. Acad. Sci. USA* **84,** 7763-7767.

Boulter, J., Evans, K., Goldman, D., Martin, G., Treco, D., Heinemann, S. and Patrick, J. (1986a). Isolation of a cDNA clone coding for a possible neural nicotinic acetylcholine receptor α-subunit. *Nature* **319,** 368-374.

Boulter, J., Evans, K. L., Martin, G., Gardner, P. D. and Conolly, J. (1986b). Mouse muscle acetylcholine receptor molecular cloning of α,β,γ and δ subunit cDNA's and expression in *Xenopus laevis* oocytes. *Soc. Neurosci. Abstr.* **12,** 40.2:146.

Boulter, J., O'Shea-Greenfield, A., Duvoisin, R. M., Connolly, J. G., Wada, E., Jensen, A., Gardner, P. D., Ballivet, M., Deneris, E. S., McKinnon, D. and et, a. (1990). Alpha 3, alpha 5, and beta 4: three members of the rat neuronal nicotinic acetylcholine receptor-related gene family form a gene cluster. *J. Biol. Chem.* **265,** 4472-82.

Boyd, R. T., Jacob, M. H., Couturier, S., Ballivet, M. and Berg, D. K. (1988). Expression and regulation of neuronal acetylcholine receptor mRNA in chick ciliary ganglia. *Neuron* **1,** 495-502.

Brake, A. J., Wagenbach, M. J. and Julius, D. (1994). New structural motif for ligand-gated ion channels defined by an ionotrophic ATP receptor. *Nature* **371,** 519-523.

Brisson, A. and Unwin, P. N. T. (1985). Quaternary structure of the acetylcholine receptor. *Nature* **315,** 474-477.

Britto, L. R., Hamassaki-Britto, D. E., Ferro, E. S., Keyser, K. T., Karten, H. J. and Lindstrom, J. M. (1992). Neurons of the chick brain and retina expressing both alpha-bungarotoxin-sensitive and alpha-bungarotoxin-insensitive nicotinic acetylcholine receptors: an immunohistochemical analysis. *Brain Res* **590,** 193-200.

Brussard, A. B., Yang, X., Doyle, J. P., Huck, S. and Role, L. W. (1994). Developmental regulation of multiple nicotinic subtypes in embryonic chick habenula neurons: Contributions of both the α2 and α4 subunit genes. *Pflügers Arch. Eur. J. Physiol.* **429,** 27-43.

Bunch, T. A., Grinblat, Y. and Goldstein, L. S. B. (1988). Characterization and use of the *Drosophila* metallothionein promoter in cultured *Drosophila melanogaster* cells. *Nucl. Acids Res.* **16,** 1043-1061.

Carbonetto, S., Fambrough, D. and Muller, K. (1978). Nonequivalence of α bungarotoxin receptors and acetylcholine receptors in chick sympathetic neurons. *Proc. Natl. Acad. Sci. USA* **75,** 1016-1020.

Castro, N. G. and Albuquerque, E. X. (1993). Brief-lifetime, fast-inactivating ion channels account for the α-bungarotoxin-sensitive nicotinic response in hippocampal neurons. *Neurosci. Lett.* **164,** 137-140.

Castro, N. G. and Albuquerque, E. X. (1995). α-Bungarotoxin-sensitive hippocampal nicotinic receptor channel has a high calcium permeability. *Biophys. J.* **68,** 516-524.

Caterina, M. J., Schumacher, M. A., Tominaga, M., Rosen, T. A., Levine, J. D. and Julius, D. (1997). The capsacian receptor: a heat-activated ion channel in the pain pathway. *Nature* **389,** 816-824.

Caulfield, M. P. (1993). Muscarinic receptors - characterization, coupling and function. *Pharmacol. Ther.* **58,** 319-379.

Changeux, J.-P., Kasai, M. and Lee, C. Y. (1970). The use of snake venom toxin to characterize the cholinergic receptor protein. *Proc. Natl. Acad. Sci. USA* **67,** 1241-1247.

Charnet, P., Labarca, C., Cohen, B. N., Davidson, N., Lester, H. A. and Pilar, G. (1992). Pharmacological and kinetic properties of α4β2 neuronal nicotinic acetylcholine receptors expressed in *Xenopus* oocytes. *J Physiol* **450,** 375-394.

Charnet, P., Labarca, C., Leonard, R. J., Vogelaar, N. J., Czyzyk, L., Gouin, A., Davidson, N. and Lester, H. A. (1990). An open-channel blocker interacts with adjacent turns of α-helices in the nicotinic acetylcholine receptor. *Neuron* **4.**

Chen, C., Bonifacino, J. S., Yuan, L. C. and Klausner, R. D. (1988). Selective degradation of T cell antigen receptor chains retained in a pre-golgi compartment. *J. Cell. Biol.* **107,** 2149-2161.

Chen, C. and Okayama, H. (1987). High-efficiency transformation of mammalian cells by plasmid DNA. *Mol. Cell. Biol.* **7,** 2745-2752.

Chen, D., Dang, H. and Patrick, J. W. (1998). Contributions of N-linked glycosylation to the expression of a functional α7-nicotinic receptor in *Xenopus* oocytes. *J. Neurochem.* **70,** 349-357.

Chen, D. and Patrick, J. W. (1997). The α-Bungarotoxin-binding nicotinic acetylcholine receptor contains only the α7 subunit. *J. Biol. Chem* **272,** 24024-24029.

Clark, P. B. S., Schwartz, R. D., Paul, S. M., Pert, C. B. and Pert, A. (1985). Nicotinic binding in rat brain: autoradiographic comparison of [^{3}H]acetylcholine, [^{3}H]nicotine, and [^{125}I]-α-bungarotoxin. *J. Neurosci.* **5,** 1307-1315.

Clarke, P., Hamill, G., Nadi, N., Jacobwitz, D. and Pert, A. (1986). ^{3}H-nicotine and ^{125}I-αbungarotoxin-labelled nicotinic receptors in the interpeduncular nucleus of rats. II. Effects of habenular deafferentation. *J. Comp. Neurol.* **251,** 407-413.

Clarke, P. B. S. and Pert, A. (1985). Autoradiographic evidence for nicotinic receptors on nigrostriatal and mesolimbic dopaminergic neurons. *Brain Res.* **348,** 355-358.

Claudio, T. (1987). Stable expression of transfected Torpedo acetylcholine receptor alpha subunits in mouse fibroblast L cells. *Proc. Natl. Acad. Sci. U S A* **84,** 5967-71.

Claudio, T. (1989). Molecular genetics of acetylcholine receptor-channels. In *Frontiers in Molecular Biology: Molecular Neurobiology* (ed. D. M. Glover and B. D. Hames), pp. 63-142. Oxford: I.R.L. Press.

Claudio, T., Ballivet, M., Patrick, J. and Heinemann, S. (1983). Nucleotide and deduced amino acid sequences of *Torpedo californica* acetylcholine receptor gamma-subunit. *Proc. Natl. Acad. Sci. USA* **80,** 1111-1115.

Claudio, T., Green, W. N., Hartman, D. S., Hayden, D., Paulson, H. L., Sigworth, F. J., Sine, S. M. and Swedlund, A. (1987). Genetic reconstitution of functional acetylcholine receptor channels in mouse fibroblasts. *Science* **238,** 1688-1694.

Colquhoun, D. and Ogden, D. C. (1988). *J. Physiol.* **395,** 131-159.

Conroy, W. G. and Berg, D. K. (1995). Neurons can maintain multiple classes of nicotinic acetylcholine receptors distinguished by different subunit compositions. *J. Biol. Chem.* **270,** 4424-4431.

Conroy, W. G., Vernallis, A. B. and Berg, D. K. (1992). The α5 gene product assembles with multiple acetylcholine receptor subunits to form distinctive receptor subtypes in brain. *Neuron* **9,** 679-691.

Conti-Tronconi, B., Dunn, S., E., B., Dolly, J., Lai, F., Ray, N. and Raferty, M. (1985). Brain and muscle nicotinic acetylcholine receptors are different but homologous proteins. *Proc. Natl. Acad. Sci. USA* **85,** 5208-5212.

Cooper, E., Couturier, S. and Ballivet, M. (1991). Pentameric structure and subunit stoichiometry of a neuronal nicotinic acetylcholine receptor. *Nature* **350,** 235-238.

Cooper, S. T. and Millar, N. S. (1997). Host cell-specific folding and assembly of the neuronal nicotinic acetylcholine receptor α7 subunit. *J. Neurochem.* **68,** 2140-2151.

Cooper, S. T. and Millar, N. S. (1998). Host cell-specific folding of the neuronal nicotinic acetylcholine receptor α8 subunit. *J. Neurochem.* **70,** 2585-2593.

Corrigall, W. A., Franklin, K. B. J., Coen, K. M. and Clarke, P. B. S. (1992). The mesolimbic dopaminergic system is implicated in the reinforcing effects of nicotine. *Psychopharmacology* **107,** 285-289.

Corringer, P.-J., Galzi, J.-L., Eliselé, J.-L., Bertrand, S., Changeux, J.-P. and Bertrand, D. (1995). Identification of a new component of the agonist binding site of the nicotinic α7 homooligomeric receptor. *J. Biol. Chem.* **270,** 11749-11752.

Corriveau, R. A. and Berg, D. K. (1993). Coexpression of multiple acetylcholine receptor genes in neurons: quantification of transcripts during development. *J Neurosci* **13,** 2662-71.

Costa, A. C. S., Patrick, J. W. and Dani, J. A. (1994). Improved technique for studying ion channels expressed in *Xenopus* oocytes, including fast superfusion. *Biophys. J.* **67,** 1-7.

Couturier, S., Bertrand, D., Matter, J. M., Hernandez, M. C., Bertrand, S., Millar, N., Valera, S., Barkas, T. and Ballivet, M. (1990a). A neuronal nicotinic acetylcholine receptor subunit (α7) is developmentally regulated and forms a homo-oligomeric channel blocked by α-BTX. *Neuron* **5,** 847-856.

Couturier, S., Erkman, L., Valera, S., Rungger, D., Bertrand, S., Boulter, J., Ballivet, M. and Bertrand, D. (1990b). α5, α3, and non-α3. Three clustered avian genes encoding neuronal nicotinic acetylcholine receptor-related subunits. *J Biol Chem* **265,** 17560-17567.

Covernton, P. J. O., Kojima, H., Sivilotti, L. G., Gibb, A. J. and Colquhoun, D. (1994). Comparison of neuronal nicotinic receptors in rat sympathetic neurones with subunit pairs expressed in *Xenopus* oocytes. *J. Physiol.* **481,** 27-34.

Cully, D. F., Vassilatis, D. K. L., K.K., Paress, P. S., Van der Ploeg, L. H. T., Schaeffer, J. M. and Arena, J. P. (1994). Cloning of an avermectin-sensitive glutamate-gated chloride channel from Caenorhabditis elegans. *Nature* **371,** 707-711.

Curtis, D. R. and Ryall, R. W. (1966). The synaptic excitation of Renshaw cells. *Exp. Brain Res.* **2,** 81-96.

Czajkowski, C. and Karlin, A. (1991). Agonist binding site of Torpedo electric tissue nicotinic acetylcholine receptor. A negatively charged region of the delta subunit within 0.9 nm of the alpha subunit binding site disulfide. *J Biol Chem* **266,** 22603-12.

Czajkowski, C., Kaufmann, C. and Karlin, A. (1993). Negatively charged amino acid residues in the nicotinic receptor delta subunit that contribute to the binding of acetylcholine. *Proc Natl Acad Sci U S A* **90,** 6285-9.

Damle, V. N., McLauglin, M. and Karlin, A. (1978). Bromo-acetylcholine as an affinity label of the acetylcholine receptor from *Torpedo californica. Biochem. Biophys. Res. Commun.* **84,** 845-851.

Dani, J. A. and Heinemann, S. (1996). Molecular and cellular aspects of nicotine abuse. *Neuron* **16,** 905-908.

Danielson, P. E., Forss-Petter, S., Brow, M. A., Calvetta, L., Douglas, J., Milner, R. J. and Sutcliffe, J. G. (1988). p1B15: a cDNA clone of the rat mRNA encoding cyclophilin. *DNA* **7,** 261-267.

Decker, E. R. and Dani, J. A. (1990). Calcium permeability of the nicotinic acetylcholine receptor: the single-channel calcium influx is significant. *J. Neurosci.* **10,** 3413-3420.

Deneris, E. S., Boulter, J., Swanson, L. W., Patrick, J. and Heinemann, S. (1989). β3: a new member of nicotinic acetylcholine receptor gene family is expressed in brain. *J. Biol. Chem.* **264,** 6268-72.

Deneris, E. S., Connolly, J., Boulter, J., Wada, E., Wada, K., Swanson, L. W., Patrick, J. and Heinemann, S. (1988). Primary structure and expression of beta 2: a novel subunit of neuronal nicotinic acetylcholine receptors. *Neuron* **1,** 45-54.

Dennis, M., Giraudat, J., Kotzyba-Hibert, F., Goeldner, M., Hirth, C., Chang, J. Y., Lazure, C., Chretien, M. and Changeux, J. P. (1988). Amino acids of the Torpedo marmorata acetylcholine receptor alpha subunit labeled by a photoaffinity ligand for the acetylcholine binding site. *Biochemistry* **27,** 2346-57.

Dineley-Miller, K. and Patrick, J. (1992). Gene transcripts for the nicotinic acetylcholine receptor subunit, beta4, are distributed in multiple areas of the rat central nervous system. *Brain Res Mol Brain Res* **16,** 339-44.

DiPaola, M., Czajkowski, C. and Karlin, A. (1989). The sideness of the COOH terminus of the acetylcholine receptor δ subunit. *J. Biol. Chem.* **264,** 15457-15463.

Dominguez Del Toro, E., Juiz, J. M., Peng, X., Lindstrom, J. and Criado, M. (1994). Immunocytochemical localization of the α7 subunit of the nicotinic acetylcholine receptor in the rat central nervous system. *J. Comp. Neurol.* **349,** 325-342.

Dunn, S. M. J., Conti-Troconi, B. M. and Raftery, M. A. (1986). Acetylcholine receptor dimers are stabilized by extracellular disulphide bonding. *Biochem. Biophys. Res. Commun.* **139,** 830-837.

Duvoisin, R. M., Deneris, E. S., Patrick, J. and Heinemann, S. (1989). The functional diversity of the neuronal nicotinic acetylcholine receptors is increased by a novel subunit: β4. *Neuron* **3,** 487-496.

Eiselé, J.-L., Bertrand, S., Galzi, J.-L., Devillers-Thiéry, A., Changeux, J.-P. and Bertrand, D. (1993). Chimaeric nicotinic-serotonergic receptor combines distinct ligand binding and channel specificities. *Nature* **366,** 479-483.

Elder, J. H. and Alexander, S. (1982). Endo-β-N-acetylglucosaminidase F; endoglycosidase from flavobacterium meningosepticum that cleaves both high mannose and complex glycoproteins. *Proc. Natl. Acad. Sci. USA* **79,** 4540-4545.

Elgoyhen, A. B., Johnson, D. S., Boulter, J., Vetter, D. E. and Heinemann, S. (1994). α9: an acetylcholine receptor with novel pharmacological properties expressed in rat cochlear hair cells. *Cell* **18,** 705-715.

Elmslie, F. V., Rees, M., Williamson, M. P., Kerr, M., Kjeldsen, M. J., Pang, K. A., Sundqvist, A., Friis, M. L., Chadwick, D., Richens, A., Covanis, A., Santos, M., Arzimanoglou, A., Panayiotopolous, C. P., Curtis, D., Whitehouse, W. P. and Gardiner, R. M. (1997). Genetic mapping of a major susceptibility locus fro juvenille myoclonic epilepsy on chromosome 15q. *Hum. Mol. Genet.* **6,** 1329-1334.

Erostegui, C., Norris, C. H. and Bobbin, R. P. (1994). *In vitro* characterisation of a cholinergic receptor on outer hair cells. *Hearing Res.* **74,** 135-147.

Felder, C. C. (1995). Muscarinic acetylcholine receptors: signal transduction through multiple effectors. *FASEB J.* **9,** 619-625.

Flores, C. M., Rogers, S. W., Pabreza, L. A., Wolfe, B. B. and Kellar, K. J. (1992). A subtype of nicotinic cholinergic receptor in rat brain is comprised of α-4 and β-2 subunits and is upregulated by chronic nicotine treatment. *Mol. Pharm,* **41,** 31-37.

Forsayeth, J. R., Franco, A., Jr., Rossi, A. B., Lansman, J. B. and Hall, Z. W. (1990). Expression of functional mouse muscle acetylcholine receptors in Chinese hamster ovary cells. *J Neurosci* **10,** 2771-9.

Forsayeth, J. R. and Kobrin, E. (1997). Formation of oligomers containing the β3 and β4 subunits of the rat nicotinic receptor. *J. Neurosci.* **17,** 1531-1538.

Frazier, C. J., Rollins, Y. D., Breese, C. R., Leonard, S., Freedman, R. and Dunwiddie, T. V. (1998). Acetylcholine activates and α-bungarotoxin-sensitive nicotinic current in rat hippocampal interneurons, but not pyramidal cells. *J. Neurosci.* **18,** 1187-1195.

Freedman, R., Coon, H., Myles-Worsley, M., Orr-Urtreger, A., Olincy, A., Davis, A., Polymeropoulos, M., Holik, J., Hopkins, J., Hoff, M., Rosenthal, J., Waldo, M. C., Reimherr, F., Wender, P., Yaw, J., Young, D. A., Breese, C. R., Adams, C.,

Patterson, D., Adler, L. E., Kruglyak, L., Leonard, S. and Byerley, W. (1997). Linkage of a neurophysiological deficit in schizophrenia to a chromosome 15 locus. *Genetics* **94,** 587-592.

Freedman, R., Hall, M., Adler, L. E. and Leonard, S. (1995). Evidence in postmortem brain tissue for decreases numbers of hippocampal nicotinic receptors in schizophrenia. *Biol. Psychiatry* **18,** 537-551.

Froehner. (1977). Subunit structure of the acetylcholine receptor from denervated rat skeletal muscle. *J. Biol. Chem.* **252,** 8589-8596.

Fuchs, P. A. and Murrow, B. W. (1992). Cholinergic inhibition of short (outer) hair cells of the chick's cochlear. *J. Neurosci.* **12,** 800-809.

Galzi, J. L., Devillers-Thiery, A., Hussy, N., Bertrand, S., Changeux, J. P. and Bertrand, D. (1992). Mutations in the channel domain of a neuronal nicotinic receptor convert ion selectivity from cationic to anionic. *Nature* **359,** 500-5.

Galzi, J. L., Revah, F., Black, D., Goeldner, M., Hirth, C. and Changeux, J. P. (1990). Identification of a novel amino acid alpha-tyrosine 93 within the cholinergic ligands-binding sites of the acetylcholine receptor by photoaffinity labeling. Additional evidence for a three-loop model of the cholinergic ligands-binding sites. *J Biol Chem* **265,** 10430-7.

Garcia-Guzman, M., Sala, F., Sala, S., Campos-Caro, A., Stuhmer, W., Gutierrez, L. M. and Criado, M. (1995). α-Bungarotoxin-sensitive nicotinic receptors on bovine chromaffin cells: molecular cloning, functional expression and alternative splicing of the α7 subunit. *Eur. J. Neurosci.* **7,** 647-655.

Gerzanich, V., Anand, R. and Lindstrom, J. (1994). Homomers of α8 and α7 subunits of nicotinic receptors exhibit similar channels but contrasting binding site properties. *Mol. Pharmacol.* **45,** 212-220.

Gerzanich, V., Kuryatov, A., Anand, R. and Lindstrom, J. (1997). "Orphan" α6 nicotinic AChR subunit can form a functional heteromeric acetylcholine receptor. *Mol. Pharmacol.* **51,** 320-327.

Gibson, R. E., O'Brien, R. D., Edelstein, S. J. and Thompson, W. R. (1976). *Biochemistry* **15,** 2377-2383.

Giraudat, J., Dennis, M., Heidmann, T., Haumont, P.-Y., Lederer, F. and Changeux, J.-P. (1987a). Structure of the high affintiy binding site for non-competitive blockers of the acetylcholine receptor: [^{3}H]-Chlorpromazine labels homologous residues in the beta and delta chains. *Biochemistry* **26,** 2410-2418.

Giraudat, J., Dennis, M., Heidmann, T., Haumont, P. Y., Lederer, F. and Changeux, J. P. (1987b). Structure of the high-affinity binding site for noncompetitive blockers of the acetylcholine receptor: [3H]chlorpromazine labels homologous residues in the beta and delta chains. *Biochemistry* **26,** 2410-8.

Giraudat, J., Gali, J., Revah, F., Changeux, J., Haumont, P. and Lederer, F. (1989). The noncompetitive blocker [(3)H]chlorpromazine labels segment M2 but not segment M1 of the nicotinic acetylcholine receptor alpha-subunit. *Febs Lett* **253,** 190-8.

Goldman, D., Deneris, E., Luyten, W., Kochhar, A., Patrick, J. and Heinemann, S. (1987). Members of a nicotinic acetylcholine receptor gene family are expressed in different regions of the mammalian central nervous system. *Cell* **48,** 965-73.

Gopalakrishnan, M., Buisson, B., Touma, E., Giordano, T., Campbell, J. E., Hu, I. C., Donnelly-Roberts, D., Arneric, S. P., Bertrand, D. and Sullivan, J. P. (1995a). Stable expression and pharmacological properties of the human α7 nicotinic acetylcholine receptor. *Eur. J. Pharmacol.* **290,** 237-246.

Gopalakrishnan, M., Monteggia, L. M., Anderson, D. J., Molinari, E. J., Piattoni-Kaplan, M., Donnelly-Roberts, D., Arneric, S. P. and Sullivan, J. P. (1995b). Stable expression, parmacologic properties and regulation of the human neuronal nicotinic acetylcholine α4β2 receptor. *J, Pharmacol. Exp. Ther.* **276,** 286-297.

Gotti, C., Hanke, W., Maury, K., Moretti, M., Ballivet, M., Clementi, F. and Bertrand, D. (1994). Pharmacology and biophysical properties of α7 and α7-α8 α-bungarotoxin receptor subtypes immunopurified from the chick optic lobe. *Eur. J. Neurosci.* **6,** 1291-1291.

Gotti, C., Hanke, W., Schlue, W. R., Briscini, L., Morett, M. and Clementi, F. (1992). A functional α-bungarotoxin receptor is present in chick cerebellum: purification and characterisation. *Neuroscience* **50,** 117-127.

Gotti, C., Moretti, M., Longhi, R., Briscini, L., Manera, E. and Clementi, F. (1993). Anti-peptide specific antibodies for the characterization of different α subunits of α-bungarotoxin binding acetylcholine receptors present in chick optic lobe. *J. Receptor Res.* **13,** 453-465.

Gotti, C., Moretti, M., Maggi, R., Longhi, R., Hanke, W., Klinke, N. and Clementi, F. (1997). α7 and α8 nicotinic receptor subtypes immunoprecipitated from chick retina have different immunological, pharmacological and functional properties. *Eur. J. Neurosci.* **9,** 1201-1211.

Grady, S., Marks, M. J., Wonnacott, S. and Collins, A. C. (1992). Characterization of nicotinic receptor-mediated [^{3}H]dopamine release from synaptosomes prepared from mouse striatum. *J. Neurochem.* **59,** 848-856.

Grady, S. R., Marks, M. J. and Collins, A. C. (1994). Desensitization of nicotine-stimulated [^{3}H]-dopamine release from mouse striatal synaptosomes. *J. Neurochem.* **62,** 1390-1398.

Gray, R., Rajan, A. S., Radcliffe, K. A., Yakehiro, M. and Dani, J. A. (1996). Hippocampal synaptic transmission enhanced by low concentrations of nicotine. *Nature* **383,** 713-716.

Green, L., Sytkowski, A., Vogel, A. and Nirenberg, M. (1973). α-Bungarotoxin used as a probe for acetylcholine receptors of cultured neurons. *Nature* **243,** 163-166.

Green, T., Stauffer, K. A. and Lummis, C. R. (1995). Expression of recombinant homo-oligomeric 5-hydroxytryptamine$_3$ receptors provides new insights into their maturation and structure. *J. Biol. Chem.* **270,** 6056-6061.

Green, W. N. and Claudio, T. (1993). Acetylcholine receptor assembly: subunit folding and oligomerization occur sequentially. *Cell* **74,** 57-69.

Green, W. N., Ross, A. F. and Claudio, T. (1991a). Acetylcholine receptor assembly is stimulated by phosphorylation of its gamma subunit. *Neuron* **7,** 659-666.

Green, W. N., Ross, A. F. and Claudio, T. (1991b). cAMP stimulation of acetylcholine receptor expression is mediated through posttranslational mechanisms. *Proc Natl Acad Sci U S A* **88,** 854-8.

Grenningloh, G., Rienitz, A., Schmitt, B., Methfessel, C., Zensen, M., Beyreuther, K., Gundelfinger, E. D. and Betz, H. (1987). The strychnine-binding subunit of the glycine receptor shows homology with nicotinic acetylcholine receptors. *Nature* **328,** 215-220.

Gross, A., Ballivet, M., Rungger, D. and Bertrand, D. (1991). Neuronal nicotinic acetylcholine receptors expressed in *Xenopus* oocytes: role of the α subunit in agonist sensitivity and desensitization. *Pflugers Arch* **419,** 545-51.

Gu, Y., Black, R. A., Ring, G. and Hall, Z. W. (1989). A C2 muscle cell variant defective in transport of the acetylcholine receptor to the cell surface. *J. Biol. Chem.* **264,** 11952-11957.

Gu, Y., Forsayeth, J. R., Verrall, S., Yu, X. M. and Hall, Z. W. (1991). Assembly of the mammalian muscle acetylcholine receptor in transfected COS cells. *J. Cell Biol.* **114,** 799-807.

Gu, Y., Franco, A., Jr., Gardner, P. D., Lansman, J. B., Forsayeth, J. R. and Hall, Z. W. (1990). Properties of embryonic and adult muscle acetylcholine receptors transiently expressed in COS cells. *Neuron* **5,** 147-57.

Gurdon, J. B., Lane, C. D., Woodland, H. R. and Marbaix, G. (1971). Use of frog eggs and oocytes for the study of messenger RNA and its translation in living cells. *Nature* **233,** 177-182.

Halvorsen, S. W. and Berg, D. K. (1990). Subunit composition of nicotinic acetylcholine receptors from chick ciliary ganglia. *J. Neurosci.* **10,** 1711-1718.

Hamilton, S. L., McLaughlin, M. and Karlin, A. (1979). Formation of disulphide linked oligomers of acetylcholine receptor in membrane from *Torpedo* electric tissue. *Biochemistry* **18,** 155-163.

Hargreaves, A. C., Lummis, S. C. R. and Taylor, C. W. (1994). Ca^{2+} permeability of cloned and native 5-hydroxytryptamine type 3 receptors. *Mol. Pharmacol.* **46,** 1120-1128.

Hartman, D. S., Millar, N. S. and Claudio, T. (1991). Extracellular synaptic factors induce clustering of acetylcholine receptors stably expressed in fibroblasts. *J Cell Biol* **115,** 165-77.

Harvey, S. C. and Luetje, C. (1996). Determinants of competitive antagonist sensitivity on neuronal nicotinic receptor β subunits. *J. Neurosci.* **16,** 3798-3806.

Hasel, K. W., Glass, J. R., Godbout, M. and Sutcliffe, J. G. (1991). An endoplasmic reticulum-specific cyclophilin. *Mol. Cell. Biol.* **11,** 3484-3491.

Helekar, S. A., Char, D., Neff, S. and Patrick, J. (1994). Prolyl isomerase requirement for the expression of functional homo-oligomeric ligand-gated ion channels. *Neuron* **12,** 179-189.

Helekar, S. A. and Patrick, J. (1997). Peptidyl prolyl cis-trans isomerase activity of cyclophilin A in functional homo-oligomeric receptor expression. *Proc. Natl. Acad. Sci. USA* **94,** 5432-5437.

Henderson, L. P., Gdovin, M. J., Liu, C., Gardner, P. D. and Maue, R. A. (1994). Nerve growth factor increases nicotinic ACh receptor gene expression and current density in wild-type and protein kinase A-deficient PC12 cells. *J. Neuroscience* **14,** 1153-1163.

Henley, J. M., Lindstrom, J. M. and Oswald, R. E. (1986). Acetylcholine receptor synthesis in retina and transport to optic tectum in goldfish. *Science* **232,** 1627-1629.

Henningfield, J. E., Miyasato, K. and Jasinski, D. R. (1983). Cigarette smokers self-administer intravenous nicotine. *Pharmacol. Biochem. Behav.* **19,** 887-890.

Hopp, T. P., Prickett, K. S., Price, V. L., Libby, R. T., March, C. J., Cerretti, D. P., Urdal, D. L. and Conlon, P. J. (1988). A short polypeptide marker sequence useful for recombinant protein identification and purification. *Biotechnology* **6,** 1204-1210.

Hucho, F., Layer, P., Kiefer, H. R. and Bandini, G. (1976). Photoaffinity labeling and quaternary structure of the acetylcholine receptor from *Torpedo californica*. *Proc. Natl. Acad. Sci. USA* **73,** 2624-2628.

Huganir, R. L., Miles, K. and Greengard, P. (1984). Phosphorylation of the nicotinic acetylcholine receptor by an endogenous tyrosine-specific kinase. *Proc Natl Acad Sci USA* **81,** 6968-6972.

Hunt, S. and Schmidt, J. (1978). Some observations on the binding patterns of α-bungarotoxin in the central nervous sytem of the rat. *Brain Res.* **157,** 213-232.

Hurtley, S. M., Bole, D. G., Hoover, L. H., Helenius, A. and Copeland, C. S. (1989). Interactions of misfolded influenza virus hemagglutinin with binding protein (BiP). *J Cell Biol* **108,** 2117-26.

Hussy, N., Ballivet, M. and Bertrand, D. (1994). Agonist and antagonist effects of nicotine on chick neuronal nicotinic receptors are defined by α and β subunits. *J Neurophysiol* **72,** 1317-1326.

Iino, M., Ozawa, S. and Tsuzuki, K. (1990). Permeation of calcium through excitatory amino acid receptor channels in cultured rat hippocampal neurons. *J. Physiol.* **424,** 151-165.

Imoto, K., Busch, C., Sakmann, B., Mishina, M., Konno, T., Nakai, J., Bujo, H., Mori, Y., Fukuda, K. and Numa, S. (1988). Rings of negatively charged amino acids determine the acetylcholine receptor channel conductance. *Nature* **335,** 645-8.

Jayawickreme, S. P., Green, W. N. and Claudio, T. (1994). Cyclic AMP-regulated AChR assembly is independent of AChR subunit phosphorylation by PKA. *J. Cell Science* **107,** 1641-1651.

Johnson, D. S., Martinez, J., Elgoyhen, A. B., Heinemann, S. F. and McIntosh, J. M. (1995). α-Conotoxin ImI exhibits subtype-specific nicotinic acetylcholine receptor blockade: preferential inhibition of homomeric α7 and α9 receptors. *Mol. Pharmacol.* **48,** 194-199.

Jones, G. M., Sahakian, B. J., Levy, R., Warburton, D. M. and Gray, J. A. (1992). Effects of acute subcutaneous nicotine on attention, information, processing and short-term memory in Alzheimer's disease. *Psychopharmacology* **108,** 485-494.

Jones, S. and Yakel, J. L. (1997). Functional nicotinic ACh receptor on interneurones in the rat hippocampus. *J. Physiol.* **504,** 603-610.

Kao, P. N., Dwork, A. J., Kaldany, R. R. J., Silver, M., Wideman, J., Stein, J. and Karlin, A. (1984). Identification of the alpha-subunit half cysteine specifically labeled by an affinity reagent for acetylcholine receptor binding site. *J. Biol. Chem.* **259,** 11662-65.

Kao, P. N. and Karlin, A. (1986). Acetylcholine receptor binding site contains a disulfide cross-link between adjacent half-cystinyl residues. *J. Biol. Chem.* **261,** 8085-8088.

Karlin, A. (1991). Explorations of the nicotinic acetylcholine receptor. *Harvey Lectures* **85,** 71-107.

Karlin, A. (1993). Structure of nicotinic acetylcholine receptors. *Curr. Opin. Neurobiol.* **3,** 299-309.

Karlin, A. and Cowburn, D. A. (1973). The affinity labeling of partially purified acetylcholine receptor from electric tissue of *Electrophorous*. *Proc. Natl. Acad. Sci. USA* **70,** 3636-3640.

Karlin, A., Holtzman, E., Yodh, N., Lobel, P., Wall, J. and Hainfeld, J. (1983). The arrangement of the subunits of the acetylcholine receptor of *Torpedo californica*. *J. Biol. Chem.* **258,** 6678-6681.

Kassner, P. D. and Berg, D. K. (1997). Differences in the fate of neuronal acetylcholine receptor protein expressed in neurons and stably transfected cells. *J. Neurobiol.* **33,** 968-982.

Katz, B. and Miledi, R. (1977). Transmitter leakage from motor nerve endings. *Proc. R. Soc. Lond. B* **196,** 59-72.

Keinanen, K., Wisden, W., Sommer, B., Werner, P., Herb, A., Verdoorn, T. A., Sakmann, B. and Seeberg, P. H. (1990). A family of AMPA-selective glutamate receptors. *Science* **249,** 556-560.

Keyser, K. T., Britto, L. R., Schoepfer, R., Whiting, P., Cooper, J., Conroy, W., Brozozowska-Prechtl, A., Karten, H. J. and Lindstrom, J. (1993). Three subtypes of alpha-bungarotoxin-sensitive nicotinic acetylcholine receptors are expressed in chick retina. *J Neurosci* **13,** 442-54.

Kienker, P., Tomaselli, G., Jurman, M. and Yellen, G. (1994). Conductance mutations of the nicotinic acetylcholine receptor do not act by a simple electrostatic mechanism. *Biophys. J.* **66,** 325-334.

Klimaschewski, L., Reuss, S., Spessert, R., Lobron, C., Wevers, A., Heym, C., Maelicke, A. and Schroder, H. (1994). Expression of nicotinic acetylcholine receptors in the rat superior cervical ganglion on mRNA and protein level. *Mol. Brain. Res.* **27,** 167-173.

Kolbilka, B. (1992). Adrenergic receptors as models for G-protein-coupled receptors. *Annu. Rev. Neurosci.* **15,** 87-114.

Kornfeld, R. and Kornfeld, S. (1985). Assembly of asparagine-linked oligosaccharides. *Annu. Rev. Biochem.* **54,** 631-664.

Kurosaki, T., Fukuda, K., Konno, T., Mori, Y., Tanaka, K., Mishina, M. and Numa, S. (1987). Functional properties of nicotinic acetylcholine receptor subunits expressed in various combinations. *Febs Lett* **214,** 253-258.

Lamar, E., Miller, K. and Patrick, J. (1990). Amplification of genome sequences identifies a new gene, α6, in the nicotinic acetylcholine receptor gene family. *Soc. Neurosci. Abstr.* **16,** 681.

Lane, C. D., Shannon, S. and Craig, R. (1979). Sequestration and turnover of guinea-pig milk proteins and chicken ovalbumin in *Xenopus* oocytes. *Eur. J. Biochem.* **101,** 485-495.

Lange, K., Wells, F., Jenner, P. and Marsden, P. (1993). Altered muscarinic and nicotinic receptor densities in cortical and subcortical regions in Parkinson's disease. *J. Neurochem.* **60,** 197-203.

Lansdell, S. J., Schmitt, B., Betz, H., Sattelle, D. B. and Millar, N. S. (1997). Temperature-sensitive expression of *Drosophila* neuronal nicotinic acetylcholine receptors. *J. Neurochem.* **68,** 1812-1819.

LaPolla, R. J., Mayne, K. M. and Davidson, N. (1984). Isolation and characterisation of a cDNA clone for the complete coding region of the δ subunit of the mouse acetylcholine receptor. *Proc. Natl. Acad. Sci. USA* **81,** 7970-7974.

Le Novère, N. and Changeux, J.-P. (1995). Molecular evolution of the nicotinic acetylcholine receptor: An example of multigene family in excitable cells. *J. Mol. Evol.* **40,** 155-172.

Le Novère, N., Zoli, M. and Changeaux, J. P. (1996). Neuronal nicotinic receptor alpha 6 mRNA is selectively concentrated in the catecholaminergic nuclei of the rat brain. *Eur. J. Neurosci.* **8,** 2428-2439.

Lee, C. Y. and Chang, C. C. (1966). Modes of actions of purified toxins from elapid venoms on neuromuscular transmission. *Mem. Inst. Butantan Sao Paulo* **33,** 555-572.

Lena, C., Changeux, J. P. and Mulle, C. (1993). Evidence for pre-terminal nicotinic receptors of GABAergic axons in the rat interpenduncular nucleus. *J. Neurosci.* **13,** 2680-2688.

Leonard, R. J., Labarca, C. G., Charnet, P., Davidson, N. and Lester, H. A. (1988). Evidence that the M2 membrane-spanning region lines the ion channel pore of the nicotinic receptor. *Science* **242,** 1578-1581.

Levin, E. D., Wilson, W., Rose, J. E. and McEvoy, J. (1996). Nicotine-haloperidol interactions and cognitive performance in schizophrenics. *Neuropsychopharmacology* **15,** 429-436.

Lewis, T. M., Harkness, P. C., Sivilotti, L. G., Colquhoun, D. and Millar, N. S. (1997). The ion channel properties of a rat recombinant neuronal nicotinic receptor are dependent on the host cell type. *J. Physiol.* **505,** 299-306.

Lindstrom. (1978). Immunization of rats with polypeptide chains from *Torpedo* acetylcholine receptor causes an autoimmune response to receptors in rat muscle. *Proc. Natl. Acad. Sci. USA* **75,** 769-773.

Lindstrom. (1979). Immunochemical similarities between subunits of acetylcholine receptors from *Torpedo*, *Electrophorous*, and mammalian muscle. *Biochemistry* **18,** 4470-4480.

Listerud, M., Brussaard, A. B., Devay, P., Colman, D. R. and Role, L. W. (1991). Functional contribution of neuronal AChR subunits revealed by antisense oligonucleotides. *Science* **254,** 1518-1521.

Lo, D. C., Pinkham, J. L. and Stevens, C. F. (1991). Role of a key cysteine residue in the gating of the acetylcholine receptor. *Neuron* **6,** 31-40.

Loring, R. H., Dahm, L. M. and Zigmond, R. E. (1985). Localization of α-bungarotoxin binding sites in the ciliary ganglion of the embryonic chick: an autoradiographic study at the light and electron microscope level. *Neuorscience* **14,** 645-660.

Luetje, C. W. and Patrick, J. (1991). Both α- and β-subunits contribute to the agonist sensitivity of neuronal nicotinic acetylcholine receptors. *J. Neurosci.* **11,** 837-45.

Lukas, R. J., Norman, S. A. and Lucero, L. (1993). Characterization of nicotinic acetylcholine receptors expressed by cells of the SH-SY5Y neuroblastoma clonal line. *Mol. Cell. Neurosci.* **4,** 1-12.

Lummis, S. C. R. and Martin, I. L. (1991). Solubilisation, purification and functional reconstitution of 5-hydroxytryptamine$_3$ receptors from NIE-115 neuroblastoma cells. *Mol. Pharmacol.* **41,** 18-23.

Maricq, A. V., Peterson, A. S., Brake, A. J., Myers, R. M. and Julius, D. (1991). Primary structure and functional expression of the 5HT$_3$ receptor, a serotonin-gated ion channel. *Science* **254,** 432-437.

Marks, M., Grady, S. and Collins, A. (1993). Downregulation of nicotinic receptor function after chronic nicotine infusion. *J. Pharmacol. Exp. Ther.* **266,** 1268-1275.

Marks, M., Pauly, J., Gross, D., Deneris, E., Hermans-Borgmeyer, I., Heinemann, S. and Collins, A. (1992). Nicotine binding and nicotinic receptor subunit mRNA after chronic nicotine treatment. *J. Neurosci.* **12,** 2765-2784.

Marks, M., Stitzel, J. and Collins, A. (1985). Time course study of the effects of chronic nicotine infusion on drug response and brain receptor. *J. Pharmacol. Exp. Ther.* **235,** 619-628.

Mathie, A., Cull-Candy, S. G. and Colquhoun, D. (1991). Conductance and kinetic properties of single nicotinic acetylcholine receptor channels in rat sympathetic neurones. *J. Physiol.* **439,** 717-750.

Mayer, M. L. and Westbrook, G. L. (1987). Permeation and block of N-methyl-D-aspartic acid receptor channels by divalent cations in mouse cultured central neurons. *J. Physiol.* **394,** 501-527.

McCrea, P., Popot, J.-L. and Engelman, D. M. (1987). Transmembrane topography of the nicotinic acetylcholine receptor δ subunit. *EMBO. J.* **6,** 3619-3626.

McGehee, D. S., Heath, M. J. S., Gelber, S., Devay, P. and Role, L. W. (1995). Nicotine enhancement of fast excitatory synaptic transmission in CNS by presynaptic receptors. *Science* **269,** 1692-1696.

McGehee, D. S. and Role, L. W. (1995). Physiological diversity of nicotinic acetylcholine receptors expressed by vertebrate neurons. *Annu. Rev. Physiol.* **57,** 521-546.

McLane, K. E., Wu, X., Lindstrom, J. M. and Conti-Tronconi, B. M. (1992). Epitope mapping of polyclonal and monoclonal antibodies against two α-bungarotoxin-binding α subunits from neuronal nicotinic receptors. *J. Neuroimmunol.* **38,** 115-128.

McMahon, L. L., Yoon, K. W. and Chiappinelli, V. A. (1994a). Electrophysiological evidence for presynaptic nicotinic receptors in the avian ventral lateral geniculate nucleus. *J. Neurophysiol.* **71,** 826-829.

McMahon, L. L., Yoon, K. W. and Chiappinelli, V. A. (1994b). Nicotinic receptor activation facilitates GABAergic neurotransmission in the avian lateral spiriform nucleus. *Neuroscience* **59,** 689-698.

Merlo Pich, E., Pagliusi, S. R., Tessari, M., Talabot-Ayer, D., Hooft van Huijsduijnen, R. and Chiamulera, C. (1997). Common neural substrates for the addictive properties of nicotine and cocaine. *Science* **275,** 83-86.

Mishina, M., Kurosaki, T., Tobimatsu, T., Morimoto, Y., Noda, M., Yamamoto, T., Terao, M., Lindstom, J., Takahashi, T., Kuno, M. and Numa, S. (1984). Expression of functional acetylcholine receptor from cloned cDNAs. *Nature* **307,** 604-608.

Mishina, M., Takai, T., Imoto, K., Noda, M., Takahashi, T., Numa, S., Methfessel, C. and Sakman, B. (1986). Molecular distinction between fetal and adult forms of muscle acetylcholine receptor. *Nature* **313,** 364-369.

Mitra, A. K., McCarthy, M. P. and Stroud, R. M. (1989). Three-dimensional structure of the nicotinic acetylcholine receptor and the location of the major associated 43-kD cytoskeletal protein, determined at 22Å by low dose electron microscopy and X-ray diffraction to 12.5Å. *J. Cell. Biol.* **109,** 755-774.

Morris, B. J., Hicks, A. A., Wisden, W., Darlison, M. G., Hunt, S. P. and Barnard, E. A. (1990). Distinct regional expression of nicotinic acetylcholine receptor genes in chick brain. *Brain Res Mol Brain Res* **7,** 305-15.

Moss, B. L., Schuetze, S. M. and Role, L. W. (1989). Functional properties and developmental regulation of nicotinic acetylcholine receptors on embryonic chicken sympathetic neurons. *Neuron* **3,** 597-607.

Mulle, C., Vidal, C., Benoit, P. and Changeux, J. P. (1991). Existence of different subtypes of nicotinic acetylcholine receptors in the rat habenulo-interpeduncular system. *J Neurosci* **11,** 2588-2597.

Nef, P., Mauron, A., Stalder, R., Alliod, C. and Ballivet, M. (1984). Structure, linkage, and sequence of the two genes encoding the δ and γ subunits of the nicotinic acetylcholine receptor. *Proc. Natl. Acad. Sci. USA* **81,** 7975-7979.

Nef, P., Oneyser, C., Alliod, C., Couturier, S. and Ballivet, M. (1988). Genes expressed in the brain define three distinct neuronal nicotinic acetylcholine receptors. *Embo J* **7,** 595-601.

Neubig, R. R. and Cohen, J. B. (1979). Equilibrium binding of [^{3}H]tubocurarine and [^{3}H]acetylcholine by *Torpedo* postsynaptic membranes: Stoichiometry and ligand interactions. *Biochemistry* **18,** 5464-5475.

Noda, M., Furutani, Y., Takahashi, H., Toyosato, M. and Tanabe, T. (1983a). Cloning and sequence analysis of calf cDNA and human genomic DNA encoding α-subunit precursor of muscle acetylcholine receptor. *Nature* **305,** 818-823.

Noda, M., Takahashi, H., Tanabe, T., Toyosato, M., Furutani, Y., Hirose, T., Asai, M., Inayama, S., Miyata, T. and Numa, S. (1982). Primary structure of α-subunit precursor of *Torpedo californica* acetylcholine receptor deduced from cDNA sequence. *Nature* **299,** 793-797.

Noda, M., Takahashi, H., Tanabe, T., Toyosato, M., Kikyotani, S., Furutana, Y., Hirose, T., Takashima, H., Inayama, S., Miyata, T. and Numa, S. (1983b). Stuctural homology of *Torpedo californica* acetylcholine receptor subunits. *Nature* **302,** 528-532.

Noda, M., Takahashi, H., Tanabe, T., Toyosato, M. and Kokyotani, S. (1983c). Primary structures of beta and delta-subunit precursors of *Torpedo Californica* acetylcholine receptor deduced from cDNA sequences. *Nature* **302,** 528-532.

Nomoto, H., Takahashi, N., Nagaki, Y., Endo, S., Arata, Y. and Hayashi, K. (1986). Carbohydrate structures of acetylcholine receptor from Torpedo californica and distribution of oligosaccharides among the subunits. *Eur. J. Biochem.* **157,** 133-142.

Norman, R. I., Mehraban, F., Barnard, E. A. and Dolly, J. O. (1982). Nicotinic acetylcholine receptor from chick optic lobe. *Proc. Natl. Acad. Sci. USA* **79,** 1321-1325.

Orr Urtreger, A., Goldner, F. M., Saeki, M., Lorenzo, I., Goldberg, L., De Biasi, M., Dani, J. A., Patrick, J. and Beaudet, A. L. (1997). Mice deficient in the α7 neuronal nicotinic acetylcholine receptor lack α-bungarotoxin binding sites and hippocampal fast nicotinic currents. *J. Neurosci.* **17,** 9165-9171.

Orr Urtreger, A., Noebels, J. L., Goldner, F. M., Patrick, J. and Beaudet, A. L. (1996). A novel hypersynchronous neocortical EEG phenotype in mice deficient in the neuronal nicotinic acetylcholine receptor (nAChR) alpha 7 subunit gene. *Am. J. Hum. Genet.* **59,** A53.

Oswald, R. E. and Freeman, J. A. (1981). α-Bungarotoxin binding and central nervous system nicotinic acetylcholine receptors. *Neuroscience* **6,** 1-14.

Palma, E., Bertrand, S., Binzoni, T. and Bertrand, D. (1996). Neuronal nicotinic α7 receptor expressed in *Xenopus* oocytes presents five putative binding sites for methyllycaconitine. *J. Physiol.* **491,** 151-161.

Papke, R. L., Boulter, J., Patrick, J. and Heinemann, S. (1989). Single-channel currents of rat neuronal nicotinic acetylcholine receptors expressed in Xenopus oocytes. *Neuron* **3,** 589-96.

Papke, R. L. and Heinemann, S. F. (1993). Partial agonist properties of cytisine on neuronal nicotinic receptors containing the β2 subunit. *Mol. Pharmacol.* **45,** 142-149.

Papke, R. L. and Heinmann, S. F. (1991). The role of the β4-subunit in determining the kinetic properties of rat neuronal nicotinic acteylcholine α3-receptors. *J. Physiol.* **440,** 95-112.

Patrick, J. and Stallcup, B. (1977a). α-Bungarotoxin binding and cholinergic receptor function on a rat sympathetic nerve line. *J. Biol. Chem.* **252,** 8629-33.

Patrick, J. and Stallcup, B. (1977b). Immunological distinction between acetylcholine receptor and the α-bungarotoxin-binding component on sympathetic neurons. *Proc. Natl. Acad. Sci. USA* **74,** 4689-464692.

Paulson, H. L., Ross, A. F., Green, W. N. and Claudio, T. (1991). Analysis of early events in acetylcholine receptor assembly. *J. Cell Biol.* **113,** 1371-84.

Pedersen, S. E. and Cohen, J. B. (1990). *d*-Tubocurarine binding sites are located at α-γ and α-δ subunit interfaces of the nicotinic acetylcholine receptor. *Proc. Natl. Acad. Sci. USA* **87,** 2785-2789.

Peng, X., Gerzanich, V., Anand, R., Whiting, P. J. and Lindstrom, J. (1994a). Nicotine-induced increase in neuronal nicotinic receptors results from a decrease in the rate of receptor turnover. *Mol. Pharmacol.* **46,** 523-530.

Peng, X., Katz, M., Gerzanich, V., Anand, R. and Lindstrom, J. (1994b). Human α7 acetylcholine receptor: cloning of the α7 subunit from the SH-SY5Y cell line and determination of pharmacological properties of native receptors and functional α7 homomers in *Xenopus* oocytes. *Mol. Pharmacol.* **45,** 546-554.

Peper, K., Bradley, R. J. and Dreyer, F. (1982). The acetylcholine receptor at the neuromuscular junction. *Physiol. Rev.* **62,** 1271-1340.

Perry, E. K., Morris, C. M., Court, J. A., Cheng, A., Fairbain, A. F., McKeith, I. G., Irving, D., Brown, A. and Perry, R. H. (1995). Alteration in nicotinic binding sites in Parkinson's disease, Lewy body dementia and Alzheimer's disease: possible index of early neuropathology. *Neuroscience* **64,** 385-395.

Picciotto, M. R., Zoli, M., Léna, C., Bessis, A., Lallemand, Y., Le Novère, N., Vincent, P., Merlo Pich, E., Brûlet, P. and Changeux, J. P. (1995). Abnormal avoidance learning in mice lacking functional high-affinity nicotine receptor in the brain. *Nature* **374,** 65-67.

Picciotto, M. R., Zoli, M., Rimondini, R., Léna, C., Marubio, L. M., Merlo Pich, E., Fuxe, K. and Changeux, J.-P. (1998). Acetylcholine receptors containing the b2 subunit are involved in the reinforcing properties of nicotine. *Nature* **391,** 173-177.

Pontieri, F. E., Tanda, G., Orzi, F. and Di Chiara, G. (1996). Effects of nicotine on the nucleus accumbens and similarity to those of addicitive drugs. *Nature* **382,** 255-257.

Popot, J.-L. and Changeux, J.-P. (1984). Nicotinic receptor of acetylcholine: structure of an oligomeric integral membrane protein. *Physiol. Rev.* **64,** 1162-1239.

Pritchett, D. B., Southeimer, H., Gorman, C. M., Ketterman, H., Seeburg, P. H. and Schofield, P. R. (1988). Transient expression shows ligand gating and allosteric potentiation of $GABA_A$ receptor subunits. *Science* **242,** 1306-1308.

Puchacz, E., Buisson, B., Bertrand, D. and Lukas, R. L. (1994). Functional expression of nicotinic acetylcholine receptors containing rat α7 subunits in human SH-SY5Y neuroblastoma cells. *FEBS Letters* **354,** 155-159.

Pugh, P. C. and Berg, D. K. (1994). Neuronal acetylcholine receptors that bind a-bungarotoxin mediate neurite retraction in a calcium dependent manner. *J. Neurosci.* **14,** 889-896.

Quik, M., Choremis, J., Komourian, J., Lukas, R. J. and Puchacz, E. (1996). Similarity between rat brain nicotinic α-bungarotoxin receptors and stably expressed α-bungarotoxin binding sites. *J. Neurochem.* **67,** 145-154.

Quik, M., Philie, J. and Choremis, J. (1997). Modulation of α7 nicotinic receptor-mediated calcium influx by nicotinic agonists. *Mol. Pharmacol.* **51,** 499-506.

Ragozzino, D., Fucile, S., Giovannelli, A., Grassi, F., Mileo, A. M., Ballivet, M., Alema, S. and Eusebi, F. (1997). Functional properties of neuronal nicotinic acetylcholine receptor channels expressed in transfected human cells. *Eur. J. Neurosci.* **9,** 480-488.

Ramirez-Latorre, J., Yu, C. R., Qu, F., Perin, F., Karlin, A. and Role, L. (1996). Functional contributions of α5 subunit to neuronal acetylcholine receptor channels. *Nature* **380,** 347-351.

Rapier, C., Lunt, G. G. and Wonnacott, S. (1990). Nicotine modulation of [3H]-dopamine release form striatal synaptosomes: pahramacological characterization. *J. Neurochem.* **54,** 937-945.

Reiter, M. J., Cowburn, D. A., Prives, J. M. and Karlin, A. (1972). Affinity labeling of the acetylcholine receptor in the electroplax: Electrophoretic separation in sodium dodecyl sulphate. *Proc. Natl. Acad. Sci. USA* **69,** 1168-1172.

Revah, F., Bertrand, D., Galzi, J. L., Devillers-Thiery, A., Mulle, C., Hussy, N., Bertrand, S., Ballivet, M. and Changeux, J. P. (1991). Mutations in the channel domain alter desensitization of a neuronal nicotinic receptor. *Nature* **353,** 846-9.

Revah, F., Galzi, J. L., Giraudat, J., Haumont, P. Y., Lederer, F. and Changeux, J. P. (1990). The noncompetitive blocker [3H]chlorpromazine labels three amino acids of the acetylcholine receptor γ subunit: implications for the α-helical organization of regions MII and for the structure of the ion channel. *Proc Natl Acad Sci U S A* **87,** 4675-9.

Reynolds, J. A. and Karlin, A. (1978). Molecular weight in a detergent solution of acetylcholine receptor from *Torpedo californica*. *Biochemistry* **17,** 2035-2038.

Rogers, S. W., Gahring, L. C., Papke, R. L. and Heinemann, S. (1991). Identification of cultured cells expressing ligand-gated cationic channels. *Protein Expr Purif* **2,** 108-16.

Rogers, S. W., Mandelzys, A., Deneris, E. S., Cooper, E. and Heinemann, S. (1992). The expression of nicotinic acetylcholine receptors by PC12 cells treated with NGF. *J Neurosci* **12,** 4611-23.

Role, L. W. (1992). Diversity in primary structure and function of neuronal nicotinic acetylcholine receptor channels. *Curr. Op. Neurobiol.* **2,** 254-262.

Role, L. W. and Berg, D. K. (1996). Nicotinic receptors in the develpopment and modulation of CNS synapses. *Neuron* **16,** 1077-1085.

Rose, J. E. and Corrigall, W. A. (1997). Nicotine self-administration in animals and humans - similarities and differences. *Psychopharmacology* **130,** 28-40.

Ross, A. F., Green, W. N., Hartman, D. S. and Claudio, T. (1991). Efficiency of acetylcholine receptor subunit assembly and its regulation by cAMP. *J Cell Biol* **113,** 623-636.

Ross, A. F., Rapuano, M., Schmidt, J. H. and Prives, J. M. (1987). Phosphorylation and assembly of nicotinic acetylcholine receptor subunits in cultured chick muscle cells. *J. Biol. Chem.* **262,** 14640-14647.

Rust, G., Burgunder, J.-M., Lauterburg, T. E. and Cachelin, A. B. (1994). Expression of neuronal nicotinic acetylcholine receptor subunit genes in the rat autonomic nervous system. *Eur. J. Neurosci.* **6,** 478-485.

Sakmann, B. and Neher, E. (1984). Patch-clamp techniques for studying ionic channels in excitable membranes. *Annu. Rev. Physiol.* **46,** 455-472.

Sambrook, J., Fritsh, E. F. and Maniatis, T. (1989). Molecular Cloning: A Laboratory Manual, vol. 2. Plainview, NY: Cold Spring Harbor Laboratory Press.

Sands, S. B., Costa, A. C. S. and Patrick, J. W. (1993). Barium permeability of neuronal nicotinic receptor α7 expressed in *Xenopus* oocyes. *Biophys. J.* **65,** 2614-2621.

Sargent, P. B. (1993). The diversity of neuronal nicotinic acetylcholine receptors. *Ann. Rev. Neurosci.* **16,** 403-443.

Schoepfer, R., Conroy, W. G., Whiting, P., Gore, M. and Lindstrom, J. (1990). Brain α-bungarotoxin binding protein cDNAs and mAbs reveal subtypes of this branch of the ligand-gated ion channel gene superfamily. *Neuron* **5,** 35-48.

Schoepfer, R., Halvorsen, S. W., Conroy, W. G., Whiting, P. and Lindstrom, J. (1989). Antisera against an acetylcholine receptor alpha 3 fusion protein bind to ganglionic but not to brain nicotinic acetylcholine receptors. *Febs Lett* **257,** 393-9.

Schoepfer, R., Whiting, P., Esch, F., Blacher, R., Shimasaki, S. and Lindstrom, J. (1988). cDNA clones coding for the structural subunit of a chicken brain nicotinic acetylcholine receptor. *Neuron* **1,** 241-8.

Schofield, P. R., Darlison, M. G., Fujita, N., Burt, D. R., Stephenson, F. A., Rodriguez, H., Rhee, L. M., Ramachandran, J., Reale, V., Glencorse, T. A., Seeburg, P. H. and Barnard, E. A. (1987). Sequence and fuctional expression of

the $GABA_A$ receptor shows a ligand-gated receptor super-family. *Nature* **328,** 221-227.

Schwartz, R. and Keller, K. (1983). Nicotinic cholinergic receptor binding sites in brain: Regulation *in vivo*. *Science* **220,** 214-216.

Schwartz, R. and Keller, K. (1985). *In vivo* regulation of [^{3}H]-acetylcholine recognition sites in brain by cholinergic drugs. *J. Neurochem.* **45,** 427-433.

Schwartz, R. D., Lehmann, J. and Kellar, K. J. (1984). Presynaptic cholinergic receptors labelled by [^{3}H]-acetylcholine on catecholamine and serotonin axons in brain. *J. Neurochem.* **42,** 1495-1498.

Seguela, P., Wadiche, J., Dineley-Miller, K., Dani, J. A. and Patrick, J. W. (1993). Molecular cloning, functional properties, and distribution of rat brain α7: a nicotinic cation channel highly permeable to calcium. *J. Neurosci.* **13,** 596-604.

Shytle, R. D., Silver, A. A., Philipp, M. K., McConville, B. J. and Sanberg, P. R. (1996). Transdermal nicointe for Tourette's syndrome. *Drug. Dev. Res.* **38,** 290-298.

Sine, S. (1993). Molecular dissection of subunit interfaces in the acetylcholine receptor: Identification of residues that determine curare selectivity. *Proc. Acad. Natl. Sci. USA* **90,** 9436-9440.

Sine, S. and Claudio, T. (1991a). γ- and δ-subunits regulate the affinity and the cooperativity of ligand binding to the acetylcholine receptor. *J. Biol. Chem.* **266,** 19369-19377.

Sine, S. M. and Claudio, T. (1991b). Stable expression of the mouse nicotinic acetylcholine receptor in mouse fibroblasts. Comparison of receptors in native and transfected cells. *J. Biol. Chem.* **266,** 13679-13689.

Sivilotti, L. G., McNeil, D. K., Lewis, T. M., Nassar, M. A., Schoepfer, R. and Colquhoun, D. (1997). Recombinant nicotinic receptors, expressed in *Xenopus* oocytes, do not resemble native rat symplathetic ganglion receptors in single-channel behaviour. *J. Physiol.* **500,** 123-138.

Smith, M. M., Lindstrom, J. and Merlie, J. P. (1987). Formation of the alpha-bungarotoxin binding site and assembly of the nicotinic acetylcholine receptor subunits occur in the endoplasmic reticulum [published erratum appears in J Biol Chem 1987 Jul 5;262(19):9428]. *J Biol Chem* **262,** 4367-76.

Steinlein, O. K., Magnusson, A., Stoodt, J., Bertrand, S., Weiland, S., Berkovic, S. F., Nakken, K. O., Propping, P. and Bertrand, D. (1997). An insertion mutation of the CHRNA4 gene in a family with autosomal dominant nocturnal frontal lobe epilepsy. *Hum. Mol. Genet.* **6,** 943-947.

Steinlein, O. K., Mulley, J. C., Propping, P., Wallace, R. H., Phillips, H. A., Sutherland, G. R., Scheffer, I. E. and Berkovic, S. F. (1995). A missense mutation in the neuronal nicotinic alpha 4 subunit is associated with autosomal dominant nocturnal frontal lobe epilepsy. *Nat. Genet.* **11,** 201-203.

Sumikawa, K., Houghton, M., Emtage, J. S., Richards, B. M. and Barnard, E. A. (1981). Active multi-subunit ACh receptor assembly by translation of heterologous mRNA in Xenopus oocytes. *Nature* **292,** 862-864.

Swanson, L., Simmons, D., Whiting, P. and Lindstrom, J. (1987). Immunohistochemical localization of neuronal nicotinic receptors in the rhodent central nervous system. *J. Neurosci.* **7,** 3334-3342.

Swick, A. G., Janicot, M., Cheneval-Kastelic, T., McLenithan, J. C. and Lane, M. D. (1992). Promoter-cDNA-directed heterologous protein expression in *Xenopus laevis* oocytes. *Proc. Natl. Acad. Sci. USA* **89,** 1812-1816.

Takai, T., Noda, M., Mishina, M., Shimizu, S., Furutani, Y., Kayano, T., Ikeda, T., Kubo, T., Takahashi, H., Takahashi, T., Kuno, M. and Numa, S. (1985). Cloning, sequencing and expression of cDNA for a novel subunit of acetylcholine receptor from calf muscle. *Nature* **315,** 761-764.

Tanabe, T., Noda, M., Furutani, Y., Takai, T., Takahashi, H., Tanaka, K., Hirose, T., Inayama, S. and Numa, S. (1984). Primary structure of the β subunit precursor of calf muscle acetylcholine receptor deduced from cDNA sequence. *Eur. J. Biochem.* **144,** 11-17.

Tarentino, A. L., Trimble, R. B. and Maley, F. (1978). Endo-β-N-acetylglucosaminidase from Streptomyces plicatus. *Methods. Enzymol.* **50,** 574-580.

Toyoshima, C. and Unwin, N. (1988). Ion channel of acetylcholine receptor reconstructed from images of postsynaptic membranes. *Nature* **336,** 247-50.

Turton, S., Gillard, N. P., Stephenson, F. A. and McKernan, R. M. (1993). Antibodies against the 5-HT_3-A receptor identify a 54 kDa protein affinity-purified from NCB20 cells. *Mol. Neuropharmacol.* **3,** 167-171.

Uetz, P., Abdelatty, F., Villaroel, A., Rappold, G., Weiss, B. and Koenen, M. (1994). Organisation of the murine 5-HT_3 receptor gene and assignment to human chromosome 11. *FEBS Lett.* **339,** 302-306.

Unwin, N. (1993). Nicotinic acetylcholine receptor at 9 Å resolution. *J. Mol. Biol.* **229,** 1101-1124.

Unwin, N. (1995). Acetylcholine receptor channel imaged in the open state. *Nature* **373,** 37-43.

Unwin, N. (1996). Projection structure of nicotinic acetylcholine receptor: distinct conformations of the α subunits. *J. Mol. Biol.* **257,** 586-596.

van der Straten, A., Johansen, H., Rosenberg, M. and Sweet, R. (1989). Introduction and constitutive expression of gene products in cultured *Drosophila* cells using hygromycin B selection. *Methods Mol. Cell. Biol.* **1,** 1-8.

Vernallis, A. B., Conroy, W. G. and Berg, D. K. (1993). Neurons assemble acetylcholine receptors with as many as three kinds of subunits while maintaining subunit segregation among receptor subtypes. *Neuron* **10,** 451-464.

Vernino, S., Amador, M., Luetje, C. W., Patrick, J. and Dani, J. A. (1992). Calcium modulation and high calcium permeability of neuronal nicotinic acetylcholine receptors. *Neuron* **8,** 127-34.

Vijayaraghavan, S., Pugh, P. C., Zhang, Z. W., Rathouz, M. M. and Berg, D. K. (1992). Nicotinic receptors that bind alpha-bungarotoxin on neurons raise intracellular free Ca2+. *Neuron* **8,** 353-62.

Villarroel, A., Herlitze, S., Loenen, M. and Sakmann, B. (1991). Location of a Threonine residue in the α-subunit M2 transmembrane segment that determines the ion flow through the acetylcholine receptor channel. *Proc. R. Soc. Lond. (B)* **243,** 69-74.

Wada, E., Wada, K., Boulter, J., Deneris, E., Heinemann, S., Patrick, J. and Swanson, L. W. (1989). Distribution of alpha 2, alpha 3, alpha 4, and beta 2 neuronal nicotinic receptor subunit mRNAs in the central nervous system: a hybridization histochemical study in the rat. *J. Comp. Neurol.* **284,** 314-335.

Wada, K., Ballivet, M., Boulter, J., Connolly, J., Wada, E., Deneris, E. S., Swanson, L. W., Heinemann, S. and Patrick, J. (1988). Functional expression of a new pharmacological subtype of brain nicotinic acetylcholine receptor. *Science* **240,** 330-4.

Wang, F., V., G., Wells, G. B., Anand, R., Peng, X., Keyser, K. and Lindstrom, J. (1996). Assembly of human neuronal nicotinic receptor α5 subunit with α3, β2, and β4 subunits. *J. Biol. Chem.* **271,** 17656-17665.

Weiland, S., Witzemann, V., Villarroel, A., Propping, P. and Steinlein, O. (1996). An amino acid exchange in the second transmembrane segment of a neuronal nicotinic receptor causes partial epilepsy by altering its desensitisation kinetics. *FEBS Lett.* **398,** 91-96.

Weill, C. L., McNamee, M. G. and Karlin, A. (1974). Affinity labeling of purified acetylcholine receptor from *Torpedo californica*. *Biochem. Biophys. Res. Commun.* **61,** 997-1003.

Wess, J. (1996). Molecular biology of muscarinic acetylcholine receptors. *Crit. Rev. Neurobiol.* **10,** 69-99.

Whitehouse, P., Martino, A., Marcus, K., Zweig, R., Singer, H., Price, D. and Kellar, K. (1988). Reduction in acetylcholine and nicotine binding in several degenerative diseases. *Arch. Neurol.* **45,** 722-724.

Whiting, P., Esch, F., Shimasaki, S. and Lindstrom, J. (1987a). Neuronal nicotinic acetylcholine receptor beta-subunit is coded for by the cDNA clone alpha 4. *FEBS Lett.* **219,** 459-63.

Whiting, P. and Lindstrom, J. (1986a). Pharmacological properties of immuno-isolated neuronal nicotinic receptors. *J. Neurosci.* **6,** 3061-69.

Whiting, P., Schoepfer, R., Lindstrom, J. and Priestley, T. (1991a). Structural and pharmacological characterization of the major brain nicotinic acetylcholine receptor subtype stably expressed in mouse fibroblasts. *Mol. Pharmacol.* **40,** 463-472.

Whiting, P. J. and Lindstrom, J. M. (1986b). Purification and characterization of a nicotinic acetylcholine receptor from chick brain. *Biochemistry* **25,** 2082-2093.

Whiting, P. J., Liu, R., Morley, B. J. and Lindstrom, J. M. (1987b). Structurally different neuronal nicotinic acetylcholine receptor subtypes purified and characterized using monoclonal antibodies. *J. Neurosci.* **7,** 4005-16.

Whiting, P. J., Schoepfer, R., Conroy, W. G., Gore, M. J., Keyser, K. T., Shimasaki, S., Esch, F. and Lindstrom, J. M. (1991b). Expression of nicotinic acetylcholine receptor subtypes in brain and retina. *Brain Res. Mol. Brain Res.* **10,** 61-70.

Willougby, J. J., Ninkima, N. N., Beech, M. M., Latchman, D. S. and Wood, J. N. (1993). Molecular cloning of a human neuronal nicotinic acetylcholine receptor β3-like subunit. *Neurosci. Lett.* **155,** 136-139.

Wilson Horch, H. L. and Sargent, P. B. (1995). Perisynaptic surface distribution of multiple classes of nicotinic acetylcholine receptors on neurons in the chicken ciliary ganglion. *J. Neurosci.* **15,** 7778-7795.

Witzemann, V., Stein, E., Barg, B., Konno, T., Koenen, M., Kues, W., Criado, M., Hofmann, M. and Sakmann, B. (1990). Primary structure and functional expression of the α-, β-, γ-, δ- and ε-subunits of the acetylcholine receptor from rat muscle. *Eur. J. Biochem.* **194,** 437-448.

Wong, E. T., Holstad, S. G., Mennerick, S. J., Hong, S. E., Zorumski, C. F. and Isenberg, K. E. (1995). Pharmacological and physiological properties of a

putative ganglionic nicotinic receptor, α3β4, expressed in transfected eucaryotic cells. *Mol. Brain Res.* **28,** 101-109.

Wonnacott, S. (1990). The paradox of nicotinic receptor upregulation by nicotine. *Trends Pharmacol. Sci.* **11,** 216-219.

Wonnacott, S. (1997). Presynaptic nicotinic ACh receptors. *Trends Neurosci.* **20,** 92-98.

Wonnacott, S., Albuquerque, E. and Bertrand, D. (1993). Methyllycaconitine: A new probe that discriminates between nicotinic receptor subclasses. *Methods Neurosci.* **12,** 263-275.

Zhang, Z.-w., Coggan, J. S. and Berg, D. K. (1996). Synaptic currents generated by neuronal acetylcholine receptors sensitive to α-bungarotoxin. *Neuron* **17,** 1231-1240.

Zhang, Z.-w., Vijayaraghavan, S. and Berg, D. K. (1994). Neuronal acetylcholine receptors that bind α-bungarotoxin with high affinity function as ligand-gated ion channels. *Neuron* **12,** 167-177.